Università degli Studi di Napoli Federico II
Facoltà di Ingegneria

Maria Cristina Pernice

FABRIC TENSOR – BASED POROELASTIC MATERIALS: A "DIRECT" APPROACH

Tesi di Dottorato
XXI ciclo

Il Coordinatore
Prof. Ing. Federico M. MAZZOLANI

Dottorato di Ricerca in Ingegneria delle Costruzioni

INDEX

INTRODUCTION

I. REMARKES ON THE THEORY OF ELASTICITY

1. Deformation Theory 3
1.1. Deformation in $\mathbb{R}^3$ 3
1.2. Volume element in deformation configuration 8
1.3. The Piola transform; area element in the deformed configuration 9
1.4. Length element in the deformed configuration; Strain Tensor 12
2. The Equation of Equilibrium 18
2.1. Applied Forces 19
2.2. The stress principle of Euler and Cauchy 21
2.3. Cauchy's theorem; The Cauchy stress tensor 23
2.4. The equation of equilibrium and the principle of virtual work in the deformed configuration 25
2.5. The Piola-Kirchhoff stress tensors 26
2.6. The equation of equilibrium and the principle of virtual work in the reference configuration 28
3. Linear Anisotropic Elastic Media 31
3.1. Elastic Stiffnesses 32
3.2. Elastic Compliances 34
3.3. Contracted Notations 35
3.4. Material Symmetry 37
3.5. The Elasticity Tensor for Materials with Symmetry Planes 39
3.6. Restrictions on Elastic Constants 44

II. HETEROGENEOUS MATERIALS

1. Inhomogeneous solids: SAS/DAS theorems 45
1.1.Stress Associated Solution (SAS) Theorem for inhomogeneous elasticity 45
1.1.a. Zero- eigenvalue stress and zero-eigenvalue strain fields 46
1.1.b. Stress Associated Solutions (SAS) Theorem 47
1.2. Generalization of the SAS theorem to piecewise defined inhomogeneities 52
1.2.a. Composite materials where φ is constant, but piecewise discontinuous 53

1.2.b. Composite materials where φ is piecewise continuous 55
1.3. Displacement Associated Solutions (DAS) Theorem for inhomogeneous elasticity 57
2. Anisotropic media: volume fraction and Fabric Tensors 65
2.1. Mean Intercept Length (MIL) Tensor 65
2.2. Orientation Distribution Function (ODF) 66
2.3. Fabric Tensor and Damage Distribution 69
2.4. Relationship between Fabric Tensor and Elasticity Tensor 74

III. THEORY OF HOMOGENIZATION

1. Thermodynamic framework and mathematically well-posed homogenization approaches 82
1.1. Representative Volume Element (RVE) 82
1.2. Localization Problem 83
1.3. The Hill-Mandel principle of macrohomogeneity 85
1.4. Example of pure elasticity 85
1.4.a. The localization problem 85
1.4.b. Case where $\mathbf{E}$ is prescribed 86
1.4.c. Case where $\mathbf{\Sigma}$ is prescribed 87
1.4.d. Equivalence between 'prescribed stress' and 'prescribed strain' 89
2. Composite heterogeneous materials: derivation of compliance and stiffness tensors 89
2.1. Direct Methods – Eshelby solution 90
2.2. Variational Methods – Hashin Shtrikman Variational Principle 94
3. Micro mechanics of porous materials: J-tensor and dilute distribution of voids cases 100
3.1. Average strain for prescribed macrostress 103
3.2. Overall compliance tensor for porous elastic solids 105
3.3. Average stress for prescribed macrostrain 106
3.4. Overall elasticity tensor for porous elastic solids 109

IV. ISOTROPIC FUNCTIONS, ENERGY DENSITY POTENTIAL AND SECOND ORDER FABRIC TENSORS FOR POROUS MEDIA

1. Evaluation of the elastic moduli for poroelastic solids: Randomly Arranged Microstructure 111
1.1. The Rho law for bone tissue 112
1.2. Generalization of the Rho law for Cubic/Isotropic Media 114
1.2.a. Finite Element Model 116

1.2.b. Model's Accuracy 118
1.2.c. Cavities of different shapes 119
1.2.d. Homogenized elastic constants 120
1.2.e. Cavity's shape influence 127
1.2.f. Algebraic formulation 130
2. Evaluation of the elastic moduli for poroelastic solids: Oriented Microstructure 132
2.1. Flugge's solution for orthotropic porous material – Low Volume Fraction (LVF) 133
2.2. Constitutive relations for LVF porous material by means of inertia tensor 137
2.3. Compliance tensors of ellipsoidal inclusions – High Volume Fraction (HVF) 140
2.4. Constitutive relations for LVF porous material by means of inertia tensor 143
2.5. Validation of the proposal for the Fabric Tensor – comparison between MIL tensor and inertia tensor 145

V. OPTIMIZATION PROBLEMS FOR ENGINEERED MATERIALS

1. Standard Topological Optimization 151
1.1. Basic problem statement 152
1.2. Isotropic models for solid-void interpolation in elasticity 154
1.3. Microstructure realizing the SIMP-model 155
2. Anisotropic Topological Optimization 157
2.1. State of – the – art 158
2.2. Stationary of the strain energy density for some classes of anisotropic solids 160
2.3. Cowin- Taliercio minimization of the strain energy involving Inertia-Fabric: an explicit strategy 167

CONCLUSIONS AND PERSPECTIVES

REFERENCES

INTRODUCTION

In the framework of the mechanics of heterogeneous media, multi-scale homogenization techniques and micromechanical approaches are widely adopted for characterizing materials that exhibit porous structure at the *nano-*, *micro-* or *macroscopic* level. These efforts are aimed to design new engineered materials and explore their possible applications in civil engineering, aerospace, mechanics, material and chemical science. Also, due to the *hierarchical* structure and the heterogeneity of biological tissues when observed at different scales, anisotropic porous materials also play a crucial role for understanding mechanical-based growth and remodelling phenomena of complex biological systems, as well as to trace new trends in biomechanics and tissue engineering.
On the other hand, it is well known the difficulty of finding closed-form solutions to problems involving anisotropic and inhomogeneous materials, needed for obtaining information about the influence of geometrical and mechanical parameters in a selected phenomenon. Analogously, no many Literature works present rational and unified formulations for estimating overall homogenized stiffness or compliance of porous materials.
In the present work, specific attention is given to porous elastic materials in which the fluid phase can be assumed inessential with reference to the estimating of the mechanical response. This is the case, for example, of drained or not-saturated porous solids, as well as the situation in which the loads are applied quasi-statically.
The porous skeleton of the RVE (Representative Volume Element) – or RVE matrix – is elastic and it can be oriented (anisotropic) or not (isotropic), and characterized by low or high volume fraction. Under these assumptions, inspired by Fabric Tensor-based micromechanical approaches, the work introduces a new consistent measure of the matrix orientation, proportional to the Inertia of the RVE mass, and then establishes a proposal for an unified constitutive elastic law for porous media, in which the inhomogeneity remains depending upon the point-wise variation of the volume fraction. The new model, validated by means of both numerical experiences and closed-form solutions for dilute concentrations of elliptical voids (High Volume Fraction, HVL) and Flugge-like arrangement of the RVE matrix (Low Volume Fraction, LVF), allows to utilize micro-geometrical information directly obtainable from standard techniques and 3D vector codes, for constructing the Fabric Tensor. This yields to avoid several difficulties present in all the previous treatments and furnishes an extremely useful tool for introducing in Finite Element-based computational strategies anisotropic and inhomogeneous characters of the porous media, straightforwardly. At the end, a possible use of the proposed model is also shown in the framework of Topological Optimization problems.

The Ph.D. dissertation is articulated in five chapters.
Chapter I furnishes some basic remarks on theory of elasticity, recalling the concepts of finite deformation and kinematical compatibility, equilibrium and Cauchy's and Piola-Kirchhoff's stress tensors, linear anisotropic elasticity.
Chapter II describes continuum mechanics approaches for heterogeneous media, also presenting some recent results aimed to obtain closed-form solutions for inhomogeneous, anisotropic elastostatic problems. At the end, a micromechanical approach based on second order Fabric Tensors is treated in detail, with reference to the most recent literature results.
Chapter III provides an introduction to the theory of homogenization. In particular, some mathematically well-posed homogenization approaches are presented such as the direct methods – Eshelby's solution – and the variational methods – based on the Hashin Shtrikman variational principles. Micromechanics of porous materials is finally shown in detail.
Chapter IV presents constitutive relations for porous elastic materials, following a way that considers three different class of porous media: with microstructure randomly arranged, with oriented microstructure and low volume fraction and with oriented microstructure and high volume fraction. In the first case, by means of numerical analyses based on Finite Element Method, constitutive relations as function of the sole volume fraction are derived, by using analytical solutions for low volume fraction (Flugge's solutions) and high volume fraction (dilute distribution of voids). In the last two cases, constitutive relations based on the fabric tensor are determined. In particular, a proposal for a direct estimation of the Fabric Tensor by means of the use of Inertia tensors is presented. Some 2D examples that validates such proposal are then illustrated.
Chapter V is devoted to isotropic and anisotropic topological optimization, involving the proposed model for porous anisotropic and inhomogeneous materials. Hence, an example application is illustrated with reference to the minimization of the strain energy where internal variables are represented by the RVE volume fraction and Inertia-Fabric tensors.

CHAPTER I

REMARKS ON THE THEORY OF ELASTICITY

1. DEFORMATION THEORY

A central problem in nonlinear, three-dimensional elasticity consists in finding the equilibrium position of an elastic body that occupies a *reference configuration* $\overline{\Omega}$ in the absence of applied forces, where Ω is a bounded open connected subset of $\mathbb{R}^3$ with a Lipschitz-continuos boundary. When subjected to applied forces, the body occupies a *deformed configuration* $\boldsymbol{\varphi}(\overline{\Omega})$, characterized by mapping $\boldsymbol{\varphi}: \overline{\Omega} \to \mathbb{R}^3$ that must be in particular *orientation-preserving* in the set $\overline{\Omega}$ and *injective* on the set Ω, in order to be physically acceptable.
Such mapping $\boldsymbol{\varphi}$ are called *deformations*, and in the next sections their *geometrical properties* are studied. It is shown in particular that the changes in *volume*, *surfaces* and *lengths* associated with a deformation $\boldsymbol{\varphi}$, are respectively governed by the scalar $\nabla\boldsymbol{\varphi}$, the matrix $\mathbf{Cof}\nabla\boldsymbol{\varphi}$ and the *right Cauchy-Green strain tensor* $\mathbf{C} = \nabla\boldsymbol{\varphi}^T\nabla\boldsymbol{\varphi}$.

1.1. Deformation in $\mathbb{R}^3$

We assume once and for all that an origin $\boldsymbol{o}$ and an orthonormal basis $\{\mathbf{e}_1, \mathbf{e}_2, \mathbf{e}_3\}$ have been chosen in three-dimensional Euclidean space, which will therefore be identified with the space $\mathbb{R}^3$. From the notational viewpoint, we identify the point $\mathbf{x}$ with the vector $\mathbf{ox}$. Whenever we consider components of vectors in $\mathbb{R}^3$, or elements of matrices in $\mathbb{M}^3$, we make the convention that Latin indices (i, j, p,….) always take their values in the set {1, 2, 3}, and we combine this rule with the standard summation convention.
Let there be given a bounded, open, connected, subset Ω of $\mathbb{R}^3$ with a sufficiently smooth boundary (specific smoothness assumptions will be made subsequently). We shall think of the closure $\overline{\Omega}$ of the set Ω as representing the volume occupied by a body "before it is deformed"; for this reason, the set $\overline{\Omega}$ is called the *reference configuration*.
A deformation of the reference configuration $\overline{\Omega}$ is a vector field:

$$\boldsymbol{\varphi}: \overline{\Omega} \to \mathbb{R}^3 \tag{1.1}$$

that is smooth enough, injective possibly on the boundary of the set Ω, and orientation–preserving.

Remarks.

1. The reason a deformation may loose its injectivity on the boundary of Ω is that "self-contact" must be allowed.
2. The expression "smooth enough" is simply a convenient way of saying that in a given definition, theorem, proof, etc. the smoothness of deformations involved is such that all arguments make sense. As a consequence, the underlying degree of smoothness varies from place to place. For instance, the existence of the deformation gradient (to be next introduced) implies that a deformation is differentiable at all points of the reference configuration; Theorem 1.1 relies on the Piola identity, which makes sense, at least in a classical setting, only for twice differentiable deformations; the characterization of rigid deformations is established for deformations that are continuously differentiable, etc.
3. Deformations are synonymously called configurations, or placements, by some authors.

We denote by $\mathbf{x}$ a generic point in the set $\bar{\Omega}$, by x_i its components with respect to the basis $\{\mathbf{e}_i\}$, and by $\partial_i = \partial/\partial x_i$ the partial derivative with respect to variable x_i. Given a deformation $\boldsymbol{\varphi} = \varphi_i \mathbf{e}_i$, we define at each point of the set Ω the matrix

$$\nabla\boldsymbol{\varphi} := \begin{pmatrix} \partial_1\varphi_1 & \partial_2\varphi_1 & \partial_3\varphi_1 \\ \partial_1\varphi_2 & \partial_2\varphi_2 & \partial_3\varphi_2 \\ \partial_1\varphi_3 & \partial_2\varphi_3 & \partial_3\varphi_3 \end{pmatrix}. \tag{1.2}$$

The matrix $\nabla\boldsymbol{\varphi}$ is called the **deformation gradient**. Since a deformation is orientation-preserving by definition, the determinant of the deformation gradient satisfies the **orientation-preserving condition**:

$$\det \nabla\boldsymbol{\varphi}(\mathbf{x}) > 0 \quad \text{for all } x \in \bar{\Omega} \tag{1.3}$$

In particular, the matrix $\nabla\boldsymbol{\varphi}(\mathbf{x})$ is invertible at all points $\mathbf{x}$ of the reference configuration $\bar{\Omega}$.

Remarks.

1. The notations $\mathbf{F} = \nabla\boldsymbol{\varphi}$ and $J = \det \nabla\boldsymbol{\varphi}$ are commonly used in the literature.
2. The notation $\nabla\boldsymbol{\varphi}$ is confusing, since the gradient of a real-valued function f is the column vector formed by the first partial derivative

$\partial_i f$, while $(\nabla \boldsymbol{\varphi})_{ij} = \partial_j \varphi_i$ (this explains why we used the notation **grad** f, and not ∇f. Indeed, the deformation gradient is simply the matrix representing the Fréchet derivative of the mapping $\boldsymbol{\varphi}$, which for real-valued functions, it is identified with the transpose of the gradient.

Together with a deformation $\boldsymbol{\varphi}$, it is often convenient to introduce the displacement $\mathbf{u}$, which is the vector field:

$$\mathbf{u} : \bar{\Omega} \to \mathbb{R}^3 \tag{1.4}$$

defined by the relation

$$\boldsymbol{\varphi} = \mathbf{id} + \mathbf{u}, \tag{1.5}$$

where **id** denotes the (restriction to $\bar{\Omega}$ of the) identity map from $\mathbb{R}^3$ onto $\mathbb{R}^3$. Notice that the displacement gradient

$$\nabla \mathbf{u} := \begin{pmatrix} \partial_1 u_1 & \partial_2 u_1 & \partial_3 u_1 \\ \partial_1 u_2 & \partial_2 u_2 & \partial_3 u_2 \\ \partial_1 u_3 & \partial_2 u_3 & \partial_3 u_3 \end{pmatrix} \tag{1.6}$$

and the deformation gradient are related by the equation

$$\nabla \boldsymbol{\varphi} = \mathbf{I} + \nabla \mathbf{u}. \tag{1.7}$$

Given a reference configuration $\bar{\Omega}$ and a deformation $\boldsymbol{\varphi} : \bar{\Omega} \to \mathbb{R}^3$, the set $\boldsymbol{\varphi}(\bar{\Omega})$ is called a **deformed configuration.** At each point

$$\mathbf{x}^{\varphi} := \boldsymbol{\varphi}(\mathbf{x}) \tag{1.8}$$

of a deformed configuration, we define the three vectors (Fig. 1.1)

$$\partial_j \boldsymbol{\varphi}(\mathbf{x}) = \partial_j \varphi_i(\mathbf{x}) \mathbf{e}_i. \tag{1.9}$$

Each vector $\partial_j \boldsymbol{\varphi}(\mathbf{x})$ measures the "local deformation in the direction of the vector $\mathbf{e}_j$" in the sense that, to within the first order with respect to dt, the vector $\mathbf{e}_j dt$ is transformed into the vector $\partial_j \boldsymbol{\varphi}(\mathbf{x}) dt$. Equivalently, the vector

$\partial_j \boldsymbol{\varphi}(\mathbf{x})$ is the tangent vector to the *j*th coordinate line passing through the point $\mathbf{x}^{\varphi}$ (i.e. the image by the deformation $\boldsymbol{\varphi}$ of a segment parallel to the vector $\mathbf{e}_j$ containing the point $\mathbf{x}$ in its interior, and parametrized by *t*). Since the vector $\partial_j \boldsymbol{\varphi}(\mathbf{x})$ is precisely the *j*th column of the matrix $\nabla \boldsymbol{\varphi}$, the knowledge of the deformation gradient completely define the local deformation to within the first order.

Remarks.

1. While the deformation gradient $\nabla \boldsymbol{\varphi}$ clearly depends upon the basis $\mathbf{e}_i$, it is possible to exhibit the intrinsic geometrical character of the deformation at the point $\mathbf{x}$, by means of the polar factorization of the matrix $\nabla \boldsymbol{\varphi}(\mathbf{x})$, which then appears as the product of a "rotation tensor" by a "stretch tensor". For details about this classical results, see for instance Germain (1972), Gurtin (1981), Truesdell&Noll (1965).
2. If the point $\mathbf{x}^{\varphi} = \boldsymbol{\varphi}(\mathbf{x})$ belongs to the interior of the deformed configuration $\boldsymbol{\varphi}(\bar{\Omega})$, the three vector $\partial_j \boldsymbol{\varphi}$ define in the terminology of differential geometry the tangent vector space at the point $\mathbf{x}$ of the manifold $\boldsymbol{\varphi}(\bar{\Omega})$. This space is of dimension three since the matrix $\nabla \boldsymbol{\varphi}(\mathbf{x})$ is invertible (by definition of a deformation).
3. The points $x \in \Omega$ and the corresponding points $\mathbf{x}^{\varphi} \in \boldsymbol{\varphi}(\Omega)$ are often called material points and spatial points respectively, and they are often denoted X and x respectively, in the continuum mechanics literature.

We next compute the volume, area, and length elements in the deformed configuration. In each case, the objective is, for a given deformation, to express quantities (volumes, surfaces, lengths) defined over the deformed configuration in terms of the same quantities, but defined over the reference configuration. To emphasize the crucial distinction between both types of quantities, we adopt the following notational device: the superscript "$\boldsymbol{\varphi}$"is systematically attached to a quantity defined over the deformed configuration, while the related quantity over the reference configuration is designed by the same letter, but without the superscript "$\boldsymbol{\varphi}$"; this rule has already been applied, for denoting a generic point $\mathbf{x} \in \bar{\Omega}$ and the corresponding point $\mathbf{x}^{\varphi} \in \boldsymbol{\varphi}(\mathbf{x}) \in \boldsymbol{\varphi}(\bar{\Omega})$.

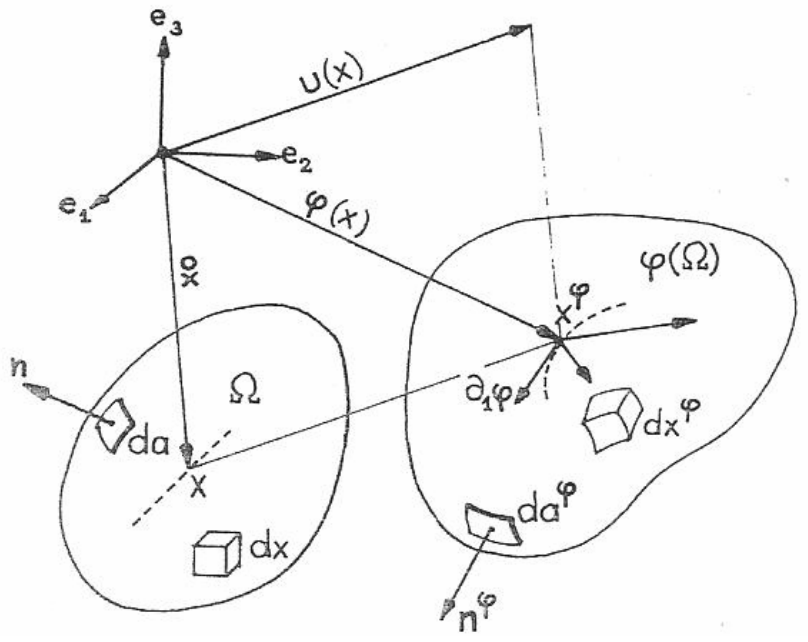

Fig. 1.1.

Geometry of a deformation: the volume element, the area element, the unit outer normal, are denoted dx, da, $\mathbf{n}$ *in the reference configuration* $\bar{\Omega}$, *and* dx^{φ}, da^{φ}, $\mathbf{n}^{\varphi}$ *in the deformed configuration* $\boldsymbol{\varphi}(\bar{\Omega})$. *The vectors* $\partial_j \boldsymbol{\varphi}(\mathbf{x})$ *define the deformation at a point* $x \in \bar{\Omega}$ *to within the first order.*

This correspondence between a quantity defined as a function of the Lagrange variable $\mathbf{x}$, and a similar quantity defined as a function of the Euler variable $\mathbf{x}^{\varphi} \in \boldsymbol{\varphi}(\mathbf{x})$, can be extended to other quantities than volume, surfaces, and lengths. As we shall see, it applies equally well to divergences of tensor fields and applied forces.

Remark.

1. This idea can be systematized through the notions of "pullback" and "push-forward", familiar in differential geometry. In this respect, see for instance Choquet-Bruhat, Dewitt-Morette and Dillard-Bleick (1977), or Marsden and Hughes (1983).

1.2. Volume element in deformation configuration

Let φ be a deformation. If dx denotes the volume element at the point $\mathbf{x}$ of the reference configuration, the volume element dx^{φ} at the point $\mathbf{x}^{\varphi} = \boldsymbol{\varphi}(\mathbf{x})$ of the deformed configuration (Fig. 1.1) is given by

$$dx^{\varphi} = \det \boldsymbol{\nabla}\boldsymbol{\varphi}(x)\, dx, \tag{1.10}$$

since $\left|\det \boldsymbol{\nabla}\boldsymbol{\varphi}(x)\right| = \det \boldsymbol{\nabla}\boldsymbol{\varphi}(x) > 0$ by assumption.

The volume element dx^{φ} is used for computing volumes in the deformed configuration: If A denotes a measurable subset of the reference configuration $\overline{\Omega}$, the volume of the set A and the volume of the deformed set $A^{\varphi} := \boldsymbol{\varphi}(A)$ are respectively given by:

$$vol\, A := \int_A dx, \quad vol\, A^{\varphi} := \int_{A^{\varphi}} dx^{\varphi} = \int_A \det \boldsymbol{\nabla}\boldsymbol{\varphi}(x)\, dx. \tag{1.11}$$

Notice that the last equality is nothing but a special case of the formula for changes of variables in multiple integrals: Let $\boldsymbol{\varphi}: A \to \boldsymbol{\varphi}(A) = A^{\varphi}$ be an injective, continuously differentiable mapping with a continuous inverse $\boldsymbol{\varphi}^{-1}: A^{\varphi} \to A$. Then a function $u: x^{\varphi} \in A^{\varphi} \to \mathbf{R}$ is dx^{φ}-integrable over the set A^{φ} if and only if the function

$$x \in A \to (u \circ \boldsymbol{\varphi})(x) \left|\det \boldsymbol{\nabla}\boldsymbol{\varphi}(x)\right| \tag{1.12}$$

is dx-integrable over the set A and if this is the case,

$$\int_{A^{\varphi} = \varphi(A)} u\left(x^{\varphi}\right) dx^{\varphi} = \int_A (u \circ \boldsymbol{\varphi})(x) \left|\det \boldsymbol{\nabla}\boldsymbol{\varphi}(x)\right| dx. \tag{1.13}$$

It should be remembered that the validity of this formula hinges critically on the assumption that the mapping $\boldsymbol{\varphi}$ is injective. Otherwise, it must be replaced by the more general relation:

$$\int_{\varphi(A)} u(x')\, card\, \boldsymbol{\varphi}^{-1}(x')\, dx' = \int_A (u \circ \boldsymbol{\varphi})(x) \left|\det \boldsymbol{\nabla}\boldsymbol{\varphi}(x)\right| dx \tag{1.14}$$

where card B denote in general the number of elements in a set B. For details, see Schwartz (1967), Rado & Reichelderfer (1955), Federer (1969), Smith

(1983), Bojarski & Iwaniec (1983), Marcus & Mizel (1973), Vodopyanov, Goldshtein & Reshetnyak (1979) for its extension to Sobolev space-valued mappings.

These properties hold in $\mathbb{R}^n$, for arbitrary *n*. The volume $\int_A dx$ of a *dx*-measurable subset of $\mathbb{R}^n$ is denoted *dx*-means *A*.

1.3. The Piola transform; area element in the deformed configuration

As a preparation for computing the area element in the deformed configuration in terms of the area element in the reference configuration, it is convenient to introduce a particular transformation between tensors defined over the reference configuration $\bar{\Omega}$ and tensors defined over the deformed configuration $\bar{\Omega}^\varphi$. Besides, this transform plays a crucial role in the definition of the first Piola-Kirchhoff tensor, following introduced.

Let us first review some definitions and results pertaining to tensor fields defined over either sets $\bar{\Omega}$ or $\bar{\Omega}^\varphi$. By a tensor, we mean here a second-order tensor

$$\mathbf{T} = \left(T_{ij}\right), \; i\text{: row index, } j\text{: column index.}$$

Since we ignore the distinction between covariant and controvariant components, the set of all such tensors will be identified with the set $\mathbb{M}^3$ of all square matrices of order three.

Given a smooth enough tensor field $\mathbf{T}: \bar{\Omega} \to \mathbb{M}^3$ defined over the reference configuration $\bar{\Omega}$, we define at each point of $\bar{\Omega}$ its divergence $\mathbf{div}\,\mathbf{T}$ as the vector whose components are the divergences of the transposes of the row vectors of the matrix $\mathbf{T}$. More explicitly,

$$\mathbf{T} = T_{ij} = \begin{pmatrix} T_{11} & T_{12} & T_{13} \\ T_{21} & T_{22} & T_{23} \\ T_{31} & T_{32} & T_{33} \end{pmatrix} \quad \Rightarrow \quad \mathbf{div}\,\mathbf{T} := \begin{pmatrix} \partial_1 T_{11} + \partial_2 T_{12} + \partial_3 T_{13} \\ \partial_1 T_{21} + \partial_2 T_{22} + \partial_3 T_{23} \\ \partial_1 T_{31} + \partial_2 T_{32} + \partial_3 T_{33} \end{pmatrix} = \partial_j T_{ij} \mathbf{e}_i \,. \qquad (1.15)$$

Of course, a similar definition holds for the divergence $\mathbf{div}^\varphi \mathbf{T}^\varphi$ of tensor fields $\mathbf{T}^\varphi : \mathbf{B}^\varphi \to \mathbb{M}^3$ defined over the deformed configuration:

$$\mathbf{T}^\varphi = \left(T_{ij}^\varphi\right) \quad \Rightarrow \quad div^\varphi T^\varphi := \partial_j^\varphi T_{ij}^\varphi \mathbf{e}_i \qquad (1.16)$$

where $\partial_j^\varphi := \partial / \partial x_j^\varphi$ denote the partial derivatives with respect to the variables x_j^φ.

A Simple application of the fundamental Green's formula over the set $\bar{\Omega}$ shows that the divergence of a tensor field satisfies:

$$\int_{\Omega} \mathbf{div}\,\mathbf{T}\,dX = \left(\int_{\Omega} \partial_j T_{ij}\,dx \right) \mathbf{e}_i = \left(\int_{\partial\Omega} T_{ij} n_j\,da \right) \mathbf{e}_i \tag{1.17}$$

or equivalently in matrix form:

$$\int_{\Omega} \mathbf{div}\,\mathbf{T}\,dx = \int_{\partial\Omega} \mathbf{T}\mathbf{n}\,da \tag{1.18}$$

Recall that a vector is always understood as a column vector when viewed as a matrix; thus the notation $\mathbf{T}\mathbf{n}$ in the previous formula represents the column vector obtained by applying the matrix $\mathbf{T}$ to the column vector $\mathbf{n}$. This Green formula is called the divergence theorem for tensor fields. A tensor field $\mathbf{T}^{\varphi} = \bar{\Omega}^{\varphi} \to \mathbb{M}^3$ likewise satisfies:

$$\int_{\Omega^{\varphi}} \mathbf{div}^{\varphi}\,\mathbf{T}^{\varphi}\,dx^{\varphi} = \int_{\partial\Omega^{\varphi}} \mathbf{T}^{\varphi}\,\mathbf{n}^{\varphi}\,da^{\varphi}\ , \tag{1.19}$$

where $\mathbf{n}^{\varphi}$ denotes the unit outer normal vector along the boundary of the deformed configuration.

We now come to an important definition. Let $\boldsymbol{\varphi}$ be a deformation that is injective on $\bar{\Omega}$, so that the matrix $\nabla\boldsymbol{\varphi}$ is invertible at all points of the reference configuration. Then if $\mathbf{T}^{\varphi}\left(\mathbf{x}^{\varphi}\right)$ is a tensor defined at the point $\mathbf{x}^{\varphi} = \boldsymbol{\varphi}(\mathbf{x})$ of the deformed configuration, we associate with $\mathbf{T}^{\varphi}\left(\mathbf{x}^{\varphi}\right)$ a tensor $\mathbf{T}(\mathbf{x})$ defined at the point $\mathbf{x}$ of the reference configuration by:

$$\begin{aligned} &\mathbf{T}(\mathbf{x}) := \left(\det \nabla\boldsymbol{\varphi}(x)\right) \mathbf{T}^{\varphi}\left(\mathbf{x}^{\varphi}\right) \nabla\boldsymbol{\varphi}(x)^{-T} = \mathbf{T}^{\varphi}\left(\mathbf{x}^{\varphi}\right) \mathbf{Cof}\left(\nabla\boldsymbol{\varphi}(x)\right), \\ &\mathbf{x}^{\varphi} = \boldsymbol{\varphi}(\mathbf{x}). \end{aligned} \tag{1.20}$$

In this fashion, a correspondence, called the Piola transform, is established between tensor fields defined over the deformed and reference configurations, respectively.

Remark.

1. It would be equally conceivable, and somehow more natural, to start with a tensor field $\mathbf{T}:\bar{\Omega}\to\mathbb{M}^3$ and to associate with it its "inverse Piola transform" $\mathbf{T}^{\varphi}:\bar{\Omega}^{\varphi}\to\mathbb{M}^3$ defined by
$$\mathbf{T}^{\varphi}\left(\mathbf{x}^{\varphi}\right):=\left(\det\nabla\boldsymbol{\varphi}(x)\right)^{-1}\mathbf{T}(\mathbf{x})\nabla\boldsymbol{\varphi}(x)^{T},\quad x\in\bar{\Omega}.$$
The reason we proceed the other way is that the starting point in elasticity is a tensor field defined over the deformed configuration (the Cauchy stress tensor field), and it is its Piola transform over three reference configuration (the first Piola –Kirchhoff stress tensor field) that subsequently plays a key role.

As shown in the next theorem, the main interest of the Piola transform is that it yields a simple relation between the divergences of the tensors $\mathbf{T}^{\varphi}$ and $\mathbf{T}$ and (as a corollary) the desires relation between corresponding area elements da^{φ} and da.

Theorem 1.1. (properties of the Piola transform). Let $\mathbf{T}:\bar{\Omega}\to\mathbb{M}^3$ denote the Piola transform of $\mathbf{T}^{\varphi}:\bar{\Omega}\to\mathbb{M}^3$. Then

$$\mathbf{div}\,\mathbf{T}(\mathbf{x})=\left(\det\nabla\boldsymbol{\varphi}(x)\right)div^{\varphi}\mathbf{T}^{\varphi}\left(\mathbf{x}^{\varphi}\right)\quad\text{for all}\quad\mathbf{x}^{\varphi}=\boldsymbol{\varphi}(\mathbf{x}),\quad x\in\bar{\Omega},\tag{1.21}$$

$$\mathbf{T}(\mathbf{x})\mathbf{n}da=\mathbf{T}^{\varphi}\left(\mathbf{x}^{\varphi}\right)\mathbf{n}^{\varphi}da^{\varphi}\quad\text{for all}\quad\mathbf{x}^{\varphi}=\boldsymbol{\varphi}(\mathbf{x}),\quad x\in\bar{\Omega}.\tag{1.22}$$

The area elements da and da^{φ} at the points $x\in\partial\Omega$ and $x^{\varphi}=\boldsymbol{\varphi}(x)\in\partial\Omega^{\varphi}$, with unit outer normal vectors $\mathbf{n}$ and $\mathbf{n}^{\varphi}$ respectively, are related by

$$\det\nabla\boldsymbol{\varphi}(x)\left|\nabla\boldsymbol{\varphi}(x)^{-T}\mathbf{n}\right|da=\left|\mathbf{Cof}\,\nabla\boldsymbol{\varphi}(x)\mathbf{n}\right|da=da^{\varphi}.\tag{1.23}$$

Remarks.

1. Of course, the conclusions of Theorem 1.1 still hold if we replace the set Ω by any sub-domain A of Ω, in which case the corresponding area elements and outer normal vectors are to be under-stood as being defined along the corresponding boundaries ∂A and $\partial A^{\varphi}=\boldsymbol{\varphi}(\partial A)$.
2. While the relation between the vectors $\mathbf{div}\,\mathbf{T}$ and $\mathbf{div}^{\varphi}\mathbf{T}^{\varphi}$ has been established here for deformations $\boldsymbol{\varphi}$ that are twice differentiable, the relations between the area elements established in Theorem (1.1) still hold under weaker regularity assumptions on the deformation.

3. The last equation in Theorem 1.1 shows that the unit outer normal vectors at the points $x^{\varphi} = \boldsymbol{\varphi}(x)$ and x are related by $\mathbf{n}^{\varphi} = \dfrac{\mathbf{Cof}\,\nabla\boldsymbol{\varphi}(x)\mathbf{n}}{\left|\mathbf{Cof}\,\nabla\boldsymbol{\varphi}(x)\mathbf{n}\right|}$.

We now have everything at our disposal to specify how areas are transformed: If Δ is a measurable subset of the boundary ∂A of a sub-domain A, the area of the deformed set $\Delta^{\varphi} = \varphi(\Delta)$ is given by

$$\text{area}\,\Delta^{\varphi} := \int_{\Delta^{\varphi}} da^{\varphi} = \int_{\Delta} (\det \nabla\boldsymbol{\varphi}) \left|\nabla\boldsymbol{\varphi}^{-T}\mathbf{n}\right| da \tag{1.24}$$

1.4. Length element in the deformed configuration; Strain Tensor

If a deformation $\boldsymbol{\varphi}$ is differentiable at a point $x \in \bar{\Omega}$, then (by definition of differentiability) we can write, for all points $x + \boldsymbol{\delta}\mathbf{x} \in \bar{\Omega}$:

$$\boldsymbol{\varphi}(x + \boldsymbol{\delta}\mathbf{x}) - \boldsymbol{\varphi}(x) = \nabla\boldsymbol{\varphi}(x)\boldsymbol{\delta}\mathbf{x} + o(\left|\boldsymbol{\delta}\mathbf{x}\right|) \tag{1.25}$$

and whence

$$\left|\boldsymbol{\varphi}(x + \boldsymbol{\delta}\mathbf{x}) - \boldsymbol{\varphi}(x)\right|^2 = \boldsymbol{\delta}\mathbf{x}^T \nabla\boldsymbol{\varphi}^T(x)\nabla\boldsymbol{\varphi}(x)\boldsymbol{\delta}\mathbf{x} + o\left(\left|\boldsymbol{\delta}\mathbf{x}\right|^2\right) \tag{1.26}$$

The symmetric tensor

$$C := \nabla\boldsymbol{\varphi}^T \nabla\boldsymbol{\varphi} \tag{1.27}$$

found in the above expression is called in elasticity the **right Cauchy-Green strain tensor**. Notice that the associated quadratic form:

$$(\boldsymbol{\xi}, \boldsymbol{\xi}) \in \mathbf{R}^3 \times \mathbf{R}^3 \to \xi^T \mathbf{C}(x)\xi = \left|\nabla\boldsymbol{\varphi}(x)\xi^2\right| \tag{1.28}$$

is positive definite at all points $x \in \bar{\Omega}$, since the deformation gradient $\nabla\boldsymbol{\varphi}$ is everywhere invertible by assumption. As expected, this quadratic form is used for computing lengths: Let

$$\gamma = f(I), \quad f : I \to \bar{\Omega}, \quad I : \text{compact interval of } \mathbb{R} \tag{1.29}$$

be a curve in the reference configuration (Fig. 1.2). Denoting by f_i the components of the mapping $\mathbf{f}$, the length of the curve γ is given by $\left(f' = df/dt\right)$:

$$\text{length } \gamma := \int_L \left|f'(t)\right| dt = \int_L \left\{f'(t) f'(t)\right\}^{1/2} dt, \tag{1.30}$$

while the length of the deformed curve $\gamma^{\varphi} : \boldsymbol{\varphi}(\gamma)$ is given by

$$\text{length } \gamma^{\varphi} := \int_L \left|\boldsymbol{\varphi} \circ f'(t)\right| dt = \int_L \left\{C_{ij}\left(f(t)\right) f'(t) f'(t)\right\}^{1/2} dt \tag{1.31}$$

Consequently, the length elements dl and dl^{φ} in the reference and deformed configurations may be symbolically written as:

$$dl = \left\{\mathbf{dx}^T \mathbf{dx}\right\}^{1/2}, \quad dl^{\varphi} = \left\{\mathbf{dx}^T \mathbf{C}\, \mathbf{dx}\right\}^{1/2}. \tag{1.32}$$

If in particular $\mathbf{dx} = dt\, \mathbf{e}_j$, the corresponding length element in the deformed configuration is $\left\{\mathbf{C}_{jj}\right\}^{1/2} dt = \left|\partial_j \boldsymbol{\varphi}\right| dt$.

Remark.

1. In the language of differential geometry, the manifold $\bar{\Omega}$ is equipped with a Riemannian structure through the data of the metric tensor $\mathbf{C} = \left(C_{ij}\right)$, often denoted $\mathbf{g} = g_{ij}$ in differential geometry, whose associated quadratic form, often denoted ds^2, is called the first fundamental form of the manifold. For details, see e.g. Lelong Ferrand(1963), Malliavin (1972).

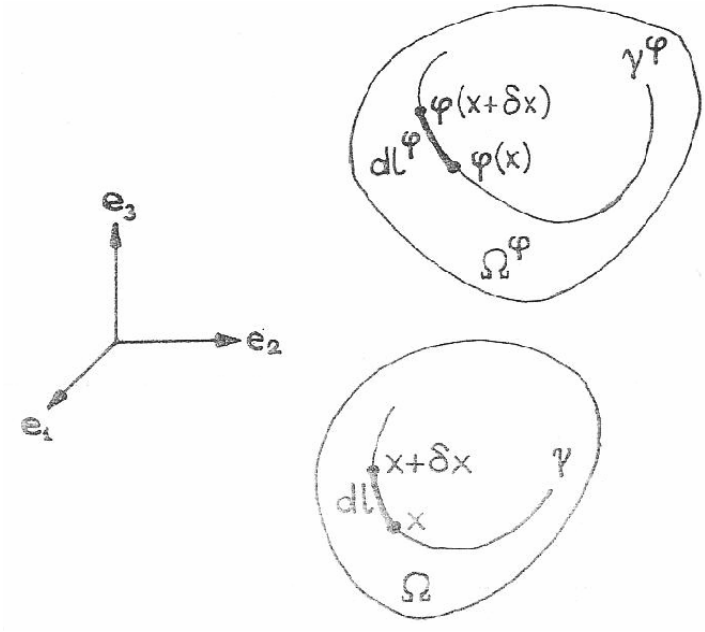

Fig. 1.2.

The length elements $dl = \{\mathbf{dx}^T \mathbf{dx}\}^{1/2}$ *and* $dl^\varphi = \{\mathbf{dx}^T \mathbf{C}\,\mathbf{dx}\}^{1/2}$ *in the reference and deformed configurations. The tensor* $\mathbf{C} = \boldsymbol{\nabla\varphi}^T \boldsymbol{\nabla\varphi}$ *is the right Cauchy-Green tensor.*

Although is has no immediate geometric interpretation, the left Cauchy-Green strain tensor

$$B : \boldsymbol{\nabla\varphi}\,\boldsymbol{\nabla\varphi}^T \tag{1.33}$$

which is also symmetric, is equally important; in particular, it plays an essential role in the representation theorem for the response function of the Cauchy stress tensor. For the time being, we simply notice that the two matrices $\mathbf{C} = \mathbf{F}^T\mathbf{F}$ and $\mathbf{B} = \mathbf{F}\mathbf{F}^T$ have the same characteristic polynomial, since this is true in general of the products $\mathbf{FG}$ and $\mathbf{GF}$ of two arbitrary matrices $\mathbf{F}$ and $\mathbf{G}$ of the same order. When $\mathbf{G} = \mathbf{F}^T$, this result is a direct consequence of the polar factorization theorem.

In view of showing that the tensor $\mathbf{C}$ is indeed a good measure of "strain", understood here in its intuitive sense of "change in form or size", let us first consider a class of deformations that induce no "strain": A deformation is called a rigid deformation if it is of the form

$$\boldsymbol{\varphi}(x) = \mathbf{a} + \mathbf{Q}\,o\,\mathbf{x}, \quad \mathbf{a} \in \mathbf{R}, \quad \mathbf{Q} \in \mathbf{O}^3_+, \quad \text{for all} \quad x \in \bar{\Omega}, \tag{1.34}$$

where $\mathbb{O}^3_+$ denotes the set of rotations in $\mathbb{R}^3$, i.e., the set of orthogonal matrices of order 3 whose determinant is +1. In other words, the corresponding deformed configuration is obtained by rotating the reference configuration around the origin by the rotation $\mathbf{Q}$ and by translating it by the vector $\boldsymbol{a}$: this indeed corresponds to the idea of a "rigid" deformation, where the reference configuration is "moved", but without any "strain" (Fig. 1.3). Observe that the rotation $\mathbf{Q}$ may be performed around any point $\tilde{\mathbf{x}} \in \mathbb{R}^3$ (Fig. 1.3), since we can also write

$$\boldsymbol{\varphi}(x) = \boldsymbol{\varphi}(\tilde{x}) + \mathbf{Q}\,\tilde{\mathbf{x}}\,\mathbf{x} \tag{1.35}$$

If $\boldsymbol{\varphi}$ is a rigid deformation, then $\nabla\boldsymbol{\varphi}(x) = \mathbf{Q} \in \mathbb{O}^3_+$ at all points $x \in \bar{\Omega}$, and therefore

$$\mathbf{C} = \mathbf{I} \quad \text{in } \bar{\Omega}, \quad \text{i.e.,} \quad \nabla\boldsymbol{\varphi}(x)^T \nabla\boldsymbol{\varphi}(x) = I \quad \text{for all} \quad x \in \bar{\Omega}. \tag{1.36}$$

It is remarkable that conversely, if $\mathbf{C} = \mathbf{I}$ in $\bar{\Omega}$ and $\det\nabla\boldsymbol{\varphi} > 0$, the corresponding deformation is necessarily rigid.

Theorem 1.2. (characterization of rigid deformations). Let Ω be an open connected subset of $\mathbb{R}^n$, and let there be given a mapping

$$\boldsymbol{\varphi} \in \mathscr{C}^1\left(\Omega, \mathbb{R}^n\right) \tag{1.37}$$

that satisfies

$$\nabla\boldsymbol{\varphi}(x)^{\mathbf{T}} \nabla\boldsymbol{\varphi}(x) = \mathbf{I} \text{ for all } \mathbf{x} \in \Omega \tag{1.38}$$

then there exists a vector $\mathbf{a} \in \mathbf{R}^n$ and an orthogonal matrix $\mathbf{Q} \in \mathbf{O}^n$ such that

$$\boldsymbol{\varphi}(x) = \boldsymbol{a} + \boldsymbol{Q}\,o\,\boldsymbol{x} \text{ for all } \mathbf{x} \in \Omega. \tag{1.39}$$

The result of theorem 1.2 can be viewed as a special case (let $\boldsymbol{\psi}$ be any rigid deformation in the theorem 1.3) of the following result, which shows that two deformations corresponding to the same tensor $\mathbf{C}$ can be obtained from one another by composition with a rigid deformation.

Theorem 1.3. Let Ω be an open connected subset of $\mathbb{R}^n$, and let here be given two mappings

$$\boldsymbol{\varphi}, \boldsymbol{\psi} \in \mathscr{C}^1\left(\Omega, \mathbb{R}^n\right) \tag{1.40}$$

such that

$$\nabla \boldsymbol{\varphi}(\boldsymbol{x})^T \cdot \nabla \boldsymbol{\varphi}(\boldsymbol{x}) = \nabla \boldsymbol{\psi}(\boldsymbol{x})^T \cdot \nabla \boldsymbol{\psi}(\boldsymbol{x}) \text{ for all } \mathbf{x} \in \Omega \tag{1.41}$$

$\boldsymbol{\psi}: \Omega \to \mathbb{R}^n$ is injective, and let $\nabla \boldsymbol{\psi}(\boldsymbol{x}) \neq 0$ for all $\mathbf{x} \in \Omega$.

Then here exist a vector $a \in \mathbb{R}^n$ and an orthogonal matrix $\mathbf{Q} \in O^n$ such that :

$$\boldsymbol{\varphi}(x) = \boldsymbol{a} + \boldsymbol{Q}\boldsymbol{\psi}(\mathbf{x}) \text{ for all } \mathbf{x} \in \Omega. \tag{1.42}$$

The previous two theorems are useful for understanding the role played by the tensor $\mathbf{C}$. First, theorem 1.2. shows that the difference

$$2\mathbf{E} \coloneqq \mathbf{C} - \mathbf{I} \tag{1.43}$$

is a measure of the "deviation" between a given deformation and a rigid deformation, since $\mathbf{C} = \mathbf{I}$ if and only if the deformation is rigid. Secondly, theorem 1.3. shows that the knowledge of the tensor field $\mathbf{C}: \Omega \to \mathbb{S}^3_>$ completely determines the deformation, up to composition with rigid deformations (the question of proving the existence of deformations for which the associated tensor field $\mathbf{C}: \Omega \to \mathbb{S}^3_>$ is equal to a given tensor field is quite another matter). These considerations are illustrated in figure 1.3.

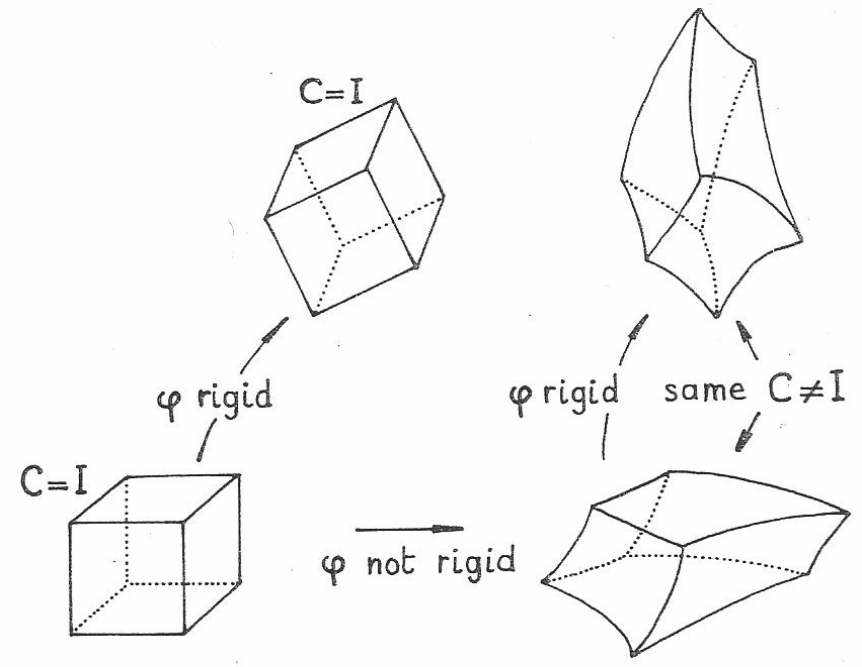

Fig. 1.3.
The right Cauchy-Green tensor $\mathbf{C}$ *is equal to* $\mathbf{I}$ *if and only if the deformation is rigid. Two deformations corresponding to the same tensor C differ by a rigid deformation.*

The tensor $\mathbf{E}$ is called the Green-St Venant strain tensor. Expressed in terms of the displacement gradient $\nabla\mathbf{u}$, in lieu of the deformation gradient $\nabla\boldsymbol{\varphi} = \mathbf{I} + \nabla\mathbf{u}$ (recall that $\boldsymbol{\varphi} = \mathbf{id} + \mathbf{u}$), the strain tensor $\mathbf{C}$ becomes

$$\mathbf{C} = \nabla\boldsymbol{\varphi}^{T}\nabla\boldsymbol{\varphi} = \mathbf{I} + \nabla\mathbf{u}^{T} + \nabla\mathbf{u} + \nabla\mathbf{u}^{T}\nabla\mathbf{u} = \mathbf{I} + 2\mathbf{E} \tag{1.44}$$

with

$$\mathbf{E}(\mathbf{u}) := \mathbf{E} = \tfrac{1}{2}\left(\nabla\mathbf{u}^{T} + \nabla\mathbf{u} + \nabla\mathbf{u}^{T}\nabla\mathbf{u}\right) \tag{1.45}$$

whose "first order" part $\frac{1}{2}\left(\nabla\mathbf{u}^{T} + \nabla\mathbf{u}\right)$ coincide with the *linearized strain tensor*, which played a key role in the earlier linearized theories that prevailed in elasticity.

2. THE EQUATION OF EQUILIBRIUM

A body occupying a deformed configuration $\bar{\Omega}^{\varphi}$, and subjected to applied body forces in its interior Ω^{φ} and to applied surfaces forces on a portion $\Gamma_1^{\varphi} = \boldsymbol{\varphi}(\Gamma_1)$ of its boundary, is in static equilibrium if the fundamental stress principle of Euler and Cauchy is satisfied. This axiom, which is the basis of continuum mechanics, implies the celebrated Cauchy theorem, according to which there exists a symmetric tensor field $\mathbf{T}^{\varphi} : \bar{\Omega}^{\varphi} \to \mathbb{S}^3$ such that

$$\begin{cases} -div^{\varphi}\mathbf{T}^{\varphi} = \boldsymbol{f}^{\varphi} & \text{in} \quad \Omega^{\varphi} \\ \mathbf{T}^{\varphi}\mathbf{n}^{\varphi} = \boldsymbol{g}^{\varphi} & \text{on} \quad \Gamma_1^{\varphi} \end{cases} \tag{1.46}$$

where $\boldsymbol{f}^{\varphi}$ and $\boldsymbol{g}^{\varphi}$ denote the densities of the applied body and surface forces respectively, and $\mathbf{n}^{\varphi}$ is the unit outer normal vector along Γ_1^{φ}. These equation are called the equilibrium over the deformed configuration, and the tensor $\mathbf{T}^{\varphi}$ is called the Cauchy stress tensor.

A remarkable feature of these equations is their "divergence structure", which makes them amenable to a variational formulation; a disadvantage is that they are expressed in terms of the unknown $\mathbf{x}^{\varphi} = \boldsymbol{\varphi}(\mathbf{x})$. In order to obviate this difficulty while retaining the divergence structure of the equations, we use the Piola transform $\mathbf{T} : \bar{\Omega} \to \mathbb{M}^3$ of the Cauchy stress tensor field, which is defined by $\mathbf{T}(\mathbf{x}) = \mathbf{T}^{\varphi}\left(\mathbf{x}^{\varphi}\right) Cof \nabla \boldsymbol{\varphi}(\mathbf{x})$. In this fashion, it is found that the equilibrium equations over $\bar{\Omega}^{\varphi}$ are equivalent to the equilibrium equations over the reference configuration $\bar{\Omega}$,

$$\begin{cases} -div\,\mathbf{T} = \boldsymbol{f} & \text{in} \quad \Omega \\ \mathbf{T}\mathbf{n} = \boldsymbol{g} & \text{on} \quad \Gamma_1 \end{cases} \tag{1.47}$$

where $\mathbf{n}$ denotes the unit outer normal vector along Γ_1, and the fields $\mathbf{f} : \Omega \to \mathbb{R}^3$ and $\boldsymbol{g} : \Gamma_1 \to \mathbb{R}^3$ are related to the fields $\boldsymbol{f}^{\varphi} : \Omega^{\varphi} \to \mathbb{R}^3$ and $\boldsymbol{g}^{\varphi} : \Gamma_1^{\varphi} \to \mathbb{R}^3$ by the simple formulas $\boldsymbol{f}\, dx = \boldsymbol{f}^{\varphi} dx^{\varphi}$ and $\boldsymbol{g}\, dx = \boldsymbol{g}^{\varphi} dx^{\varphi}$. Because they are still in divergence form, these equations can be given a variational formulation, known as the principle of virtual work. This principle plays a key role as the starting point of the theory of hyperelastic materials, as well in the asymptotic theory of two-dimensional plate models.

The tensor $\mathbf{T}$ is called the first Piola-Kirchhoff stress tensor. We also introduce the symmetric second Piola-Kirchhoff stress tensor $\boldsymbol{\Sigma} = \nabla \boldsymbol{\varphi}^{-1} \mathbf{T}$, which naturally arises in the expression of the constitutive equations of elastic materials.

2.1. Applied Forces

We assume that in the deformed configuration $\bar{\Omega}^{\varphi}$ associated with an arbitrary deformation $\boldsymbol{\varphi}$, the body is subjected to applied forces of two types:

(i) applied **body forces**, defined by a vector field

$$\boldsymbol{f}^{\varphi} : \Omega^{\varphi} \to \mathbb{R}^3, \tag{1.48}$$

called the density of the applied body forces per unit volume in the deformed configuration;

(ii) applied **surface forces**, defined by a vector field

$$\boldsymbol{g}^{\varphi} : \Gamma_1^{\varphi} \to \mathbb{R}^3 \tag{1.49}$$

on a da^{φ}-measurable subset Γ_1^{φ} of the boundary

$$\Gamma^{\varphi} := \partial\Omega^{\varphi} \tag{1.50}$$

called the density of the applied surface force per unit area in the deformed configuration.

Let $\rho^{\varphi} : \Omega^{\varphi} \to \mathbb{R}$ denote the mass density in the deformed configuration, so that the mass of every dx^{φ}-measurable subset A^{φ} of $\bar{\Omega}^{\varphi}$ is given by the integral $\int_{A^{\varphi}} \rho^{\varphi}\left(x^{\varphi}\right) dx^{\varphi}$. We assume that

$$\rho^{\varphi}\left(x^{\varphi}\right) > 0 \quad \text{for all} \quad x^{\varphi} \in \Omega \tag{1.51}$$

The applied body forces can be equivalently defined by their density $\mathbf{b}^{\varphi} : \Omega^{\varphi} \to \mathbb{R}^3$ per unit mass in the deformed configuration, which is related to the density $\boldsymbol{f}^{\varphi}$ by the equation

$$\boldsymbol{f}^{\varphi} = \rho^{\varphi}\,\mathbf{b}^{\varphi} \tag{1.52}$$

The applied forces describe the action of the outside world on the body: An elementary force $\boldsymbol{f}^{\varphi}\left(x^{\varphi}\right) dx^{\varphi}$ is exerted on the elementary volume dx^{φ} at each point x^{φ} of the deformed configuration. For example, this is the case of the gravity field, for which $\boldsymbol{f}\left(x^{\varphi}\right) = -g\rho^{\varphi}\left(x^{\varphi}\right)\mathbf{e}_3$ for all $x^{\varphi} \in \Omega^{\varphi}$ (assuming that

the vector $\mathbf{e}_3$ is vertical and oriented "upward"), where g is the gravitational constant. Another example is given by the action of electrostatic forces.

Likewise, an elementary force $\boldsymbol{g}^{\varphi}\left(x^{\varphi}\right)dx^{\varphi}$ is exerted on the elementary area da^{φ} at each point x^{φ} of the subset Γ_1^{φ} of the boundary of the deformed configuration (Fig. 1.3). Such forces generally represent the action of another body (whatever its nature its may be) along the portion Γ_1^{φ} of the boundary.

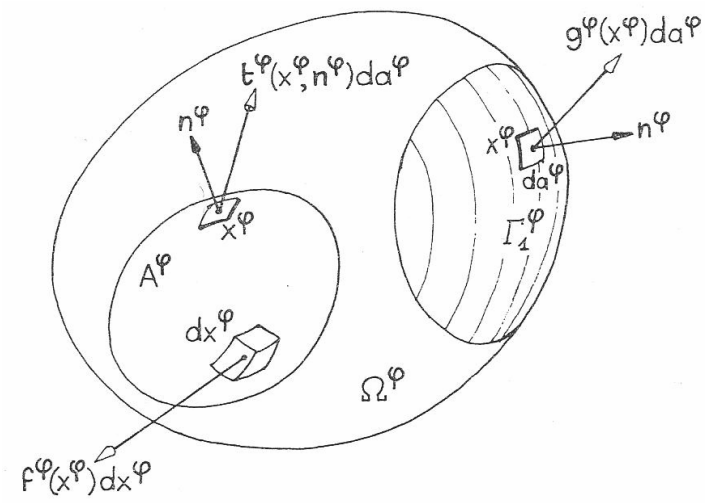

Fig. 1.3.

Applied forces comprise applied body forces $\boldsymbol{f}^{\varphi}\left(x\right)dx^{\varphi}$, $x^{\varphi}\in\Omega^{\varphi}$ *and applied surface forces* $\boldsymbol{g}^{\varphi}\left(x\right)da^{\varphi}$, $x^{\varphi}\in\Gamma_1^{\varphi}$. *The stress principle of Euler and Cauchy asserts in addition the existence of elementary surface forces* $\mathbf{t}^{\varphi}\left(\mathbf{x}^{\varphi},\mathbf{n}^{\varphi}\right)da^{\varphi}$, $x^{\varphi}\in\partial A^{\varphi}$, *along the boundary* ∂A^{φ}, *with unit outer normal vector* $\mathbf{n}^{\varphi}$, *of any sub-domain* A^{φ} *of the deformed configuration* $\bar{\Omega}^{\varphi}$.

Remark.

1. In order to avoid introducing too many notations, we use the same symbol to denote distinct quantities in the same figure. For instance in Fig. 1.3. the symbol x^{φ} stands fro three different points, and the symbols da^{φ} and $\mathbf{n}^{\varphi}$ stand for two different area elements and normal vectors.

Applied surface forces that are only "partially" specified (for instance, only the normal component $\boldsymbol{g}^{\varphi}\left(x\right)\cdot\boldsymbol{n}^{\varphi}$ could be prescribed along Γ_1^{φ}) are not excluded from our analysis; but in order to simplify the exposition, we solely considered

at this stage the "extreme" cases where either the density $\boldsymbol{g}^{\varphi}$ is fully known on Γ_1^{φ}, or is left completely unspecified, as on the remaining portion

$$\Gamma_0^{\varphi} := \Gamma^{\varphi} - \Gamma_1^{\varphi} \tag{1.53}$$

of the boundary of the deformed configuration. This being the case, we shall see that it is the deformation itself that should be specified on the corresponding portion $\Gamma_0 := \boldsymbol{\varphi}^{-1}\left(\Gamma_0^{\varphi}\right)$ of the boundary of the reference configuration, in order that the problem be well posed.

2.2. The stress principle of Euler and Cauchy

Continuum mechanics for static problems is founded on the following axiom, named after the fundamental contributions of Euler (1757,1771) and Cauchy (1823,1827a). Note that the exterior product in $\mathbb{R}^3$ is denoted $\wedge$.

Axiom 1. (stress principle of Euler and Cauchy). Consider a body occupying a deformed configuration $\bar{\Omega}^{\varphi}$, and subjected to applied forces represented by densities $\boldsymbol{f}^{\varphi} := \Omega^{\varphi} \to \mathbb{R}^3$ and $\boldsymbol{g}^{\varphi} := \Omega^{\varphi} \to \mathbb{R}^3$. Then there exists a vector field

$$\mathbf{t}^{\varphi} : \Omega^{\varphi} \times S_1 \to \mathbb{R}^3, \quad \text{where} \quad S_1 = \left\{ v \in \mathbb{R}^3 ; \left| \mathbf{v} \right| = 1 \right\}, \tag{1.54}$$

such that:

(a) For any sub-domain A^{φ} of $\bar{\Omega}^{\varphi}$, and at any point $\mathbf{x}^{\varphi} \in \Gamma_1^{\varphi} \cap \partial A^{\varphi}$ where the unit outer normal vector $\boldsymbol{n}^{\varphi}$ to $\Gamma_1^{\varphi} \cap \partial A^{\varphi}$ exists: $\mathbf{t}^{\varphi}\left(\mathbf{x}^{\varphi}, \mathbf{n}^{\varphi}\right) = \mathbf{g}^{\varphi}\left(\mathbf{x}^{\varphi}\right)$.

(b) Axiom of **force balance**: For any sub-domain A^{φ} of $\bar{\Omega}^{\varphi}$,

$$\int_{A^{\varphi}} \mathbf{f}^{\varphi}\left(\mathbf{x}^{\varphi}\right) dx^{\varphi} + \int_{\partial A^{\varphi}} \mathbf{t}^{\varphi}\left(\mathbf{x}^{\varphi}, \mathbf{n}^{\varphi}\right) dx^{\varphi} = \mathbf{0} \tag{1.55}$$

where $\boldsymbol{n}^{\varphi}$ denotes the unit outer normal vector along ∂A^{φ}.

(c) Axiom of **moment balance**: For any sub-domain A^{φ} of $\bar{\Omega}^{\varphi}$,

$$\int_{A^{\varphi}} \mathbf{ox}^{\varphi} \wedge \mathbf{f}^{\varphi}\left(\mathbf{x}^{\varphi}\right) dx^{\varphi} + \int_{\partial A^{\varphi}} \mathbf{ox}^{\varphi} \wedge \mathbf{t}^{\varphi}\left(\mathbf{x}^{\varphi}, \mathbf{n}^{\varphi}\right) dx^{\varphi} = \mathbf{0}. \tag{1.56}$$

The stress principle thus first asserts the existence of elementary **surface forces** $\mathbf{t}^{\varphi}\left(\mathbf{x}^{\varphi},\mathbf{n}^{\varphi}\right)da^{\varphi}$ along the boundaries of all domains of the reference configuration (Fig. 1.3.).

Secondly, the stress principle asserts that at a point $\mathbf{x}^{\varphi}$ of the boundary ∂A^{φ} of a sub-domain A^{φ}, the elementary surface force depends on the sub-domain A^{φ}, only via the normal vector $\boldsymbol{n}^{\varphi}$ to ∂A^{φ} at $\mathbf{x}^{\varphi}$. While it would be equally conceivable a priori that the elementary surface force at $\mathbf{x}^{\varphi}$ be also dependent on other geometrical properties of the sub-domain A^{φ}, for instance the curvature of ∂A^{φ} at $\mathbf{x}^{\varphi}$, etc., it is possible to rigorously rule out such further geometrical dependences by constructing a general theory of surfaces forces, as shown by Noll (1959).

Thirdly, the stress principle asserts that any sub-domain A^{φ} of the deformed configuration $\bar{\Omega}^{\varphi}$, including $\bar{\Omega}^{\varphi}$ itself, is in static equilibrium, in the sense that the torsor formed by the elementary forces $\mathbf{t}^{\varphi}\left(\mathbf{x}^{\varphi},\mathbf{n}^{\varphi}\right)da^{\varphi}$, $x^{\varphi}\in\partial A^{\varphi}$, $\mathbf{n}^{\varphi}$ normal to ∂A^{φ} at $\mathbf{x}^{\varphi}$, and the body forces $\mathbf{f}^{\varphi}\left(\mathbf{x}^{\varphi}\right)d\mathbf{x}^{\varphi}$, $\mathbf{x}^{\varphi}\in A^{\varphi}$, is equivalent to zero. This means that its resultant vector vanishes (axiom of force balance) and that its resulting moment with respect to the origin (and thus with respect to any other point, by a classical property of torsos) vanishes (axiom of moment balance).

Hence the stress principle mathematically express, in the form of an axiom, the intuitive idea that the static equilibrium of any sub-domain A^{φ} of $\bar{\Omega}^{\varphi}$, already subjected to given applied body forces $\mathbf{f}^{\varphi}\left(\mathbf{x}^{\varphi}\right)d\mathbf{x}^{\varphi}$, $\mathbf{x}^{\varphi}\in A^{\varphi}$, and (possibly) to given applied surface forces $\mathbf{g}^{\varphi}\left(\mathbf{x}^{\varphi}\right)da^{\varphi}$ at those points $\mathbf{x}^{\varphi}\in\Gamma_1^{\varphi}\cap\partial A^{\varphi}$ where the outer normal vector to $\Gamma_1^{\varphi}\cap\partial A^{\varphi}$ exists, is made possible by the added effect of elementary surfaces forces of the specific form indicated, acting on the remaining part of the boundary ∂A^{φ}.

Remark.

1. Gurtin (1981a, 1981b) calls system of forces the set formed by the applied bodu forces, corresponding to the vector field $\boldsymbol{f}^{\varphi}:=\Omega^{\varphi}\to\mathbb{R}^3$ and by the surface forces, corresponding to the vector field $\boldsymbol{t}^{\varphi}:=\Omega^{\varphi}\times S_1\to\mathbb{R}^3$.

Let $\mathbf{x}^{\varphi}$ be a point of the deformed configuration. The vector $\mathbf{t}^{\varphi}\left(\mathbf{x}^{\varphi},\mathbf{n}^{\varphi}\right)$ is called the Cauchy stress vector across an oriented surface element with normal $\mathbf{n}^{\varphi}$, or the density of the surface force per unit area in the deformed configuration.

2.3. Cauchy's theorem; The Cauchy stress tensor

We now derive consequences of paramount importance from the stress principle. The first one, due to Cauchy (1823,1827a), is one of the most important results in continuum mechanics. It asserts that the dependence of the Cauchy stress vector $\mathbf{t}^{\varphi}\left(\mathbf{x}^{\varphi},\mathbf{n}^{\varphi}\right)$ with respect to its second argument $\mathbf{n}\in S_1$ is linear, i.e., at each point $\mathbf{x}^{\varphi}\in\Omega^{\varphi}$, there exists a tensor $\mathbf{T}^{\varphi}\left(\mathbf{x}^{\varphi}\right)\in\mathbb{M}^3$ such that $\mathbf{t}^{\varphi}\left(\mathbf{x}^{\varphi},\mathbf{n}^{\varphi}\right)=\mathbf{T}^{\varphi}\left(\mathbf{x}^{\varphi}\right)\mathbf{n}$ for all $\mathbf{n}\in S_1$; the second one asserts that at each point $\mathbf{x}^{\varphi}\in\Omega^{\varphi}$, the tensor $\mathbf{T}^{\varphi}\left(\mathbf{x}^{\varphi}\right)$ is symmetric; the third one, again due to Cauchy (1827b, 1828), is that the tensor field $\mathbf{T}^{\varphi}:\Omega^{\varphi}\to\mathbb{M}^3$ and the vector fields $\boldsymbol{f}^{\varphi}:\Omega^{\varphi}\to\mathbb{R}^3$ and $\boldsymbol{g}^{\varphi}:=\Gamma_1^{\varphi}\to\mathbb{R}^3$ are related by a partial differential equation in Ω^{φ}, and by a boundary condition on Γ_1^{φ}, respectively.

Theorem 1.2. (Cauchy's theorem). Assume that the applied body force density $\boldsymbol{f}^{\varphi}:\Omega^{\varphi}\to\mathbb{R}^3$ is continuous, and that the Cauchy stress vector field

$$\mathbf{t}^{\varphi}:\left(\mathbf{x}^{\varphi},\mathbf{n}^{\varphi}\right)\in\bar{\Omega}^{\varphi}\times S_1\to\mathbf{t}^{\varphi}\left(\mathbf{x}^{\varphi},\mathbf{n}\right)\in\mathbb{R}^3 \tag{1.57}$$

is continuously differentiable with respect to the variable $\mathbf{x}^{\varphi}\in\bar{\Omega}^{\varphi}$ for each $\mathbf{n}\in S_1$ and continuous with respect to the variable $\mathbf{n}\in S_1$ for each $\mathbf{x}^{\varphi}\in\bar{\Omega}^{\varphi}$. Then the axioms of force and moment balance imply that there exists a continuously differentiable tensor field

$$\mathbf{T}^{\varphi}:\mathbf{x}^{\varphi}\in\bar{\Omega}^{\varphi}\to\mathbf{T}^{\varphi}\left(\mathbf{x}^{\varphi}\right)\in\mathbb{M}^3, \tag{1.58}$$

such that the Cauchy stress vector satisfies

$$\mathbf{t}^{\varphi}\left(\mathbf{x}^{\varphi},\mathbf{n}\right)=\mathbf{T}^{\varphi}\left(\mathbf{x}^{\varphi}\right)\mathbf{n}\quad\text{for all }\mathbf{x}^{\varphi}\in\bar{\Omega}^{\varphi}\quad\text{and all }\mathbf{n}\in S_1, \tag{1.59}$$

and such that

$$-div^{\varphi}\mathbf{T}^{\varphi}\left(\mathbf{x}^{\varphi}\right)=\mathbf{f}^{\varphi}\left(\mathbf{x}^{\varphi}\right)\quad\text{for all }\mathbf{x}^{\varphi}\in\Omega^{\varphi}, \tag{1.60}$$

$$\mathbf{T}^{\varphi}\left(\mathbf{x}^{\varphi}\right)=\mathbf{T}^{\varphi}\left(\mathbf{x}^{\varphi}\right)^{T}\quad\text{for all }\mathbf{x}^{\varphi}\in\bar{\Omega}^{\varphi}, \tag{1.61}$$

$$\mathbf{T}^{\varphi}\left(\mathbf{x}^{\varphi}\right)\mathbf{n}^{\varphi}=\mathbf{g}^{\varphi}\left(\mathbf{x}^{\varphi}\right)\quad\text{for all }\mathbf{x}^{\varphi}\in\Gamma_1^{\varphi} \tag{1.62}$$

where $\mathbf{n}^{\varphi}$ is the unit outer normal vector along Γ_1^{φ}.

The symmetry tensor $\mathbf{T}^{\varphi}$ is called the Cauchy stress tensor at the point $\mathbf{x}^{\varphi} \in \bar{\Omega}^{\varphi}$. It is helpful to keep in mind the interpretation of its elements $\mathbf{T}_{ij}^{\varphi}\left(\mathbf{x}^{\varphi}\right)$: Since $\mathbf{t}^{\varphi}\left(x^{\varphi}, \mathbf{e}_j\right) = \mathbf{T}_{ij}^{\varphi}\left(\mathbf{x}^{\varphi}\right) \cdot \mathbf{e}_i$, the elements of the j-th row of the tensor $\mathbf{T}^{\varphi}\left(x^{\varphi}\right)$ represent the components of the Cauchy stress vector $\mathbf{t}^{\varphi}\left(x^{\varphi}, \mathbf{n}\right)$ at the point $\mathbf{x}^{\varphi}$ corresponding to the particular choice $\mathbf{n} = \mathbf{e}_j$ (Fig. 1.4. where the case j=1 is considered). The knowledge of the three vectors $\mathbf{t}^{\varphi}\left(x^{\varphi}, \mathbf{e}_j\right)$ in turn completely determines the Cauchy stress vector $\mathbf{t}^{\varphi}\left(x^{\varphi}, \mathbf{n}\right)$ for an arbitrary vector $\mathbf{n} = n_i \mathbf{e}_i \in S_1$, since

$$\mathbf{t}^{\varphi}\left(x^{\varphi}, \mathbf{n}\right) = n_j \mathbf{t}^{\varphi}\left(x^{\varphi}, \mathbf{e}_j\right) \tag{1.63}$$

This observation is used in the drawing of figures, where the Cauchy stress vector is often represented on three mutually perpendicular faces of a rectangular parallelepiped.

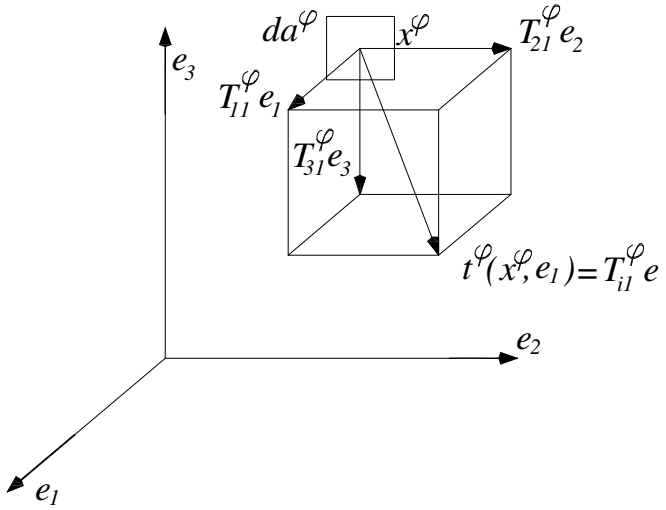

Fig. 1.4.

Interpretation of the elements $\mathbf{T}_{i1}^{\varphi}$ *of the Cauchy stress tensor* $\mathbf{T}^{\varphi} = \left(T_{ij}^{\varphi}\right)$.

2.4. The equation of equilibrium and the principle of virtual work in the deformed configuration

As shown un Theorem 1.2., the axioms of force and moment balance imply that the Cauchy stress tensor field $\mathbf{T}^{\varphi}:\bar{\Omega}^{\varphi}\to\mathbb{S}^3$ satisfies a boundary value problem expressed in terms of the Euler variable x^{φ} over the deformed configuration , comprising the partial differential equation $-div^{\varphi}\mathbf{T}^{\varphi}=\mathbf{f}^{\varphi}$ in Ω^{φ} and the boundary condition $\mathbf{T}^{\varphi}\mathbf{n}^{\varphi}=\mathbf{g}^{\varphi}$ on Γ_1^{φ}. A remarkable property of this boundary value problem, due to its " divergence form", is that it can be given a variational formulation, as we now show . In what follows, $\mathbf{u}\cdot\mathbf{v}=u_iv_i$ denotes the Euclidean vector inner product, $\mathbf{A}:\mathbf{B}=A_{ij}B_{ji}=tr\,\mathbf{A}^T\mathbf{B}$ denotes the matrix inner product, and $\nabla^{\varphi}\boldsymbol{\theta}^{\varphi}$ denotes the matrix $\left(\partial_j^{\varphi}\theta_i^{\varphi}\right)$.

Theorem 1.3. The boundary value problem:

$$\begin{aligned} -div^{\varphi}\mathbf{T}^{\varphi}&=\mathbf{f}^{\varphi} \quad \text{in} \quad \Omega^{\varphi}\\ \mathbf{T}^{\varphi}\mathbf{n}^{\varphi}&=\mathbf{g}^{\varphi} \quad \text{on} \quad \Gamma_1^{\varphi}\end{aligned} \tag{1.64}$$

Is formally equivalent to the variational equations:

$$\int_{\Omega^{\varphi}}\mathbf{T}^{\varphi}:\nabla^{\varphi}\theta^{\varphi}dx^{\varphi}=\int_{\Omega^{\varphi}}\mathbf{f}^{\varphi}\cdot\boldsymbol{\theta}^{\varphi}dx^{\varphi}+\int_{\Gamma_1^{\varphi}}\mathbf{g}^{\varphi}\cdot\boldsymbol{\theta}^{\varphi}dx^{\varphi} \tag{1.65}$$

valid for all smooth enough vector fields: $\boldsymbol{\theta}^{\varphi}:\Omega^{\varphi}\to\mathbb{R}^3$ that satisfy

$$\boldsymbol{\theta}^{\varphi}=\mathbf{0} \quad \text{on} \quad \Gamma_o^{\varphi}:=\Gamma^{\varphi}-\Gamma_1^{\varphi}. \tag{1.66}$$

The equation

$$\begin{aligned} -div^{\varphi}\mathbf{T}^{\varphi}&=\mathbf{f}^{\varphi} \quad \text{in} \quad \Omega^{\varphi},\\ \mathbf{T}^{\varphi}&=\left(\mathbf{T}^{\varphi}\right)^T \quad \text{in} \quad \Omega^{\varphi},\\ \mathbf{T}^{\varphi}\mathbf{n}^{\varphi}&=\mathbf{g}^{\varphi} \quad \text{on} \quad \Gamma_1^{\varphi},\end{aligned} \tag{1.67}$$

are called the equations of equilibrium in the deformed configuration, while the associated variational equations (1.65) of Theorem 1.3. constitute the principle of virtual work in the deformed configuration .

2.5. The Piola-Kirchhoff stress tensors

Our final objective is to determine the deformation field and the Cauchy stress tensor field that arise in a body subjected to a given system of applied forces. In this respect, the equations of equilibrium in the deformed configuration are of not much avail, since they are expressed in terms of the Euler variable $\mathbf{x}^{\varphi} = \varphi(x)$, which is precisely on of the unknows. To obviate this difficulty, we shall rewrite these equations in terms of the Lagrange variable x that is attached to the reference configuration, which is considered as being given once and for all. More specifically, we shall transform the left-hand sides $div^{\varphi}\mathbf{T}^{\varphi}$ and $\mathbf{T}^{\varphi}\mathbf{n}^{\varphi}$ and the right-hand sides $\boldsymbol{f}^{\varphi}$ and $\boldsymbol{g}^{\varphi}$ appearing in the equations of equilibrium over $\bar{\Omega}^{\varphi}$ into similar expressions over $\bar{\Omega}$.
We defined the Piola transform: $\mathbf{T}:\bar{\Omega}\to\mathbb{M}^3$ of a tensor field $\mathbf{T}^{\varphi}:\bar{\Omega}^{\varphi}=\varphi(\bar{\Omega})\to\mathbb{M}^3$ by letting

$$\mathbf{T}(x)=\left(\det\nabla\boldsymbol{\varphi}(x)\right)\boldsymbol{T}^{\varphi}\left(x^{\varphi}\right)\nabla\boldsymbol{\varphi}(x)^{-T},\quad x^{\varphi}=\boldsymbol{\varphi}(x). \tag{1.68}$$

We shall therefore apply this transform to the Cauchy stress tensor $\mathbf{T}^{\varphi}$, in which case its Piola transform $\mathbf{T}$ is called the first Piola-Kirchhoff stress tensor. As shown in theorem 1 (chapter 1a), the main advantage of this transform is to induce a particularly simple between the divergences of both tensors:

$$div\mathbf{T}(x)=\left(\det\nabla\boldsymbol{\varphi}(x)\right)div^{\varphi}\mathbf{T}^{\varphi}\left(\mathbf{x}^{\varphi}\right),\quad x^{\varphi}=\varphi(x). \tag{1.69}$$

As a consequence, the equations of equilibrium over the deformed configuration will be transformed into equations over the reference configuration that have a similar divergence structure. This property in turn makes it possible to write these partial differential equations in variational form.
On can likewise transform the Cauchy stress vector $\mathbf{t}^{\varphi}\left(x^{\varphi},\mathbf{n}\right)=\mathbf{T}^{\varphi}\left(x^{\varphi}\right)\mathbf{n}^{\varphi}$ into a vector $\mathbf{t}(x,\mathbf{n})$ in such a way that the relation

$$\mathbf{t}(x,\mathbf{n})=\mathbf{T}(x)\mathbf{n}, \tag{1.70}$$

holds, where $\mathbf{T}(x)$ is the first Piola-Kirchhoff stress tensor and where $\mathbf{n}$ and $\mathbf{n}^{\varphi}$ are the corresponding normal vectors at the points x and $\mathbf{x}^{\varphi}=\varphi(x)$ of the boundaries of corresponding sub-domains A and $A^{\varphi}=\varphi(A)$. Notice that there is no ambiguity in this process since the normal vector $\mathbf{n}^{\varphi}$ at the point

$\mathbf{x}^{\varphi} = \boldsymbol{\varphi}(x)$ is the same for all sub-domains whose boundary passes through the point x with $\mathbf{n}$ as the normal vector there. In view of the relation $\mathbf{T}(x)\mathbf{n}da = \mathbf{T}^{\varphi}\left(x^{\varphi}\right)\mathbf{n}^{\varphi}da^{\varphi}$ established in Theorem 1.1., it suffices to define the vector $\mathbf{t}(x,\mathbf{n})$ by the relation:

$$\mathbf{t}(x,\mathbf{n})da = t^{\varphi}\left(x^{\varphi},\mathbf{n}^{\varphi}\right)da^{\varphi}. \tag{1.71}$$

Since $\mathbf{t}^{\varphi}\left(x^{\varphi},\mathbf{n}\right) = \mathbf{T}^{\varphi}\left(x^{\varphi}\right)\mathbf{n}^{\varphi}$ by Cauchy's theorem, the desired relation $\mathbf{t}(x,\mathbf{n}) = \mathbf{T}(x)\mathbf{n}$ holds.

The vector $\mathbf{t}(x,\mathbf{n})$ is called the **first Piola-Kirchhoff stress vector** at the point x of the reference configuration, across the oriented surface element with normal $\mathbf{n}$. The vector field $\mathbf{t}:\bar{\Omega}\times S_1 \to \mathbb{R}^3$ defined in this fashion thus measures the density of the surface force per unit area in the reference configuration.

While the Cauchy stress tensor $\mathbf{T}^{\varphi}\left(x^{\varphi}\right)$ is symmetric (Theorem 1.2.) the first Piola-Kirchhoff stress tensor $\mathbf{T}(x)$ is not symmetric in general; instead one has:

$$\mathbf{T}(x)^{T} = \nabla\boldsymbol{\varphi}(x)^{-1}\mathbf{T}(x)\nabla\boldsymbol{\varphi}(x)^{-T}. \tag{1.72}$$

It is nevertheless desirable to define a symmetric stress tensor in the reference configuration, essentially because the constitutive equation in the reference configuration then takes a simpler form. More specifically, we define the **second Piola-Kirchhoff stress tensor** $\boldsymbol{\Sigma}(x)$ by letting

$$\boldsymbol{\Sigma}(x) = \nabla\boldsymbol{\varphi}(x)^{-1}\boldsymbol{T}(x) = \left(\det\nabla\boldsymbol{\varphi}(x)\right)\nabla\boldsymbol{\varphi}(x)^{-1}\boldsymbol{T}^{\varphi}\left(x^{\varphi}\right)\nabla\boldsymbol{\varphi}(x)^{-T}, \quad x^{\varphi} = \boldsymbol{\varphi}(x) \tag{1.73}$$

Remarks.

(1) In fact, the question of whether or not the matrix $\mathbf{T}(x)$ is symmetric does not make sense for, as a tensor, it has one index attached to the reference configuration and one index attached to the deformed configuration. A complete discussion of these aspect can be found in Marsden & Hughes (1983)-

(2) Historical reference on the Piola-Kirchhoff stress tensors are given in Truesdell & Toupin (1960).

The Piola-Kirchhoff stress tensor $\mathbf{T}(x)$ and $\boldsymbol{\Sigma}(\mathbf{x})$ both depend on the deformation $\boldsymbol{\varphi}$, first through the Piola transform itself, secondly because the Cauchy stress tensor also dependent on $\boldsymbol{\varphi}$.

2.6. The equation of equilibrium and the principle of virtual work in the reference configuration

It remains to transform the applied forces densities that appear in the equilibrium equations over the deformed configuration. First, with the density $\boldsymbol{f}^{\varphi}:\Omega^{\varphi}\to\mathbb{R}^3$ of the applied force per unit volume in the deformed configuration, we associate a vector field $\boldsymbol{f}:\Omega\to\mathbb{R}^3$ in such a way that

$$\boldsymbol{f}(x)dx=\boldsymbol{f}^{\varphi}\left(x^{\varphi}\right)dx^{\varphi} \text{ for all } x^{\varphi}=\boldsymbol{\varphi}(x)\in\Omega^{\varphi} \tag{1.74}$$

where dx and dx^{φ} denote the corresponding volume elements. Since

$$dx^{\varphi}=\left(\det\boldsymbol{\nabla}\boldsymbol{\varphi}(x)\right)\boldsymbol{f}^{\varphi}\left(x^{\varphi}\right),\quad x^{\varphi}=\boldsymbol{\varphi}(x), \tag{1.75}$$

so that the vector $\boldsymbol{f}(x)$ depends on the deformation $\boldsymbol{\varphi}$, via the factor $\det\boldsymbol{\nabla}\boldsymbol{\varphi}(x)$ on the one hand, and via the possible dependence of the density $\boldsymbol{f}^{\varphi}$ on the deformation $\boldsymbol{\varphi}$ on the other hand. Notice that this relation displays the same factor $\det\boldsymbol{\nabla}\boldsymbol{\varphi}(x)$ as the relation between the vectors $\mathbf{div}\,\mathbf{T}(x)$ and $\mathbf{div}^{\varphi}\mathbf{T}^{\varphi}\left(x^{\varphi}\right)$.

The vector field $\boldsymbol{f}:\Omega\to\mathbb{R}^3$ measures the density of the applied body force per unit volume in the reference configuration; the vector $\boldsymbol{f}(x)$ is defined in such a way that the elementary vector $\boldsymbol{f}(x)dx$ is equal to the elementary body force $\boldsymbol{f}\left(x^{\varphi}\right)dx^{\varphi}$ acting on the corresponding volume element dx^{φ} at the point $x^{\varphi}=\boldsymbol{\varphi}(x)$ (Figure 1.5.).

Let: $\rho:\Omega\to\mathbb{R}$ denote the mass density in the reference configuration. Expressing that the mass of the elementary volumes dx and $dx^{\varphi}=\det\boldsymbol{\nabla}\boldsymbol{\varphi}(x)dx$ is the same, we find the mass densities $\rho:\Omega\to\mathbb{R}$ and $\rho^{\varphi}:\Omega^{\varphi}\to\mathbb{R}$ are related by the equation

$$\rho(x)=\det\boldsymbol{\nabla}\boldsymbol{\varphi}(x)\rho^{\varphi}\left(x^{\varphi}\right),\quad x^{\varphi}=\boldsymbol{\varphi}(x). \tag{1.76}$$

Incidentally, this relation also shows that, regardless of any consideration concerning the preservation of orientation, the Jacobian $\det \nabla \boldsymbol{\varphi}(x)$ should not vanish in an actual deformation, since mass density is always >0, at least macroscopically.

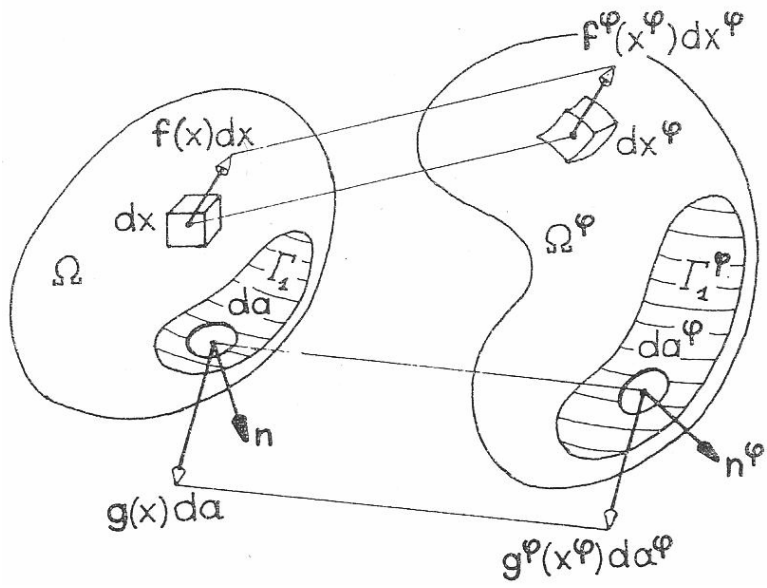

Fig. 1.5.
The applied body force and surface force densities in the deformed configuration and in the reference configuration

Then if we define the density $\mathbf{b}:\Omega\to\mathbb{R}^3$ of the applied body forces per unit mass in the reference configuration by letting

$$\boldsymbol{f}(x)=\rho(x)\mathbf{b}(x) \text{ for all } x\in\Omega \tag{1.77}$$

it follows that the densities of the applied force per unit mass are related by

$$\mathbf{b}(x)=\mathbf{b}^{\varphi}\left(x^{\varphi}\right),\quad x^{\varphi}=\boldsymbol{\varphi}(x). \tag{1.78}$$

Secondly, in order to transform the boundary condition $\mathbf{T}^{\varphi}\mathbf{n}^{\varphi}=\mathbf{g}^{\varphi}$ over $\Gamma_1^{\varphi}=\boldsymbol{\varphi}(\Gamma_1)$ into a similar condition over Γ_1, it suffices to use the first Piola-Kirchhoff stress vector, which was precisely defined for this purpose: With the

density $\mathbf{g}^{\varphi}:\Gamma_1^{\varphi}\to\mathbb{R}^3$ of the applied surface force per unit area in the deformed configuration, we associate the vector field $\mathbf{g}:\Gamma_1\to\mathbb{R}^3$ defined by

$$\mathbf{g}(x)\,da=\mathbf{g}^{\varphi}\left(x^{\varphi}\right)da^{\varphi}\ \text{ for all }\ x^{\varphi}=\boldsymbol{\varphi}(x)\in\Gamma_1^{\varphi} \tag{1.79}$$

where da and da^{φ} are the corresponding area elements. Hence by Theorem 1.1 (Properties of the Piola transform), the vector $\mathbf{g}(x)$ is given by

$$\mathbf{g}(x)=\det\boldsymbol{\nabla\varphi}(x)\left|\boldsymbol{\nabla\varphi}(x)^{-T}\mathbf{n}\right|\mathbf{g}^{\varphi}\left(\mathbf{x}^{\varphi}\right). \tag{1.80}$$

Notice that the vector $\mathbf{g}(x)$ depends on the deformation $\boldsymbol{\varphi}$, via the formula relating the corresponding area elements on the one hand and via the possible dependence of the density, $\mathbf{g}^{\varphi}$ on the deformation $\boldsymbol{\varphi}$ on the other hand. The vector field $\mathbf{g}:\Gamma_1\to\mathbb{R}^3$ measures the density of the applied surface force per unit area in the reference configuration; it is defined in such a way that the elementary vector $\mathbf{g}(x)da$ is equal to the elementary surface force $\mathbf{g}^{\varphi}\left(x^{\varphi}\right)da^{\varphi}$ acting on the corresponding area element da^{φ} at the point $x^{\varphi}=\varphi(x)$ (Fig. 1.5).
We can now establish the analogous of Theorem 1.3 over the reference configuration:

Theorem 1.4. The first Piola-Kirchhoff stress tensor

$$\mathbf{T}(x)=\left(\det\boldsymbol{\nabla\varphi}(x)\right)\mathbf{T}^{\varphi}\left(\mathbf{x}^{\varphi}\right)\boldsymbol{\nabla\varphi}(x)^{-T} \tag{1.81}$$

satisfies the following equations in the reference configuration $\overline{\Omega}$:

$$\begin{aligned}
&-\mathbf{div}\,\mathbf{T}(x)=\boldsymbol{f}(x),\quad x\in\Omega,\\
&\boldsymbol{\nabla\varphi}(x)\mathbf{T}(x)^{T}=\mathbf{T}(x)\boldsymbol{\nabla\varphi}(x)^{T},\quad x\in\Omega,\\
&\mathbf{T}(x)\mathbf{n}=\mathbf{g}(x),\quad x\in\Gamma_1
\end{aligned} \tag{1.82}$$

where $\mathbf{f}\,dx=\mathbf{f}^{\varphi}dx^{\varphi}$, $\mathbf{g}\,da=\mathbf{g}^{\varphi}da^{\varphi}$. The first and third equations are together equivalent to the variational equations:

$$\int_{\Omega}\mathbf{T}:\boldsymbol{\nabla\theta}\,dx=\int_{\Omega}\boldsymbol{f}\cdot\boldsymbol{\theta}\,dx+\int_{\Gamma_1}\boldsymbol{g}\cdot\boldsymbol{\theta}\,da, \tag{1.83}$$

valid for all smooth enough vector fields $\boldsymbol{\theta}: \overline{\Omega} \to \mathbb{R}^3$ that satisfy

$$\boldsymbol{\theta} = \mathbf{0} \quad \text{on} \quad \Gamma_0 = \Gamma - \Gamma_1. \tag{1.84}$$

In terms of the second Piola-Kirchhoff stress tensor, the above result becomes:
Theorem 1.5. The second Piola-Kirchhoff stress tensor

$$\boldsymbol{\Sigma}(x) = \left(\det \nabla \boldsymbol{\varphi}(x)\right) \nabla \boldsymbol{\varphi}(x)^{-1} \boldsymbol{T}^{\varphi}\left(x^{\varphi}\right) \nabla \boldsymbol{\varphi}(x)^{-T} \tag{1.85}$$

satisfies the following equations in the reference configuration $\overline{\Omega}$:

$$\begin{aligned} &-\mathbf{div}\left(\nabla \boldsymbol{\varphi}(x) \boldsymbol{\Sigma}(x)\right) = \boldsymbol{f}(x), \quad x \in \overline{\Omega}, \\ &\boldsymbol{\Sigma}(x) = \boldsymbol{\Sigma}(x)^T, \quad x \in \Omega, \\ &\nabla \boldsymbol{\varphi}(x) \boldsymbol{\Sigma}(x) \mathbf{n} = \mathbf{g}(x), \quad x \in \Gamma_1 \end{aligned} \tag{1.86}$$

The first and third equations are together equivalent to the variational equations

$$\int_{\Omega} \nabla \varphi \Sigma : \nabla \boldsymbol{\theta} \, dx = \int_{\Omega} \boldsymbol{f} \cdot \boldsymbol{\theta} \, dx + \int_{\Gamma_1} \boldsymbol{g} \cdot \boldsymbol{\theta} \, da \tag{1.87}$$

valid for all smooth enough maps $\boldsymbol{\theta}: \overline{\Omega} \to \mathbb{R}^3$ that satisfy

$$\boldsymbol{\theta} = \mathbf{0} \quad \text{on} \quad \Gamma_0 = \Gamma - \Gamma_1 \tag{1.88}$$

The equations satisfied over Ω and Γ_1 by either stress tensor are called the equations of equilibrium in the reference configuration, and their associated variational equations constitute the principal of virtual work in the reference configuration. The equation on Γ_1 is called a boundary condition of traction.

3. LINEAR ANISOTROPIC ELASTIC MEDIA

The relation between stress and strain in an anisotropic elastic material are presented in this section. A linear anisotropic elastic material can have as many as 21 elastic constants. This number is reduced when the material possesses a certain material symmetry. The number of elastic constants is also reduced, in most cases, when a two-dimensional deformation is considered. An important condition on elastic constants is that the strain energy must be positive. This condition implies that the 6x6 matrices of elastic constants presented herein must be positive definite.

3.1. Elastic Stiffnesses

Referring to a fixed rectangular coordinate system x_1, x_2, x_3, let σ_{ij} and ε_{ij} be the stress and strain, respectively, in an anisotropic elastic material. The stress-strain law can be written as

$$\sigma_{ij} = C_{ijkl}\varepsilon_{kl} \tag{1.89}$$

in which C_{ijhk}, are the *elastic stiffnesses* which are components of a fourth rank tensor. They satisfy the full symmetry conditions

$$C_{ijkl} = C_{jikl}, \quad C_{ijkl} = C_{ijlk}, \quad C_{ijkl} = C_{klij}. \tag{1.90}$$

Before we present justifications for the three conditions in (1.90), we show that $(1.90)_1$ and $(1.90)_3$ imply $(1.90)_2$. Using $(1.90)_3$, $(1.90)_1$ and $(1.90)_3$ in that order we have

$$C_{ijkl} = C_{klij} = C_{lkij} = C_{ijlk}$$

which proves $(1.90)_2$. Therefore the three conditions in (1.90) are written as

$$C_{ijkl} = C_{jikl} = C_{klij}. \tag{1.91}$$

One can also show that $(1.90)_2$ and $(1.90)_3$ imply $(1.90)_1$.
The first equation of (1.90) follows directly from the symmetry of the stress tensor $\sigma_{ij} = \sigma_{ji}$. The second equation of (1.90) does *not* follow directly from the symmetry of the strain tensor $\varepsilon_{ij} = \varepsilon_{ji}$. However, if the C_{ijkl} in (1.90) do not satisfy $(1.90)_2$, we rewrite (1.90) as

$$\sigma_{ij} = \tfrac{1}{2}C_{ijkl}\varepsilon_{kl} + \tfrac{1}{2}C_{ijkl}\varepsilon_{kl} = \tfrac{1}{2}C_{ijkl}\varepsilon_{kl} + \tfrac{1}{2}C_{ijlk}\varepsilon_{lk}$$

or since $\varepsilon_{lk} = \varepsilon_{kl}$,

$$\sigma_{ij} = \tfrac{1}{2}\left(C_{ijkl} + C_{ijlk}\right)\varepsilon_{kl}. \tag{1.92}$$

The coefficients of ε_{kl} are symmetric with the subscripts *kl*. We can therefore redefine the coefficients of ε_{kl} in (1.92) as the new C_{ijkl} which satisfy $(1.90)_2$.

The third equation follows from the consideration of strain energy. The strain energy W per unit volume of the material is

$$W = \int_0^{\varepsilon_{pq}} \sigma_{ij} d\varepsilon_{ij} = \int_0^{\varepsilon_{pq}} C_{ijkl} \varepsilon_{kl} d\varepsilon_{ij} \,. \tag{1.93}$$

We demand that the integral be independent of the path ε_{ij} takes from 0 to ε_{pq}. If not, say path 1 yields a larger integral than path 2, one can consider loading the material from 0 to ε_{pq} through path 1, and unloading from ε_{pq} to 0 through the reverse of path 2. The energy gained is the difference between the W 's for path 1 and path 2. If we repeat the process we can extract unlimited amount of energy from the material, which is physically impossible for a real material. Therefore the integral in (1.93) must be independent of the path taken by ε_{ij}, and W depends on the final strain ε_{pq} only. This implies that the integrand must be the total differential dW, i.e.,

$$C_{ijkl} \varepsilon_{kl} d\varepsilon_{ij} = dW = \frac{\partial W}{\partial \varepsilon_{ij}} d\varepsilon_{ij} \,. \tag{1.94}$$

Since $d\varepsilon_{ij}$ is arbitrary we must have

$$\sigma_{ij} = C_{ijkl} \varepsilon_{kl} = \frac{\partial W}{\partial \varepsilon_{ij}} \tag{1.95}$$

in which the first equality follows from (1.89). Differentiation of (1.95) with ε_{kl} leads to

$$C_{ijkl} = \frac{\partial^2 W}{\partial \varepsilon_{kl} \partial \varepsilon_{ij}}$$

The double differentiations on the right are interchangeable. Therefore

$$C_{ijkl} = C_{klij}$$

is the condition for the integral in (1.93) to be Independent of the loading path.

This proves $(1.90)_3$. With $(1.90)_3$, (1.94) is written as

$$dW = C_{ijkl}\varepsilon_{kl}d\varepsilon_{ij} = \tfrac{1}{2}d\left(C_{ijkl}\varepsilon_{ij}\varepsilon_{kl}\right).$$

Hence

$$W = \tfrac{1}{2}C_{ijkl}\varepsilon_{ij}\varepsilon_{kl} = \tfrac{1}{2}\sigma_{ij}\varepsilon_{ij}\,. \tag{1.96}$$

and since the strain energy must be positive, it results

$$C_{ijkl}\varepsilon_{ij}\varepsilon_{kl} > 0 \tag{1.97}$$

for any real, nonzero, symmetric tensor ε_{kl}.

3.2. Elastic Compliances

The inverse of (1.89) is written as

$$\varepsilon_{ij} = S_{ijkl}\sigma_{kl} \tag{1.98}$$

where S_{ijkl} are the elastic compliance which are components of a four rank tensor. They also possess the full symmetry

$$S_{ijkl} = S_{jikl}\,, \quad S_{ijkl} = S_{ijlk}\,, \quad S_{ijkl} = S_{klij} \tag{1.99}$$

or, as in (1.91)

$$S_{ijkl} = S_{jikl} = S_{klij}\,. \tag{1.100}$$

The justifications of the first and second equations in (1.101) are similar to their counterparts in (1.102). The justification of $(1.103)_3$ also follows from the energy consideration. Integration by parts of $(1.104)_1$ leads to

$$W = \sigma_{pq}\varepsilon_{pq} - \int_0^{\sigma_{pq}} \varepsilon_{ij}d\sigma_{ij} = \sigma_{pq}\varepsilon_{pq} - \int_0^{\sigma_{pq}} S_{ijkl}\sigma_{kl}d\sigma_{ij}\,.$$

If *W* depends on the final strain ε_{pq} it depends on the final stress σ_{pq}. The last integral which represents the *complementary energy* must be independent of the path σ_{ij} takes from 0 to the final stress σ_{pq}. Following a similar argument for

C_{ijkl}, we deduce that $(1.105)_3$ must hold for the integral to be path independent. Since the strain energy must be positive, the substitution of the (1.98) into the (1.96) yields

$$S_{ijkl}\sigma_{ij}\sigma_{kl} > 0 \tag{1.106}$$

3.3. Contracted Notations

Introducing the contracted notation (Voigt, 1928; Lekhnitskii, 1963; Christensen, 1979)

$$\begin{aligned} &\sigma_{11} = \sigma_1, \quad \sigma_{22} = \sigma_2, \quad \sigma_{33} = \sigma_3, \\ &\sigma_{32} = \sigma_4, \quad \sigma_{31} = \sigma_5, \quad \sigma_{12} = \sigma_6, \end{aligned} \tag{1.107}$$

$$\begin{aligned} &\varepsilon_{11} = \varepsilon_1, \quad \varepsilon_{22} = \varepsilon_2, \quad \varepsilon_{33} = \varepsilon_3, \\ &2\varepsilon_{32} = \varepsilon_4, \quad 2\varepsilon_{31} = \varepsilon_5, \quad 2\varepsilon_{12} = \varepsilon_6, \end{aligned} \tag{1.108}$$

the stress-strain law (1.89) and (1.90) can be written as

$$\sigma_\alpha = C_{\alpha\beta}\varepsilon_\beta, \quad C_{\alpha\beta} = C_{\beta\alpha}, \tag{1.109}$$

or, in matrix notation,

$$\boldsymbol{T} = \mathbb{C}\boldsymbol{E}, \quad \mathbb{C} = \mathbb{C}^T. \tag{1.110}$$

In the above $\boldsymbol{T}$ and $\boldsymbol{E}$ are 6×1 column matrices and $\mathbb{C}$ is the 6×6 symmetric matrix given by

$$\mathbb{C} = \begin{bmatrix} C_{11} & C_{12} & C_{13} & C_{14} & C_{15} & C_{16} \\ C_{12} & C_{22} & C_{23} & C_{24} & C_{25} & C_{26} \\ C_{13} & C_{23} & C_{33} & C_{34} & C_{35} & C_{36} \\ C_{14} & C_{24} & C_{34} & C_{44} & C_{45} & C_{46} \\ C_{15} & C_{25} & C_{35} & C_{45} & C_{55} & C_{56} \\ C_{16} & C_{26} & C_{36} & C_{46} & C_{56} & C_{66} \end{bmatrix} \tag{1.111}$$

The transformation between C_{ijkl} and $C_{\alpha\beta}$ is accomplished by replacing the subscripts *ij* (or *kl*) by α (or β) using the following rules:

$$\begin{aligned} ij(\text{or } kl) &\leftrightarrow \alpha(\text{or } \beta) \\ 11 &\leftrightarrow 1 \\ 22 &\leftrightarrow 2 \\ 33 &\leftrightarrow 3 \\ 32 \text{ or } 23 &\leftrightarrow 4 \\ 31 \text{ or } 13 &\leftrightarrow 5 \\ 12 \text{ or } 21 &\leftrightarrow 6 \end{aligned} \tag{1.112}$$

The presence of the factor 2 in $(1.108)_{4\text{-}5\text{-}6}$ but not in $(1.107)_{4\text{-}5\text{-}6}$ 6 is necessary for the symmetry of $\mathbb{C}$.
Analogously, with reference to the equation (1.107) and(1.108), the stress-strain law in the form (1.98) may be expressed in a matrix form, as it follows:

$$\boldsymbol{E} = \mathbb{S}\boldsymbol{T}, \quad \mathbb{S} = \mathbb{S}^T \tag{1.113}$$

where the compliance tensor $\mathbb{S}$. is expressed in form of the 6×6 symmetric matrix, given by:

$$\mathbb{S} = \begin{bmatrix} S_{11} & S_{12} & S_{13} & S_{14} & S_{15} & S_{16} \\ S_{12} & S_{22} & S_{23} & S_{24} & S_{25} & S_{26} \\ S_{13} & S_{23} & S_{33} & S_{34} & S_{35} & S_{36} \\ S_{14} & S_{24} & S_{34} & S_{44} & S_{45} & S_{46} \\ S_{15} & S_{25} & S_{35} & S_{45} & S_{55} & S_{56} \\ S_{16} & S_{26} & S_{36} & S_{46} & S_{56} & S_{66} \end{bmatrix} \tag{1.114}$$

Note that the transformation between S_{ijkl} and $S_{\alpha\beta}$ is similar to that one between C_{ijkl} and $C_{\alpha\beta}$ except the following:

$$\begin{aligned} &S_{ijhk} = S_{\alpha\beta} \quad \text{if both} \quad \alpha,\beta \le 3 \\ &2S_{ijhk} = S_{\alpha\beta} \quad \text{if either} \quad \alpha \text{ or } \beta \le 3 \\ &4S_{ijhk} = S_{\alpha\beta} \quad \text{if both} \quad \alpha,\beta > 3. \end{aligned} \tag{1.115}$$

From $(1.110)_1$ and $(1.113)_1$, it is obtained the expression of the strain energy, the strain energy W becomes:

$$W = \tfrac{1}{2}\mathbf{T}^T\,\mathbf{E} = \tfrac{1}{2}\mathbf{E}^T\mathbb{C}\,\mathbf{E} = \mathbf{T}^T\,\mathbb{S}\,\mathbf{T} \tag{1.116}$$

and, for the positiveness of W, it must be:

$$\begin{aligned}\mathbf{E}^T\mathbb{C}\,\mathbf{E} > 0\\ \mathbf{T}^T\mathbb{S}\,\mathbf{T} > 0\end{aligned} \tag{1.117}$$

This implies that the matrices $\mathbb{C}$ and $\mathbb{S}$ are both positive definite. Moreover, the substitution of the $(1.113)_1$ into the $(1.110)_1$ yields:

$$\mathbb{C}\,\mathbb{S} = \mathbb{I} = \mathbb{S}\mathbb{C} \tag{1.118}$$

where the second equality follows from the first one which says that $\mathbb{C}$ and $\mathbb{S}$ are the inverses of each other and, hence their product commute.

3.4. Material Symmetry

The 6×6 matrices $\mathbb{C}$ and $\mathbb{S}$ contain 21 independent elastic constants. The number of independent constants is reduced when the material possesses a certain material symmetry.
Under an orthogonal transformation

$$x_i^* = Q_{ij}x_j \quad \text{or} \quad \boldsymbol{x}^* = \mathbf{Q}\,\boldsymbol{x} \tag{1.119}$$

in which $\mathbf{Q}$ is an orthogonal matrix that satisfies the that satisfies the relations:

$$\mathbf{Q}\cdot\mathbf{Q}^T = \mathbf{I} = \mathbf{Q}^T\mathbf{Q}\,, \tag{1.120}$$

the four rank elasticity tensor C_{ijkl}^*, referred to the x_i^* coordinate system becomes

$$\mathrm{C}_{ijkl}^* = Q_{ip}Q_{jq}Q_{kr}Q_{ls}\mathrm{C}_{pqrs} \tag{1.121}$$

If it results $C_{ijkl}^* = C_{ijkl}$, i.e.,

$$\mathrm{C}_{ijkl} = Q_{ip}Q_{jq}Q_{kr}Q_{ls}\mathrm{C}_{pqrs} \tag{1.122}$$

material is said to possess a *symmetry* with respect to $\mathbf{Q}$.
An anisotropic material possesses the symmetry of *central inversion* if (1.122) is satisfied for

$$\mathbf{Q} = \begin{bmatrix} -1 & 0 & 0 \\ 0 & -1 & 0 \\ 0 & 0 & -1 \end{bmatrix} = -\mathbf{I}. \tag{1.123}$$

It is obvious that the (1.122) is satisfied by the $\mathbf{Q}$ given in the (1.123) for any C_{ijkl}. Therefore, all the anisotropic materials have the symmetry of central inversion.
If $\mathbf{Q}$ is a proper orthogonal matrix, the transformation (1.119) represents a rigid body rotation about an axis. So, an anisotropic material is said to possess a *rotational symmetry* if the (1.122) is satisfied for:

$$\mathbf{Q}^r(\theta) = \begin{bmatrix} \cos\theta & \sin\theta & 0 \\ -\sin\theta & \cos\theta & 0 \\ 0 & 0 & 1 \end{bmatrix} \tag{1.124}$$

which represents, for example, a rotation about the $\boldsymbol{x}_3$-axis an angle θ.
An orthogonal transformation $\mathbf{Q}$ is a *reflection* if

$$\mathbf{Q} = \mathbf{I} - 2\mathbf{n} \otimes \mathbf{n}^T \tag{1.125}$$

where $\mathbf{n}$ is a unit vector normal to the reflection plane. If $\boldsymbol{m}$ is any vector on the plane,

$$\mathbf{Q}\mathbf{n} = -\mathbf{n}, \quad \mathbf{Q}\mathbf{m} = -\mathbf{m}. \tag{1.126}$$

Thus a vector normal to the reflection plane reverses its direction after the transformation while a vector on the reflection place remains unchanged. When (1.122) is satisfied by the $\mathbf{Q}$ of (1.125), the material is laid to possess a *symmetry plane.* For example, let

$$\mathbf{n}^T = [\cos\theta, \sin\theta, 0] \tag{1.127}$$

the symmetry plane. In this case, the orthogonal matrix $\mathbf{Q}$ of the (1.125) has the following expression

$$\mathbf{Q}(\theta)=\begin{bmatrix} 2+\cos 2\theta & \sin 2\theta & 0 \\ \sin 2\theta & 2-\cos 2\theta & 0 \\ 0 & 0 & 1 \end{bmatrix}, \quad -\frac{\pi}{2}<\theta\le\frac{\pi}{2}, \qquad (1.128)$$

which is an improper orthogonal matrix. Since θ and $\theta+\pi$ represent the same plane, θ is limited to the range shown in $(1.128)_2$.
When $\theta=0$, $\mathbf{Q}$ becomes:

$$\mathbf{Q}(0)=\begin{bmatrix} -1 & 0 & 0 \\ 0 & 1 & 0 \\ 0 & 0 & 1 \end{bmatrix} \qquad (1.129)$$

which represents a reflection about the plane $\boldsymbol{x}_1=0$. When (1.122) is satisfied by (1.129), the material has a symmetry plane at $x_1=0$. If (1.122) is satisfied by (1.128) for any θ, the material is *transversely isotropic*. The x_3-axis is the *axis of symmetry*. Two extreme cases of anisotropic elastic materials are *triclinic materials* and *isotropic materials*. A triclinic material possesses no rotational symmetry or a plane of reflection symmetry. An isotropic material possesses infinitely many rotational symmetries and planes of reflection symmetry.

3.5. The Elasticity Tensor for Materials with Symmetry Planes

Depending on the number of rotations and/or reflection symmetry a crystal possesses, Voigt (1928) has classified crystals into 32 classes. (See also Gurtin, 1972; Cowin and Mehrabadi, 1987; and Mehrabadi and Cowin. 1990). In terms of the 6×6 matrix $\mathbb{C}$ however there are only 8 basic groups. For a non-crystalline material the structure of $\mathbb{C}$ can also be represented by one of the 8 basic groups. We list below the 8 basic groups for $\mathbb{C}$ according to the number of symmetry planes that each group has. Consideration of rotational symmetry does not change the structure of $\mathbb{C}$ in each group. Without loss in generality we choose the symmetry plane (or planes) to coincide with the coordinate planes whenever possible. We will therefore employ the orthogonal matrix $\mathbf{Q}$ (1.128) which represents a reflection with respect to a plane whose normal is on the

(x_1, x_2) plane making an angle θ with the x_1-axis. We will also employ the orthogonal matrix

$$\hat{\mathbf{Q}}(\psi) = \begin{bmatrix} 1 & 0 & 0 \\ 0 & -\cos 2\psi & -\sin 2\psi \\ 0 & -\sin 2\psi & \cos 2\psi \end{bmatrix}, \quad -\frac{\pi}{2} < \psi \leq \frac{\pi}{2} \tag{1.130}$$

which represents a reflection with respect to a plane whose normal is on the (x_2, x_3) plane making an angle ψ with the x_2-axis, (Fig. 1.6.). The plane $x_2 = 0$ can be represented by either $\theta = \pi/2$ or $\psi = 0$.

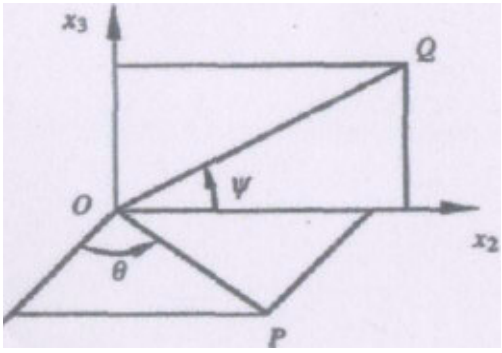

Fig. 1.6.

I. *Triclinic Materials.* No symmetry planes exist.

$$\mathbb{C} = \begin{bmatrix} C_{11} & C_{12} & C_{13} & C_{14} & C_{15} & C_{16} \\ C_{12} & C_{22} & C_{23} & C_{24} & C_{25} & C_{26} \\ C_{13} & C_{23} & C_{33} & C_{34} & C_{35} & C_{36} \\ C_{14} & C_{24} & C_{34} & C_{44} & C_{45} & C_{46} \\ C_{15} & C_{25} & C_{35} & C_{45} & C_{55} & C_{56} \\ C_{16} & C_{26} & C_{36} & C_{46} & C_{56} & C_{66} \end{bmatrix} \quad n = 21 \tag{1.131}$$

II. *Monoclinic Materials*. One symmetry plane.

(a) Symmetry plane at $x_1 = 0$, i.e., $\theta = 0$.

$$\mathbb{C} = \begin{bmatrix} C_{11} & C_{12} & C_{13} & C_{14} & 0 & 0 \\ C_{12} & C_{22} & C_{23} & C_{24} & 0 & 0 \\ C_{13} & C_{23} & C_{33} & C_{34} & 0 & 0 \\ C_{14} & C_{24} & C_{34} & C_{44} & 0 & 0 \\ 0 & 0 & 0 & 0 & C_{55} & C_{56} \\ 0 & 0 & 0 & 0 & C_{56} & C_{66} \end{bmatrix} \quad n = 13 \qquad (1.132)$$

(b) Symmetry plane at $x_2 = 0$, i.e., $\theta = \pi/2$ or $\psi = 0$.

$$\mathbb{C} = \begin{bmatrix} C_{11} & C_{12} & C_{13} & 0 & C_{15} & 0 \\ C_{12} & C_{22} & C_{23} & 0 & C_{25} & 0 \\ C_{13} & C_{23} & C_{33} & 0 & C_{35} & 0 \\ 0 & 0 & 0 & C_{44} & 0 & C_{46} \\ C_{15} & C_{25} & C_{35} & 0 & C_{55} & 0 \\ 0 & 0 & 0 & C_{46} & 0 & C_{66} \end{bmatrix} \quad n = 13 \qquad (1.133)$$

(c) Symmetry plane at $x_3 = 0$, i.e., $\psi = \pi/2$.

$$\mathbb{C} = \begin{bmatrix} C_{11} & C_{12} & C_{13} & 0 & 0 & C_{16} \\ C_{12} & C_{22} & C_{23} & 0 & 0 & C_{26} \\ C_{13} & C_{23} & C_{33} & 0 & 0 & C_{36} \\ 0 & 0 & 0 & C_{44} & C_{45} & 0 \\ 0 & 0 & 0 & C_{45} & C_{55} & 0 \\ C_{16} & C_{26} & C_{36} & 0 & 0 & C_{66} \end{bmatrix} \quad n = 13 \qquad (1.134)$$

II. *Orthotropic (or Rhombic) Materials*. The three coordinate planes $\theta = 0$, $\pi/2$, and $\psi = \pi/2$ are the symmetry planes.

$$\mathbb{C} = \begin{bmatrix} C_{11} & C_{12} & C_{13} & 0 & 0 & 0 \\ C_{12} & C_{22} & C_{23} & 0 & 0 & 0 \\ C_{13} & C_{23} & C_{33} & 0 & 0 & 0 \\ 0 & 0 & 0 & C_{44} & 0 & 0 \\ 0 & 0 & 0 & 0 & C_{55} & 0 \\ 0 & 0 & 0 & 0 & 0 & C_{66} \end{bmatrix} \quad n = 9 \qquad (1.135)$$

III. *Trigonal Materials*. Three symmetry planes at $\theta = 0$ and $\pm\pi/3$.

$$\mathbb{C} = \begin{bmatrix} C_{11} & C_{12} & C_{13} & C_{14} & 0 & 0 \\ C_{12} & C_{11} & C_{13} & -C_{14} & 0 & 0 \\ C_{13} & C_{13} & C_{33} & 0 & 0 & 0 \\ C_{14} & -C_{14} & 0 & C_{44} & 0 & 0 \\ 0 & 0 & 0 & 0 & C_{44} & C_{14} \\ 0 & 0 & 0 & 0 & C_{14} & \frac{C_{11}-C_{12}}{2} \end{bmatrix} \quad n = 6 \qquad (1.136)$$

IV. *Tetragonal Materials*. Five symmetry planes at $\theta = 0$ $\pm\pi/4$, $\pi/2$ and $\psi = \pi/2$.

$$\mathbb{C} = \begin{bmatrix} C_{11} & C_{12} & C_{13} & 0 & 0 & 0 \\ C_{12} & C_{11} & C_{13} & 0 & 0 & 0 \\ C_{13} & C_{13} & C_{33} & 0 & 0 & 0 \\ 0 & 0 & 0 & C_{44} & 0 & 0 \\ 0 & 0 & 0 & 0 & C_{44} & 0 \\ 0 & 0 & 0 & 0 & 0 & C_{66} \end{bmatrix} \quad n = 6 \qquad (1.137)$$

V. *Transversely Isotropic (or Hexagonal) Materials*. The symmetry planes are the $x_3 = 0$ plane and any plane that contains the x_3-axis. The x_3-axis is the axis of symmetry.

$$\mathbb{C} = \begin{bmatrix} C_{11} & C_{12} & C_{13} & 0 & 0 & 0 \\ C_{12} & C_{11} & C_{13} & 0 & 0 & 0 \\ C_{13} & C_{13} & C_{33} & 0 & 0 & 0 \\ 0 & 0 & 0 & C_{44} & 0 & 0 \\ 0 & 0 & 0 & 0 & C_{44} & 0 \\ 0 & 0 & 0 & 0 & 0 & \frac{C_{11}-C_{12}}{2} \end{bmatrix} \quad n = 5 \qquad (1.138)$$

VI. *Cubic Materials*. Nine planes of symmetry whose normals are on the three coordinate axes and on the coordinate planes making an angle $\pi/4$ with the coordinate axes.

$$\mathbb{C} = \begin{bmatrix} C_{11} & C_{12} & C_{12} & 0 & 0 & 0 \\ C_{12} & C_{11} & C_{12} & 0 & 0 & 0 \\ C_{12} & C_{12} & C_{11} & 0 & 0 & 0 \\ 0 & 0 & 0 & C_{44} & 0 & 0 \\ 0 & 0 & 0 & 0 & C_{44} & 0 \\ 0 & 0 & 0 & 0 & 0 & C_{44} \end{bmatrix} \quad n = 3 \qquad (1.139)$$

VII. *Isotropic Materials*. Any plane is a symmetry plane.

$$\mathbb{C} = \begin{bmatrix} C_{11} & C_{12} & C_{12} & 0 & 0 & 0 \\ C_{12} & C_{11} & C_{12} & 0 & 0 & 0 \\ C_{12} & C_{12} & C_{11} & 0 & 0 & 0 \\ 0 & 0 & 0 & \frac{C_{11}-C_{12}}{2} & 0 & 0 \\ 0 & 0 & 0 & 0 & \frac{C_{11}-C_{12}}{2} & 0 \\ 0 & 0 & 0 & 0 & 0 & \frac{C_{11}-C_{12}}{2} \end{bmatrix} \quad n = 2 \qquad (1.140)$$

Note that while the number of nonzero elements in $\mathbb{C}$ may increase when different coordinate system are employed, the number of independent elastic constants *n* does not depend on the choice of the coordinate systems.

3.6. Restrictions on Elastic Constants

As shown above, the positiveness of the strain energy, yields that the stiffness tensor $\mathbb{C}$ is positive defined, as well as, the positive definiteness of the stress energy, yields that the compliance tensor $\mathbb{S}$ is defined positive. In particular, in the contracted notation, the (1.97) is equivalent to the $(1.117)_1$ which implies that the 6×6 matrix $\mathbb{C}$ is also positive definite and, therefore, all its principal minors are positive, i.e.:

$$
\begin{gathered}
C_{ii} > 0 \quad (i \text{ not summed}), \\
\begin{vmatrix} C_{ii} & C_{ij} \\ C_{ij} & C_{jj} \end{vmatrix} > 0 \quad (i, j \text{ not summed}), \\
\begin{vmatrix} C_{ii} & C_{ij} & C_{ih} \\ C_{ij} & C_{jj} & C_{jh} \\ C_{ih} & C_{jh} & C_{hh} \end{vmatrix} > 0 \quad (i, j, k \text{ not summed}), \\
\vdots
\end{gathered}
$$

where i, j, h are distinct integers which can have any value from 1 to 6.
In particular, according to the theorem which states that a real symmetric matrix is positive definite if and only if its *leading* principal minors are positive, the *necessary* and *sufficient conditions* for the 6×6 matrix $\mathbb{C}$ to be positive definite are the positivity of its 6 *leading* principal minors. Same considerations may be applied to the compliance tensor $\mathbb{S}$. By imposing these conditions of positivity on the minors of the matrices, some restrictions on the elastic coefficients can be found.

CHAPTER II

HETEROGENEOUS MATERIALS

1. INHOMOGENEOUS SOLIDS: SAS/DAS THEOREMS

It is well known the difficulty to find solutions to anisotropic inhomogeneous material problems. A very few restricted classes of these problems are solved in a general way.
One example of these solutions is for cylinders subjected to pure torsion and possessing cylindrical orthotropy, with a variation of the shear moduli with the local normal direction to the family of curves of which the lateral boundary is a member (Cowin, 1987). This solution is a generalization, to a set of arbitrary cross-sectional shapes, of a problem solved by Voigt (Voigt, 1928) for a circular cross-section with radial variation of its cylindrical anisotropy. These cylinders are said to possess *shape intrinsic orthotropy* since it is the boundary of the cylinder that establishes the possible directional variation of the elastic moduli.
A second example was given by Chung & Ting (Chung & Ting, 1995) who presented an exact solution for the case of an anisotropic half-space with elastic moduli dependent upon one coordinate, the angle θ, when the loads on the half-space are represented by a straight line of force. These kinds of problems were called *angularly inhomogeneous problems* by the authors. Closely related to these solutions is a third example called *radially inhomogeneous problems* (Alshits and Kirchner, 2001). As the name suggests, the variation of the elastic constants is in the radial direction in this case.
In spite of this difficulty, in the last years, it has been a growing interest about the mechanical behaviour of anisotropic and inhomogeneous solids, above all in biomechanics. Moreover, the necessity to build thermodynamically consistent theories for this kind of materials, by means the employment of the mathematical theory of the *homogenization,* has determined the necessity to find exact analytical solutions in the ambit of this more complex section of the theory of elasticity, (Lions, 1985), (Maugin, 1993).
In the next sections, it is presented a useful method enables one to find solutions for inhomogeneous, anisotropic elastostatic problems under particular conditions by means of the use of two theorems, *S.A.S. theorem* and *D.A.S. theorem* (Fraldi and Cowin, 2004).

1.1. Stress Associated Solutions (SAS) Theorem for inhomogeneous elasticity

The Stress Associated Solution Theorem lets to find solutions for inhomogeneous, anisotropic elastostatic problems if two conditions are satisfied:

(1) a knowledge of the solution for a homogeneous elastic *reference* problem (the *associated problem*) whose solution has a stress state with a zero eigenvalue everywhere in the domain of the problem, and (2) an inhomogeneous anisotropic elastic tensor related to the homogeneous anisotropic elastic tensor of (1) by

$$\mathbb{C}^I = \varphi(\boldsymbol{x})\mathbb{C}^H, \qquad \varphi(\boldsymbol{x}) \mid \forall \boldsymbol{x} \in B,\ \varphi(\boldsymbol{x}) > \alpha > 0,\ \alpha \in \mathbb{R}^+ \tag{2.1}$$

where $\mathbb{C}^H = \mathbb{C}^{H^T}$ is the elasticity tensor of a generic anisotropic homogeneous elastic material of the *reference problem*, $\mathbb{C}^I$ is the elasticity tensor of the corresponding anisotropic inhomogeneous elastic problem, B is the domain occupied by both the homogeneous object B^H and the inhomogeneous one B^I, $\alpha \in \mathbb{R}^+$ is an arbitrary positive real number, while $\varphi(\boldsymbol{x})$ is a $C^2(B)$ scalar function. The assumption (2.1) means that the inhomogeneous character of the material is due to the presence of a scalar parameter producing the inhomogeneity in the elastic coefficients.
This method makes it possible to find analytical solutions for an *inhomogeneous* anisotropic elastic problem if the elastic solution of the corresponding *homogeneous* anisotropic *reference* problem is known and characterized everywhere by a stress state with a zero eigenvalue. The solutions to the *inhomogeneous* anisotropic elastic problem are called the *associated solutions* of the *homogeneous problem.*

1.1.a. Zero-eigenvalue stress and zero-eigenvalue strain fields

A zero-eigenvalue stress state (zero-eigenvalue strain state) is characterized by the condition that the determinant of the stress (strain) is zero

$$\det \boldsymbol{T} = 0, \qquad (\det \boldsymbol{E} = 0)\,. \tag{2.2}$$

It is easy to show that a zero-eigenvalue stress (strain) state is a necessary condition for a plane stress (strain) state. The components of the stress tensor $\boldsymbol{T}$ (strain tensor $\boldsymbol{E}$) are denoted by σ_{ij} (ε_{ij}). The strain tensor $\boldsymbol{E}$ is related to the displacement field $\boldsymbol{u}$ by

$$\boldsymbol{E} = \frac{1}{2}[(\nabla \otimes \boldsymbol{u}) + (\nabla \otimes \boldsymbol{u})^T] = sym \nabla \otimes \boldsymbol{u} \qquad \forall \boldsymbol{x} \in B \tag{2.3}$$

in which $grad\, \boldsymbol{u} = (\nabla \otimes \boldsymbol{u})$ and the symbol $\otimes$ represents the *tensor product*. In components we have

$$\varepsilon_{ij} = \frac{1}{2}(u_{i,j} + u_{j,i}), \tag{2.4}$$

where the comma denotes differentiation and $\boldsymbol{u}$ is the displacement field.

1.1.b. Stress Associated Solutions (SAS) Theorem

Consider the following mixed boundary-value elastostatic homogeneous and anisotropic problem P^H in the absence of action-at-a-distance forces

$$\nabla \cdot \boldsymbol{T}(\boldsymbol{u}) = \boldsymbol{0} \quad \text{in } B^H,\ \boldsymbol{T}(\boldsymbol{u}) \cdot \boldsymbol{n} = \boldsymbol{t} \text{ on } \partial B_t^H,\ \boldsymbol{u} = \boldsymbol{u}_0 \text{ on } \partial B_u^H \tag{2.5}$$

where B^H is the domain occupied by the homogeneous elastic object, $\partial B^H = \{\partial B_t^H \cup \partial B_u^H\}$ is its boundary and $\boldsymbol{t}$ and $\boldsymbol{u}_0$ are the traction field and the displacements assigned on the corresponding partition of the boundary, respectively (Barber, 1992; Gurtin, 1972). The notation for the divergence of the stress tensor is $\nabla \cdot \boldsymbol{T}(\boldsymbol{u}) = div\,\boldsymbol{T}(\boldsymbol{u})$, where the *del operator* is a vectorial differential operator defined by $\nabla \equiv \partial_i \boldsymbol{e}_i$, $\partial_i \equiv \partial / \partial x_i = (*)_{,i}$ is the partial differential operator and $\boldsymbol{e}_i$ is the base unit vector of the *i*-axis.
The anisotropic Hooke's law is written

$$\boldsymbol{T}(\boldsymbol{u}) = \mathbb{C}^H : \boldsymbol{E}(\boldsymbol{u}) = \mathbb{C}^H : sym(\nabla \otimes \boldsymbol{u}) = \mathbb{C}^H : (\nabla \otimes \boldsymbol{u}) \tag{2.6}$$

or, in components

$$\sigma_{ij} = C_{ijhk}^H \varepsilon_{hk} = C_{ijhk}^H u_{h,k}. \tag{2.7}$$

Let $\mathfrak{S}^H = \{\boldsymbol{u}^H, \boldsymbol{E}^H, \boldsymbol{T}^H\}$ be the solution of the homogeneous problem (2.5).
Consider now an associated anisotropic elastic inhomogeneous problem P^I, described by modifying the system (2.5), with $\boldsymbol{t}^I = \boldsymbol{\varphi t}$ representing the traction field applied on ∂B_t^I and the inhomogeneous anisotropic elasticity tensor given by (2.1), thus

$$\nabla \cdot \boldsymbol{T}(\boldsymbol{u}) = \boldsymbol{0} \quad \text{in } B^I,\ \boldsymbol{T}(\boldsymbol{u}) \cdot \boldsymbol{n} = \boldsymbol{t}^I \text{ on } \partial B_t^I,\ \boldsymbol{u} = \boldsymbol{u}_0 \text{ on } \partial B_u^I \tag{2.8}$$

The solid domains B^H and B^I, as well as their corresponding boundary partitions made on ∂B^H and ∂B^I, are geometrically the same in the homogeneous and inhomogeneous problems. Then, if we expand the equation $(2.8)_1$ it is possible to write

$$\begin{aligned} \nabla \cdot \boldsymbol{T}(\boldsymbol{u}) &= \nabla \cdot \left[\varphi(\boldsymbol{x})\mathbb{C}^H : \boldsymbol{E}(\boldsymbol{u})\right] = \\ &= \varphi(\boldsymbol{x})\nabla \cdot \left[\mathbb{C}^H : \boldsymbol{E}(\boldsymbol{u})\right] + \left[\mathbb{C}^H : \boldsymbol{E}(\boldsymbol{u})\right] \cdot \nabla\varphi(\boldsymbol{x}) = \boldsymbol{0} \end{aligned} \tag{2.9}$$

where $\nabla(*) = grad(*)$ is the gradient operator applied on a generic scalar-valued function $(*)$. Consider now the situation in which the displacements are equal for the homogeneous and inhomogeneous problems. Then, by substituting the displacement solution $\boldsymbol{u}^H$ obtained for the homogeneous problem P^H in (2.9) in place of the displacement vector $\boldsymbol{u}$, we have that

$$\nabla \cdot \boldsymbol{T}(\boldsymbol{u}^H) = \varphi(\boldsymbol{x})\left[\nabla \cdot \boldsymbol{T}^H(\boldsymbol{u}^H)\right] + \left[\boldsymbol{T}^H(\boldsymbol{u}^H)\right] \cdot \nabla\varphi(\boldsymbol{x}) = \boldsymbol{0} \tag{2.10}$$

But, since $\nabla \cdot [\boldsymbol{T}^H(\boldsymbol{u}^H)] = \nabla \cdot [\mathbf{C}^H : \boldsymbol{E}(\boldsymbol{u}^H)] = \boldsymbol{0}$, it follows that

$$[\boldsymbol{T}^H(\boldsymbol{u}^H)] \cdot \nabla\varphi(\boldsymbol{x}) = \boldsymbol{0} \qquad \forall \boldsymbol{x} \in B^I \tag{2.11}$$

By excluding the trivial case in which $\varphi(\boldsymbol{x}) = \text{constant}$, it follows that

$$\det \boldsymbol{T}^H = 0, \qquad \forall \boldsymbol{x} \in B^H \tag{2.12}$$

This means that the stress state at $\boldsymbol{x}$ of the *reference* homogeneous problem is required to be a zero eigenvalue stress state everywhere in the domain. To investigate the geometrical meaning of the equation (2.11), since (2.11) must be true everywhere in B^I, we consider, without loss of generality, the *local principal stress reference system* $\{\xi_1, \xi_2, \xi_3\}$, in which the stress tensor $\boldsymbol{T}^H$ takes the component form

$$\mathrm{T}^{\mathrm{H}} = \begin{bmatrix} \sigma^{\mathrm{H}}_{\xi_1} & 0 & 0 \\ 0 & \sigma^{\mathrm{H}}_{\xi_2} & 0 \\ 0 & 0 & \sigma^{\mathrm{H}}_{\xi_3} \end{bmatrix}. \tag{2.13}$$

Representing the gradient of the scalar function φ as

$$\nabla\varphi(\boldsymbol{\xi})^{\mathrm{T}} = \left[\varphi_{,\xi_1} \quad \varphi_{,\xi_2} \quad \varphi_{,\xi_3}\right], \tag{2.14}$$

the three scalar equations implied by (2.11) are written as

$$\sigma^H_{\xi_1}\varphi_{,\xi_1} = 0, \quad \sigma^H_{\xi_2}\varphi_{,\xi_2} = 0, \quad \sigma^H_{\xi_3}\varphi_{,\xi_3} = 0. \tag{2.15}$$

The system (2.15) is satisfied if the stress tensor $\boldsymbol{T}^H$ for the reference homogeneous problem P^H is, at each internal point $\boldsymbol{x} \in B^H$, a locally variable *zero eigenvalue stress* state. If there is only one zero eigenvalue, say in the ξ_3-direction, the only non-zero component of the vector $\nabla\varphi$, is $\varphi_{,\xi_3}$ at the corresponding points $\boldsymbol{x} \in B^I$. If there are two zero eigenvalues there can be two non-zero components of $\nabla\varphi$. The case of three zero eigenvalues of the stress tensor $\boldsymbol{T}^H$ is trivial and will not be mentioned further. It follows that, at each internal point, the equipotential surfaces of φ admit as a tangent plane the plane whose normal is coaxial with the eigenvector associated with the zero stress eigenvalue (or a direction, in the case of two zero stress eigenvalues). This is illustrated in Figure 2.1. for the case of one zero eigenvalue of stress.

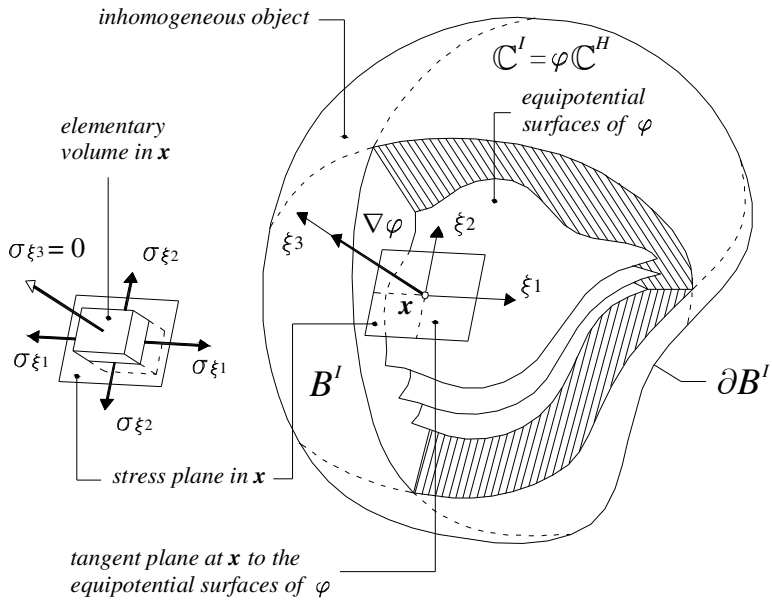

Fig. 2.1.
Geometrical interpretation of the relationship between the equipotential surfaces of φ and the distribution of the planes of stresses in the associated anisotropic problem

The geometrical relationship (2.11) between the stress tensor $\boldsymbol{T}^H$ and the vector $\nabla\varphi$ may be rewritten in the form

$$\{\boldsymbol{T}^H \cdot \nabla\varphi = \boldsymbol{0}\} \Leftrightarrow \{\forall \boldsymbol{v} \in V, \quad \boldsymbol{T}^H : (\nabla\varphi \otimes \boldsymbol{v}) = 0\} \tag{2.16}$$

where $\boldsymbol{v}$ is any unit vector defined in the three-dimensional Euclidean space $\mathbb{E}^3$ and V represents the corresponding vector space. It follows that the stress vector on the plane whose normal is $\boldsymbol{v}$ is always orthogonal to the vector $\nabla\varphi$.
Then, it is possible to establish the following theorem:

Stress Associated Solution (SAS) Theorem. *Consider two geometrically identical elastic objects* B^H *and* B^I, *one homogeneous and the other inhomogeneous, respectively*. Let $\mathbb{C}^H$ *and* $\mathbb{C}^I = \varphi(\boldsymbol{x})\mathbb{C}^H$ *be the corresponding elasticity tensors* (Figure 2.2.). *The two elastostatic problems associated with the two objects are*

$$P^H: \ \{\boldsymbol{\nabla}\cdot\boldsymbol{T}(\boldsymbol{u}) = \boldsymbol{0} \quad \text{in } B^H,\ \boldsymbol{T}(\boldsymbol{u})\cdot\boldsymbol{n} = \boldsymbol{t} \ \text{ on } \partial B_t^H,\ \boldsymbol{u} = \boldsymbol{u}^0 \ \text{ on } \partial B_u^H\},$$
$$P^I: \ \{\boldsymbol{\nabla}\cdot\boldsymbol{T}(\boldsymbol{u}) = \boldsymbol{0} \quad \text{in } B^I,\ \boldsymbol{T}(\boldsymbol{u})\cdot\boldsymbol{n} = \varphi\boldsymbol{t} \ \text{ on } \partial B_t^I,\ \boldsymbol{u} = \boldsymbol{u}^0 \ \text{ on } \partial B_u^I\},$$

where

$$\varphi(\boldsymbol{x}) \in C^2(B) \,\big|\ \forall \boldsymbol{x} \in B,\ \varphi(\boldsymbol{x}) > \alpha > 0, \quad \alpha \in \mathbb{R}^+.$$

If $\boldsymbol{u}^H$ *is the solution of the homogeneous problem* P^H, *then* $\boldsymbol{u}^I = \boldsymbol{u}^H$ *if and only if* $\{\boldsymbol{T}^H\!: \ (\boldsymbol{\nabla}\varphi \otimes \boldsymbol{v}) = 0, \quad \forall \boldsymbol{v} \in V\}$, *i.e.*

$$\{\forall \boldsymbol{x} \in B^I,\ \forall \boldsymbol{v} \in V,\ \boldsymbol{T}^H\!:(\boldsymbol{\nabla}\varphi \otimes \boldsymbol{v}) = 0\} \ \Leftrightarrow\ \boldsymbol{u}^I = \boldsymbol{u}^H.$$

<u>*Proof*</u>. The *necessary condition* has been established in the preamble. To prove the *sufficient condition*:

$$\{\forall \boldsymbol{v} \in V,\ \boldsymbol{T}^H\!:(\boldsymbol{\nabla}\varphi \otimes \boldsymbol{v}) = 0\} \ \Rightarrow\ \boldsymbol{u}^I = \boldsymbol{u}^H,$$

we first recall (2.16). Consequently, if $\boldsymbol{u}^H$ is the displacement solution of the homogeneous problem P^H, we can write

$$\begin{aligned}
&\{\boldsymbol{\nabla}\cdot[\boldsymbol{T}^H(\boldsymbol{u}^H)] = \boldsymbol{0},\ [\boldsymbol{T}^H(\boldsymbol{u}^H)]\cdot\boldsymbol{\nabla}\varphi = \boldsymbol{0}\} \Rightarrow \\
&\Rightarrow \{\boldsymbol{\nabla}\cdot[\mathbb{C}^H\!:(\boldsymbol{\nabla}\otimes\boldsymbol{u}^H)] = \boldsymbol{0},\ [\mathbb{C}^H:(\boldsymbol{\nabla}\otimes\boldsymbol{u}^H)]\cdot\boldsymbol{\nabla}\varphi = \boldsymbol{0}\} \Rightarrow \\
&\Rightarrow \varphi\boldsymbol{\nabla}\cdot[\mathbb{C}^H\!:(\boldsymbol{\nabla}\otimes\boldsymbol{u}^H)] + [\mathbb{C}^H:(\boldsymbol{\nabla}\otimes\boldsymbol{u}^H)]\cdot\boldsymbol{\nabla}\varphi = \boldsymbol{0},
\end{aligned}$$

from which it follows that

$$\boldsymbol{\nabla}\cdot[\mathbb{C}^I:(\boldsymbol{\nabla}\otimes\boldsymbol{u}^H)] = \boldsymbol{0},$$

when (2.1) is considered. Then, if we rewrite the inhomogeneous elastostatic problem P^I in terms of displacements, that is

$$P^I : \{\nabla \cdot [\mathbb{C}^I : (\nabla \otimes \boldsymbol{u}^I)] = \mathbf{0} \quad \text{in } B^I,\ [\mathbb{C}^I : (\nabla \otimes \boldsymbol{u}^I)] \cdot \boldsymbol{n} = \varphi \boldsymbol{t} \ \text{ on } \partial B_t^I,\ \boldsymbol{u}^I = \boldsymbol{u}^0 \ \text{ on } \partial B_u^I\}$$

we can observe that $\boldsymbol{u}^H$ satisfies all these field and boundary equations. Therefore, from the uniqueness theorem, it follows that $\boldsymbol{u}^I = \boldsymbol{u}^H$ and, consequently, $\boldsymbol{T}^I = \varphi\, \mathbb{C}^H : (\nabla \otimes \boldsymbol{u}^H) = \varphi \boldsymbol{T}^H$. This proves the sufficiency condition.

It is convenient to increase the similarity between the elastic problems for the homogeneous and the inhomogeneous materials by writing the boundary conditions in the same way. Thus we substitute for the prescribed boundary tractions a corresponding prescribed displacement field; this converts the portion of the boundary upon which the surface tractions are prescribed to a portion of the boundary upon which the displacements are prescribed. Due to uniqueness of solution, this is always possible in a linear elastic problem. Then, the two problems may be written in the equivalent forms as

$$P^H : \ \{\nabla \cdot \boldsymbol{T}(\boldsymbol{u}) = \mathbf{0} \quad \text{in } B^H,\ \boldsymbol{u} = \boldsymbol{u}^t \ \text{ on } \partial B_t^H,\ \boldsymbol{u} = \boldsymbol{u}^0 \ \text{ on } \partial B_u^H\},$$
$$P^I : \ \{\nabla \cdot \boldsymbol{T}(\boldsymbol{u}) = \mathbf{0} \quad \text{in } B^I,\ \boldsymbol{u} = \boldsymbol{u}^t \ \text{ on } \partial B_t^I,\ \boldsymbol{u} = \boldsymbol{u}^0 \ \text{ on } \partial B_u^I\},$$

where $\boldsymbol{u}^t$ represents the prescribed displacement on ∂B_t and where, now, the tractions $\boldsymbol{t}$ and $\varphi \boldsymbol{t}$ represent the reactions of the constraints on ∂B_t specified by $\boldsymbol{u}^t$. It follows that, when a solution $\mathfrak{S}^H = \{\boldsymbol{u}^H, \boldsymbol{E}^H, \boldsymbol{T}^H\}$ for an anisotropic homogeneous elastic problem P^H is known, the *Stress Associated Solution Theorem* yields the corresponding solution for an inhomogeneous problem P^I as $\mathfrak{S}^I = \{\boldsymbol{u}^H, \boldsymbol{E}^H, \varphi \boldsymbol{T}^H\}$, if and only if $\boldsymbol{T}^H \cdot \nabla \varphi = \mathbf{0}$ everywhere in the object and the displacement boundary conditions are the same for both the homogeneous and the inhomogeneous objects. Thus the solution $\mathfrak{S}^H = \{\boldsymbol{u}^H, \boldsymbol{E}^H, \boldsymbol{T}^H\}$ is used to construct a solution of the associated inhomogeneous problem.

Finally we note that the restriction (2.1) may be relaxed in many different ways. For example the *Associated Solutions* could involve only some selected elastic moduli of the homogeneous elasticity tensor, so that the solutions do not depend on all stiffness coefficients. This means that it is possible to extend the validity of the proposed theorem by rewriting the assumption (2.1) in the weaker form

$$\hat{C}_{ijhk}^I = \varphi \hat{C}_{ijhk}^H,$$

where $\hat{C}^H_{ijhk}$ represents only those elastic coefficients explicitly involved in the specific anisotropic homogeneous problem used to construct the associated solution. In the next section it is shown that components of the elasticity tensor not involved in the solution of the homogeneous problem will not be involved in the solution of the associated inhomogeneous problem.

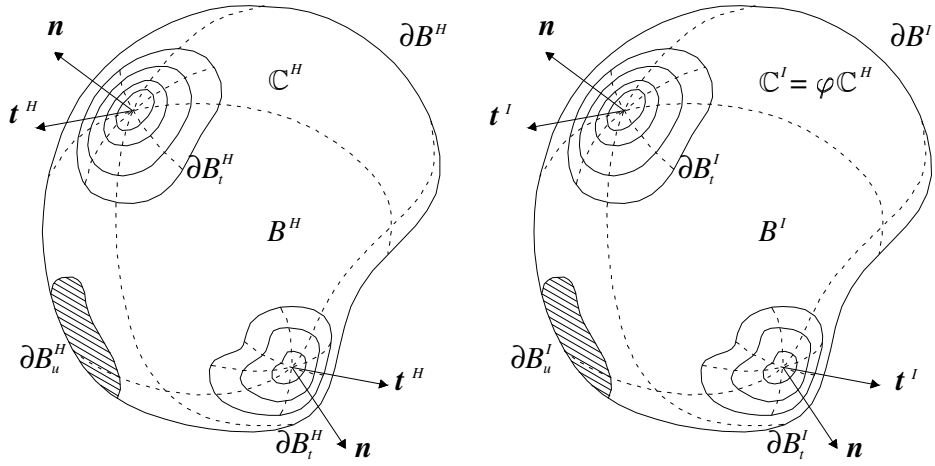

Homogeneous object Inhomogeneous object

Fig. 2.2.
The homogeneous and inhomogeneous bodies with their boundary conditions

1.2. Generalization of the SAS theorem to piecewise defined inhomogeneities

Two types of composite materials are considered in this section, one in which φ is *constant*, but piecewise *discontinuous* and another in which φ is a *piecewise continuous function*. These two cases extend the domain of applicability of the condition (2.1), and therefore the domain of applicability of the SAS theorem. In the first case the extension is to composite materials for which each phase is characterized by elastic moduli that are constant within their own phase, but are different from the constant elastic moduli of the other phases. In the second case

the extension is to composite materials for which each phase is characterized by the possibility of each phase having variable elastic coefficients inside the phase domain and discontinuous elastic coefficients across phase boundaries.

1.2.a. Composite materials where φ is constant, but piecewise discontinuous

In the following two sections we extend the SAS theorem to heterogeneous materials where there is not a smooth variation of the elastic moduli. To achieve this, we will make reference to some results obtained previously and formulate new hypotheses about the features of composite inhomogeneous bodies considered. In particular, for each phase p present of a composite material, we will assume here that the elasticity tensor can be written as

$$\mathbb{C}_p^H = \varphi_p \mathbb{C}^H, \qquad p = \{1, 2, ..., n\} \subset \mathbb{N} \tag{2.17}$$

where $\mathbb{C}^H$ is the elasticity tensor of a reference isotropic or anisotropic homogeneous material and φ_p is a positive scalar parameter. This hypothesis does not constitute the most general case for describing the relation between the elastic tensors of the different phases for a composite material, but it is widely utilized in literature because many artificial and natural composites exhibit mechanical properties that are well represented by the proposed assumption (Lekhnitskii, 1963; Ting, 1996; Fraldi and Guarracino, 2001; Nemat-Nasser and Hori, 1993).

Let us consider a partition of the inhomogeneous body $\{\Omega_p(B) \,\big|\, B \equiv \bigcup_{p=1}^{n} \Omega_p(B)\}$, where $\partial\Omega_{(p,q)}$ represents the interface boundary between two generic sub-domains Ω_p and Ω_q of the partition, with elasticity tensors $\mathbb{C}_p^H$ and $\mathbb{C}_q^H$, respectively.

If we assume that the solution for the anisotropic homogeneous reference problem is known, and the geometries of the homogeneous and composite material objects are the same, we can study the conditions under which the stress tensor for the inhomogeneous material (multi-phase material) assumes the form

$$\boldsymbol{T}_p^H = \varphi_p \boldsymbol{T}^H, \qquad \forall \boldsymbol{x} \in \Omega_p(B) \tag{2.18}$$

required by the SAS theorem. Note that the stress (2.18) satisfies the equilibrium equations in each sub-domain of the partition,

$$\boldsymbol{\nabla} \cdot \boldsymbol{T}_p^H = \varphi_p \boldsymbol{\nabla} \cdot \boldsymbol{T}^H = \boldsymbol{0}, \quad \forall \boldsymbol{x} \in \Omega_p(B). \tag{2.19}$$

Moreover, by virtue of the assumed constitutive relationships,

$$\boldsymbol{E}_p^H = \mathbb{C}_p^{H-1}\boldsymbol{T}_p^H = \mathbb{C}^{H-1}\boldsymbol{T}^H = \boldsymbol{E}^H, \quad \{\forall p \in \mathbf{N}, \forall \boldsymbol{x} \in \Omega_p\} \tag{2.20}$$

the satisfaction of the compatibility condition on the surfaces of discontinuity between the different materials of the composite object is automatic. From the force equilibrium on the interfaces between two adjacent phases, it follows that

$$\boldsymbol{T}_p^H \cdot \boldsymbol{n}_{(p,q)} = \boldsymbol{T}_q^H \cdot \boldsymbol{n}_{(p,q)}, \quad \{\forall \{p,q\} \in \mathbf{N}, \forall \boldsymbol{x} \in \partial\Omega_{(p,q)}\} \tag{2.21}$$

where $\boldsymbol{n}_{(p,q)}$ is the unit normal vector to the interface between the phases p and q. By virtue of (2.18), the equation (2.21) is satisfied if

$$\boldsymbol{T}^H \cdot \boldsymbol{n}_{(p,q)} = \boldsymbol{0}, \quad \forall \boldsymbol{x} \in \partial\Omega_{(p,q)}. \tag{2.22}$$

Equation (2.22) requires that for each point belonging to the interface surfaces between two phases, the stress tensor $\boldsymbol{T}^H$ must possess at least one zero-eigenvalue, that is $\{\det \boldsymbol{T}^H = 0, \quad \forall \boldsymbol{x} \in \partial\Omega_{(p,q)}\}$. This hypothesis is necessary in order to orient the plane of the stress on the interface surfaces such that the eigenvector associated with a zero eigenvalue of the stress tensor is coaxial with the unit normal vector to the tangent plane to the interface. For structures sometimes consistent with this hypothesis one can consider the interfaces between layers of certain plant structures, for example, onions and leeks. In the literature of this subject examples that conform to this hypothesis include the piece-wise angularly inhomogeneous elastic wedges considered by Ting (Ting, 1996a), the intrinsically orthotropic layered cylinders under torsion, described by Cowin (Cowin, 1987), as well as in other examples analyzed by Lekhnitskii (Lekhnitskii, 1963).

To complete the elastic solution for the composite material (2.17) using the known solution of a homogeneous reference problem, we note the satisfaction of the compatibility and equilibrium conditions on the external boundary. The satisfaction of the compatibility conditions is easily verified by virtue of (2.20). The equilibrium equation on the part of the external boundary where the tractions are prescribed is given by

$$\boldsymbol{T}_e^H \cdot \boldsymbol{n} = \boldsymbol{t}_e^H = \varphi_e \boldsymbol{t}^H, \quad \forall \boldsymbol{x} \in \partial B_{t(e)} \tag{2.23}$$

where $\partial B_{t(e)}$ represents a typical element of the partition of the external boundary on which the tractions $\boldsymbol{t}^H$ are prescribed in the homogeneous reference problem. The total stress boundary is the sum over all the typical

distinct boundaries, $\partial B_t = \bigcup_{e=1}^{k} \partial B_{t(e)}$, where k represents the total number of phases that have a projection of their boundary on the external boundary on which the tractions are assigned. Then, if the conditions (2.22) and (2.23) are satisfied, we can build the elastic solution of composite multi-phase materials from a knowledge of the displacements and the stresses for a homogeneous object with analogous geometry using the extension of the SAS theorem.
Note that, in order to utilize the results of the proposed theorem for inhomogeneous materials in which φ was assumed to be a continuous scalar function, the stress tensor $\boldsymbol{T}^H$ had to exhibit a zero-eigenvalue at each point of the body. However, in order to generalize the SAS theorem to composite materials where φ is constant, but piecewise discontinuous, it is sufficient that the stress tensor $\boldsymbol{T}^H$ related to the associated homogeneous problem possesses a zero-eigenvalue $\left(\det \boldsymbol{T}^H = 0\right)$ only in the points belonging to the internal interfaces between the different phases. This means that, in the case of materials where φ is a constant, but piecewise discontinuous, $\boldsymbol{T}^H$ can be a three-dimensional stress field in any other point of the solid domain.

1.2.b. Composite materials where φ is piecewise continuous

In this subsection we consider the new and more general situation in which each phase p of the heterogeneous solid (composite material) can be represented by the following elasticity tensor

$$\mathbb{C}_p^H = \varphi_p(\boldsymbol{x}_p)\mathbb{C}^H, \quad \forall \boldsymbol{x}_p \in \Omega_p \subset B \tag{2.24}$$

where $\mathbb{C}^H$ is the elasticity tensor of a homogeneous reference material, while φ_p is now a positive scalar function, not necessarily constant, but continuous inside each phase (or sub-domain defined by the partition described above). We relax some of the hypotheses for the situation when φ is constant, but retain the previous notation; $\{\Omega_p(B) \,\big|\, B \equiv \bigcup_{p=1}^{n} \Omega_p(B)\}$ is again the partition of the inhomogeneous object, with $\partial\Omega_{(p,q)}$ representing the interface boundary between two generic adjacent sub-domains Ω_p and Ω_q of the partition whose elasticity tensors are $\mathbb{C}_p^H$ and $\mathbb{C}_q^H$, respectively, see Figure 2.3.. The representation of the stress tensor of the phase p required by the SAS theorem is

$$\boldsymbol{T}_p^H = \varphi_p(\boldsymbol{x}_p)\boldsymbol{T}^H, \qquad \forall \boldsymbol{x}_p \in \Omega_p(B). \tag{2.25}$$

Equilibrium is satisfied if the divergence of the stress for each phase is zero;

$$\nabla \cdot \boldsymbol{T}_p^H = \varphi_p \nabla \cdot \boldsymbol{T}^H + \boldsymbol{T}^H \cdot \nabla \varphi_p = \boldsymbol{0} \Rightarrow \boldsymbol{T}^H \cdot \nabla \varphi_p = \boldsymbol{0}, \quad \forall \boldsymbol{x}_p \in \Omega_p(B) \tag{2.26}$$

From this result it follows, using (2.17) and (2.20), that $\boldsymbol{E}_p^H = \boldsymbol{E}^H$, $\{\forall p \in \mathbf{N}, \forall \boldsymbol{x}_p \in \Omega_p\}$. The equilibrium conditions (2.21)-(2.22) across the interface between two phases are then satisfied as well the external boundary conditions (2.23) considered previously. This means that, in order to extend the SAS theorem to piecewise continuous composite materials, one has to first establish two facts about the stress tensor $\boldsymbol{T}^H$, namely: 1) at each internal point of each phase *p*, the stress tensor $\boldsymbol{T}^H$ possesses at least one zero-eigenvalue and 2) at every point in the interface between two adjacent phases the normal to the tangent plane has to be coincident with the direction of the eigenvector associated with the zero eigenvalue.

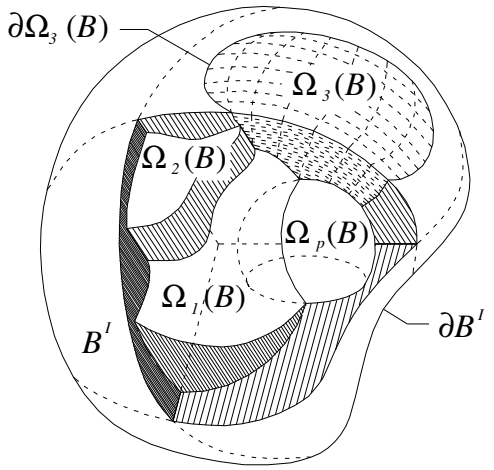

Fig. 2.3.
A representation of a possible spatial distribution of the phases inside a piecewise inhomogeneous material.

1.3. Displacement Associated Solutions (DAS) Theorem for inhomogeneous elasticity

Analogously to the SAS theorem, the *Displacement Associated Solution* (D.A.S.) theorem lets to find solutions for inhomogeneous anisotropic elastostatic problems, if two conditions are satisfied, (Fraldi, Cowin, 2004): (3) the solution of the homogeneous elastic *reference* problem *(the associated* one) is known and it has a local plane strain state, with a zero eigenvalue everywhere in the domain of the problem and (4) the inhomogeneous anisotropic compliance tensor is in relation with the homogeneous associated one according to the following equation:

$$\mathbb{S}^I = \frac{1}{\varphi(\boldsymbol{x})}\mathbb{C}^{H^{-1}} = \lambda(\boldsymbol{x})\mathbb{S}^H, \qquad \lambda(\boldsymbol{x})\big|\ \forall \boldsymbol{x} \in B,\ \lambda(\boldsymbol{x}) > \beta > 0,\ \beta \in \mathbb{R}^+ \quad (2.27)$$

where $\mathbb{S}^H = \mathbb{S}^{H^T}$ is the compliance tensor of the anisotropic homogeneous elastic *reference problem*, $\mathbb{S}^I$ is the compliance tensor of the corresponding anisotropic inhomogeneous elastic problem, B is the domain occupied by both the homogeneous object B^H and the inhomogeneous one B^I, $\beta \in \mathbb{R}^+$ is an arbitrary positive real number, while $\lambda(\boldsymbol{x})$ is a $C^2(B)$ scalar function.
The second condition implies that the inhomogeneous character of the material is due to the presence of a scalar parameter, $\lambda(\boldsymbol{x})$, producing the inhomogeneity in the compliance coefficients. It can be also relaxed and, so, written in a weaker form:

$$\hat{S}^I_{ijhk} = \lambda \hat{S}^H_{ijhk} \quad (2.28)$$

where $\hat{S}^H_{ijhk}$ represents only those compliance coefficients explicitly involved in the specific anisotropic homogeneous problem used to construct the associated solution.
This means that components of the compliance tensor not involved in the solution of the homogeneous problem will not be involved in that one of the associated inhomogeneous problem.
If the conditions (3) and (4) are satisfied, starting from the known solution of the homogeneous problem, the *associated solution,* that is the solution to the inhomogeneous problem, is derived.
In particular, the stress field solution is identical with the stress field of the homogeneous reference solution, while the strain field of the inhomogeneous problem is equal to $\lambda(\boldsymbol{x})$ times the strain field of the homogeneous problem.
The advantage of this method is in the fact that its use yields exact solutions for several new interesting inhomogeneous and anisotropic problems.

More in detail, let us to consider an anisotropic homogeneous elastic object, that occupies a volume B^H, with mixed boundary-value (see Figure 2.2.a).
In presence of action-at-a-distance forces and taking into account the compatibility of the solution by writing the equilibrium equations in terms of displacements, the following equilibrium equations can be written

$$\begin{aligned} &\nabla \cdot \boldsymbol{T}(\boldsymbol{u}) = \boldsymbol{0} \quad \text{in } B^H \\ &\boldsymbol{T}(\boldsymbol{u}) \cdot \boldsymbol{n} = \boldsymbol{t} \quad \text{on } \partial B_t^H \\ &\boldsymbol{T}(\boldsymbol{u}) \cdot \boldsymbol{n} = \boldsymbol{0} \quad \text{on } \partial B_0^H \end{aligned} \tag{2.29}$$

where $\nabla = \partial_i \boldsymbol{e}_i$ is a vectorial differential operator, ∂B_t^H is the boundary partition of the homogeneous continuum on which the traction field is assigned, ∂B_0^H is the boundary partition of the homogeneous continuum in absence of both traction and displacements fields.
On the boundary partition on which the displacements field is assigned, the following relation has to be satisfied

$$\boldsymbol{u} = \boldsymbol{0} \quad \text{on } \partial B_u^H \tag{2.30}$$

where ∂B_u^H is the boundary partition of the homogeneous continuum on which the displacements field is assigned.
The anisotropic Hooke's law, in a linear elastic stress-strain relation, is written in the form

$$\boldsymbol{T}(\boldsymbol{u}) = \mathbb{C}^H : \boldsymbol{E}(\boldsymbol{u}) = \mathbb{C}^H : sym(\nabla \otimes \boldsymbol{u}) = \mathbb{C}^H : (\nabla \otimes \boldsymbol{u}) \tag{2.31}$$

or

$$sym(\nabla \otimes \boldsymbol{u}) = \boldsymbol{E}(\boldsymbol{u}) = \mathbb{S}^H : \boldsymbol{T}(\boldsymbol{u}) \tag{2.32}$$

in components

$$\sigma_{ij} = C_{ijhk}^H \varepsilon_{hk} = C_{ijhk}^H u_{h,k} \tag{2.33}$$

or

$$\varepsilon_{ij} = S_{ijhk}^H \sigma_{hk} \,. \tag{2.34}$$

Let us to consider, now, an anisotropic inhomogeneous elastic object, that occupies a volume B^I, geometrically the same of B^H, with mixed boundary-value (see Figure 2.2.b).
In presence of action-at-a-distance forces and taking into account the compatibility of the solution by writing the equilibrium equations in terms of displacements, in an analogous manner to what has been done before, the following equilibrium equations can be written

$$\begin{aligned} &\nabla \cdot \boldsymbol{T}(\boldsymbol{u}) = -\mathbf{b} \quad \text{in } B^I \\ &\boldsymbol{T}(\boldsymbol{u}) \cdot \boldsymbol{n} = \boldsymbol{t} \quad \text{on } \partial B_t^I \\ &\boldsymbol{T}(\boldsymbol{u}) \cdot \boldsymbol{n} = \boldsymbol{0} \quad \text{on } \partial B_0^I \end{aligned} \tag{2.35}$$

where ∂B_t^I is the boundary partition of the inhomogeneous continuum on which the traction field is assigned. It is geometrically the same of that one in the homogeneous problem and ∂B_0^I is the boundary partition of the inhomogeneous continuum in absence of both traction and displacements fields. It is geometrically the same of that one in the homogeneous problem.
On the boundary partition on which the displacements field is assigned, the following relation has to be satisfied

$$\boldsymbol{u} = \boldsymbol{0} \quad \text{on } \partial B_u^I \tag{2.36}$$

where ∂B_u^I is the boundary partition of the inhomogeneous continuum on which the displacements field is assigned. It is geometrically the same of that one in the homogeneous problem.
Let us to assume the stress tensor $\boldsymbol{T}^H$ as the solution for the homogeneous problem, and let us to assume, also, the hypothesis that

$$\boldsymbol{T}^I = \boldsymbol{T}^H . \tag{2.37}$$

In this way, the equations in the differential system (2.29) are automatically satisfied. Moreover, if $\boldsymbol{T}^H$ is the solution of the first anisotropic and homogeneous problem, we have that the compatibility condition

$$\nabla \times \left[\nabla \times \left(\mathbb{S}^H : \boldsymbol{T}^H \right) \right] = \mathbf{0} \tag{2.38}$$

have to be also satisfied. As well-known, this ensures that a displacement field $\boldsymbol{u}^H$ exists. So, it is possible to write the strain-displacement relationship

$$\boldsymbol{E}^H = \mathbb{S}^H : \boldsymbol{T}^H = sym\left(\nabla \otimes \boldsymbol{u}^H\right) \tag{2.39}$$

where $\boldsymbol{u}^H$ is displacements field, solution of the homogeneous problem. Then, in order to accept the hypothesis (2.37), the following equation

$$\nabla \times \left[\nabla \times \left(\mathbb{S}^I : \boldsymbol{T}^I\right)\right] = \nabla \times \left[\nabla \times \left(\lambda \mathbb{S}^H : \boldsymbol{T}^H\right)\right] = \boldsymbol{0} \tag{2.40}$$

becomes necessary and sufficient condition for the existence of a displacement field $\boldsymbol{u}^I$, where $\boldsymbol{u}^I$ is the displacements field, solution of the inhomogeneous problem, and it is given by

$$sym\left(\nabla \otimes \boldsymbol{u}^I\right) = \boldsymbol{E}^I = \mathbb{S}^I : \boldsymbol{T}^I = \lambda \mathbb{S}^H : \boldsymbol{T}^H . \tag{2.41}$$

The compatibility condition (2.40), in general, is not satisfied. Therefore, it is necessary to find the conditions under whose it becomes true, (Fraldi, Cowin, 2004). Without loss of generality, let us consider

$$\lambda = \lambda(\boldsymbol{x}_3) \tag{2.42}$$

that means that the $\boldsymbol{x}_3$ is the direction locally coaxial with the gradient of λ, i.e.,

$$\nabla \lambda^T = \left[0, 0, \partial\lambda / \partial x_3\right]. \tag{2.43}$$

So, by recalling that $\boldsymbol{u}^H$ is the solution of the homogeneous problem, and by operating some algebraic manipulations, the set of compatibility equations (2.40) can be reduced to five differential equations as it is shown

$$\begin{cases} \lambda_{,33} u^H_{1,1} + \lambda_{,3}\left(u^H_{1,3} - u^H_{3,1}\right)_{,1} = 0 \\ \lambda_{,33} u^H_{2,2} + \lambda_{,3}\left(u^H_{2,3} - u^H_{3,2}\right)_{,2} = 0 \\ \lambda_{,3}\left(u^H_{1,2} - u^H_{2,1}\right)_{,1} = 0 \\ \lambda_{,3}\left(u^H_{1,2} - u^H_{2,1}\right)_{,2} = 0 \\ \lambda_{,33}\left(u^H_{1,2} + u^H_{2,1}\right) + \lambda_{,3}\left[\left(u^H_{1,3} - u^H_{3,1}\right)_{,2} + \left(u^H_{2,3} - u^H_{3,2}\right)_{,1}\right] = 0 \end{cases} \tag{2.44}$$

where, obviously, is absent any prescribed constrain about the relation between the first and the second derivatives of the parameter λ.
It can be noted that the terms in the parentheses represent the skew components of the $\nabla \otimes \boldsymbol{u}^H$, that are local rotations, while the only present strain components are $(1-\delta_{i3})(1-\delta_{j3})u^H_{i,j}$, having indicated with δ_{hk} the standard Kronecker operator.
It has to be noted that:

1. the displacement field for the reference homogeneous problem has to be related, at each internal point $\boldsymbol{x} \in B^H$, with a local plane strain field, where any plane with support the axis $\boldsymbol{x}_3$ can be the plane of the strains
2. $$\det \boldsymbol{E}^H = 0\,; \tag{2.45}$$
3. the vector $\nabla\lambda$, the corresponding points $\boldsymbol{x} \in B^I$, has to be coaxial with the support axis $\boldsymbol{x}_3$ of plane of the strains in the homogeneous problem;
4. $curl\left(\boldsymbol{u}^H\right)$ must be independent from $\boldsymbol{x}_3$-direction, i.e. the $\nabla\lambda$-direction.

In the previous statements, analogously to what has been done with the stress state, it has been implicitly considered the definition about the *"plane strain":* a strain state will be *said plane* if, in a fixed point $\boldsymbol{x}$ of the solid, there is *a plane of the strains* to which all the strain components ε_{ij} belong. It is easy to demonstrate that this plane exists if the strain tensor $\boldsymbol{E}$ has a zero eigenvalue. So, if $\{\xi_1, \xi_2, \xi_3\}$ is the orthogonal *principal* reference frame of the strain tensor $\boldsymbol{E}$ and if ξ_3 is assumed, for example, as the eigenvector associated to the zero eigenvalue of $\boldsymbol{E}$, *the plane of the strains* must coincide with $\xi_1 - \xi_3$ plane.
It follows that a necessary and sufficient condition for the existence of a *plane strain* is given by

$$\det \boldsymbol{E} = 0\,. \tag{2.46}$$

It has to be noted that the satisfaction of the compatibility condition (2.40) yields that the displacements field of the homogeneous problem has to satisfy the equations (2.44).
This compatibility condition (2.40), therefore, may be rewritten in the form

$$\begin{aligned} &\left\{curl\left[curl\left(\lambda\,\mathbb{S}^H : \boldsymbol{T}^H\right)\right] = \boldsymbol{0}\right\} \Leftrightarrow \\ &\left\{\forall \boldsymbol{h} \in V : \nabla\lambda \cdot \boldsymbol{h} = 0,\, \left(\nabla \otimes curl\,\boldsymbol{u}^H\right)\boldsymbol{h} = \boldsymbol{0},\, sym\left(\nabla \otimes \boldsymbol{u}^H\right)\boldsymbol{h} \cdot \boldsymbol{h} = 0\right\} \end{aligned} \tag{2.47}$$

where $\lambda(\boldsymbol{x}) \in C^2(B) \,|\, \forall \boldsymbol{x} \in B,\ \lambda(\boldsymbol{x}) > \alpha > 0,\ \alpha \in \mathbb{R}^+$, $\boldsymbol{h}$ is any unit vector defined in the three-dimensional Euclidean space $\mathbb{E}^3$ and V is the corresponding vector space.
Moreover, it is worth to note that the assumed position (2.27) and the hypothesis (2.37), that is true if the equation (2.40) is satisfied, imply

$$\boldsymbol{E}^I = \lambda \boldsymbol{E}^H . \tag{2.48}$$

So, at this point, it can be stated that any anisotropic and homogeneous elastic problem that possesses a solution represented by the displacement equations can be considered a *Displacement Auxiliary Solution* for the corresponding dual inhomogeneous elastic problem.
In other words, it can be possible to demonstrate the following theorem:
Displacement Associated Solution (DAS) Theorem
Consider two geometrically identical anisotropic elastic objects, one homogeneous, B^H, and the other inhomogeneous, B^I, respectively. Let be $\mathbb{S}^H$ and $\mathbb{S}^I = \lambda(\boldsymbol{x})\mathbb{S}^H$ the corresponding compliance tensors. The two elastostatic Cauchy problems associated with the two objects, in presence of the body forces and of mixed boundary-value, are

$$\begin{aligned} P^H :\{&\boldsymbol{\nabla}\cdot\boldsymbol{T}(\boldsymbol{u}) = -\mathbf{b} \text{ in } B^H,\ \boldsymbol{T}(\boldsymbol{u})\cdot\boldsymbol{n} = \boldsymbol{t} \text{ on } \partial B_t^H,\ \boldsymbol{T}(\boldsymbol{u})\cdot\boldsymbol{n} = \mathbf{0} \text{ on } \partial B_0^H,\ \boldsymbol{u} = \mathbf{0} \text{ on } \partial B_u^H\},\\ P^I :\{&\boldsymbol{\nabla}\cdot\boldsymbol{T}(\boldsymbol{u}) = -\mathbf{b} \text{ in } B^I,\ \boldsymbol{T}(\boldsymbol{u})\cdot\boldsymbol{n} = \boldsymbol{t} \text{ on } \partial B_t^I,\ \boldsymbol{T}(\boldsymbol{u})\cdot\boldsymbol{n} = \mathbf{0} \text{ on } \partial B_0^H,\ \boldsymbol{u} = \mathbf{0} \text{ on } \partial B_u^H\}. \end{aligned} \tag{2.49}$$

If $\boldsymbol{T}^H$ is the solution of the homogeneous problem p^H, then $\boldsymbol{T}^I = \boldsymbol{T}^H$ if and only if the second part of the equation (2.47) is verified, i.e. if

$$\boldsymbol{w}^H = curl\,\boldsymbol{u}^H \,|\, \forall \boldsymbol{v},\ skew\left(\nabla \otimes \boldsymbol{u}^H\right)\boldsymbol{v} = \boldsymbol{w}^H \wedge \boldsymbol{v}$$

we have that

$$\forall \boldsymbol{h} \in V \,|\, \nabla\lambda\cdot\boldsymbol{h} = 0, \left\{\left(\nabla \otimes curl\,\boldsymbol{u}^H\right)\boldsymbol{h} = \mathbf{0},\ sym\left(\nabla \otimes \boldsymbol{u}^H\right)\boldsymbol{h}\cdot\boldsymbol{h} = 0\right\} \Leftrightarrow \left\{\boldsymbol{T}^I = \boldsymbol{T}^H\right\}. \tag{2.50}$$

In other words, when a solution $\mathscr{R}_\varepsilon^H = \left\{\boldsymbol{u}^H, \boldsymbol{E}^H, \boldsymbol{T}^H\right\}$ for an anisotropic homogeneous elastic problem p^H is known, the DAS theorem yields the

corresponding solution for an inhomogeneous elastic problem p^I as $\mathscr{R}_\varepsilon^I = \{\lambda \boldsymbol{E}^H, \boldsymbol{T}^H\}$, if and only if the anisotropic and homogeneous elastic problem possesses, everywhere in the object, a displacement solution satisfying the equations (2.44) and if the displacements boundary conditions are the same for both the homogeneous and inhomogeneous objects.

The solution $\boldsymbol{u}^I$, for the inhomogeneous problem, in general, have to be integrated with reference to the specific case.

It is worth to underline that in the case where displacement boundary-value $\boldsymbol{u}$ is not equal to zero, the elastic mixed problem can be rewritten as the corresponding first type one, in which only the traction and reaction fields are considered.

For more details on D.A.S. demonstration, see (Fraldi, Cowin, 2004).

It is useful to underline, now and again, the geometrical interpretation of the result of the theorem, constituted by the observation that, in order to find an analytical solution for a given elastic inhomogeneous and anisotropic body in the form $\mathscr{R}_\varepsilon^I = \{\lambda \boldsymbol{E}^H, \boldsymbol{T}^H\}$, a necessary and sufficient condition is that the displacement solution for the corresponding anisotropic and homogeneous problem is related with a local plane strain field that has as plane of the strains any plane with support an axis coaxial with the gradient of λ, with rotational part depending on this gradient direction, only.

The D.A.S. theorem can be generalized to comprise different types of composite materials. For example, it is possible to consider the case of a multi-linear law for λ, i.e.:

$$\lambda = \lambda_0 + \lambda_1 \boldsymbol{x}_1 + \lambda_2 \boldsymbol{x}_2 + \lambda_3 \boldsymbol{x}_3 \tag{2.51}$$

with λ_i, $i = \{0,...,3\}$ arbitrary constants.

In this case, it is obtained that the second derivatives of the differential system (2.44) go to zero, therefore, the compatibility equation system becomes as it follows

$$\begin{cases} \lambda_1\left(u^*_{1,2}-u^*_{2,1}\right)_{,2}=\lambda_2\left(u^*_{1,2}-u^*_{2,1}\right)_{,1} \\ \lambda_2\left(u^*_{2,3}-u^*_{3,2}\right)_{,3}=\lambda_3\left(u^*_{2,3}-u^*_{3,2}\right)_{,2} \\ \lambda_3\left(u^*_{1,3}-u^*_{3,1}\right)_{,1}=\lambda_1\left(u^*_{1,3}-u^*_{3,1}\right)_{,3} \\ \lambda_1\left[\left(u^*_{1,2}-u^*_{2,1}\right)_{,3}+\left(u^*_{1,3}-u^*_{3,1}\right)_{,2}\right]=\lambda_2\left(u^*_{1,3}-u^*_{3,1}\right)_{,1}+\lambda_3\left(u^*_{1,2}-u^*_{2,1}\right)_{,1} \\ \lambda_2\left[\left(u^*_{2,1}-u^*_{1,2}\right)_{,3}+\left(u^*_{1,3}-u^*_{3,1}\right)_{,1}\right]=\lambda_1\left(u^*_{2,3}-u^*_{3,2}\right)_{,2}+\lambda_3\left(u^*_{2,1}-u^*_{1,2}\right)_{,2} \\ \lambda_3\left[\left(u^*_{3,1}-u^*_{1,3}\right)_{,2}+\left(u^*_{3,2}-u^*_{2,3}\right)_{,1}\right]=\lambda_1\left(u^*_{3,2}-u^*_{2,3}\right)_{,3}+\lambda_2\left(u^*_{3,1}-u^*_{1,3}\right)_{,3} \end{cases} \tag{2.52}$$

Because of the arbitrary of the assumption about the constants in the λ law, by setting to zero all skew components of $\nabla\otimes\boldsymbol{u}^H$, a very closed solution of the system can be found in the classical *strain potential* form, (Barber, 1992), that is

$$\boldsymbol{u}^H=\nabla\phi \tag{2.53}$$

where $\phi=\phi(\boldsymbol{x})$ is a scalar function. The displacement in the form of the equation (2.52) produces, as well-known, an irrotational deformation field and constitutes the irrotational part of the Papkovich-neuber representation in the isotropic elasticity, (Barber, 1992). The reason for which this particular case could result very useful is related to the fact that many fundamental solutions in isotropic and anisotropic elasticity have a representation as described in (2.52), as the axisymmetric, thermoelastic and heat-conduction problems.
It is, also, interesting to observe that, for the case of multi-linear law of λ, not any prescription on the form of the strain tensor $\boldsymbol{E}^H$ is necessary and, so, it is possible to use as *Displacement Associated Solutions* all the three dimensional solutions about anisotropic elasticity, satisfying the equation (2.52), that is, all the three dimensional solutions that satisfy the equation

$$curl\,\boldsymbol{u}^H=\boldsymbol{0} \tag{2.54}$$

For the examples of applicability of the DAS theorem and for more details on its formulation, let us to send to the references being in literature, (Fraldi, Cowin, 2004).
It is worth to note that the DAS theorem, like the SAS one, yields the possibility to find a closed-form solution for some inhomogeneous materials and it evidences that this possibility depends, in general, on the relation between the geometry of the strain distribution in the homogeneous material and the structural gradient, $\nabla\lambda$, of the inhomogeneous material.

2. ANISOTROPIC MEDIA: VOLUME FRACTION AND FABRIC TENSORS

In multiphase or damage materials, mechanical properties are closely related to the underlying microstructure or crack distribution. Although the volume fraction is the primary parameter in the geometric characterization of the microstructure of such materials, it does not provide information about the arrangement and the orientation of the microstructure. It is therefore necessary to introduce further parameters able to describe such orientations. The approach commonly use to modelling the material microstructure consists on introducing tensors of higher rank which characterize the microstructural architecture. In particular, in many application, microstructural anisotropy seems to be sufficiently well described by a scalar and a symmetric second rank fabric tensor, which restricts the material symmetry to orthotropy.
Fabric tensors may be defined in a wide number of ways but it is required to be a positive define tensor that is a quantitative stereological measure of the microstructural architecture, a measure whose principal axes are coincident with the principal microstructural direction and whose eigenvalues are proportional to the distribution of the microstructure in the associated principal direction. The fabric tensor may be measure on a finite test volume and it is considered a continuous function of the position in the material. It should be highlight that since the fabric tensor is a continuum point property, its applicability to solve real problem is really difficult because would require a wide number of measures. In other words it would be necessary evaluate the fabric tensor in each point of the material.
In the next sections, some way to construct fabric tensors proposed in scientific literature are illustrate.

2.1. Mean Intercept Length (MIL) Tensor

In order to characterize the microstructural anisotropy in orthotropic materials, Harrigan and Mann (1984) proposed a particular second order tensor – the so-called mean intercept length (MIL) tensor – related to the stereological measurement of the microstructural arrangement. In particular, the MIL in a material is define as the average distance, measured along a particular straight line, between two interfaces of the two different constituents. The value of the MIL is a function of the slope θ of the line along which the measurement is made in a specific plane. If, by plotting in a polar diagram the MIL – measured in the selected plane passing through a particular point in the specimen – as function of θ, the polar diagram produced ellipses (see Figure 2.4), than the values of all MILs in the plane may be represented by a second-order tensor in two dimension. By extending these consideration to a three-dimensional case, the MILs in all direction would be represented by an ellipsoid that is by a positive define second rank tensor $\boldsymbol{M}$ which is commonly related to the mean

intercept length $L(\boldsymbol{n})$ by the relationship $1/L^2(\boldsymbol{n}) = \boldsymbol{n} \cdot \boldsymbol{M}\boldsymbol{n}$, where $\boldsymbol{n}$ is the unit vector in the direction of the mean intercept length measurement.

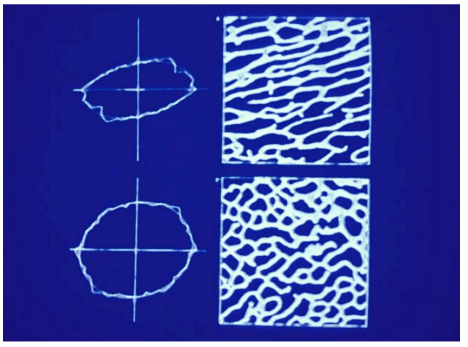

Fig. 2.4.
Polar diagram of the Mean Intercept Length function of a cancellous bone

The MIL approach as well as other stereological methods – e.g. the volume orientation method, the star volume distribution method – were proposed to construct the fabric tensor for biphasic materials, with particular reference to a specific porous material, the cancellous bone (Odgaard *et al.*, 1997). However, it is worth to highlight that for particular microstructure – e.g. planar fibre networks or materials made of a set of plates – the MIL distribution is not in general elliptic and so it may not be analytically expressed in terms of a second-order tensor (Tözeren and Skalak, 1989).
Cowin (Cowin,1986) defined a fabric tensor $\boldsymbol{H}$ related to the MIL tensor $\boldsymbol{M}$ by $\boldsymbol{H} = \boldsymbol{M}^{-1/2}$. Such tensor is well defined being the positive square root of the inverse of the positive define symmetric tensor $\boldsymbol{M}$. The difference between $\boldsymbol{H}$ and $\boldsymbol{M}$ is in the shape of ellipsoid while the principal axes coincide.

2.2. Orientation Distribution Function (ODF)

Let φ be some macroscopic scalar property of a material. At a given instant, φ generally depends on the material point, identified with the reference position vector $\boldsymbol{x}$, and on the orientation, specified by the unit vector $\boldsymbol{n}$; that is, $\varphi = \varphi(\boldsymbol{x}, \boldsymbol{n})$. Since only the dependence of φ on $\boldsymbol{n}$ is concerned in subsequent investigations, it is convenient to consider $\boldsymbol{x}$ as fixed and drop the dependence of φ on $\boldsymbol{x}$. Then we write

$$\varphi = f(\boldsymbol{n}), \qquad f : \mathscr{S} \to \mathscr{R} \tag{2.55}$$

and call f, the scalar-valued function defined on the unit sphere $\mathscr{S}$, the *orientation distribution function* (ODF) of the property φ. Concretely φ may be the effective surface density of the microdefects, Young's modulus, the wave speed, the electrical resistivity, the fatigue limit, etc. (Lemaitre *et al.*, 1987).
The function $f(\boldsymbol{n})$ must satisfy the condition

$$f(\boldsymbol{n}) = f(-\boldsymbol{n}), \qquad \forall \boldsymbol{n} \in \mathscr{S}, \tag{2.56}$$

because any material property φ in a direction is independent of the geometrical choice made between $\boldsymbol{n}$ and $-\boldsymbol{n}$ for defining that direction. It is possible to prove that the invariance requirement (2.56) is satisfied if and only if there exists a function $\hat{f}$ from $\mathscr{N} = \mathscr{S} \otimes \mathscr{S}$ to $\mathscr{R}$ such that

$$f(\boldsymbol{n}) = \hat{f}(\boldsymbol{n} \otimes \boldsymbol{n}) = \hat{f}(\boldsymbol{N}), \qquad \forall \boldsymbol{n} \in \mathscr{S}. \tag{2.57}$$

In the following we only consider the function $\hat{f}(\boldsymbol{N})$ for which the condition (2.56) is verified.
Assume $\hat{f}(\boldsymbol{N})$ to be squre-integrable:

$$\int_{\mathscr{S}} \left| \hat{f}(\boldsymbol{N}) \right|^2 da < +\infty, \tag{2.58}$$

where $da = \sin\theta \, d\theta \, d\phi$ is an infinitesimal surface element of the unit sphere $\mathscr{S}$.
It is that known (Vilenkin, 1969; Bunge, 1982; Jones, 1985) that $\hat{f}(\boldsymbol{N})$ can be expanded in the following Fourier series:

$$\begin{aligned} \hat{f}(\boldsymbol{N}) &= f_0(\boldsymbol{N}) + f_1(\boldsymbol{N}) + f_2(\boldsymbol{N}) + \ldots \\ &= g + \boldsymbol{G}' : \boldsymbol{F}(\boldsymbol{N}) + \mathbb{G}' :: \mathbb{F}(\boldsymbol{N}) + \ldots, \qquad \forall \boldsymbol{N} \in \mathscr{N}, \end{aligned} \tag{2.59}$$

which is convergent in mean, i.e.

$$\lim_{n \to \infty} \int_{\mathscr{S}} \left| \hat{f}(\boldsymbol{N}) - s_n(\boldsymbol{N}) \right|^2 da = 0, \quad s_n(\boldsymbol{N}) := f_0(\boldsymbol{N}) + f_1(\boldsymbol{N}) + \ldots + f_n(\boldsymbol{N}). \tag{2.60}$$

In the equation (2.59), $\{\boldsymbol{I}, \boldsymbol{F}(\boldsymbol{N}), \mathbb{F}(\boldsymbol{N}), \ldots\}$ are generalized spherical harmonics (Kanatani, 1984; Onat, 1984; Jones, 1985) and form a complete orthogonal basis for the squere-integrable functions on $\mathscr{S}$.

The first two tensor spherical harmonics $\boldsymbol{F}(\boldsymbol{N})$ and $\mathbb{F}(\boldsymbol{N})$ are of particular interest. In view of the tensor products of Kronecker-type, they may be written in the coordinate-free forms:

$$\boldsymbol{F}(\boldsymbol{N}) = \boldsymbol{N} - \frac{1}{3}\boldsymbol{I} \tag{2.61}$$

$$\begin{aligned}\mathbb{F}(\boldsymbol{N}) = \boldsymbol{N}\otimes\boldsymbol{N} - \tfrac{1}{7}\big(\boldsymbol{I}\otimes\boldsymbol{N} + \boldsymbol{N}\otimes\boldsymbol{I} + \boldsymbol{I}\underline{\otimes}\boldsymbol{N} + \boldsymbol{N}\underline{\otimes}\boldsymbol{I} + \boldsymbol{I}\overline{\otimes}\boldsymbol{N} + \boldsymbol{N}\overline{\otimes}\boldsymbol{I}\big) + \\ \tfrac{1}{35}\big(\boldsymbol{I}\otimes\boldsymbol{I} + \boldsymbol{I}\underline{\otimes}\boldsymbol{I} + \boldsymbol{I}\overline{\otimes}\boldsymbol{I}\big)\end{aligned} \tag{2.62}$$

The orthogonality of the basis functions $\{\boldsymbol{I}, \boldsymbol{F}(\boldsymbol{N}), \mathbb{F}(\boldsymbol{N}), ...\}$ means that

$$\begin{aligned}&\int_{\mathscr{S}} \boldsymbol{F}(\boldsymbol{N})\,da = \boldsymbol{0}, \qquad \int_{\mathscr{S}} \mathbb{F}(\boldsymbol{N})\,da = \mathbb{O} \\ &\int_{\mathscr{S}} \boldsymbol{F}(\boldsymbol{N})\otimes\mathbb{F}(\boldsymbol{N})\,da = \int_{\mathscr{S}} \mathbb{F}(\boldsymbol{N})\otimes\boldsymbol{F}(\boldsymbol{N})\,da = \mathbb{O}_6, ...\end{aligned} \tag{2.63}$$

where $\mathbb{O}_6$ denotes the sixth-order zero tensor. It is important to remark that $\boldsymbol{F}(\boldsymbol{N})$ is symmetric and traceless:

$$\boldsymbol{F}^T = \boldsymbol{F}\,; \quad \boldsymbol{I}:\boldsymbol{F} = 0\,, \tag{2.64}$$

and that $\mathbb{F}(\boldsymbol{N})$ is completely symmetric and traceless:

$$\mathbb{F} = \big(\boldsymbol{I}\overline{\otimes}\boldsymbol{I}\big)\mathbb{F} = \mathbb{F}^T; \quad \big(\boldsymbol{Y}\overline{\otimes}\boldsymbol{X}\big)::\mathbb{F} = \big(\boldsymbol{Y}\overline{\otimes}\boldsymbol{X}^T\big)::\mathbb{F}, \quad \forall \boldsymbol{X},\boldsymbol{Y}\in\mathscr{L}; \quad \mathbb{F}\boldsymbol{I} = \boldsymbol{0}\,. \tag{2.65}$$

The first three expansion coefficients of equation (2.59) can be determined from $f(\boldsymbol{n})$ via the integrals (Kanatani, 1984):

$$\begin{aligned}&g = \frac{1}{4\pi}\int_{\mathscr{S}} \hat{f}(\boldsymbol{N})\,da, \quad \boldsymbol{G}' = \frac{15}{8\pi}\int_{\mathscr{S}} \hat{f}(\boldsymbol{N})\boldsymbol{F}(\boldsymbol{N})\,da, \\ &\mathbb{G}' = \frac{315}{32\pi}\int_{\mathscr{S}} \hat{f}(\boldsymbol{N})\mathbb{F}(\boldsymbol{N})\,da.\end{aligned} \tag{2.66}$$

Due to equations (2.64) and (2.65), $\boldsymbol{G}'$ turns out to be symmetric and traceless and $\mathbb{G}'$ to be completely symmetric and traceless. With these properties, in the most general case, $\boldsymbol{G}'$ and $\mathbb{G}'$ contain five and nine independent components, respectively.

It is readily seen from equations (2.59) and (2.60) that any square-integrable ODF $\hat{f}(\boldsymbol{N})$ is fully characterized by its scalar and tensor expansion coefficients $\{g, \boldsymbol{G}', \mathbb{G}', ...\}$. If only the leading terms (for example, the first three ones) of the series expansion, (2.59), are retained, a finite or discrete description is then obtained for $\hat{f}(\boldsymbol{N})$. Theoretically speaking, the accuracy of such a description increases with the number of the leading terms being employed; in practice, the maximum value of this number is determined by the degree of accuracy with which the directional data of the property φ are experimentally acquired.
The importance of this result resides in the fact that only the tensors of zero or even orders are usable for a finite description of the ODF of a scalar-valued physical or mechanical property φ.

2.3. Fabric Tensor and Microcrack Distribution

In the characterization of mechanical response of damaged materials, a central problem is represented by the development of the formalism which enables a traditional continuum representation of the statistical distribution of microcracks compiled from the stereological data measured on a statistically homogeneous volume of damaged microstructure. The selection of the damage parameter approximating the measured data is not unique due to the contradictory requirements of accuracy and simplicity.
In the framework of damage mechanics, the effective continuum theories (Krajcinovic, 1996) are based on the assumption that the exact location of a microcrack within a representative volume element is not very important for the determination of the effective properties. This statement is, rigorously speaking, valid only in the dilute concentration limit. In other case, it is necessary to determine the distribution of crack surface densities as a function, for example, of the orientation of their bedding planes. For this purpose, the damage at a material point x is defined by a finite set of doublets $[\rho_i, n_i]$ $(i = 1, 2, ..., m)$ where ρ_i, is the microcrack density in a plane with normal n_i. Geometrically this set of doublets represents a binned histogram. Each bin defines the microcrack density in planes with orientations belonging to a particular range of angles. To determine the density of microcracks sharing a particular orientation (defined by a normal $\boldsymbol{n}$ to their bedding plane) it is necessary to make a large number of parallel cuts through a representative volume element of the actual material which maps on the observed material point in the effective continuum. In the limit of a very large number of orientations the density function $\rho(\boldsymbol{n})$ tends to a continuous distribution of the densities of microcracks in planes with normals $\boldsymbol{n}$ passing through the material point $\boldsymbol{x}_0$ (Ilankamban and Krajcinovic 1987, Curran, *et al.* 1987).

The principal problem in the formulation of an analytical representation of the experimental data is related to the representation of the raw statistical data in a frame indifferent (objective) manner. This question was explored and answered by Kanatani (1984) and later elaborated upon in connection to the damage distribution by Budiansky and O'Connell (1976), Onat and Leckie (1984), Wong (1985) and Lubarda and Krajcinovic (1993). The central task is to establish a procedure relating a measured distribution of microcrack densities as a function of their orientation $\rho(\boldsymbol{n})$ to an appropriate damage measure in form of a tensor invariant to coordinate transformations. This procedure must provide a criterion needed to measure the fit between the experimental data and various analytical descriptions of the microcrack distributions. The empirical function $\rho(\boldsymbol{n})$, typically determined for a limited number of bedding planes and samples, is seldom smooth. Depending on the heterogeneity of the material, size of the representative volume element, experimental technique, available equipment and finally the chance itself the function $\rho(\boldsymbol{n})$ may substantially change from one sample to the other. A large number of samples and sections may be needed for a statistically valid characterization of the function $\rho(\boldsymbol{n})$. In most cases a task like this is not cheap enough to be feasible. It is possible to utilize the measured or conjectured directional dependence of the crack surface area density $\rho(\boldsymbol{n})$ directly into an appropriately formulated computational model (Ilankamban and Krajcinovic 1987, Curran, *et al.* 1987). For the present purposes it is obviously advantageous to use a tensor function which approximates the distribution $\rho(\boldsymbol{n})$ with sufficient accuracy. The procedure, shown in the previous section, is developed in order to derive a tensor approximation of the raw data arranged into the histogram, expanding the function $\rho(\boldsymbol{n})$ into a Fourier-type series of certain families of Laplace spherical harmonics (Kanatani 1984, Onat and Leckie 1988) which represent the dyadic products of the unit vector $\boldsymbol{n}$ and the Kronecker delta tensor $\boldsymbol{\delta}$. Since a surface is defined by an axial vector the analytical expression for the distribution $\rho(\boldsymbol{n})$ can involve only even order tensors. A rigorous approximation of an empirical or actually measured function $\rho(\boldsymbol{n})$ involves an infinite series of tensors of even order. In many cases the details of this distribution may not have a discernible effect on the macro properties and may not be reproducible when testing "identical" specimens under "identical" circumstances. For purely practical purposes this series must be truncated to a rather moderate number of terms limited to the lowest order tensors. The truncation introduces inevitable errors into the selected representation and some non-physical effects which were not noticed until recently.

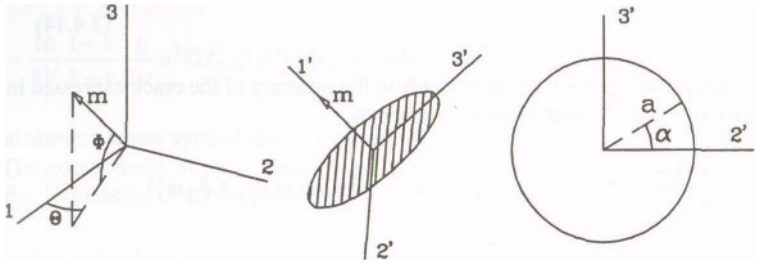

Fig. 2.5.
Geometry of a penny-shaped crack

With reference to penny-shaped cracks defined by their radii a and two Euler angles (θ,ϕ), shown in Figure 2.5., it is possible to write (Krajcinovic, 1996) the average crack density within a selected unit sphere centered at a material point as

$$\overline{w}=\frac{1}{4\pi}\int_{a^-}^{a^+}a^3\vartheta(a)\,da\int_0^{2\pi}\int_{-\pi/2}^{\pi/2}\rho(\phi,\theta)\cos\phi\;d\theta d\phi=$$
$$\frac{1}{4\pi}N\left\langle a^3\right\rangle\int_0^{2\pi}\int_{-\pi/2}^{\pi/2}\rho(\phi,\theta)\cos\phi\;d\theta d\phi=N\left\langle a^3\right\rangle\overline{\rho}(\boldsymbol{n}) \tag{2.67}$$

where $N\left\langle a^3\right\rangle=\int_{a^-}^{a^+}a^3\vartheta(a)\,da$ is the non-dimensional microcracks density. To be able to compare different microcrack distributions with respect to the orientations $w(\boldsymbol{n})=N\left\langle a^3\right\rangle\rho(\boldsymbol{n})=N\left\langle a^3\right\rangle\rho(\phi,\theta)$ the product $N\left\langle a^3\right\rangle=1$ will be fixed in the sequel.

Scalar Representation of the Damage Variable. The microcrack distribution can be assumed to be approximately isotropic when the microcrack density is a weak function of the plane orientation (defined by the normal $\boldsymbol{n}$ to the bedding plane through the material point). In this special case (which is preferred primarily by analysts if not by the geometry, nature and the physics of defect nucleation and growth) the microcrack distribution is fully defined by a single scalar ρ_0 which represents the total microcrack density or by the density $\overline{\rho}$ averaged over the solid angle. These two scalar measures of the crack distribution are related by the well known formula

$$\rho^0\equiv D^0=\int_\Omega\rho(n)\,d\Omega=4\pi\overline{\rho}\,. \tag{2.68}$$

The integration in (2.68) is extended over all orientations within the solid angle $\Omega = 4\pi$. In this, simplest of all cases, the damage is defined by a single parameter ρ^0 (microcrack density). All symmetries of the original solid are preserved. The scalar damage variable (2.68) is introduced for the sake of consistency and uniformity. Due to its simplicity the scalar damage variable representation has been extensively utilized in the past (see, for example, Lemaitre and Chaboche 1978, Lemaitre 1986, 1992).

Second Order Tensor Representation of the Damage Variable. The isotropic distribution of microcracks is a relatively rare phenomenon which may occur in rocks in crustal conditions (i.e. well confined in all directions) which are exposed to large temperatures and internal pressures and/or expansive exothermic reactions. In a general case the microcracks distribution is characterized by a varying degree of anisotropy. In a frequently encountered class of problems and tests the microcrack distribution may render the specimen statistically (macro) orthotropic. The orthotropy may also be a function of the variations of strength and stiffness with direction. This may happen in sedimentary rocks characterized by a strong dependence of the cohesive strength on the primary depositional petrofabric and also in laminate composites made of fiber reinforced laminae. The microcrack induced orthotropy can also be stress induced. The damage density in an initially isotropic solid subjected to proportional loading will reach maximum densities in the planes perpendicular to the largest principal stress. Similarly, the microcrack densities will be minimal in planes which are orthogonal to the minimum principal stress. The principal planes of the damage density will often be perpendicular assuming that the state of stress is simple and the loads proportional. This class of microcrack distributions may be adequately represented by a second order tensor. The microcrack density in planes with a normal $\boldsymbol{n}$ can be in this case defined by the expression

$$\rho(\boldsymbol{n}) = \rho_{ij} n_i n_j \tag{2.69}$$

(Lubarda, Krajcinovic 1993) where ρ_{ij} is a symmetric second order tensor. Integrating (2.69) over the entire solid angle, and using the identity

$$\int_{\Omega} n_i n_j d\Omega = \frac{4\pi}{3} \delta_{ij} \tag{2.70}$$

where δ_{ij} is the Kronecker (identity) delta tensor, it follows that the first invariant (trace) of the second order tensor ρ_{ij} is

$$\rho_{kk} = \frac{3}{4\pi}\rho^0 \tag{2.71}$$

The scalar damage variable ρ^0 in (2.71) is defined by (2.68). Multiplying both sides of (2.69) by $n_m n_n$ and integrating the product over the solid angle while making use of the identity

$$\int_\Omega n_i n_j n_m n_n d\Omega = \frac{4\pi}{5} I_{ijmn} \tag{2.72}$$

leads to the following expression

$$\frac{8\pi}{15}\left(\rho_{ij} + \frac{1}{2}\rho_{kk}\delta_{ij}\right) = \int_\Omega \rho(n) n_i n_j d\Omega\,. \tag{2.73}$$

The fourth order tensor $\mathbb{I}$ in (2.72) is defined by the tensor products of two delta second order tensors as

$$I_{ijmn} = \frac{1}{3}\left(\delta_{ij}\delta_{mn} + \delta_{im}\delta_{jn} + \delta_{in}\delta_{jm}\right) \tag{2.74}$$

The microcrack density tensor can now be derived by substituting (2.71) into (2.73)

$$\rho_{ij} = \frac{15}{8\pi}\left(D_{ij} - \frac{\rho^0}{5}\delta_{ij}\right) \tag{2.75}$$

where

$$D_{ij} = \int_\Omega \rho(n) n_i n_j d\Omega \tag{2.76}$$

is referred to as the second order damage tensor. The microcrack density distribution (2.69) is, in view of (2.75), a function of the scalar and second order tensor damage parameters

$$\rho(n) = \frac{15}{8\pi} n_i n_j D_{ij} - \frac{3}{8\pi} D^0\,. \tag{2.77}$$

2.4. Relationship between Fabric Tensor and Elasticity Tensor

From a mathematical point of view, identifying the dependence of the elastic behaviour of the material on its microstructure consists in analyzing the formal relationship between the fabric tensor and the elasticity tensor.
The main attempt to relate a fabric tensor describing microstructure to a fourth rank elasticity tensor – with specific reference to porous materials – is due to Cowin (Cowin, 1985). He proposed a model based on a normalized second rank fabric tensor and developed a general representation of $\bar{\boldsymbol{C}}$ as a function of the solid volume fraction γ and of the invariants of the fabric tensor $\boldsymbol{H}$ based on the notion that the matrix material of the porous elastic solid is isotropic and that the anisotropy of the porous elastic solid itself is due only to the geometry of microstructure represented by the fabric tensor. The mathematical statement of this notion is that the stress tensor $\boldsymbol{T}$ is an isotropic function of the strain tensor $\boldsymbol{E}$ and the fabric tensor $\boldsymbol{H}$ as well as the solid volume fraction γ. Thus, the tensor valued function

$$\boldsymbol{T} = \boldsymbol{T}\left(\gamma, \boldsymbol{E}, \boldsymbol{H}\right) \tag{2.78}$$

has the property that

$$\boldsymbol{Q}\boldsymbol{T}\boldsymbol{Q}^{T} = \boldsymbol{T}\left(\gamma, \boldsymbol{Q}\boldsymbol{E}\boldsymbol{Q}^{T}, \boldsymbol{Q}\boldsymbol{H}\boldsymbol{Q}^{T}\right) \tag{2.79}$$

for all orthogonal tensors $\boldsymbol{Q}$. This definition of an isotropic tensor valued function is given, for example, by Truesdell and Noll (1965). In accord with the isotropy assumption, the stress tensor $\boldsymbol{T}$ has the representation

$$\begin{aligned}\boldsymbol{T} = {} & f_1\boldsymbol{I} + f_2\boldsymbol{H} + f_3\boldsymbol{H}^2 + f_4\boldsymbol{E} + f_5\boldsymbol{E}^2 + f_6\left(\boldsymbol{H}\boldsymbol{E} + \boldsymbol{E}\boldsymbol{H}\right) \\ & + f_7\left(\boldsymbol{H}^2\boldsymbol{E} + \boldsymbol{E}\boldsymbol{H}^2\right) + f_8\left(\boldsymbol{H}\boldsymbol{E}^2 + \boldsymbol{E}^2\boldsymbol{H}\right) + f_9\left(\boldsymbol{H}^2\boldsymbol{E}^2 + \boldsymbol{E}^2\boldsymbol{H}^2\right)\end{aligned} \tag{2.80}$$

where f_1 through f_9 are function of the ten invariants $Tr\boldsymbol{H}$, $Tr\boldsymbol{H}^2$, $Tr\boldsymbol{H}^3$, $Tr\boldsymbol{E}$, $Tr\boldsymbol{E}^2$, $Tr\boldsymbol{E}^3$, $Tr\boldsymbol{H}\boldsymbol{E}$, $Tr\boldsymbol{H}^2\boldsymbol{E}$, $Tr\boldsymbol{H}\boldsymbol{E}^2$, $Tr\boldsymbol{E}^2\boldsymbol{H}^2$. This representation is reduced by the requirement that $\boldsymbol{T}$ be linear in $\boldsymbol{E}$ and that $\boldsymbol{T}$ vanish when $\boldsymbol{E}$ vanishes, thus

$$\boldsymbol{T} = f_1\boldsymbol{I} + f_2\boldsymbol{H} + f_3\boldsymbol{H}^2 + f_4\boldsymbol{E} + f_6\left(\boldsymbol{H}\boldsymbol{E} + \boldsymbol{E}\boldsymbol{H}\right) + f_7\left(\boldsymbol{H}^2\boldsymbol{E} + \boldsymbol{E}\boldsymbol{H}^2\right) \tag{2.81}$$

where f_1, f_2, f_3 must be of the form

$$\begin{aligned} f_1 &= a_1 Tr\boldsymbol{E} + a_2 Tr\boldsymbol{HE} + a_3 Tr\boldsymbol{H}^2\boldsymbol{E}, \\ f_2 &= d_1 Tr\boldsymbol{E} + b_1 Tr\boldsymbol{HE} + b_2 Tr\boldsymbol{H}^2\boldsymbol{E}, \\ f_3 &= d_2 Tr\boldsymbol{E} + d_3 Tr\boldsymbol{HE} + b_3 Tr\boldsymbol{H}^2\boldsymbol{E}, \end{aligned} \tag{2.82}$$

and where a_1, a_2, a_3, b_1, b_2, b_3, d_1, d_2 and d_3, are function of $Tr\boldsymbol{H}$, $Tr\boldsymbol{H}^2$ and $Tr\boldsymbol{H}^3$. It follows then that

$$\begin{aligned} \boldsymbol{T} = {} & \boldsymbol{I}\left(a_1 Tr\boldsymbol{E} + a_2 Tr\boldsymbol{HE} + a_3 Tr\boldsymbol{H}^2\boldsymbol{E}\right) + \boldsymbol{H}\left(d_1 Tr\boldsymbol{E} + b_1 Tr\boldsymbol{HE} + b_2 Tr\boldsymbol{H}^2\boldsymbol{E}\right) \\ & + \boldsymbol{H}^2\left(d_2 Tr\boldsymbol{E} + d_3 Tr\boldsymbol{HE} + b_3 Tr\boldsymbol{H}^2\boldsymbol{E}\right) + 2c_1\boldsymbol{E} + 2c_2\left(\boldsymbol{HE} + \boldsymbol{EH}\right) \\ & + 2c_3\left(\boldsymbol{H}^2\boldsymbol{E} + \boldsymbol{EH}^2\right) \end{aligned} \tag{2.83}$$

where we have set $f_4 = 2c_1$, $f_6 = 2c_2$ and $f_7 = 2c_3$. This result may be expressed in indicial notation as

$$\begin{aligned} T_{ij} = {} & \delta_{ij}\left(a_1 E_{kk} + a_2 H_{rp}E_{pr} + a_3 H_{rq}H_{qp}E_{pr}\right) + H_{ij}\left(d_1 E_{kk} + b_1 H_{rp}E_{pr} + b_2 H_{rq}H_{qp}E_{pr}\right) \\ & + H_{is}H_{sj}\left(d_2 E_{kk} + d_3 H_{rp}E_{pr} + b_3 H_{rq}H_{qp}E_{pr}\right) + 2c_1 E_{ij} + 2c_2\left(H_{ir}E_{rj} + E_{ir}H_{rj}\right) \\ & + 2c_3\left(H_{ip}H_{pr}E_{rj} + E_{ir}H_{rp}H_{pj}\right) \end{aligned} \tag{2.84}$$

Comparison of this result with the constitutive equation $T_{ij} = C_{ijhk}E_{hk}$ suggests that C_{ijhk} should be of the form

$$\begin{aligned} C_{ijhk} = {} & \left(a_1\delta_{ij} + d_1 H_{ij} + d_2 H_{is}H_{sj}\right)\delta_{hk} + \left(a_2\delta_{ij} + b_1 H_{ij} + d_3 H_{is}H_{sj}\right)H_{hk} \\ & + \left(a_3\delta_{ij} + b_2 H_{ij} + b_3 H_{is}H_{sj}\right)H_{hq}H_{qk} + 2c_1\delta_{hi}\delta_{kj} \\ & + 2c_2\left(H_{ih}\delta_{kj} + \delta_{ih}H_{kj}\right) + 2c_3\left(H_{ip}H_{pk}\delta_{kj} + \delta_{ih}H_{kp}H_{ps}\right). \end{aligned} \tag{2.85}$$

In order to satisfy the symmetry conditions (1.90) we must set $d_1 = a_2$, $d_2 = a_3$, and $d_3 = b_2$ and take the symmetric parts of the terms multiplied by $2c_1$, $2c_2$, and $2c_3$ with respect to *hk* and *ij*. The final results may be express as follow

$$
\begin{aligned}
C_{ijhk} = {} & a_1\delta_{ij}\delta_{hk} + a_2(H_{ij}\delta_{ij} + H_{hk}\delta_{hk}) + a_3(\delta_{ij}H_{hq}H_{qk} + \delta_{hk}H_{iq}H_{qj}) + \\
& + b_1H_{ij}H_{hk} + b_2(H_{ij}H_{hq}H_{qk} + H_{is}H_{sj}H_{hk}) + b_3H_{is}H_{sj}H_{hq}H_{qk} + \\
& + c_1(\delta_{hi}\delta_{kj} + \delta_{ki}\delta_{hj}) + c_2(H_{ih}\delta_{kj} + H_{hj}\delta_{ki} + H_{ik}\delta_{hj} + H_{kj}\delta_{hi}) + \\
& + c_3(H_{ir}H_{rh}\delta_{kj} + H_{rj}H_{hr}\delta_{ki} + H_{ir}H_{rk}\delta_{hj} + H_{kr}H_{rj}\delta_{ih})
\end{aligned}
\tag{2.86}
$$

where a_1, a_2, a_3, b_1, b_2, b_3, c_1, c_2 and c_3 are functions of γ and $Tr\boldsymbol{H}$, $Tr\boldsymbol{H}^2$ and $Tr\boldsymbol{H}^3$.

It is possible to show that the representation (2.86) for the fourth rank elasticity tensor is not capable of representing all possible elastic material symmetry. The last material symmetry that may be represented by is orthotropy. In fact, expanding in indicial notation in the coordinate system that diagonalized the fabric tensor ($H_{12} = H_{13} = H_{23} = 0$), only the following nine components of the elastic tensor are non-zero and are function of the nine coefficient a_1, a_2, a_3, b_1, b_2, b_3, c_1, c_2, c_3 and of the three eigenvalues of $\boldsymbol{H}$, H_{11}, H_{22} and H_{33}

$$
\begin{aligned}
C_{1111} &= a_1 + 2c_1 + 2(a_2 + 2c_2)H_{11} + (2a_3 + b_1 + 4c_3)H_{11}^2 + 2b_2H_{11}^3 + b_3H_{11}^4 \\
C_{2222} &= a_1 + 2c_1 + 2(a_2 + 2c_2)H_{22} + (2a_3 + b_1 + 4c_3)H_{22}^2 + 2b_2H_{22}^3 + b_3H_{22}^4 \\
C_{3333} &= a_1 + 2c_1 + 2(a_2 + 2c_2)H_{33} + (2a_3 + b_1 + 4c_3)H_{33}^2 + 2b_2H_{33}^3 + b_3H_{33}^4 \\
C_{1122} &= a_1 + a_2(H_{11} + H_{22}) + a_3(H_{11}^2 + H_{22}^2) + b_1H_{11}H_{22} + b_2(H_{11}H_{22}^2 + H_{22}H_{11}^2) \\
&\quad + b_3H_{11}^2H_{22}^2 \\
C_{1133} &= a_1 + a_2(H_{11} + H_{33}) + a_3(H_{11}^2 + H_{33}^2) + b_1H_{11}H_{33} + b_2(H_{11}H_{33}^2 + H_{33}H_{11}^2) \\
&\quad + b_3H_{11}^2H_{33}^2 \\
C_{3322} &= a_1 + a_2(H_{33} + H_{22}) + a_3(H_{33}^2 + H_{22}^2) + b_1H_{33}H_{22} + b_2(H_{33}H_{22}^2 + H_{22}H_{33}^2) \\
&\quad + b_3H_{33}^2H_{22}^2 \\
C_{1212} &= c_1 + c_2(H_{11} + H_{22}) + c_3(H_{11}^2 + H_{22}^2) \\
C_{1313} &= c_1 + c_2(H_{11} + H_{33}) + c_3(H_{11}^2 + H_{33}^2) \\
C_{3232} &= c_1 + c_2(H_{33} + H_{22}) + c_3(H_{33}^2 + H_{22}^2)
\end{aligned}
\tag{2.87}
$$

Note that these nine components of the elasticity tensor are distinct if and only if the eigenvalues of $\boldsymbol{H}$ are distinct. In fact, it is easy to see that by setting $H_{22} = H_{33}$ in the (2.87), only the following six constants are different

$$
\begin{aligned}
&C_{1111} = a_1 + 2c_1 + 2(a_2 + 2c_2)H_{11} + (2a_3 + b_1 + 4c_3)H_{11}^2 + 2b_2H_{11}^3 + b_3H_{11}^4 \\
&C_{2222} = C_{3333} = a_1 + 2c_1 + 2(a_2 + 2c_2)H_{22} + (2a_3 + b_1 + 4c_3)H_{22}^2 + 2b_2H_{22}^3 + b_3H_{22}^4 \\
&C_{1122} = C_{1133} = a_1 + a_2(H_{11} + H_{22}) + a_3(H_{11}^2 + H_{22}^2) + b_1H_{11}H_{22} + b_2(H_{11}H_{22}^2 + H_{22}H_{11}^2) \\
&\qquad + b_3H_{11}^2H_{22}^2 \\
&C_{3322} = a_1 + a_2(H_{33} + H_{22}) + a_3(H_{33}^2 + H_{22}^2) + b_1H_{33}H_{22} + b_2(H_{33}H_{22}^2 + H_{22}H_{33}^2) \\
&\qquad + b_3H_{33}^2H_{22}^2 \\
&C_{1212} = C_{1313} = c_1 + c_2(H_{11} + H_{22}) + c_3(H_{11}^2 + H_{22}^2) \\
&C_{3232} = c_1 + c_2(H_{33} + H_{22}) + c_3(H_{33}^2 + H_{22}^2)
\end{aligned}
\tag{2.88}
$$

and only five of which are independent being $C_{2222} = C_{2233} + 2C_{2323}$. Thus, the represented material symmetry is the transversely isotropy. In the same way, if the eigenvalues of $\boldsymbol{H}$ are all equal the represented material symmetry is the isotropy, being only the following three constant different

$$
\begin{aligned}
C_{1111} = C_{2222} = C_{3333} &= a_1 + 2c_1 + 2(a_2 + 2c_2)H_{11} + (2a_3 + b_1 + 4c_3)H_{11}^2 \\
&\quad + 2b_2H_{11}^3 + b_3H_{11}^4 \\
C_{1122} = C_{1133} = C_{2233} &= a_1 + a_2(H_{11} + H_{22}) + a_3(H_{11}^2 + H_{22}^2) + b_1H_{11}H_{22} \\
&\quad + b_2(H_{11}H_{22}^2 + H_{22}H_{11}^2) + b_3H_{11}^2H_{22}^2 \\
C_{1212} = C_{1313} = C_{3232} &= c_1 + c_2(H_{11} + H_{22}) + c_3(H_{11}^2 + H_{22}^2)
\end{aligned}
\tag{2.89}
$$

and only two of which are independent, being $C_{1111} = C_{1122} + 2C_{1212}$.
The nine functions a_1, a_2, a_3, b_1, b_2, b_3, c_1, c_2 and c_3 depending upon γ, $Tr\boldsymbol{H}$, $Tr\boldsymbol{H}^2$ and $Tr\boldsymbol{H}^3$, can be determine by means of experimental tests.

Following this method, Zysset and Curnier (1995) introduce a general approach for relating the material microstructure to the four rank elasticity tensor. In particular, they describe the microstructure by means of a scalar and a symmetric, traceless second rank fabric tensor. By using a representation theorem for anisotropic function with tensorial arguments, they derive a general expression for the elastic free energy and discuss the resulting material symmetry in terms of the fabric tensor.
Specifically, they hypothesize that the mechanical anisotropy of the material is identical to that of a single microstructural property $f = f(\boldsymbol{N}) > 0$, where $\boldsymbol{N} = \boldsymbol{n} \otimes \boldsymbol{n}$ is the dyadic product of the unit vector $\boldsymbol{n}$ specifying the orientation (He *et al.*, 1995). By following the procedure shown in section 2.2, assuming

that the function f to be square integrable, it can be expanded in a convergent Fourier series

$$f(\boldsymbol{N}) = g \cdot \boldsymbol{I} + \boldsymbol{G} : \boldsymbol{F}(\boldsymbol{N}) + \mathbb{G} :: \mathbb{F}(\boldsymbol{N}) + ..., \qquad \forall \boldsymbol{N} \tag{2.90}$$

where $\boldsymbol{I}$, $\boldsymbol{F}(\boldsymbol{N})$ and $\mathbb{F}(\boldsymbol{N})$ are even ranked tensorial basis functions – in particular $\boldsymbol{I}$ is the second order unit tensor, while $\boldsymbol{F}(\boldsymbol{N})$ and $\mathbb{F}(\boldsymbol{N})$ are given by the (2.61) and (2.62), respectively – and g, $\boldsymbol{G}$ and $\mathbb{G}$ are the corresponding even ranked tensorial coefficients, called fabric tensor and given by the equations (2.66). As highlight in section 2.2., the accuracy of the series expansion improves with the number of retained leading terms. However, in most applications, the first and second terms provide a sufficient description of material anisotropy. So, the orientation distribution function f is approximate with

$$f(\boldsymbol{N}) = g \cdot \boldsymbol{I} + \boldsymbol{G} : \boldsymbol{F}(\boldsymbol{N}) \tag{2.91}$$

which implies a restriction on material symmetry – that can be orthotropy if all three eigenvalues of $\boldsymbol{G}$ are distinct, transerse isotropy if only two eigenvalues of $\boldsymbol{G}$ are distinct or isotropy if the tensor $\boldsymbol{G}$ vanishes.
By using the second rank tensor representation $\boldsymbol{Q}$ of the orthogonal group *Orth*, the material symmetry group *G* can be characterized by the fabric tensors:

$$\boldsymbol{Q} \in G \Leftrightarrow \begin{cases} \boldsymbol{Q}^T g \boldsymbol{I} \boldsymbol{Q} = g \boldsymbol{I} \\ \boldsymbol{Q}^T \boldsymbol{G} \boldsymbol{Q} = \boldsymbol{G} \\ (\boldsymbol{Q} \underline{\otimes} \boldsymbol{Q})^T \mathbb{G} (\boldsymbol{Q} \underline{\otimes} \boldsymbol{Q}) = \mathbb{G} \\ \cdots \end{cases} \tag{2.92}$$

Following this hypothesis, a scalar valued function $\psi(\boldsymbol{E})$ invariant with respect to the elements of the symmetry group *G* can be identified with an isotropic function $\hat{\psi}(\boldsymbol{E}, g, \boldsymbol{G}, \mathbb{G}, \ldots)$ of the same argument and the corresponding fabric tensor (Boehler, 1987)

$$\psi(\boldsymbol{E}) = \psi\left(\boldsymbol{Q}^T \boldsymbol{E} \boldsymbol{Q}\right), \qquad \forall \boldsymbol{Q} \in G,$$
$$\hat{\psi}(\boldsymbol{E}, g, \boldsymbol{G}, \mathbb{G}, \ldots) = \hat{\psi}\left(\boldsymbol{Q}^T \boldsymbol{E} \boldsymbol{Q}, g, \boldsymbol{Q}^T \boldsymbol{G} \boldsymbol{Q}, (\boldsymbol{Q} \underline{\otimes} \boldsymbol{Q})^T \mathbb{G} (\boldsymbol{Q} \underline{\otimes} \boldsymbol{Q})\right), \qquad \forall \boldsymbol{Q} \in Orth.$$

Representation theorems then provide the most general form of the isotropic scalar function $\hat{\psi}(\boldsymbol{E}, g, \boldsymbol{G}, \mathbb{G}, \ldots)$ in terms of invariants of the arguments.

For a scalar g and two second rank tensor arguments $\boldsymbol{E}$ and $\boldsymbol{G}$, with $\boldsymbol{G}$ being traceless, a set of irreducible invariants is given by (Boehler, 1987) $Tr(\boldsymbol{E})$, $Tr(\boldsymbol{E}^2)$, $Tr(\boldsymbol{E}^3)$, g, $Tr(\boldsymbol{G}^2)$, $Tr(\boldsymbol{G}^3)$, $Tr(\boldsymbol{EG})$, $Tr(\boldsymbol{E}^2\boldsymbol{G})$, $Tr(\boldsymbol{E}\boldsymbol{G}^2)$, $Tr\left((\boldsymbol{EG})^2\right)$. Retaining only quadratic terms in $\boldsymbol{E}$ to come up with linear elasticity, general form of the elastic free energy is

$$\begin{aligned}\psi = \psi(\boldsymbol{E}, g, \boldsymbol{G}) = {} & \frac{c_1}{2}Tr^2(\boldsymbol{E}) + \frac{c_2}{2}Tr(\boldsymbol{E}^2) + \frac{c_3}{2}Tr^2(\boldsymbol{EG}) \\ & + c_4 Tr(\boldsymbol{E}^2\boldsymbol{G}) + \frac{c_5}{2}Tr^2(\boldsymbol{E}\boldsymbol{G}^2) + \frac{c_6}{2}Tr\left((\boldsymbol{EG})^2\right) + c_7 Tr(\boldsymbol{E})Tr(\boldsymbol{EG}) \\ & + c_8 Tr(\boldsymbol{EG})Tr(\boldsymbol{E}\boldsymbol{G}^2) + c_9 Tr(\boldsymbol{E})Tr(\boldsymbol{E}\boldsymbol{G}^2)\end{aligned} \tag{2.93}$$

where c_i are functions of g and the two invariants of $\boldsymbol{G}$.
The constitutive equation for the stress tensor is obtained by derivation of the free energy potential ψ with respect to the strain $\boldsymbol{E}$

$$\begin{aligned}\boldsymbol{T} = \frac{\partial \psi}{\partial \boldsymbol{E}}(\boldsymbol{E}, g, \boldsymbol{G}) = {} & c_1 Tr(\boldsymbol{E})\boldsymbol{I} + c_2\boldsymbol{E} + c_3 Tr(\boldsymbol{EG})\boldsymbol{G} + c_4(\boldsymbol{EG} + \boldsymbol{GE}) \\ & + c_5 Tr(\boldsymbol{E}\boldsymbol{G}^2)\boldsymbol{G}^2 + c_6(\boldsymbol{GEG}) + c_7\left(Tr(\boldsymbol{EG})\boldsymbol{I} + Tr(\boldsymbol{E})\boldsymbol{G}\right) \\ & + c_8\left(Tr(\boldsymbol{E}\boldsymbol{G}^2)\boldsymbol{G} + Tr(\boldsymbol{EG})\boldsymbol{G}^2\right) + c_9\left(Tr(\boldsymbol{E}\boldsymbol{G}^2)\boldsymbol{I} + Tr(\boldsymbol{E})\boldsymbol{G}^2\right).\end{aligned} \tag{2.94}$$

The elasticity tensor is obtained by further derivation

$$\begin{aligned}\mathbb{C} = {} & \frac{\partial^2 \psi}{\partial \boldsymbol{E}^2}(\boldsymbol{E}, g, \boldsymbol{G}) \\ & = c_1\boldsymbol{I}\otimes\boldsymbol{I} + c_2\boldsymbol{I}\underline{\overline{\otimes}}\boldsymbol{I} + c_3\boldsymbol{G}\underline{\overline{\otimes}}\boldsymbol{G} + c_4\left(\boldsymbol{G}\underline{\overline{\otimes}}\boldsymbol{I} + \boldsymbol{I}\underline{\overline{\otimes}}\boldsymbol{G}\right) + c_5\boldsymbol{G}^2\otimes\boldsymbol{G}^2 + c_6\boldsymbol{G}\underline{\overline{\otimes}}\boldsymbol{G} \\ & + c_7\left(\boldsymbol{I}\otimes\boldsymbol{G} + \boldsymbol{G}\otimes\boldsymbol{I}\right) + c_8\left(\boldsymbol{G}\otimes\boldsymbol{G}^2 + \boldsymbol{G}^2\otimes\boldsymbol{G}\right) + c_9\left(\boldsymbol{I}\otimes\boldsymbol{G}^2 + \boldsymbol{G}^2\otimes\boldsymbol{I}\right).\end{aligned} \tag{2.95}$$

The material symmetry represented by the elasticity tensor in the form (2.95), like which one in (2.86), is at least the orthotropy that may degenerate into transverse isotropy when two eigenvalues of $\boldsymbol{G}$ are identical and into isotropy when the fabric tensor $\boldsymbol{G}$ vanishes.
By using the spectral decomposition of $\boldsymbol{G}$:

$$\boldsymbol{G} = g_i\boldsymbol{G}_i,\ \boldsymbol{G}_i = \boldsymbol{g}_i\otimes\boldsymbol{g}_i,$$

where g_i are the eigenvalues and $\boldsymbol{g}_i$ are the unit orthogonal eigenvectors of $\boldsymbol{G}$, and the property $\boldsymbol{G}_1+\boldsymbol{G}_2+\boldsymbol{G}_3=\boldsymbol{I}$, the elasticity tensor (2.95) may be translated in the general orthotropic form

$$\mathbb{S}=\lambda_{ii}\boldsymbol{G}_i\otimes\boldsymbol{G}_i+\lambda_{ij}^{*}\left(\boldsymbol{G}_i\otimes\boldsymbol{G}_j+\boldsymbol{G}_j\otimes\boldsymbol{G}_i\right)+2\mu_{ij}\left(\boldsymbol{G}_i\overline{\underline{\otimes}}\boldsymbol{G}_j+\boldsymbol{G}_j\overline{\underline{\otimes}}\boldsymbol{G}_i\right), \qquad (2.96)$$

where summation is performed for $i<j$ due to symmetrization of tensor products. The identification of the coefficients leads

$$\begin{aligned}
\lambda_{ii}&=c_1+c_2+c_3g_i^2+2c_4g_i+c_5g_i^4+c_6g_i^2+2c_7g_i+c_8g_i^3+2c_9g_i^2,\\
\lambda_{ij}^{*}&=c_1+c_3g_ig_j+c_5g_i^2g_j^2+c_7\left(g_i+g_j\right)+c_8\left(g_ig_j^2+g_jg_i^2\right)+c_9\left(g_i^2+g_j^2\right),\\
\mu_{ij}&=\tfrac{1}{2}c_2+\tfrac{1}{2}c_4\left(g_i+g_j\right)+\tfrac{1}{2}c_6g_ig_j.
\end{aligned} \qquad (2.97)$$

At this stage, additional assumption are necessary to guide the choice of the nine function c_i. The hypothesis they made, consists in introducing a homogeneity property for the set of fabric tensor $\{g,\boldsymbol{G}\}$, which means that anisotropy of the elastic constitutive law is independent of the size or physical units of the microstructural properties $\mathbb{S}(\lambda\boldsymbol{G})=\lambda^k\mathbb{S}(g,\boldsymbol{G}),\forall\lambda>0$, where $k\neq 0$ is the degree of the homogeneity property.

By considering the isotropic elasticity tensor, $\mathbb{S}=\lambda_c\boldsymbol{I}\otimes\boldsymbol{I}+2\mu_c\boldsymbol{I}\overline{\underline{\otimes}}\boldsymbol{I}$, and substituting the identity tensor $\boldsymbol{I}$ by the tensor $g\boldsymbol{I}+\boldsymbol{G}$:

$$\mathbb{S}=\lambda_c\left(g\boldsymbol{I}+\boldsymbol{G}\right)\otimes\left(g\boldsymbol{I}+\boldsymbol{G}\right)+2\mu_c\left(g\boldsymbol{I}+\boldsymbol{G}\right)\overline{\underline{\otimes}}\left(g\boldsymbol{I}+\boldsymbol{G}\right) \qquad (2.98)$$

where λ_c and μ_c are Lamé like constants, a particular form of the previous model is provided:

$$\begin{aligned}
&c_1=\lambda_cg^2, && c_2=2\mu_cg^2, && c_3=\lambda_c,\\
&c_4=2\mu_cg, && c_5=0, && c_6=2\mu_c,\\
&c_7=\lambda_cg, && c_8=0, && c_9=0.
\end{aligned} \qquad (2.99)$$

In the principal reference frame of $\boldsymbol{G}$:

$$\begin{aligned}
\mathbb{S}(g,\boldsymbol{G})=&\left(\lambda_c+2\mu_c\right)\left(g+g_i\right)^2\left(\boldsymbol{G}_i\otimes\boldsymbol{G}_i\right)\\
&+\lambda_c\left(g+g_i\right)\left(g+g_j\right)\left(\boldsymbol{G}_i\otimes\boldsymbol{G}_j+\boldsymbol{G}_j\otimes\boldsymbol{G}_i\right)\\
&+2\mu_c\left(g+g_i\right)\left(g+g_j\right)\left(\boldsymbol{G}_i\overline{\underline{\otimes}}\boldsymbol{G}_j+\boldsymbol{G}_j\overline{\underline{\otimes}}\boldsymbol{G}_i\right)
\end{aligned} \qquad (2.100)$$

Comparison with the general orthotropic form gives

$$\begin{aligned}
\lambda_{ii} &= \left(\lambda_c + 2\mu_c\right)\left(g + g_i\right)^2, \quad \forall i, \\
\lambda_{ij}^* &= \lambda_c \left(g + g_i\right)\left(g + g_j\right), \quad \forall i, j \ \ (i < j), \\
\mu_{ij} &= \mu_c \left(g + g_i\right)\left(g + g_j\right), \quad \forall i, j \ \ (i < j).
\end{aligned} \tag{2.101}$$

Sufficient but not necessary to satisfy the homogeneity condition, the substitution (2.98) provides the most simple orthotropic model that degenerates into transverse isotropy if two eigenvalues of $\boldsymbol{G}$ are identical and into isotropy if $\boldsymbol{G} = 0$.

In order to generalize the previous approach, it is considered now the substitution (2.98) for an arbitrary strictly positive power k of the tensor $g\boldsymbol{I} + \boldsymbol{G}$. In the principal reference frame of $\boldsymbol{G}$, the elasticity tensor becomes:

$$\begin{aligned}
\mathbb{S}\left(g, \boldsymbol{G}\right) = &\left(\lambda_c + 2\mu_c\right) m_i^{2k} \left(\boldsymbol{G}_i \otimes \boldsymbol{G}_i\right) \\
&+ \lambda_c m_i^k m_j^k \left(\boldsymbol{G}_i \otimes \boldsymbol{G}_j + \boldsymbol{G}_j \otimes \boldsymbol{G}_i\right) \\
&+ 2\mu_c m_i^k m_j^k \left(\boldsymbol{G}_i \underline{\overline{\otimes}} \boldsymbol{G}_j + \boldsymbol{G}_j \underline{\overline{\otimes}} \boldsymbol{G}_i\right)
\end{aligned} \tag{2.102}$$

where $m_i = g + g_i$. The coefficient exhibit the more general form:

$$\begin{aligned}
\lambda_{ii} &= \left(\lambda_c + 2\mu_c\right) m_i^{2k}, \quad \forall i, \\
\lambda_{ij}^* &= \lambda_c m_i^k m_j^k, \quad \forall i, j \ \ (i < j), \\
\mu_{ij} &= \mu_c m_i^k m_j^k, \quad \forall i, j \ \ (i < j).
\end{aligned} \tag{2.103}$$

In this case, the anisotropic elastic behaviour of the material is completely described by the two constants λ_c and μ_c, the exponent k and the fabric tensor $\{g, \boldsymbol{G}\}$ and the overall elasticity tensor assumes the form:

$$\mathbb{S} = \begin{pmatrix}
\left(\lambda_c + 2\mu_c\right) m_1^{2k} & \lambda_c m_1^k m_2^k & \lambda_c m_1^k m_3^k & 0 & 0 & 0 \\
\lambda_c m_2^k m_1^k & \left(\lambda_c + 2\mu_c\right) m_2^{2k} & \lambda_c m_2^k m_3^k & 0 & 0 & 0 \\
\lambda_c m_3^k m_1^k & \lambda_c m_3^k m_2^k & \left(\lambda_c + 2\mu_c\right) m_3^{2k} & 0 & 0 & 0 \\
0 & 0 & 0 & 2\mu_c m_2^k m_3^k & 0 & 0 \\
0 & 0 & 0 & 0 & 2\mu_c m_3^k m_1^k & 0 \\
0 & 0 & 0 & 0 & 0 & 2\mu_c m_1^k m_2^k
\end{pmatrix}. \tag{2.104}$$

CHAPTER III

THEORY OF HOMOGENIZATION

1. THERMODYNAMIC FRAMEWORK AND MATHEMATICALLY WELL-POSED HOMOGENIZATION APPROACHES

Homogenization is the modelling of a heterogeneous medium by means of a *unique* continuous medium. A heterogeneous medium is a medium of which material properties (e. g., elasticity coefficients) vary pointwise in a continuous or discontinuous manner, in a periodic or nonperiodic way, deterministically or randomly. While, obviously, homogenization is a modelling technique that applies to all fields of macroscopic physics governed by nice partial differential equations, we focus more particularly on the mechanics of deformable bodies.

1.5. Representative Volume Element (RVE)

Two different scales are used in the description of heterogeneous media. One of these is a **macroscopic** (x) scale at which homogeneities are weak. The other one is the scale of inhomogeneities and is referred to as the **microscopic** (y) scale. The latter defines the size of the representative volume element (Fig. 3.1). The basic cell of a periodic composite is an example of RVE.

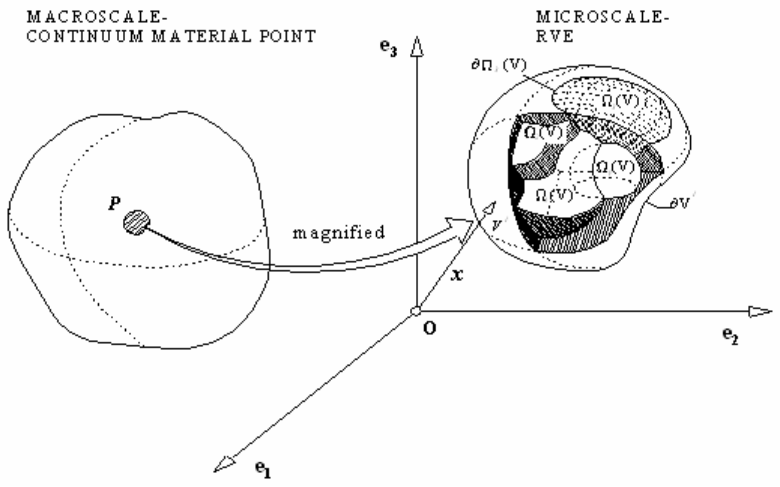

Fig. 3.1.
Representative Volume Element

From the experimental point of view, we can say that there exists a kind of statistical homogeneity in the sense that any RVE at a specific point looks very much like any other RVE taken at random at another point.
The mathematical problem presents itself in the following manner. Let $\boldsymbol{\sigma}(y)$ and $\boldsymbol{\varepsilon}(y)$ be the stress and strain at the micro scale in the framework of small-perturbation hypothesis. We denote by $\boldsymbol{\Sigma}$ and $\mathbf{E}$ the same notion at the macro scale. Let $\langle ... \rangle$ indicate the *averaging operator*. For a volume averaging we have

$$\begin{aligned} \boldsymbol{\Sigma}(\boldsymbol{x}) &= \langle \boldsymbol{\sigma} \rangle = \frac{1}{|V|} \int_V \boldsymbol{\sigma}(x, y)\, dy \\ \mathbf{E}(\boldsymbol{x}) &= \langle \boldsymbol{\varepsilon} \rangle = \frac{1}{|V|} \int_V \boldsymbol{\varepsilon}(x, y)\, dy \end{aligned} \tag{3.1}$$

where V is the volume of the RVE.
It is important to notice that any quantity that is an additive function is averaged in the micro-macro transition. Thus, if $\overline{\rho} = \langle \rho \rangle$ denotes the averaged density, then we have

$$\begin{aligned} \overline{\rho} E &= \langle \rho e \rangle, \quad \text{internal energy,} \\ \overline{\rho} S &= \langle \rho \eta \rangle, \quad \text{entropy,} \\ \Phi &= \langle \phi \rangle, \quad \text{dissipation.} \end{aligned} \tag{3.2}$$

1.2. Localization Problem

We can state the following

- the process that relates $(\boldsymbol{\Sigma}, \mathbf{E})$ by means of equations (3.1) and (3.2) and the microscopic constitutive equations is called **homogenization**;
- the inverse process that consists in determining $\boldsymbol{\sigma}(y)$ and $\boldsymbol{\varepsilon}(y)$ from $\boldsymbol{\Sigma}$ and $\mathbf{E}$ is called **localization**.

Therefore, the data are $\boldsymbol{\Sigma}$ and $\mathbf{E}$ in the localization process which corresponds to the following problem:

$$(\mathscr{P}\mathscr{L}) \begin{cases} \langle \boldsymbol{\sigma} \rangle = \boldsymbol{\Sigma} \\ \langle \boldsymbol{\varepsilon} \rangle = \mathbf{E} \\ \operatorname{div} \boldsymbol{\sigma} = \mathbf{0} \end{cases} \tag{3.3}$$

This problem is original, because of the following two reasons:

i. the load is the averaged value of a field and not a prescription at points in the bulk or at a limiting surface;
ii. there are *no* boundary conditions.

It follows from (ii) that the problem (3.3) is *ill-posed*. The missing boundary condition must, in some way, reproduce the internal state of the RVE in the most satisfactory manner. They therefore depend on the choice of RVE, more specifically on its size. As a rule, different choices of RVE will provide different macroscopic laws.

The following give some examples of boundary conditions:

$$\boldsymbol{\sigma}\cdot\boldsymbol{n}=\boldsymbol{\Sigma}\cdot\boldsymbol{n} \quad \text{on } \partial V \quad - \quad \text{uniform traction on } \partial V\ ; \tag{3.4}$$

$$\boldsymbol{u}=\mathbf{E}\cdot\boldsymbol{y} \quad \text{on } \partial V \quad - \quad \text{uniform traction on } \partial V\ . \tag{3.5}$$

With this and $\operatorname{div}\boldsymbol{\sigma}=\mathbf{0}$, in V, it is verified that (3.1) holds good. Indeed, for (3.5) we have

$$\frac{1}{2}\int_V\left(\frac{\partial u_i}{\partial y_j}+\frac{\partial u_j}{\partial y_i}\right)dv=\frac{1}{2}\int_{\partial V}\left(u_i n_j+u_j n_i\right)ds=\frac{1}{2}\int_{\partial V}\left(\mathrm{E}_{ik}\,y_k n_j+\mathrm{E}_{jk}\,y_k n_i\right)ds \tag{3.6}$$

or

$$\left\langle\boldsymbol{\varepsilon}(\boldsymbol{u})\right\rangle=\mathbf{E} \tag{3.7}$$

The proof for (3.4) is self-evident.

The above reasoning does not apply to the case of a periodic structure. In that case, $\boldsymbol{\sigma}$ and $\boldsymbol{\varepsilon}$ are locally periodic (they are only quasi-periodic for a large sample) and the periodicity condition read as follows:

- the traction $\boldsymbol{\sigma}\cdot\boldsymbol{n}$ are opposite on opposite faces of ∂V (where $\boldsymbol{n}$ corresponds to $-\boldsymbol{n}$);
- the local strain $\boldsymbol{\varepsilon}(\boldsymbol{u})$ is made of two part, the mean $\mathbf{E}$ and the fluctucation part $\boldsymbol{\varepsilon}(\boldsymbol{u}^*)$ such that

$$\boldsymbol{\varepsilon}(\boldsymbol{u})=\mathbf{E}+\boldsymbol{\varepsilon}(\boldsymbol{u}^*),\quad \left\langle\boldsymbol{\varepsilon}(\boldsymbol{u}^*)\right\rangle=0\,, \tag{3.8}$$

where $\boldsymbol{u}^*$ can be shown to be periodic. Therefore, the condition are

$$\begin{cases}\boldsymbol{\sigma}\cdot\boldsymbol{n} & \text{is antiperiodic,}\\ \boldsymbol{u}=\mathbf{E}\cdot\boldsymbol{y}+\boldsymbol{u}^*,\boldsymbol{u}^* & \text{periodic.}\end{cases} \tag{3.9}$$

On account of (3.4), (3.5) and (3.9), the problem (3.3) now is theoretically well-posed, but this must be verified for each constitutive behaviour.

1.3. The Hill-Mandel principle of macrohomogeneity

Let $\bar{\boldsymbol{\sigma}}$ and $\bar{\boldsymbol{u}}$ be, respectively, a statistically admissible (SA) stress field and a kinematically admissible (KA) displacement field. Then it is possible to prove that

$$\left\langle \bar{\boldsymbol{\sigma}} : \boldsymbol{\varepsilon}\left(\bar{\boldsymbol{u}}\right)\right\rangle = \bar{\boldsymbol{\Sigma}} : \bar{\mathbf{E}} . \tag{3.10}$$

The remarkable expression (3.10) is called the *prinpiple of macrohomogeneity of Hill and Mandel* (Hill, 1965a, Mandel 1971) or the *Hill-Mandel* relation between micro and macro scales. In statistical theories this condition is viewed as an ergodic hypothesis. This condition, in fact, plays in the end a much more important role than the boundary conditions applied at the RVE.

1.4. The example of pure elasticity

In this section the localization problem in the case of *anisotropic linear elastic* components are examined.

1.4.a. The localization problem

This problem is written in the following form (here $\mathbb{C}(y)$ is the tensor of elasticity coefficient at the micro scale):

$$\begin{cases} \boldsymbol{\sigma}(y) = \mathbb{C}(y) : \boldsymbol{\varepsilon}(y) = \mathbb{C}(y) : \left[\mathbf{E} + \boldsymbol{\varepsilon}\left(\boldsymbol{u}^*(y)\right)\right] \\ \operatorname{div}\boldsymbol{\sigma} = \mathbf{0} \\ \text{boundary conditions} \end{cases} \tag{3.11}$$

where $\mathbf{E}$ or $\boldsymbol{\Sigma}$ is prescribed. Accordingly, the fluctuation displacement $\boldsymbol{u}^*$ is the solution of the following problem:

$$\begin{cases} \operatorname{div}\left(\mathbb{C} : \boldsymbol{\varepsilon}\left(\boldsymbol{u}^*\right)\right) = -\operatorname{div}\left(\mathbb{C} : \mathbf{E}\right) \\ \text{boundary conditions} \end{cases} \tag{3.12}$$

Whenever $\mathbf{E}$ is constant for each constituent component, it can be shown that

$$\operatorname{div}\left(\mathbb{C} : \mathbf{E}\right) = \left(\left[\!\left[\mathbb{C}\right]\!\right] : \mathbf{E}\right)\boldsymbol{n}\delta(S), \tag{3.13}$$

where $[\![\mathbb{C}]\!] = \mathbb{C}^+ - \mathbb{C}^-$, $\delta(S)$ is Dirac's distribution, and $\boldsymbol{n}$ is the unit normal oriented from the '$-$' to the '$+$' side of the surface S separating components. Then we can state the following:

Proposition. Under classical working hypotheses applying to $\mathbb{C}$ (symmetry and positivity), the problem (3.12) admits a unique solution for all three types of boundary condition.

To prove this we must distinguish whether it is $\mathbf{E}$ or $\boldsymbol{\Sigma}$ which is prescribed.

1.4.b. Case where $\mathbf{E}$ *is prescribed*

For the existence and uniqueness proofs one can see Suquet (1981b). We shall only give the representation of the solution. As the problem is linear, the solution $\boldsymbol{\varepsilon}(\boldsymbol{u}^*)$ depends linearly on the prescribed field $\mathbf{E}$. The latter can be decomposed into six elementary states of macroscopic strains (stretch in three directions and three shears). Let $\boldsymbol{\varepsilon}(\boldsymbol{\chi}_{kl})$ be the fluctation strain field induced by these six elementary states at the microscopic level. The solution $\boldsymbol{\varepsilon}(\boldsymbol{u}^*)$ for a general macrostrain $\mathbf{E}$ is the superposition of the six elementary solutions, so that we can write (summation over k and l)

$$\boldsymbol{\varepsilon}(\boldsymbol{u}^*) = \mathrm{E}_{kl}\boldsymbol{\varepsilon}(\boldsymbol{\chi}_{kl}). \tag{3.14}$$

In all we have

$$\boldsymbol{\varepsilon}(\boldsymbol{u}) = \mathbf{E} + \boldsymbol{\varepsilon}(\boldsymbol{u}^*) = \mathbf{E}\big(\mathbf{I} + \boldsymbol{\varepsilon}(\boldsymbol{\chi})\big) \tag{3.15}$$

or, in components,

$$\varepsilon_{ij}(\boldsymbol{u}) = D_{ijkl}\mathrm{E}_{kl} = (\boldsymbol{D} : \mathbf{E})_{ij} \tag{3.16}$$

where

$$D_{ijkl} = I_{ijkl} + \varepsilon_{ij}(\boldsymbol{\chi}_{kl}) \tag{3.17}$$

Here $I_{klij} = \frac{1}{2}\big(\delta_{ik}\delta_{jl} + \delta_{il}\delta_{jk}\big)$ is the tensorial representation in $\mathbb{R}^3$ of the unity of $\mathbb{R}^6$ and D_{ijkl} is called, depending on the author, the **tensor of strain localization**, or **tensor of concentrations** (Mandel, 1971) or the **tensor of influence** (Hill, 1967).

Homogenization
We can write in an obvious manner

$$\boldsymbol{\Sigma} = \langle \boldsymbol{\sigma} \rangle = \langle \mathbb{C} : \boldsymbol{\varepsilon}(\boldsymbol{u}) \rangle = \langle \mathbb{C} : \boldsymbol{D} : \mathbf{E} \rangle = \langle \mathbb{C} : \boldsymbol{D} \rangle : \mathbf{E} \tag{3.18}$$

so that

$$\boldsymbol{\Sigma} = \mathbb{C}^{\text{hom}} : \mathbf{E}, \quad \mathbb{C}^{\text{hom}} = \langle \mathbb{C} : \boldsymbol{D} \rangle . \tag{3.19}$$

We note that

$$\langle \boldsymbol{D} \rangle = \boldsymbol{I} , \quad \langle \boldsymbol{D}^T \rangle = \boldsymbol{I} .$$

Equation $(3.19)_2$ shows that the tensor of 'macro' elasticity coefficients is obtained by taking the average of 'micro' elasticity coefficients, the latter being *weighted* by the tensor of strain localization. It is possible to prove that the tensor $\mathbb{C}^{\text{hom}}$ is symmetric. For a direct proof we compute $\langle \boldsymbol{D}^T : \bar{\boldsymbol{\sigma}} \rangle$ for an admissible field $\bar{\boldsymbol{\sigma}}$, obtaining thus

$$\langle \boldsymbol{D}^T : \bar{\boldsymbol{\sigma}} \rangle_{ij} = \langle D^T_{ijkl} : \bar{\sigma}_{kl} \rangle = \langle \left[I_{ijkl} + \varepsilon_{kl}(\chi_{ij}) \right] \bar{\sigma}_{kl} \rangle = \bar{\Sigma}_{ij}$$

i.e.,

$$\boldsymbol{\Sigma} = \langle \boldsymbol{D}^T : \boldsymbol{\sigma} \rangle = \langle \boldsymbol{D}^T : \mathbb{C} : \boldsymbol{\varepsilon}(\boldsymbol{u}) \rangle = \langle \boldsymbol{D}^T : \mathbb{C} : \boldsymbol{D} \rangle : \mathbf{E} ,$$

so that

$$\mathbb{C}^{\text{hom}} = \langle \boldsymbol{D}^T : \mathbb{C} : \boldsymbol{D} \rangle , \tag{3.20}$$

which is symmetric.

1.4.c. Case where $\boldsymbol{\Sigma}$ is prescribed

The localization problem than reads

$$\begin{cases} \boldsymbol{\varepsilon}(\boldsymbol{u}) = \boldsymbol{\varepsilon}(\boldsymbol{u}^*) + \mathbf{E} = \mathbb{S} : \boldsymbol{\sigma} \\ \operatorname{div} \boldsymbol{\sigma} = \mathbf{0} \\ \langle \boldsymbol{\sigma} \rangle = \boldsymbol{\Sigma} \\ \text{boundary conditions} \end{cases} \tag{3.21}$$

where $\mathbb{S}$ is the tensor of the 'micro' elastic compliance and $\mathbf{E}$ is an unknown. The existence and uniqueness of the solution may be proved (Suquet, 1981b). Thus, here, we assume that a unique solution $\boldsymbol{\sigma}$ exists. This solution depends linearly on data by virtue of the linearity of the problem. Let us call S_{kl} the solution of the problem (3.21) for the datum $\boldsymbol{\Sigma} = \boldsymbol{I}_{kl}$ - note that $I_{ijkl} = (\boldsymbol{I}_{kl})_{ij}$.
Then the general solution, obtained by superposition, is written

$$\begin{aligned} &\boldsymbol{\sigma} = \boldsymbol{A} : \boldsymbol{\Sigma}, \quad \text{i.e.,} \quad \boldsymbol{\sigma}(y) = \Sigma_{kl} A_{kl}(y), \\ &\text{or} \quad \sigma_{ij} = A_{ijkl} \Sigma_{kl}, \quad A_{ijkl} = (\boldsymbol{A}_{kl})_{ij}, \end{aligned} \tag{3.22}$$

***where A is the* tensor of stress localization.**
The homogenized compliance tensor $\mathbb{S}^{\text{hom}}$ is evaluated thus. We have directly

$$\mathbf{E} = \langle \boldsymbol{\varepsilon}(\boldsymbol{u}) \rangle = \langle \mathbb{S} : \boldsymbol{\sigma} \rangle = \langle \mathbb{S} : \boldsymbol{A} \rangle : \boldsymbol{\Sigma} = \mathbb{S}^{\text{hom}} : \boldsymbol{\Sigma}, \tag{3.23}$$

whence

$$\mathbb{S}^{\text{hom}} = \langle \mathbb{S} : \boldsymbol{A} \rangle. \tag{3.24}$$

We note that

$$\langle \boldsymbol{A}^{\mathrm{T}} \rangle = \boldsymbol{I}, \tag{3.25}$$

and for any admissible field $\langle \boldsymbol{\varepsilon}(\bar{\boldsymbol{u}}) \rangle$ we can write

$$\langle \boldsymbol{A}^{\mathrm{T}} : \boldsymbol{\varepsilon}(\bar{\boldsymbol{u}}) \rangle_{ij} = \langle A^{\mathrm{T}}_{ijkl} \, \varepsilon_{kl}(\bar{\boldsymbol{u}}) \rangle = \langle (A_{ij})_{kl} \, \varepsilon_{kl}(\bar{\boldsymbol{u}}) \rangle = \langle (A_{ij})_{kl} \rangle \langle \varepsilon_{kl}(\bar{\boldsymbol{u}}) \rangle = \bar{\mathrm{E}}_{ij}$$

so that

$$\mathbf{E} = \langle \boldsymbol{A}^{\mathrm{T}} : \boldsymbol{\varepsilon}(\boldsymbol{u}) \rangle = \langle \boldsymbol{A}^{\mathrm{T}} : \mathbb{S} : \boldsymbol{\sigma} \rangle = \langle \boldsymbol{A}^{\mathrm{T}} : \mathbb{S} : \boldsymbol{A} \rangle : \boldsymbol{\Sigma},$$

hence

$$\mathbb{S}^{\text{hom}} = \left\langle \boldsymbol{A}^{\mathrm{T}} : \mathbb{S} : \boldsymbol{A} \right\rangle \tag{3.26}$$

and thus $\mathbb{S}^{\text{hom}}$ is symmetric.

1.4.d. Equivalence between 'prescribed stress' and 'prescribed strain'

First we note that $\mathbb{C}^{\text{hom}}$ and $\mathbb{S}^{\text{hom}}$ are *inverse* tensors (in $\mathbb{R}^6$) of one another if they correspond to the *same* choice of boundary conditions in the localization problem. Indeed, using the symmetry of $\mathbb{C}^{\text{hom}}$ we can write

$$\mathbb{C}^{\text{hom}} : \mathbb{S}^{\text{hom}} = \left(\mathbb{C}^{\text{hom}}\right)^{T} : \mathbb{S}^{\text{hom}} = \left\langle \boldsymbol{D}^{T} : \mathbb{C} \right\rangle : \left\langle \mathbb{S} : \boldsymbol{A} \right\rangle \tag{3.27}$$

in which the first factor is an admissible stress field (from the definition of $\boldsymbol{D}$ and $\boldsymbol{A}$) and the second factor is an admissible strain field. The principle (3.10) therefore applies and we can write $\left(\mathbb{C} : \mathbb{S} = \mathbb{I}\right)$

$$\mathbb{C}^{\text{hom}} : \mathbb{S}^{\text{hom}} = \left\langle \boldsymbol{D}^{T} : \mathbb{C} : \mathbb{S} : \boldsymbol{A} \right\rangle = \left\langle \boldsymbol{D}^{T} : \boldsymbol{A} \right\rangle = \left\langle \boldsymbol{D}^{T} \right\rangle : \left\langle \boldsymbol{A} \right\rangle = \boldsymbol{I} . \tag{3.28}$$

However, if *different* boundary conditions are used, one then has the estimate of Hill (1967) and Mandel (1971),

$$\mathbb{C}^{\text{hom}} : \mathbb{S}^{\text{hom}} = \mathbb{I} + O\left(\left(d/l\right)^{3}\right), \tag{3.29}$$

where $\mathbb{C}^{\text{hom}}$ is evaluated by using the condition (3.5), while $\mathbb{S}^{\text{hom}}$ is computed through use of the condition (3.4), d is a characteristic size of an inhomogeneity and l is the typical size of the RVE. If $l \gg d$, then the choice of boundary condition is hardly important. For *periodic* media where $d/l = O(1)$, this choice is most important.

2. COMPOSITE HETEROGENEOUS MATERIALS: DERIVATION OF COMPLIANCE AND STIFFNESS TENSORS

The overall properties of a composite material depends not only upon the constitutive properties of each phases, but also on the microstructural architecture and define a relationship between the overall field variables – such as the deformation and the stress. The determination of the overall deformation

and stress obviously needs of the preventive determination of the deformation and stress, and than the solution of an elastic PDE problem which involves the equilibrium, compatibility and constitutive equations of each phase, as well as the continuity conditions of the interphase. In other words, between two different phases – called here (1) and (2) – it must results

$$\boldsymbol{u}^{(1)} = \boldsymbol{u}^{(2)}, \quad \boldsymbol{\sigma}^{(1)}\boldsymbol{n} = \boldsymbol{\sigma}^{(2)}\boldsymbol{n} \tag{3.30}$$

being $\boldsymbol{u}^{(i)}$ the displacement field of the *i*-phase, $\boldsymbol{\sigma}^{(i)}$ the stress field of the *i*-phase and $\boldsymbol{n}$ is the outer normal vector of a point on the interphase. From such procedure – which may be see as a direct approach to the homogenization problem – seems clear that the homogenized properties depend upon the microstructure architecture. Consequently, this procedure is often extremely difficult to apply because of the equations (3.30), and may be developed only in vary particular – and often ideal – cases.
In the following section, alternative approaches to determine the overall properties of composite materials are presented. In particular, the **direct approach** requires the exact evaluation of the microscopic fields for some specific geometries, and so it is the more efficient, the more the microstructural geometry is similar to that one used in the model.
The **variational approaches** are always able to furnish upper and lower bounds of the overall properties of the composite materials. In particular, such approaches are the only ones that may solve the homogenization problem when the microstructural geometries are particular irregular or not completely known. Obviously, the wider the range defined by the upper and lower bounds gets, the less the practical utility of these methods is.

2.1. Direct Methods – Eshelby solution

Let consider an homogeneous, linearly elastic and infinitely extended medium, subjected to a uniform prescribed strain $\mathbf{E}^*$ on the domain Ω. Generally, the resulting strain $\mathbf{E}$ is variable on Ω, but Eshelby proved that if Ω is an ellipsoid then the resulting strain $\mathbf{E}$ and hence the stress $\mathbf{T}$, are also uniform in Ω, the former being given by

$$\mathbf{E} = \mathbb{P}\mathbf{E}^* \tag{3.31}$$

where the four-order tensor $\mathbb{P}$ is called Eshelby's tensor and it shows the following propeties:

- it is symmetric with respect to the first two indices and the second two indices, $P_{ijkl} = P_{jikl} = P_{ijlk}$, while, in general, it is not symmetric with respect to the exchange of ij and kl, i. e., in general, $P_{ijkl} \neq P_{klij}$;
- it is independent of the material properties of the inclusion Ω;

- it is completely defined in terms of the aspect ratios of the ellipsoidal inclusion Ω, and the elastic parameters of the surrounding matrix;
- when the surrounding matrix is isotropic, then $\mathbb{P}$ depends only on the Poisson's ratio of the matrix and the aspect ratios of Ω.

In the following this results is proving in the case of isotropic matrix with Poisson's ratio ν and shear modulus μ.

Let

$$u_i(\boldsymbol{x}) = -C_{jkmn}\varepsilon^*_{mn}\int_\Omega G_{ij/k}(\boldsymbol{x}-\boldsymbol{x}')\,d\boldsymbol{x}' \tag{3.32}$$

be the solution of the PDE problem of the considered problem, where the Green function $\boldsymbol{G}(\boldsymbol{x}-\boldsymbol{x}')$ for the homogeneous and isotropic medium is

$$\boldsymbol{G}(\boldsymbol{x}-\boldsymbol{x}') = \frac{1}{16\pi\mu(1-\nu)}\left[\frac{(3-4\nu)\boldsymbol{I}}{|\boldsymbol{x}-\boldsymbol{x}'|} + \frac{(\boldsymbol{x}-\boldsymbol{x}')\otimes(\boldsymbol{x}-\boldsymbol{x}')}{|\boldsymbol{x}-\boldsymbol{x}'|^3}\right] \tag{3.33}$$

where $\boldsymbol{I}$ is the second order identity tensor. Being Ω an ellipsoid of equation

$$\frac{x_1^2}{a_1^2} + \frac{x_2^2}{a_2^2} + \frac{x_3^2}{a_3^2} \le 1 \tag{3.34}$$

through simple algebraic manipulation it result

$$u_i(\boldsymbol{x}) = \frac{-\varepsilon^*_{jk}}{8\pi(1-\nu)}\int_\Omega g_{ijk}(\boldsymbol{l})\frac{d\boldsymbol{x}'}{|\boldsymbol{x}-\boldsymbol{x}'|^2} \tag{3.35}$$

where

$$g_{ijk}(\boldsymbol{l}) = (1-2\nu)\left(\delta_{ij}l_k + \delta_{ik}l_j - \delta_{jk}l_i\right) + 3l_il_jl_k \tag{3.36}$$

being $\boldsymbol{l}$ the versor of $(\boldsymbol{x}'-\boldsymbol{x})/|\boldsymbol{x}'-\boldsymbol{x}|$.

By assuming that the point $\boldsymbol{x}$ is inside the region Ω, the integral into the (3.35) may be explicitly calculated. To achieve this goal, the volume element $d\boldsymbol{x}'$ may be written as $r^2 dr d\omega$, being $r = |\boldsymbol{x}-\boldsymbol{x}'|$ and $d\omega$ the superficial element of a unit sphere centred in $\boldsymbol{x}$. The integration of the (3.35) with respect to *r*, yields

$$u_i(\boldsymbol{x}) = \frac{-\varepsilon^*_{jk}}{8\pi(1-\nu)}\int_\Sigma r(\boldsymbol{l})\,g_{ijk}(\boldsymbol{l})\,d\omega\,, \tag{3.37}$$

where $r(\boldsymbol{l})$ is the positive root of

$$\left(x_1 + rl_1\right)^2 / a_1^2 + \left(x_2 + rl_1\right)^2 / a_2^2 + \left(x_3 + rl_3\right)^2 / a_3^2 = 1, \tag{3.38}$$

that is

$$r(\boldsymbol{l}) = -f/g + \sqrt{f^2/g^2 + e/g} \tag{3.39}$$

with

$$\begin{aligned} g &= l_1^2/a_1^2 + l_2^2/a_2^2 + l_3^2/a_3^2 \\ f &= l_1 x_1/a_1^2 + l_2 x_2/a_2^2 + l_3 x_3/a_3^2 \\ e &= 1 - x_1^2/a_1^2 - x_2^2/a_2^2 - x_3^2/a_3^2. \end{aligned} \tag{3.40}$$

By posing $\lambda_i = l_i/a_i^2$, the (3.37) becomes

$$u_i(\boldsymbol{x}) = \frac{x_m \varepsilon_{jk}^*}{8\pi(1-\nu)} \int_\Sigma \frac{\lambda_m g_{ijk}}{g} d\omega \tag{3.41}$$

from which the strain inside Ω may be calculated

$$\varepsilon_{ij}(\boldsymbol{x}) = \frac{\varepsilon_{mn}^*}{16\pi(1-\nu)} \int_\Sigma \frac{\lambda_i g_{jmn} + \lambda_j g_{imn}}{g} d\omega \tag{3.42}$$

which depends upon $\boldsymbol{x} \in \Omega$.
So, the components of Eshelby's tensor $\mathbb{P}$ introduced in the equation (3.31) are:

$$\begin{aligned} P_{1111} &= \frac{3}{8\pi(1-\nu)} a_1^2 I_{11} + \frac{1-2\nu}{8\pi(1-\nu)} I_1 \\ P_{1122} &= \frac{1}{8\pi(1-\nu)} a_2^2 I_{12} - \frac{1-2\nu}{8\pi(1-\nu)} I_1 \\ P_{1133} &= \frac{1}{8\pi(1-\nu)} a_3^2 I_{13} - \frac{1-2\nu}{8\pi(1-\nu)} I_1 \\ P_{1212} &= \frac{a_1^2 + a_2^2}{16\pi(1-\nu)} I_{12} + \frac{1-2\nu}{16\pi(1-\nu)} (I_1 + I_2) \end{aligned} \tag{3.43}$$

with

$$I_1 = \int_\Sigma \frac{l_1^2}{a_1^2 g} d\omega$$
$$I_{11} = \int_\Sigma \frac{l_1^4}{a_1^4 g} d\omega \tag{3.44}$$
$$I_{12} = 3\int_\Sigma \frac{l_1^2 l_2^2}{a_1^2 a_2^2 g} d\omega.$$

All the other non-zero components may be obtained through a cyclic permutation of the indexes (1, 2, 3).
Such solution may be particularized for many cases of practical interest. By means of the solution (3.43), it is possible to determine the concentration strain tensor in an ellipsoidal inclusion of elasticity tensor $\mathbb{C}^{(2)}$ embedded in a homogeneous, isotropic and infinitely extended medium of elasticity tensor $\mathbb{C}^{(1)}$. Then, under the uniform strain field $\mathbf{E}^0$, the medium, supposed homogeneous, would be subjected to a uniform stress $\mathbf{T} = \mathbb{C}^{(1)}\mathbf{E}^0$. This uniform stress field is perturbed by the presence of the inclusion. But the stress field $\mathbf{T}^{(2)} = \mathbb{C}^{(2)}\mathbf{E}^{(2)}$ in a generic point of the inclusion is the same that we would have in the inclusion imagining to substitute the inclusion with the matrix subjected to $\mathbf{E}^0$ as well as to the strain $\mathbf{E}^*$, such as

$$\mathbb{C}^{(2)}\mathbf{E}^{(2)} = \mathbb{C}^{(1)}\left(\mathbf{E}^{(2)} - \mathbf{E}^*\right). \tag{3.45}$$

As proved by Eshelby, a uniform strain $\mathbf{E}^*$ applied on an ellipsoidal region yields – as unique equilibrated and compatible solution – a uniform strain in the region given by the equation (3.31). In this case, being also $\mathbf{E}^0$, it results

$$\mathbf{E}^{(2)} = \bar{\mathbf{E}}^{(2)} = \mathbf{E}^0 + \mathbb{P}\mathbf{E}^*. \tag{3.46}$$

The (3.46) and (3.45), yield

$$\mathbf{E}^{(2)} = \left[\mathbb{I} + \mathbb{P}\left(\mathbb{C}^{(1)}\right)^{(-1)}\left[\mathbb{C}^{(2)} - \mathbb{C}^{(1)}\right]\right]^{-1}\mathbf{E}^0. \tag{3.47}$$

Being $\mathbf{E}^{(2)}$ uniform in Ω, the concentration strain tensor into the inclusion is

$$\mathbb{A}^{(2)} = \left[\mathbb{I} + \mathbb{P}\left(\mathbb{C}^{(1)}\right)^{(-1)}\left[\mathbb{C}^{(2)} - \mathbb{C}^{(1)}\right]\right]^{-1}. \tag{3.48}$$

2.2. Variational Methods – Hashin Shtrikman Variational Principle

The homogenization problem of an heterogeneous RVE is equivalent to solve one of the following variational problems:

$$\begin{aligned}\frac{1}{2}\bar{\mathbb{C}}\bar{\mathbf{E}}\cdot\bar{\mathbf{E}} &= \inf_{E^d\in E}\frac{1}{V}\int_V\frac{1}{2}\mathbb{C}\left(\bar{\mathbf{E}}+\mathbf{E}^d\right)\cdot\left(\bar{\mathbf{E}}+\mathbf{E}^d\right)dV \\ \frac{1}{2}\bar{\mathbb{S}}\bar{\mathbf{T}}\cdot\bar{\mathbf{T}} &= \inf_{T^d\in T}\frac{1}{V}\int_V\frac{1}{2}\mathbb{S}\left(\bar{\mathbf{T}}+\mathbf{T}^d\right)\cdot\left(\bar{\mathbf{T}}+\mathbf{T}^d\right)dV\end{aligned} \tag{3.49}$$

where: $\mathbf{E}$ is compatible periodic strain field space, whose average value is equal to zero, $\mathbf{T}$ is equilibrated periodic stress field space, whose average value is equal to zero, $\bar{\mathbb{C}}$ is homogenized stiffness tensor, $\bar{\mathbb{S}}$ is homogenized compliance tensor, $\bar{\mathbf{T}}$ is the generic symmetric stress field, and $\bar{\mathbf{E}}$ is the generic symmetric strain field.
The first members of the $(3.49)_1$ and $(3.49)_2$ represent the elastic energy density and the complementary energy density of the homogenized material. In particular, solving the first problem of the $(3.49)_1$ is equivalent to determine, among the compatible strain fields, whose prescribed average value is $\bar{\mathbf{E}}$, the sole one that is also equilibrated. On the contrary, solving the $(3.49)_2$ is equivalent of determining, among the equilibrated stress fields, whose prescribed average value is $\bar{\mathbf{T}}$, the sole one that is also compatible.
It is possible to demonstrate that, if the stiffness tensor $\mathbb{C}$. and the compliance one $\mathbb{S}$. have, uniformly in V, all the eigenvalues lower down bounded by a positive constant, then the equations (3.49) admit one and only one solution.
Since the functionals in the first members of the (3.49) are conjugate each other, (Giangreco, 2003), it follows that the homogenized properties of the material are well defined, hence:

$$\bar{\mathbb{S}} = \bar{\mathbb{C}}^{-1}. \tag{3.50}$$

In this framework, the basic physic idea of the Hashin and Shtrikman's principles is to substitute the heterogeneous medium with a reference homogeneous one, having a stiffness tensor, $\mathbb{C}^H$, and a compliance tensor, $\mathbb{S}^H$.
In order to simulate the actual micro-structure, eigenstress and eigenstrain fields are prescribed on the reference homogeneous medium, as already seen in the previous section. So, the Hashin and Shtrikman's variational principles are characterized from two tumbled variational problems:

- the first problem, defined as auxiliary problem, is related to the elastostatic response of the reference homogeneous solid, subjected to a prescribed field of polarization (eigenstress or eigenstrain);

- the second problem, defined as optimization problem, has the objective to found the unknown field of polarization.

In the follows, the four classic Hashin and Shtrikman's variational principles are reported. It is worth to underline that two of these are minimum principles, while the other two are saddle principles. Obviously, the minimum principles are particularly useful, because each numeric approximation of them, for example by using the Finite Element Method, represents an upper estimation of the solution.

In particular, consider a reference homogeneous material which is more deformable than each phase included in the heterogeneous RVE, such that $\mathbb{C}-\mathbb{C}^H$ is positive definite everywhere in *V*. Hence, the following identity is verified:

$$\int_V \left(\frac{1}{2}\mathbb{C}\,\mathbf{E}\cdot\mathbf{E}-\frac{1}{2}\mathbb{C}^H\,\mathbf{E}\cdot\mathbf{E}\right)dV=\sup_{\mathbf{T}^*\in\mathbf{H}}\left\{\int_V \mathbf{T}^*\cdot\mathbf{E}-\frac{1}{2}\left(\mathbb{C}-\mathbb{C}^H\right)\mathbf{T}^*\cdot\mathbf{T}^*dV\right\} \quad (3.51)$$

where $\mathbf{H}$ is the space of symmetric second-order periodic tensors, $\mathbf{T}^*$ is polarization field (eigenstress) prescribed on the reference homogeneous medium in order to simulate the actual micro-structure of the heterogeneous RVE.

In particular, by taking:

$$\mathbf{E}=\overline{\mathbf{E}}+\hat{\mathbf{E}} \quad (3.52)$$

where $\overline{\mathbf{E}}\in Sym$ and $\hat{\mathbf{E}}\in\mathbf{E}$, and by remembering that $\mathbb{C}^H$ is constant in *V*, the (3.51) assumes the following form:

$$\begin{aligned}&\int_V\left[\frac{1}{2}\mathbb{C}\left(\overline{\mathbf{E}}+\hat{\mathbf{E}}\right)\left(\overline{\mathbf{E}}+\hat{\mathbf{E}}\right)-\frac{1}{2}\mathbb{C}^H\overline{\mathbf{E}}\cdot\overline{\mathbf{E}}\right]dV=\\&=\sup_{\mathbf{T}^*\in\mathbf{H}}\left\{\int_V\left[\left\langle\mathbf{T}^*\right\rangle\cdot\overline{\mathbf{E}}-\frac{1}{2}\left(\mathbb{C}-\mathbb{C}^H\right)^{-1}\mathbf{T}^*\cdot\mathbf{T}^*\right]dV\right\}+\int_V\left(\mathbf{T}^*\cdot\hat{\mathbf{E}}+\frac{1}{2}\mathbb{C}^H\hat{\mathbf{E}}\cdot\hat{\mathbf{E}}\right)dV\end{aligned} \quad (3.53)$$

where $\left\langle\mathbf{T}^*\right\rangle$ denotes the average value of $\mathbf{T}^*$ in *V*.

Therefore, by considering the lower bound with respect to $\hat{\mathbf{E}}$, changing the minimization with the maximization and by dividing for *V*, it is obtained:

$$\frac{1}{2}\bar{\mathbb{C}}\bar{\mathbf{E}}\cdot\bar{\mathbf{E}}-\frac{1}{2}\mathbb{C}^{H}\bar{\mathbf{E}}\cdot\bar{\mathbf{E}}=\frac{1}{V}\sup_{\mathbf{T}^{*}\in\mathbf{H}}\left\{\int_{V}\left(\left\langle\mathbf{T}^{*}\right\rangle\cdot\bar{\mathbf{E}}-\frac{1}{2}\left(\mathbb{C}-\mathbb{C}^{H}\right)^{-1}\mathbf{T}^{*}\cdot\mathbf{T}^{*}\right)dV+\inf_{\hat{\mathbf{E}}\in\mathbf{E}}F_{C''}^{\mathbf{T}^{*}}\right\} \tag{3.54}$$

where the quadratic functional $F_{C''}^{\mathbf{T}^{*}}$ is defined by:

$$F_{C''}^{\mathbf{T}^{*}}=\hat{\mathbf{E}}\in E\rightarrow\int_{V}\left(\mathbf{T}^{*}\cdot\hat{\mathbf{E}}+\frac{1}{2}\mathbb{C}^{H}\hat{\mathbf{E}}\cdot\hat{\mathbf{E}}\right)dV\,. \tag{3.55}$$

Consider, now, a reference homogeneous material which is stiffer than each phase included in the heterogeneous RVE, such that $\mathbb{C}-\mathbb{C}^{H}$ is negative definite everywhere in *V*. Hence, in analogous manner, it is obtained the following equation:

$$\frac{1}{2}\bar{\mathbb{C}}\bar{\mathbf{E}}\cdot\bar{\mathbf{E}}-\frac{1}{2}\mathbb{C}^{H}\bar{\mathbf{E}}\cdot\bar{\mathbf{E}}=\frac{1}{V}\inf_{\mathbf{T}^{*}\in\mathbf{H}}\left\{\int_{V}\left(\left\langle\mathbf{T}^{*}\right\rangle\cdot\bar{\mathbf{E}}-\frac{1}{2}\left(\mathbb{C}-\mathbb{C}^{H}\right)^{-1}\mathbf{T}^{*}\cdot\mathbf{T}^{*}\right)dV+\inf_{\hat{\mathbf{E}}\in\mathbf{E}}F_{C''}^{\mathbf{T}^{*}}\right\} \tag{3.56}$$

The equations (3.54) and (3.56) represent the Hashin and Shtrikman's variational principles, based on the eigenstress. In particular, the (3.54) is a saddle principle, while the (3.56) is a minimum principle. From them, by imposing stationariness principles with respect to $\mathbf{T}^{*}$, it is obtained:

$$\left(\mathbb{C}-\mathbb{C}^{H}\right)^{-1}\mathbf{T}^{*}=\hat{\mathbf{E}}+\bar{\mathbf{E}} \tag{3.57}$$

that confirms that stress field $\mathbf{T}^{*}$ is the correction which has to be prescribed to the reference homogeneous material stress field $\mathbb{C}^{H}\left(\hat{\mathbf{E}}+\bar{\mathbf{E}}\right)$ in order to obtain the stress field in the actual material $\mathbb{C}\left(\hat{\mathbf{E}}+\bar{\mathbf{E}}\right)$.

It is possible to obtain other two variational principles, having similar expressions to the (3.54) and the (3.56) and involving the overall compliance tensor $\mathbb{S}$. About them, the sole results will be shown, directly, since they are reached with similar considerations to those ones already done.

Therefore, consider a reference homogeneous material which is stiffer than each phase included in the heterogeneous RVE, such that $\mathbb{S}-\mathbb{S}^{H}$ is positive definite

everywhere in *V*. Hence, in analogous manner, it is obtained the following equation:

$$\frac{1}{2}\overline{\mathbb{S}}\,\overline{\mathbf{T}}\cdot\overline{\mathbf{T}}-\frac{1}{2}\overline{\mathbb{S}}^{H}\,\overline{\mathbf{T}}\cdot\overline{\mathbf{T}}=\frac{1}{V}\sup_{\mathbf{E}^{*}\in\mathbf{H}}\left\{\int_{V}\left(\left\langle\mathbf{E}^{*}\right\rangle\cdot\overline{\mathbf{T}}-\frac{1}{2}\left(\mathbb{S}-\mathbb{S}^{H}\right)^{-1}\mathbf{E}^{*}\cdot\mathbf{E}^{*}\right)dV+\inf_{\hat{\mathbf{T}}\in T}F_{S''}^{\mathbf{E}^{*}}\right\} \tag{3.58}$$

where the quadratic functional $F_{S''}^{\mathbf{E}^{*}}$ is defined by:

$$F_{S''}^{\mathbf{E}^{*}}=\hat{\mathbf{T}}\in T\rightarrow\int_{V}\left(\mathbf{E}^{*}\cdot\hat{\mathbf{T}}+\frac{1}{2}\mathbb{S}^{H}\hat{\mathbf{T}}\cdot\hat{\mathbf{T}}\right)dV \tag{3.59}$$

and where $\mathbf{H}$ is the space of symmetric second-order periodic tensors, $\mathbf{E}^{*}_{.}$ is polarization field (eigenstrain) prescribed on the reference homogeneous medium in order to simulate the actual micro-structure of the heterogeneous RVE.

Consider, on the contrary, a reference homogeneous material which is more deformable than each phase included in the heterogeneous RVE, such that $\mathbb{S}-\mathbb{S}^{H}$ is positive definite everywhere in *V*. Hence, in similar form, it is obtained the following equation:

$$\frac{1}{2}\overline{\mathbb{S}}\,\overline{\mathbf{T}}\cdot\overline{\mathbf{T}}-\frac{1}{2}\overline{\mathbb{S}}^{H}\,\overline{\mathbf{T}}\cdot\overline{\mathbf{T}}=\frac{1}{V}\inf_{\mathbf{E}^{*}\in\mathbf{H}}\left\{\int_{V}\left(\left\langle\mathbf{E}^{*}\right\rangle\cdot\overline{\mathbf{T}}-\frac{1}{2}\left(\mathbb{S}-\mathbb{S}^{H}\right)^{-1}\mathbf{E}^{*}\cdot\mathbf{E}^{*}\right)dV+\inf_{\hat{\mathbf{T}}\in T}F_{S''}^{\mathbf{E}^{*}}\right\} \tag{3.60}$$

The equations (3.58) and (3.60) represent the Hashin and Shtrikman's variational principles, based on the eigenstrain. In particular, the (3.58) is a saddle principle, while the (3.60) is a minimum principle. From them, by imposing stationariness principles with respect to $\mathbf{E}^{*}_{.}$, it is obtained:

$$\left(\mathbb{S}-\mathbb{S}^{H}\right)^{-1}\mathbf{E}^{*}=\hat{\mathbf{T}}+\overline{\mathbf{T}} \tag{3.61}$$

that confirms that strain field $\mathbf{E}^{*}_{.}$ is the correction which has to be prescribed to the reference homogeneous material strain field $\mathbb{S}^{H}\left(\hat{\mathbf{T}}+\overline{\mathbf{T}}\right)$ in order to obtain the strain field in the actual material $\mathbb{S}\left(\hat{\mathbf{T}}+\overline{\mathbf{T}}\right)$.

It has to be considered that the Hashin and Shtrikman's variational principles involve auxiliary problems, consisting in the minimization of the functionals, $F_{C''}^{\mathbf{T}^*}$ (or $F_{S''}^{\mathbf{E}^*}$). The goal is to solve an equilibrium (or a compatibility) problem, for the reference homogeneous solid, subject to a prescribed eigenstress, $\mathbf{T}_\cdot^*$, (or an eigenstrain $\mathbf{E}^*$). For such problem, however, only few particular cases has a solution.

In particular, it can be remembered the Eshelby's solution for the case in which the polarization field is constant and different from zero, only in an ellipsoidal region. This solution lets to use the Hashin and Shtrikman's variational principles for determining the homogenized properties of a biphasic composite, with a low concentration of inclusions. In order to do it, the same matrix or the inclusions can be chosen as reference homogeneous material, but the matrix and the inclusions have to be well ordered, that means, $\mathbb{C}^M - \mathbb{C}^\Omega$ has to be defined in sign.

In case of periodic composite, the auxiliary problem is easier to solve, because it is possible to transform the RVE domain into a Fourier domain. It is not our interest to expose this procedure, so the interested reader is referred to (Giangreco, 2003).

The calculation of the elastic energy density and of the complementary one, according to the two equations (3.49), requires the execution of very difficult minimization with respect of functionals, that are defined on unbounded space. Operating such minimizations is equivalent to solve the elastostatic problem for the RVE, in the cases of displacements approach and tractions approach, respectively. A numeric minimization, obtained, for example, by using the Element Finite Method, can be employed on finite subspaces, E_f and T_f, of the above mentioned spaces, **E** and **T**.

Consequently, numeric minimization will yield the following expressions of the tensors, $\mathbb{C}_\cdot^+$ and $\mathbb{S}^+$:

$$\begin{aligned}\frac{1}{2}\mathbb{C}^+\overline{\mathbf{E}}\cdot\overline{\mathbf{E}} &= \inf_{\mathbf{E}^d\in E_f}\frac{1}{V}\int_V\frac{1}{2}\mathbb{C}\left(\overline{\mathbf{E}}+\mathbf{E}^d\right)\left(\overline{\mathbf{E}}+\mathbf{E}^d\right)dV\\ \frac{1}{2}\mathbb{S}^+\overline{\mathbf{T}}\cdot\overline{\mathbf{T}} &= \inf_{\mathbf{T}^d\in T_f}\frac{1}{V}\int_V\frac{1}{2}\mathbb{S}\left(\overline{\mathbf{T}}+\mathbf{T}^d\right)\left(\overline{\mathbf{T}}+\mathbf{T}^d\right)dV\end{aligned} \tag{3.62}$$

which, for constructions, satisfy the following inequalities:

$$\begin{aligned}\frac{1}{2}\overline{\mathbb{C}}\,\overline{\mathbf{E}}\cdot\overline{\mathbf{E}} &\le \frac{1}{2}\mathbb{C}^+\,\overline{\mathbf{E}}\cdot\overline{\mathbf{E}}\\ \frac{1}{2}\overline{\mathbb{S}}\,\overline{\mathbf{T}}\cdot\overline{\mathbf{T}} &\le \frac{1}{2}\mathbb{S}^+\,\overline{\mathbf{T}}\cdot\overline{\mathbf{T}}.\end{aligned} \tag{3.63}$$

By naming with $\mathbb{C}^-_{\cdot}$ and $\mathbb{S}^-_{\cdot}$, respectively, the inverse of the tensors $\mathbb{S}^+_{\cdot}$ and $\mathbb{C}^+_{\cdot}$, the upper and lower limitations for the elastic energy, and the complementary one, of the homogenized material are obtained, as given by:

$$\begin{aligned} &\frac{1}{2}\mathbb{C}^-\,\overline{\mathbf{E}}\cdot\overline{\mathbf{E}} \le \frac{1}{2}\overline{\mathbb{C}}\,\overline{\mathbf{E}}\cdot\overline{\mathbf{E}} \le \frac{1}{2}\mathbb{C}^+\,\overline{\mathbf{E}}\cdot\overline{\mathbf{E}} \\ &\frac{1}{2}\mathbb{S}^-\,\overline{\mathbf{T}}\cdot\overline{\mathbf{T}} \le \frac{1}{2}\overline{\mathbb{S}}\,\overline{\mathbf{T}}\cdot\overline{\mathbf{T}} \le \frac{1}{2}\mathbb{S}^+\,\overline{\mathbf{T}}\cdot\overline{\mathbf{T}}. \end{aligned} \tag{3.64}$$

Elementary estimations on $\overline{\mathbb{C}}_{\cdot}$ and $\overline{\mathbb{S}}_{\cdot}$ are obtained by choosing the simplest E_f and T_f, i.e., coinciding with the space constituted by the sole null tensor. In this way, the well known Voigt and Reuss' estimations are reached; in particular, for a biphasic composite, they are:

$$\begin{aligned} &\left(f_M\mathbb{S}_M + f_\Omega\mathbb{S}_\Omega\right)^{-1} \le \overline{\mathbb{C}} \le f_M\mathbb{C}_M + f_\Omega\mathbb{C}_\Omega \\ &\left(f_M\mathbb{C}_M + f_\Omega\mathbb{C}_\Omega\right)^{-1} \le \overline{\mathbb{S}} \le f_M\mathbb{S}_M + f_\Omega\mathbb{S}_\Omega \end{aligned} \tag{3.65}$$

with:

$$\begin{aligned} &\left(f_M\mathbb{C}_M + f_\Omega\mathbb{C}_\Omega\right)^{-1} = \left(\mathbb{C}^+\right)^V, \quad \left(f_M\mathbb{C}_M + f_\Omega\mathbb{C}_\Omega\right)^{-1} = \left(\mathbb{S}^-\right)^V \\ &\left(f_M\mathbb{S}_M + f_\Omega\mathbb{S}_\Omega\right)^{-1} = \left(\mathbb{C}^-\right)^R, \quad \left(f_M\mathbb{S}_M + f_\Omega\mathbb{S}_\Omega\right)^{-1} = \left(\mathbb{S}^+\right)^R \end{aligned} \tag{3.66}$$

where the superscript V and R stands for Voigt and Reuss.
At the same manner, the Hashin and Shtrikman's variational principles (3.54), (3.56), (3.58) and (3.60) yield estimations on the stiffness and compliance tensors, if the optimization with regard to the polarization fields is employed above a finite underspace H_f, of the above unbounded mentioned space H of all possible polarization fields.
In particular, it results

$$\frac{1}{2}\overline{\mathbb{C}}\,\overline{\mathbf{E}}\cdot\overline{\mathbf{E}} - \frac{1}{2}\mathbb{C}^H\overline{\mathbf{E}}\cdot\overline{\mathbf{E}} \ge \frac{1}{V}\sup_{\mathbf{T}^*\in H_f}\left\{\int_V\left(\left\langle\mathbf{T}^*\right\rangle\cdot\overline{\mathbf{E}} - \frac{1}{2}\left(\mathbb{C}-\mathbb{C}^H\right)^{-1}\mathbf{T}^*\cdot\mathbf{T}^*\right)dV + \inf_{\hat{\mathbf{E}}\in E} F_{C''}^{\mathbf{T}^*}\right\} \tag{3.67}$$

and

$$\frac{1}{2}\bar{\mathbb{S}}\,\bar{\mathbf{T}}\cdot\bar{\mathbf{T}}-\frac{1}{2}\mathbb{S}^{H}\,\bar{\mathbf{T}}\cdot\bar{\mathbf{T}}\le\frac{1}{V}\inf_{\mathbf{E}^{*}\in H_{f}}\left\{\int_{V}\left(\left\langle\mathbf{E}^{*}\right\rangle\cdot\bar{\mathbf{T}}-\frac{1}{2}\left(\mathbb{S}-\mathbb{S}^{H}\right)^{-1}\mathbf{E}^{*}\cdot\mathbf{E}^{*}\right)dV+\inf_{\hat{\mathbf{T}}\in T}F_{S''}^{\mathbf{E}^{*}}\right\} \tag{3.68}$$

if the reference homogeneous material is more deformable than each phase included in the heterogeneous RVE; on the contrary, it results

$$\frac{1}{2}\bar{\mathbb{C}}\,\bar{\mathbf{E}}\cdot\bar{\mathbf{E}}-\frac{1}{2}\mathbb{C}^{H}\bar{\mathbf{E}}\cdot\bar{\mathbf{E}}\le\frac{1}{V}\inf_{\mathbf{T}^{*}\in H}\left\{\int_{V}\left(\left\langle\mathbf{T}^{*}\right\rangle\cdot\bar{\mathbf{E}}-\frac{1}{2}\left(\mathbb{C}-\mathbb{C}^{H}\right)^{-1}\mathbf{T}^{*}\cdot\mathbf{T}^{*}\right)dV+\inf_{\hat{\mathbf{E}}\in E}F_{C''}^{\mathbf{T}^{*}}\right\} \tag{3.69}$$

and

$$\frac{1}{2}\bar{\mathbb{S}}\,\bar{\mathbf{T}}\cdot\bar{\mathbf{T}}-\frac{1}{2}\mathbb{S}^{H}\,\bar{\mathbf{T}}\cdot\bar{\mathbf{T}}\ge\frac{1}{V}\sup_{\mathbf{E}^{*}\in H_{f}}\left\{\int_{V}\left(\left\langle\mathbf{E}^{*}\right\rangle\cdot\bar{\mathbf{T}}-\frac{1}{2}\left(\mathbb{S}-\mathbb{S}^{H}\right)^{-1}\mathbf{E}^{*}\cdot\mathbf{E}^{*}\right)dV+\inf_{\hat{\mathbf{T}}\in T}F_{S''}^{\mathbf{E}^{*}}\right\} \tag{3.70}$$

if the reference homogeneous material is stiffer than each phase included in the heterogeneous RVE.

A numeric estimation of the inferior extreme of $F_{C''}^{\mathbf{T}^{*}}$ and of $F_{S''}^{\mathbf{E}^{*}}$ implies that only the minimum principles (3.68) and (3.69) yield upper estimations for the density of the elastic complementary energy and for the elastic one, respectively, for the homogenized material. The saddle principles (3.67) and (3.70), instead, are able to yield an estimation that cannot be read as an upper or lower estimation.

3. MICROMECHANICS OF POROUS MATERIALS: J-TENSOR AND DILUTE DISTRIBUTION OF VOIDS CASES

In this section, the overall stress-strain/strain stress relations are developed with reference to an RVE consisting of a linearly elastic material which contains stress-free cavities.

Consider an RVE with total volume *V*, bounded *externally* by surface ∂V . On this surface, either uniform tractions,

$$\boldsymbol{t}^{0}=\boldsymbol{n}\cdot\boldsymbol{\sigma}^{0}\qquad\text{on }\partial V\,, \tag{3.71}$$

or linear displacements,

$$\boldsymbol{u}^0 = \boldsymbol{x} \cdot \boldsymbol{\varepsilon}^0 \qquad \text{on } \partial V\,, \tag{3.72}$$

are assumed to be prescribed, where $\boldsymbol{\sigma}^0$ and $\boldsymbol{\varepsilon}^0$ are second-order symmetric *constant* stress and strain tensors for the macro-element. It is emphasized that either (3.71) or (3.72) (4.1.1 a), but not both, can be prescribed. In other words, if the traction boundary data (3.71) corresponding to the constant macrostress $\boldsymbol{\Sigma} = \boldsymbol{\sigma}^0$, are prescribed, then the surface displacements on ∂V, corresponding to these tractions, in general, are *not* spatially linear, being affected by the microstructure of the RVE. Similarly, if the linear displacement boundary data (3.72) corresponding to the constant macrostrain $\mathbf{E} = \boldsymbol{\varepsilon}^0$, are prescribed, then the surface tractions on ∂V, produced by these displacements, are *not,* in general, spatially uniform. In the sequel, therefore, the two cases are treated separately and independently, and then the relation between the results is discussed.

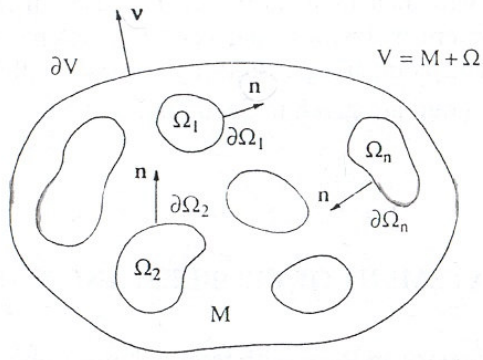

Fig. 3.2.
Matrix M and microcavities Ω_α

Assume that the material of the RVE is linearly elastic and *homogeneous* (but not necessarily isotropic). The inhomogeneity, therefore, stems solely from the presence of cavities. Denote a typical cavity by Ω_α, with the boundary $\partial\Omega_\alpha$ $(\alpha = 1,2,...,\mathrm{n})$, so that there are a total of n individual cavities in *V*. The union of these cavities is denoted by Ω, having the boundary $\partial\Omega$ which is the union of all $\partial\Omega_\alpha$, i.e.,

$$\Omega \equiv \cup_{\alpha=1}^{n} \Omega_\alpha \qquad \partial\Omega \equiv \cup_{\alpha=1}^{n} \partial\Omega_\alpha \tag{3.73}$$

The remainder of the RVE (i.e, when Ω is excluded) is called the *matrix*. The matrix is denoted by M. The boundary of M is the sum of ∂V and $\partial\Omega$, Figure 3.2.,

$$M \equiv V - \Omega \qquad \partial M \equiv \partial V - \partial\Omega\,. \tag{3.74}$$

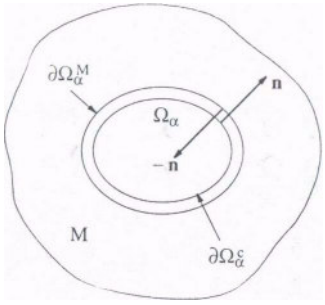

Fig. 3.3.
$\partial\Omega_\alpha^M$ *and* $\partial\Omega_\alpha^c$

The total boundary surface of the RVE can include some portion of $\partial\Omega$. For simplicity, however, exclude this possibility. Thus, all cavities are within the RVE, each being fully surrounded by the matrix material. For a typical cavity, Ω_α, two faces of its surface boundary, $\partial\Omega_\alpha$, may be distinguished, as follows:

- the *exterior* face of the cavity, denoted by $\partial\Omega_\alpha^{\mathrm{c}}$ which is the face toward the matrix material, denned by the direction of the exterior unit normal $\boldsymbol{n}$ of the cavity;
- the *exterior* face of the *surrounding matrix,* denoted by $\partial\Omega_\alpha^{\mathrm{M}}$, which is the face toward the interior of the cavity, denned by the direction of the exterior unit normal $(-\boldsymbol{n})$ of the matrix (i.e., the interior unit normal of the cavity). $\partial\Omega_\alpha$ coincides with $\partial\Omega_\alpha^{\mathrm{c}}$, for the cavity Ω_α, while $\partial\mathrm{M}$ at the cavity Ω_α coincides with $\partial\Omega_\alpha^{\mathrm{M}}$ (Fig. 3.3). In view of this convention, the integral of a surface quantity taken over $\partial\mathrm{M}$ can always be decomposed as
-

$$\begin{aligned}\int_{\partial\mathrm{M}}(.)\,dS &= \int_{\partial V}(.)\,dS + \sum_{\alpha=1}^{\mathrm{n}}\int_{\partial\Omega_\alpha^{\mathrm{M}}}(.)\,dS = \\ &= \int_{\partial V}(.)\,dS - \sum_{\alpha=1}^{\mathrm{n}}\int_{\partial\Omega_\alpha^{\mathrm{c}}}(.)\,dS = \int_{\partial V}(.)\,dS - \int_{\partial\Omega}(.)\,dS.\end{aligned} \tag{3.75}$$

Thus $\partial\Omega$ always stands for the union of $\partial\Omega_\alpha^c$ $(\alpha = 1,2,...,\mathrm{n})$.
To distinguish the boundary of M at the cavities from that at the exterior of the RVE, which is ∂V, the exterior unit normal on ∂V is systematically denoted by $\boldsymbol{n}$ (as before), and the *exterior* unit normal on the surface $\partial\Omega_\alpha$ for a typical cavity Ω_α, by $\boldsymbol{n}$, *pointing from the inside of the cavity toward the matrix* M.
The matrix material is linearly elastic and homogeneous. Denote the corresponding constant elasticity tensor by $\mathbb{C}$ and the compliance tensor by $\mathbb{S}$.

3.1. Average strain for prescribed macrostress

Suppose that uniform tractions $\boldsymbol{t}^0 = \boldsymbol{n}\cdot\boldsymbol{\sigma}^0$ are prescribed on ∂V, associated with the constant symmetric macrostress $\boldsymbol{\Sigma} = \boldsymbol{\sigma}^0$. If the RVE is homogeneous, having *no* cavities, then the corresponding average strain associated with the average stress $\boldsymbol{\sigma}^0$ would be

$$\boldsymbol{\varepsilon}^0 = \mathbb{S} : \boldsymbol{\sigma}^0, \tag{3.76}$$

and hence, in conjunction with $\bar{\boldsymbol{\sigma}} = \boldsymbol{\sigma}^0$, the average strain would be $\boldsymbol{\varepsilon}^0$. The presence of cavities disturbs the uniform stress and strain fields, producing the variable stress field $\boldsymbol{\sigma} = \boldsymbol{\sigma}(\boldsymbol{x})$ and strain field $\boldsymbol{\varepsilon} = \boldsymbol{\varepsilon}(\boldsymbol{x})$, in M, with $\boldsymbol{\sigma} = \boldsymbol{0}$ in Ω. Nevertheless, from the (3.1)

$$\bar{\boldsymbol{\sigma}} = \langle\boldsymbol{\sigma}\rangle = \frac{1}{V}\int_V \boldsymbol{\sigma}\, dv = \frac{1}{V}\int_M \boldsymbol{\sigma}\, dv = \boldsymbol{\sigma}^0. \tag{3.77}$$

On the other hand, the average strain is *not,* in general, equal to $\boldsymbol{\varepsilon}^0$. Instead,

$$\bar{\boldsymbol{\varepsilon}} = \langle\boldsymbol{\varepsilon}\rangle = \boldsymbol{\varepsilon}^0 + \bar{\boldsymbol{\varepsilon}}^c, \tag{3.78}$$

where $\boldsymbol{\varepsilon}^0$ is *defined* by (3.76), and $\bar{\boldsymbol{\varepsilon}}^c$ is the additional strain due to the presence of cavities.
To calculate the additional strain $\bar{\boldsymbol{\varepsilon}}^c$ due to cavities, one may apply the reciprocal theorem, as follows. Consider two sets of loads, one defined by

$$\boldsymbol{t}^{(1)} = \begin{cases} \boldsymbol{n}\cdot\delta\boldsymbol{\sigma}^0 & \text{on } \partial V \\ -\boldsymbol{n}\cdot\delta\boldsymbol{\sigma}^0 & \text{on } \partial\Omega \end{cases} \tag{3.79}$$

which corresponds to uniform *virtual* stress $\delta\boldsymbol{\sigma}^0$ and strain $\delta\boldsymbol{\varepsilon}^0 = \mathbb{S} : \delta\boldsymbol{\sigma}^0$ within the entire RVE (as illustrated in Figure 3.3, $-\boldsymbol{n}$ is the *interior* unit normal on the

cavity surface $\partial\Omega$, or the *exterior* unit normal to the boundary of the *matrix)*, and the other defined by

$$\boldsymbol{t}^{(2)} = \begin{cases} \boldsymbol{n}\cdot\boldsymbol{\sigma}^0 & \text{on } \partial V \\ \boldsymbol{0} & \text{on } \partial\Omega \end{cases} \tag{3.80}$$

which is the actual loading considered for the RVE.
Denote the displacement, strain, and stress fields associated with the first loading (3.79) by

$$\left\{\boldsymbol{u}^{(1)},\boldsymbol{\varepsilon}^{(1)},\boldsymbol{\sigma}^{(1)}\right\} = \left\{\left(\boldsymbol{x}\,.\,\delta\boldsymbol{\varepsilon}^0\right),\delta\boldsymbol{\varepsilon}^0,\delta\boldsymbol{\sigma}^0\right\} \tag{3.81}$$

which follows from the fact that, for loading (3.79), the strain and stress fields are both uniform throughout the matrix M. And denote the fields associated with the second (i.e., the actual) loading (3.80) by

$$\left\{\boldsymbol{u}^{(2)},\boldsymbol{\varepsilon}^{(2)},\boldsymbol{\sigma}^{(2)}\right\} = \left\{\boldsymbol{u},\boldsymbol{\varepsilon},\boldsymbol{\sigma}\right\}. \tag{3.82}$$

From the reciprocal theorem, it follows that

$$\int_{\partial V}\left(\boldsymbol{n}\cdot\boldsymbol{\sigma}^0\right)\cdot\left(\boldsymbol{x}\,.\,\delta\boldsymbol{\varepsilon}^0\right)ds = \int_{\partial V}\left(\boldsymbol{n}\cdot\delta\boldsymbol{\sigma}^0\right)\cdot\boldsymbol{u}\,ds - \int_{\partial\Omega}\left(\boldsymbol{n}\cdot\delta\boldsymbol{\sigma}^0\right)\cdot\boldsymbol{u}\,ds \tag{3.83}$$

which can be written as

$$\delta\boldsymbol{\sigma}^0 : \left\{\int_{\partial V}\mathbb{S} : \left\{\left(\boldsymbol{x}\otimes\boldsymbol{n}\right)\cdot\boldsymbol{\sigma}^0\right\}ds - \int_{\partial V}\boldsymbol{n}\otimes\boldsymbol{u}\,ds + \int_{\partial\Omega}\boldsymbol{n}\otimes\boldsymbol{u}\,ds\right\} = 0\,. \tag{3.84}$$

Since $\delta\boldsymbol{\sigma}^0$ is an arbitrary symmetric tensor, the symmetric part of the quantity within the braces must vanish identically. Noting that the first integral within the braces yields

$$\frac{1}{V}\int_{\partial V}\mathbb{S} : \left\{\left(\boldsymbol{x}\otimes\boldsymbol{n}\right)\cdot\boldsymbol{\sigma}^0\right\}ds = \mathbb{S} : \left\{\boldsymbol{I}\cdot\boldsymbol{\sigma}^0\right\} = \boldsymbol{\varepsilon}^0, \tag{3.85}$$

and using the averaging scheme, it follows that

$$\bar{\boldsymbol{\varepsilon}} = \frac{1}{V}\int_V\frac{1}{2}\left\{\nabla\otimes\boldsymbol{u} + \left(\nabla\otimes\boldsymbol{u}\right)^T\right\}dv = \boldsymbol{\varepsilon}^0 + \frac{1}{V}\int_{\partial\Omega}\frac{1}{2}\left(\boldsymbol{n}\otimes\boldsymbol{u} + \boldsymbol{u}\otimes\boldsymbol{n}\right)ds\,. \tag{3.86}$$

Comparison with (3.78) shows that the additional strain $\bar{\boldsymbol{\varepsilon}}^c$ due to cavities, is given by

$$\bar{\boldsymbol{\varepsilon}}^c = \frac{1}{V}\int_{\partial\Omega}\frac{1}{2}\left(\boldsymbol{n}\otimes\boldsymbol{u}+\boldsymbol{u}\otimes\boldsymbol{n}\right)ds\,. \tag{3.87}$$

3.2. Overall compliance tensor for porous elastic solids

Define *the overall compliance* $\bar{\mathbb{S}}$ of the porous RVE with a linearly elastic homogeneous matrix, through

$$\bar{\boldsymbol{\varepsilon}} = \bar{\mathbb{S}}:\bar{\boldsymbol{\sigma}} = \bar{\mathbb{S}}:\boldsymbol{\sigma}^0\,, \tag{3.88}$$

where the macrostress, $\boldsymbol{\Sigma}=\boldsymbol{\sigma}^0$, is regarded prescribed, and the average strain is given by (3.78). To obtain the overall compliance in an explicit form, the strain $\bar{\boldsymbol{\varepsilon}}^c$ due to cavities will now be expressed in terms of the applied stress $\boldsymbol{\sigma}^0$. Since the matrix of the RVE is linearly elastic, for a given microstructure the displacement $\boldsymbol{u}(\boldsymbol{x})$ at a point $\boldsymbol{x}$ on $\partial\Omega$ is linearly dependent on the uniform overall stress $\boldsymbol{\sigma}^0$, as show following. By remembering that the displacement field may be expressed in terms of Green function as

$$\boldsymbol{u}(\boldsymbol{x}) = \int_{\partial V}\boldsymbol{G}(\boldsymbol{x},\boldsymbol{y})\cdot\boldsymbol{t}(\boldsymbol{y})\,ds \tag{3.89}$$

where $\boldsymbol{t}(\boldsymbol{y})$ are the self-equilibrating surface traction prescribed on the boundary ∂V of the RVE, if the applied tractions (3.71) are substituting into (3.89), to arrive at

$$\boldsymbol{u}(\boldsymbol{x}) = \int_{\partial V}\boldsymbol{G}(\boldsymbol{x},\boldsymbol{y})\cdot\left\{\boldsymbol{n}(\boldsymbol{y})\cdot\boldsymbol{\sigma}^0\right\}ds\,, \tag{3.90}$$

where the integration is taken with respect to $\boldsymbol{y}$ over the boundary ∂V of the RVE. Since $\boldsymbol{\sigma}^0$ is a symmetric constant tensor, (3.90) can be expressed as

$$u_i(\boldsymbol{x}) = K_{ijk}(\boldsymbol{x})\sigma^0_{jk} \tag{3.91}$$

where the third-order tensor,

$$K_{ijk}(\boldsymbol{x}) = K_{ijk}(\boldsymbol{x}) = \int_{\partial V}\frac{1}{2}\left\{G_{ij}(\boldsymbol{x},\boldsymbol{y})n_k(\boldsymbol{y})+G_{ik}(\boldsymbol{x},\boldsymbol{y})n_j(\boldsymbol{y})\right\}dS\,, \tag{3.92}$$

depends on the geometry and the elastic properties of the matrix of the RVE.
To obtain the additional overall strain, $\bar{\boldsymbol{\varepsilon}}^c$, due to the presence of cavities in terms of the prescribed overall stress, $\boldsymbol{\sigma}^0$, substitute from (3.92) into (3.87), to arrive at

$$\bar{\varepsilon}_{ij}^c = H_{ijkl}\sigma_{kl}^0, \tag{3.93}$$

where the *constant* fourth-order tensor, $\mathbb{H}$, is given by

$$H_{ijkl} \equiv H_{jikl} \equiv H_{ijlk} \equiv \frac{1}{V}\int_{\partial\Omega}\frac{1}{2}\left\{n_i(\boldsymbol{x})K_{jkl}(\boldsymbol{x}) + n_j(\boldsymbol{x})K_{ikl}(\boldsymbol{x})\right\}dS\,. \tag{3.94}$$

Hence, for an RVE with a linearly elastic matrix containing cavities *of arbitrary shapes and sizes,* the following general result is obtained, when the overall macrostress is regarded prescribed (Horii and Nemat-Nasser, 1983):

$$\bar{\boldsymbol{\varepsilon}}^c = \mathbb{H} : \boldsymbol{\sigma}^0\,. \tag{3.95}$$

It should be noted that this exact result is valid whether or not the linearly elastic constituent of the RVE is homogeneous. The requirements are:

- the matrix of the RVE is linearly elastic;
- the microstructure of the RVE remains unchanged under the applied macrostress $\boldsymbol{\Sigma} = \boldsymbol{\sigma}^0$.

To obtain the overall elastic compliance tensor $\bar{\mathbb{S}}$, in terms of the constant compliance of the matrix, $\mathbb{S}$, and the *constant* tensor $\mathbb{H}$, substitute (3.76), (3.88) and (3.95) into (3.78), and noting that the resulting equation must hold for any macrostress $\boldsymbol{\sigma}^0$, arrive at

$$\bar{\mathbb{S}} = \mathbb{S} + \mathbb{H}\,, \tag{3.96}$$

Note that in many situation, the tensor $\mathbb{H}$ can be computer directly, using the (3.87).

3.3. Average stress for prescribed macrostrain

Suppose that the linear displacements $\boldsymbol{u}^0 = \boldsymbol{x}\cdot\boldsymbol{\varepsilon}^0$ (associated with the constant symmetric macrostrain $\mathbf{E} = \boldsymbol{\varepsilon}^0$) are prescribed on ∂V. The matrix of the RVE is assumed to be homogeneous, as marked before. *In the absence of cavities,* the corresponding average stress associated with the prescribed macrostrain, $\boldsymbol{\varepsilon}^0$, would be

$$\boldsymbol{\sigma}^0 = \mathbb{C} : \boldsymbol{\varepsilon}^0 . \tag{3.97}$$

Due to the presence of cavities, the actual field quantities are nonuniform. From the (3.6),

$$\boldsymbol{\varepsilon} = \langle \boldsymbol{\varepsilon} \rangle = \frac{1}{V}\int_V \boldsymbol{\varepsilon} dv = \frac{1}{V}\int_{\partial V} \frac{1}{2}\left(\boldsymbol{n}\otimes\boldsymbol{u} + \boldsymbol{u}\otimes\boldsymbol{n}\right) ds = \boldsymbol{\varepsilon}^0 \tag{3.98}$$

which is valid for any RVE of any material and microstructure. Note that the surface integral in (3.98) extends over the exterior boundary, ∂V, of the RVE only. It does *not* include the cavity boundaries $\partial\Omega$. Equation (3.98) is the direct consequence of the fact that the average strain for an RVE is given in terms of its boundary displacements which are prescribed here to be $\boldsymbol{u}^0 = \boldsymbol{x}\cdot\boldsymbol{\varepsilon}^0$.
In general, for a prescribed macrostrain, the average stress is not equal to $\boldsymbol{\sigma}^0$ but

$$\bar{\boldsymbol{\sigma}} = \langle \boldsymbol{\sigma} \rangle = \boldsymbol{\sigma}^0 + \bar{\boldsymbol{\sigma}}^c , \tag{3.99}$$

where $\boldsymbol{\sigma}^0$ is *defined* by (3.97), and $\bar{\boldsymbol{\sigma}}^c$ is the decrement in the overall stress due to the presence of cavities.
As in Subsection 3.1., the reciprocal theorem will be applied to calculate the average stress a in (3.99). To this end, a third set of boundary data defined by

$$\begin{aligned} \boldsymbol{u}^{(3)} &= \boldsymbol{n}\cdot\boldsymbol{\sigma}^0 \qquad \text{on } \partial V \\ \boldsymbol{t}^{(3)} &= \boldsymbol{0} \qquad\qquad \text{on } \partial\Omega. \end{aligned} \tag{3.100}$$

The displacement, strain, and stress fields associated with these boundary conditions are denoted by

$$\left\{\boldsymbol{u}^{(3)}, \boldsymbol{\varepsilon}^{(3)}, \boldsymbol{\sigma}^{(3)}\right\} = \left\{\boldsymbol{u}, \boldsymbol{\varepsilon}, \boldsymbol{\sigma}\right\} \tag{3.101}$$

which are actual fields, in general, different from those given by (3.82) for the boundary conditions (3.80). The actual tractions on the boundary of the RVE now are

$$\boldsymbol{t}(\boldsymbol{x}) = \boldsymbol{n}(\boldsymbol{x})\cdot\boldsymbol{\sigma}(\boldsymbol{x}) , \tag{3.102}$$

where $\boldsymbol{x}$ is on ∂V. These tractions are required in order to impose the boundary displacements prescribed by (3.100).
Applying the reciprocal theorem to the two sets of loads, (3.79) and (3.100), it follows that

$$\int_{\partial V} \boldsymbol{t}\cdot\left(\boldsymbol{x}.\delta\boldsymbol{\varepsilon}^0\right)ds=\int_{\partial V}\left(\boldsymbol{n}\cdot\delta\boldsymbol{\sigma}^0\right)\cdot\left(\boldsymbol{x}.\delta\boldsymbol{\varepsilon}^0\right)ds-\int_{\partial\Omega}\left(\boldsymbol{n}\cdot\delta\boldsymbol{\sigma}^0\right)\cdot\boldsymbol{u}\,ds \tag{3.103}$$

which can be written as

$$\delta\boldsymbol{\varepsilon}^0:\left\{\int_{\partial V}\boldsymbol{t}\otimes\boldsymbol{x}\,ds-\int_{\partial V}\mathbb{C}:\left\{\left(\boldsymbol{x}\otimes\boldsymbol{n}\right)\cdot\boldsymbol{\varepsilon}^0\right\}ds+\int_{\partial\Omega}\mathbb{C}:\left(\boldsymbol{n}\otimes\boldsymbol{u}\right)ds\right\}=0 \tag{3.104}$$

where, in using loading (3.81), the quantity $\delta\boldsymbol{\varepsilon}^0$ is regarded as a virtual spatially constant strain field with the corresponding stress field, $\delta\boldsymbol{\sigma}^0=\mathbb{C}:\delta\boldsymbol{\varepsilon}^0$. Since $\delta\boldsymbol{\varepsilon}^0$ is an arbitrary symmetric tensor, the symmetric part of the quantity within the braces in (3.104) must vanish identically. Noting that the second integral within the parentheses can be expressed as

$$\frac{1}{V}\int_{\partial V}\mathbb{C}:\left\{\left(\boldsymbol{x}\otimes\boldsymbol{n}\right)\cdot\boldsymbol{\varepsilon}^0\right\}ds=\mathbb{C}:\left\{\boldsymbol{I}\cdot\boldsymbol{\varepsilon}^0\right\}=\boldsymbol{\sigma}^0, \tag{3.105}$$

and using the averaging procedure, it now follows that

$$\bar{\boldsymbol{\sigma}}=\frac{1}{V}\int_{\partial V}\boldsymbol{t}\otimes\boldsymbol{x}\,ds=\boldsymbol{\sigma}^0-\mathbb{C}:\left\{\frac{1}{V}\int_{\partial\Omega}\frac{1}{2}\left(\boldsymbol{n}\otimes\boldsymbol{u}+\boldsymbol{u}\otimes\boldsymbol{n}\right)ds\right\} \tag{3.106}$$

Comparison with (3.99) shows that the decremental stress $\bar{\boldsymbol{\sigma}}^c$ due to the presence of cavities, is given by

$$\bar{\boldsymbol{\sigma}}^c=-\mathbb{C}:\bar{\boldsymbol{\varepsilon}}^c \tag{3.107}$$

where $\bar{\boldsymbol{\varepsilon}}^c$ is the strain due to the presence of cavities given by (3.87), which now must be computed for the prescribed boundary displacements $\boldsymbol{u}^0=\boldsymbol{x}\cdot\boldsymbol{\varepsilon}^0$.

3.4. Overall elasticity tensor for porous elastic solids

When the overall macrostrain is regarded prescribed, $\mathbf{E}=\boldsymbol{\varepsilon}^0$, designate the overall elasticityJensor of the porous RVE with a-linearly elastic and homogeneous matrix, by $\bar{\mathbb{C}}$, and define it through

$$\bar{\boldsymbol{\sigma}}=\bar{\mathbb{C}}:\boldsymbol{\varepsilon}^0. \tag{3.108}$$

Substitution of (3.97), (3.107), and (3.108) into (3.99) then yields

$$\left(\bar{\mathbb{C}}-\mathbb{C}\right):\boldsymbol{\varepsilon}^0+\mathbb{C}:\bar{\boldsymbol{\varepsilon}}^c=\mathbf{0}. \tag{3.109}$$

For a given microstructure (i.e., for existing cavities with fixed shapes, sizes, and distribution), the response of the RVE is linear. Hence, the displacement field anywhere within the linearly elastic matrix of the RVE is a linear and homogeneous function of the prescribed overall constant strain $\boldsymbol{\varepsilon}^0$. Therefore, in line with results (3.91) and (3.92) for the case when the macrostresses were considered to be prescribed, at a typical point $\boldsymbol{x}$ on the boundary of the cavities, $\partial\Omega$,

$$u_i(\boldsymbol{x}) = L_{ijk}(\boldsymbol{x})\varepsilon^0_{jk} \tag{3.110}$$

where $\boldsymbol{L}(\boldsymbol{x})$ is a is a third-order tensor-valued function with the symmetry property, $L_{ijk} = L_{ikj}$. Now, from the definition of $\overline{\boldsymbol{\varepsilon}}^c$, given by the (3.87),

$$\overline{\varepsilon}^c_{ij} = J_{ijkl}\varepsilon^0_{kl}, \tag{3.111}$$

where the *constant* fourth-order tensor, $\mathbb{J}$, is given by

$$J_{ijkl} \equiv J_{jikl} \equiv J_{ijlk} \equiv \frac{1}{V}\int_{\partial\Omega}\frac{1}{2}\left\{n_i(\boldsymbol{x})J_{jkl}(\boldsymbol{x}) + n_j(\boldsymbol{x})J_{ikl}(\boldsymbol{x})\right\}dS. \tag{3.112}$$

Hence, for an RVE with a linearly elastic matrix (whether homogeneous or not) containing cavities of arbitrary shapes and sizes, the following general result is obtained, when the overall macrostrains are regarded prescribed:

$$\overline{\boldsymbol{\varepsilon}}^c = \mathbb{J} : \boldsymbol{\varepsilon}^0. \tag{3.113}$$

To obtain an expression for the overall elastic moduli of the porous RVE, substitute (3.113) into (3.109) and, noting that the resulting expression must be valid for any constant symmetric macrostrain $\boldsymbol{\varepsilon}^0$, arrive at

$$\overline{\mathbb{C}} = \mathbb{C} - \mathbb{C} : \mathbb{J}. \tag{3.114}$$

It should be noted that in many practical problems the tensor J, similarly to the tensor $\mathbb{H}$, can be calculated *directly* from (3.87), and therefore, the overall elastic moduli can be estimated from (3.114).
It may, however, be instructive to seek to construct the tensor $\mathbb{J}$ in terms of the Green functions $\boldsymbol{G}(\boldsymbol{x},\boldsymbol{y})$ and $\boldsymbol{G}^{-1}(\boldsymbol{x},\boldsymbol{y})$.

To this end, for the linear displacements, $\boldsymbol{u}^0 = \boldsymbol{z} \cdot \boldsymbol{\varepsilon}^0$, *prescribed* on the outer boundary ∂V of the RVE, by remembering that the *resulting* tractions, $\boldsymbol{t}(\boldsymbol{y})$, may be written as

$$\boldsymbol{t}(\boldsymbol{y}) = \int_{\partial V} \boldsymbol{G}^{-1}(\boldsymbol{y},\boldsymbol{z}) \cdot \left(\boldsymbol{z} \cdot \boldsymbol{\varepsilon}^0\right) ds\,, \tag{3.115}$$

where the integration is taken with respect to $\boldsymbol{z}$ over the outer boundary ∂V (excluding the traction-free cavity boundaries) of the RVE. Substituting (3.115) into (3.89), the displacement field for points on $\partial\Omega$ is obtained in terms of the prescribed macrostrain $\boldsymbol{\varepsilon}^0$, as

$$\boldsymbol{u}(\boldsymbol{x}) = \int_{\partial V} \boldsymbol{G}(\boldsymbol{x},\boldsymbol{y}) \cdot \left\{ \int_{\partial V} \boldsymbol{G}^{-1}(\boldsymbol{y},\boldsymbol{z}) \cdot \left(\boldsymbol{z} \cdot \boldsymbol{\varepsilon}^0\right) ds \right\} ds \tag{3.116}$$

where both the $\boldsymbol{y}$- and $\boldsymbol{z}$-integral are taken over ∂V. Noting that $\boldsymbol{\varepsilon}^0$ is a symmetric tensor, tensor $\boldsymbol{L}$ in (3.110) may now be written in terms of $\boldsymbol{G}$ and $\boldsymbol{G}^{-1}$, as

$$L_{ijk}(\boldsymbol{x}) = \int_{\partial V} G_{im}(\boldsymbol{x},\boldsymbol{y}) \left\{ \int_{\partial V} \frac{1}{2} \left\{ G^{-1}_{mj}(\boldsymbol{y},\boldsymbol{z})\, z_k + G^{-1}_{mk}(\boldsymbol{y},\boldsymbol{z})\, z_j \right\} ds \right\} ds\,. \tag{3.117}$$

Therefore, from comparison of (3.113) with (3.117), a fourth-order tensor, $\boldsymbol{j}(\boldsymbol{x},\boldsymbol{y})$, can be introduced as

$$j_{ijkl} = \int_{\partial V} \frac{1}{4} \begin{Bmatrix} n_i(\boldsymbol{x}) G_{jm}(\boldsymbol{x},\boldsymbol{y}) G^{-1}_{mk}(\boldsymbol{y},\boldsymbol{z})\, z_l + n_i(\boldsymbol{x}) G_{jm}(\boldsymbol{x},\boldsymbol{y}) G^{-1}_{ml}(\boldsymbol{y},\boldsymbol{z})\, z_k + \\ n_j(\boldsymbol{x}) G_{im}(\boldsymbol{x},\boldsymbol{y}) G^{-1}_{mk}(\boldsymbol{y},\boldsymbol{z})\, z_l + n_j(\boldsymbol{x}) G_{im}(\boldsymbol{x},\boldsymbol{y}) G^{-1}_{ml}(\boldsymbol{y},\boldsymbol{z})\, z_k + \end{Bmatrix} dS, \tag{3.118}$$

where the integral is taken with respect to $\boldsymbol{z}$ over ∂V. The constant tensor $\mathbb{J}$ in (3.113) now becomes

$$\mathbb{J} = \frac{1}{V} \int_{\partial\Omega} \int_{\partial V} \boldsymbol{j}(\boldsymbol{x},\boldsymbol{y})\, ds\, ds\,, \tag{3.119}$$

where the $\boldsymbol{y}$-integration is over ∂V, and the $\boldsymbol{x}$-integration is over $\partial\Omega$.

CHAPTER IV

ISOTROPIC FUNCTIONS, ENERGY DENSITY POTENTIAL AND SECOND ORDER FABRIC TENSORS FOR POROUS MEDIA

1. EVALUATION OF THE ELASTIC MODULI FOR POROELASTIC SOLIDS: RANDOMLY ARRANGED MICROSTRUCTURE

The micromechanical characterization of porous materials is of primary importance in the study of biomaterials, in many problems of tissue mechanics as well as in the application of engineering of materials.
In fact, porous media made by a solid matrix and isolated or linked voids – which determine the porosity of the medium – form the microstructure of a wide number of materials such as the geotechnical materials (soils and rocks), cellular conglomerates, ceramic materials, synthetic biomaterials or biological tissues (e.g. cancellous bone, soft tissue). The mechanical interpretation of the elastic and ultra-elastic behaviour of such materials requires the homogenization of the overall physic and geometrical properties inside RVE of the considered poro-elastic solid. In this way, it is than possible to establish the constitutive relationship for such solids, to analyze the structural response under specific load conditions as well as – in biomedical circles – to have mathematical models useful to simulate problems of permeability or drug delivery.
If the volume fraction is strongly variable inside the considered solid, it is not possible apply standard homogenization procedure which usually require periodic microstructure, namely constant porosity.
With specific reference to cancellous bone, many author determined the elatic moduli and the strength as function of the volume fraction by means of mechanical experimental tests on a large number of bone specimens taken *in situ*.
In particular, Rho (1995) – by means of experimental tests – obtained interpolation functions between the stiffness and the volume fraction of the bone that sometimes show a too high value of standard deviation. The dispersion of the results and the dependence upon the specific type of bone are the main limits of such experimental relations.
Besides, further studies are based on numerical approaches. Analyses based on Finite Element (FE) method are implemented on micro-models whose micro-architecture has been accurately reconstructed. Unfortunately, this kind of analysis do not furnish general relations between the elastic moduli and the density because of the dependence of the results upon the specific densitometry of the specimen.

1.1. The Rho law for bone tissue

Most FE models of bone have used one average Young's modulus for cortical bone and typically less than six average values for different cancellous areas even if it is well known that the mechanical properties among species and among bones are extremely variable. Beyond relying on average mechanical properties, better approximations of bone elasticity have been obtained through correlation with density. From the densities measured on the particular bone, the elastic properties are calculated by means of published correlations of elasticity with bone density. Many author (Edidin *et al.*, 1991; Keyak *et al.*, 1990; Marom *et al.*) used CT numbers to predict the mechanical properties needed for a finite element model by founding a relationship between CT numbers and the apparent density. In particular, Rho derived specific relationships between various properties of bone for each different bone type and different direction in the same bone type by means of experimental investigations on a wide number of human bone specimens. The bone specimens were CT scanned transversely in the proximal-to-distal direction. Raw CT values were obtained from the same anatomic position as cubic specimens cut for the measurement of mechanical properties. The raw CT values were converted into Hounsfield Units (H) by relating the bone values to nearby water $(H=0)$ and air values $(H=-1000)$[14] through the formula, $H=1000\dfrac{\mathrm{CT}-\mathrm{CT_w}}{\mathrm{CT_w}-\mathrm{CT_a}}$ where $\mathrm{CT_w}$ and $\mathrm{CT_a}$ are the CT values of water and air, respectively. Bone density is defined as mean value expressed in Hounsfield units in each pixel. The density of cortical bone was determined by Archimedes' principle, while the apparent density of cancellous bone was determined by wet weight divided by volume of the overall physical dimensions of the specimens. The elastic properties of each specimen was estimated through ultrasonic techniques which offer some advantages over mechanical testing such as the ultrasonic specimens can be smaller and several anisotropic properties can be evaluated from one specimens. Both advantages are significant due to the inhomogeneity, anisotropy and limited size of bone. The experimental results were interpolated by linear ($y=c+bx$) and power ($y=bx^a$) relations. Their predictive capabilities were evaluated using *t*-test of the estimated coefficients of the general nonlinear ($y=c+bx^a$) relation which included both power (if $c=0$) and linear (if $a=1$) models.

For cortical bone, the linear relationship between axial modulus and density was found to be the best fit based on the *t*-tests of the estimated coefficients of the general nonlinear relationship for the data obtained from all examined type of bone – tibia, femur, humerus, mandible.

Bones	Dependent variable	Independent variable	Regression equations	r2
Tibia	E_3	ρ	E_3=-3.842+0.013ρ	0.53
Femur	E_1	ρ	E_1=-6.087+0.010ρ	0.61
	E_2	ρ	E_2=-4.007+0.009ρ	0.47
	E_3	ρ	E_3=-6.142+0.014ρ	0.77
Humerus	E_1	ρ	E_1=-9.212+0.011ρ	0.69
	E_2	ρ	E_2=-8.540+0.011ρ	0.66
	E_3	ρ	E_3=-6.326+0.015ρ	0.72
Mandible	E_1	ρ	E_1=-13.05+0.013ρ	0.54
	E_3	ρ	E_3=-23.93+0.024ρ	0.37

Tab. 4.1.

Linear relationship for cortical bone between elastic modulus and density obtained by Rho (1995). Values of elastic modulus (E) are expressed in GPa and the density (ρ) in kg/m^3. Subscripts 1, 2 and 3 indicate the radial circumferential and superior-inferior direction, respectively.

On the other hand, for cancellous bone the power model for moduli and apparent density had a statistically better fit based on *t*-tests of the estimated coefficients of the general nonlinear relationship for data obtained from the proximal tibia, proximal femur, and distal femur.

Both power and linear model for moduli and apparent density produced good fits for the humerus and patella, while for the lumbar spine the linear model was better than the power one.

Bones	Dependent variable	Independent variable	Regression equations	r2
Proximal Femur	E_1	ρ	E_1=-657+3.91ρ	0.9
	E_2	ρ	E_2=-506+3.64ρ	0.89
	E_3	ρ	E_3=-331+4.56ρ	0.9
	E_1	ρ	$E_1=0.004\rho^{2.01}$	0.91
	E_2	ρ	$E_2=0.01\rho^{1.86}$	0.89
	E_3	ρ	$E_3=0.58\rho^{1.30}$	0.94
	E_3	CT#	E_3=269+4.86CT#	0.8
	ρ	CT#	ρ=131+1.067CT#	0.84

Tab. 4.2.

The relations between the mechanical properties and apparent density of the proximal femur cancellous bone obtained by Rho (1995). Values of elastic modulus (E) are expressed in MPa, the apparent density (ρ) in kg/m^3, and the CT number in Hounsfield values. Subscripts 1, 2 and 3 indicate the anterior-posterior, medial-lateral and superior-inferior direction, respectively.

1.2. Generalization of the Rho law for Cubic/Isotropic Media

As recalled in the previous sections, the determination of the elastic constant of porous material such as the bone tissue is a complex problem. The relations between elastic constants and apparent density obtained by fitting experimental data often show a not negligible dispersion of the results. It is probably due to the fact that being the density a scalar quantity, it is not able to describe other microstructural features such as the orientation. Moreover, the Rho's laws depend upon the specific type of bone. On the other hand, FEM-analyses of micro-models whose micro-architecture has been accurately reconstructed require too heavy computer's elaborations and, moreover, do not furnish general relationships between the elastic moduli and the density because of the dependence of the results upon the specific densitometry of the specimen.
In order to overcome this problems, many authors also employ analysis based on the finite element method on micro-models with a regularized micro-geometry (Wagner and Gibson, 2000; Kouznetsova et al., 2001; Gonzáles et al., 2004). This approach permits to simulate mechanical tests on three-dimensional RVE by introducing both material and geometrical non-linearities, in order to predict the elastic moduli of the heterogeneous media, the yield strengths as well as possible post-elastic stress-strain curves.

However, no explicit investigations are available on the determination of overall elastic response of porous RVEs with strongly variable volume fraction, i.e., RVEs characterized by the presence of symmetrically arranged voids growing from low porosity to low volume fraction of the matrix.
Thus, with the aim of establishing a closed relationship between averaged moduli and volume fraction for porous materials, FE analyses are performed to estimate the mechanical properties of a three-dimensional cubic anisotropic porous material, whose micro-structure is geometrically modelled as periodic arrangement of cubic cells with a centred void. The shape of such voids is a cube with smoothed corner, called here *dice cavity* (see Fig. 4.1.). The matrix of the RVE is supposed to be isotropic.

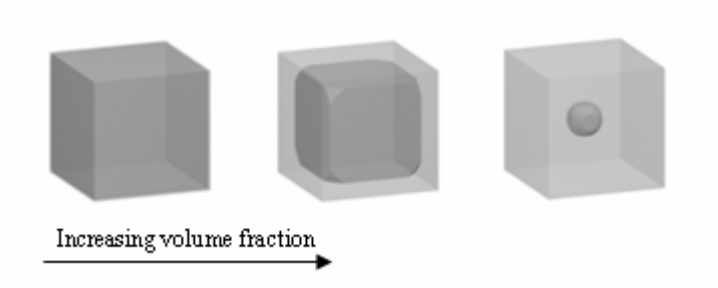

Fig. 4.1.
3D representation of the dice void porous RVE.

In particular, the upper and lower bounds of the effective elastic constants as a function of the volume fraction are evaluated, by considering displacement and traction-prescribed boundary conditions.
More in detail, a wide number of FE simulations on the 3D models with increasing dimension of the void are examined, and, for each value of the volume fraction, elastic analyses are performed to obtain overall elastic moduli as a function of the cell density. For each isotropic elastic constant, the corresponding set of computational data is interpolated by means of a specific analytical function, in order to relate density to moduli in a closed form. This law is based on the third polynomial regression and is solved through limit conditions defined to make it obeying to the Flugge's theory – in case of high porosity – and to the theory of dilute distribution of voids – valid in the case of high volume fraction.
Moreover, in order to also evaluate the influence of the shape of cavities on the overall mechanical properties of the RVE at a fixed value of the volume fraction, voids of three different shapes are considered, that is a sole centred spherical void, eight overlapping spherical voids and seven overlapping ellipsoidal voids (see Figure 4.2.). For reaching lowest volume fractions, in the last mentioned

case, voids are able to intersect RVE sides, to describe the mechanical response for more complicated shapes of the porous material.

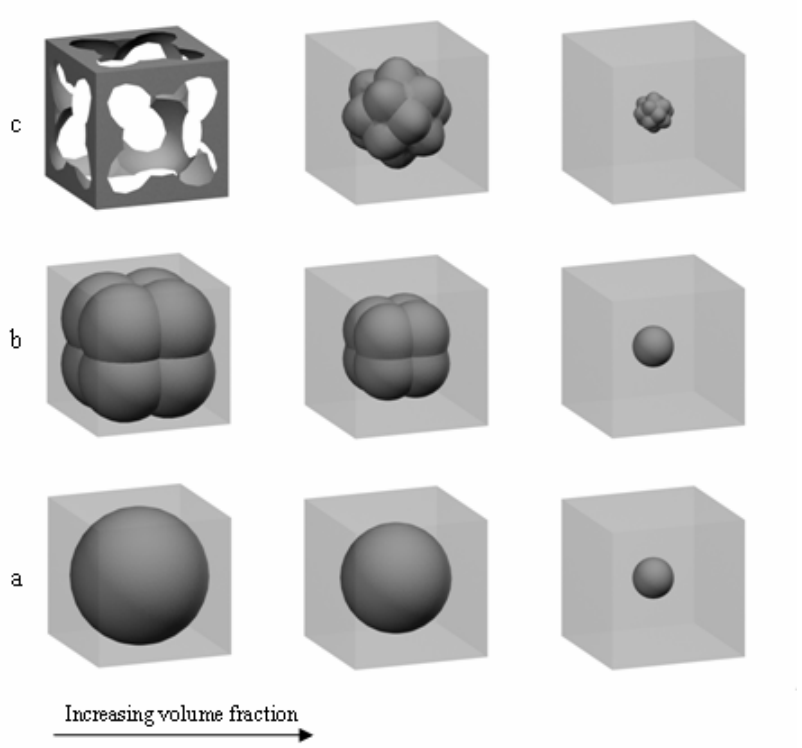

Fig. 4.2.

3D representation of cubic RVEs showing different types of cavities and with increasing volume fraction: a) single sphere void porous RVE, b) eight spheres void porous RVE, c)seven ellipsoids void porous RVE.

1.2.a. Finite Element Model

Starting from an heterogeneous porous material, homogenization criteria can be developed through different ways. To predict homogenized behaviour of a porous cubic symmetric material, it is useful to adopt a cubic cell RVE oriented towards material symmetry direction, in way to obtain a cubic symmetric RVE. By the shape and distribution of voids investigated in this work, two different cubic symmetric RVE are available: a cubic cell centred on void and cubic cell with voids eroding its corners, Fig 4.3.

3D representative sketches of cells eroded symmetrically at the eight corners by decreasing volume voids with dice form are shown in Fig. 4.4.

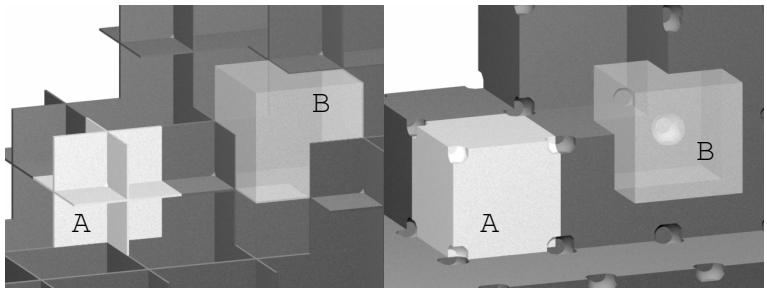

Fig. 4.3.
3D representation of cubic RVE position in a porous material with periodic voids arrangement, for $\gamma \to 0$ *on the left, for* $\gamma \to 1$ *on the right. Type A) corner eroded, type B) void centred.*

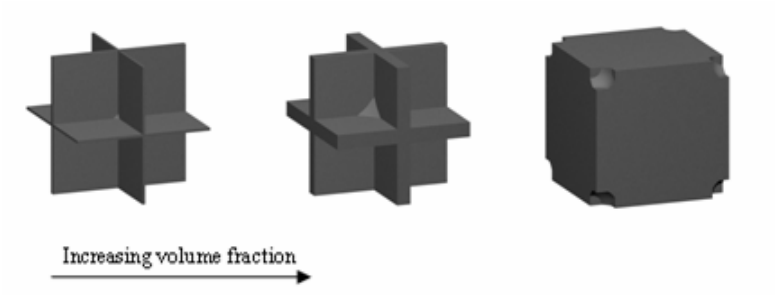

Fig. 4.4.
3D representation of corner eroded void porous RVE through increasing volume fraction sketches.

Therefore, in order to estimate the influence of the volume fraction on the overall mechanical behaviour of the porous media, a model of cubic porous RVE centred on void is studied, namely the cubic RVE introduced above (Fig 4.1.). Model's density varies within a characteristic voids length. Smoothed edge cubic volume is subtracted from the RVE and the diagonal of the subtracted cubic volume varies from $L/2$ to $\sqrt{3}\cdot L/2$, where L is the length of the RVE's side. Thanks to symmetrical subtractions, the varying density of the cell keeps cubic anisotropy in every porous configuration. The volume fraction of the models, γ, varies in the range $[0.06,1]$. In particular, a typical dilute porous material arrangement is obtained when γ is close to 1, while a structure made of orthogonal linked shells – like the Flugge's porous material model (Flugge, 1972) – is obtained γ tends to 0, see Fig. 4.3. Material properties of the matrix of cubic cell is assumed to be linear, elastic and isotropic, characterized by the Young modulus $E_0 = 17200MPa$ and the Poisson's ratio $\nu_0 = 0.3$.

The 3D model is meshed by using ten nodes three dimensional isoparametric tetrahedral elements which have a quadratic displacement shape function and thus are well suited to model irregular geometry.
A routine for the automatic generation of both geometric models and mesh is created. In particular, the algorithm allows the automatic generation of a wide number of FE models, in which the dimension of the voids progressively increases, in a way able to obtain a population of results sufficient to draw with accuracy the relations between average mechanical properties and volume fraction. Representation sketches of FE mesh is shown in figure 4.5. where, for a better voids visualization, corner eroded RVE type is reported.
Two different load conditions are considered, that is uniform tractions and uniform displacements prescribed on cubic cell surfaces. In both cases, over three of the others faces of the cubic cell, symmetric boundary conditions in terms of displacements are applied.

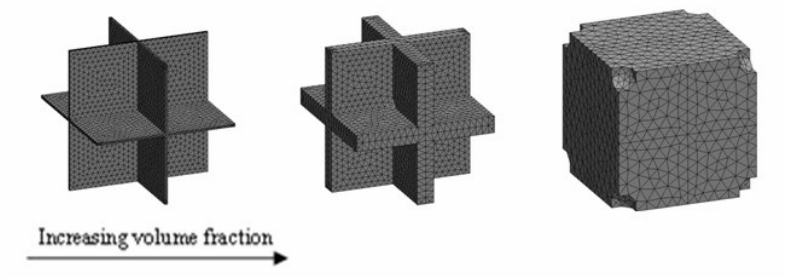

Fig. 4.5.
3D representation of meshed FE model of corner eroded RVE trough increasing volume fraction sketches.

1.2.b. Model's accuracy

Fine element local population defines fidelity both of geometrical and material model behaviours. FEM model mesh accuracy is generally intended to assure an high precision of the performed analysis results. Principal mesh thickness upper bound is marked by solving process time directly related to clock speed of implemented machine. Fixing results error tolerance, finite element mesh is to be lower populated as possible, in way to obtain an easily handling model.
An error tolerance percentage of 3% is assumed here, model mesh densities is tested to ensure this accuracy level and it shows less than 35.600 elements for cases of highest complexity of cavity geometry (see fig 4.6.). So, it is able to perform a large number of analyses.
The geometry of the porous modelled RVE varies with a single geometrical parameter, in way to obtain a variable RVE's density. For each value of such

parameter a specific routine aims to obtain the generation of a local parametric. In no one case a wall of less than three finite elements thickness appears and the generally coarse mesh becomes automatically more and more fine whereas the cavity surface curvature drastically increase.

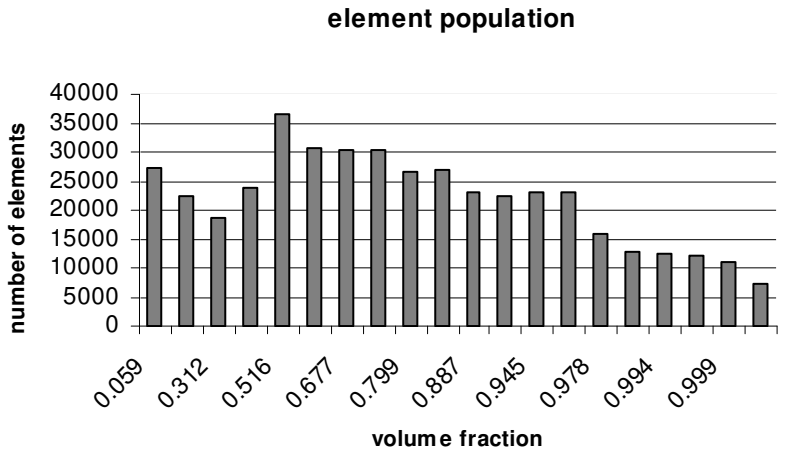

Fig. 4.6.
Finite Element population in modelled dice void RVE.

1.2.c. Cavities of different shapes

The mechanical behaviour of the RVE is generally related to shape and direction of voids. In way to investigate this aspect three different cavity types are adopted to model cell's porosity. Cubic symmetry is at least preserved over all three types, and different volume fraction range is allowed for each of them. The density for each model varies within a characteristic voids length. Models reproduce a cubic cell with constant length side, L, with different types of cavity. The three cavity types are: one centred spherical cavity, eight centred overlapping spherical cavity of the same radius and finally seven centred overlapping ellipsoidal cavity of common dimensions, Fig. 4.2.
In the first model, the centre of the spherical void coincides with the centre of cubic cell and the radius increases from the minimum value of $L/20$ until the maximum value of L, where L is the length of the RVE cubic cell side, and the related volume fraction varies in the range $[0.5,1]$, (see fig.4.2.a.).
In the second model, eight overlapping spherical voids are considered. Every sphere has the centre located on the semi-diagonal of the cubic cell and passes for its centre, that is the position of the centre of each sphere depends on their radius, (see fig.4.2.b). The volume fraction of this model varies in the range

$[0.48,1]$. The increasing sphere radius r must satisfy the inequality $r < L/323$ in order to avoid intersection between cubic cell surface and cavity.
In the last model, the centre of each of the seven ellipsoidal cavities is placed at the centre of the cell, the major diameters of three of them lying on the three axis orthogonal to the cell faces, and the other four ellipsoids major diameters lie on the four RVE diagonals. The major ellipsoidal axes varies between $L/20$ and $L/1.21$. The upper limit of axes length value is imposed by the geometrical consistency of the model and for this cavity type the intersections with the faces of the cubic cell are allowed, (see fig.4.2.c). In this way, a wider range of the volume fraction is obtained, in fact it is included in the range $[0.14,1]$.
The matrix of the cubic cell is assumed to be linear, elastic and isotropic, characterized by the Young modulus $E_0 = 17200MPa$ and the Poisson's ratio $\nu_0 = 0.3$.

1.2.d. Homogenized elastic constants

Numerical mechanical tests are performed on the L side cubic cell with a centred dice cavity which gives to the RVE a cubic symmetry. Thus, to define its elastic behaviour, three elastic constants are needed. The variation of the dimension of the cavity produces a variation of the volume fraction in a wide range of value, and so it is possible to obtain all the homogenized elastic properties as function of the volume fraction.
The model is tested both under uniform tractions and uniform displacements normal to a face of the RVE cubic cell. Moreover, cubic symmetric RVE models are even tested both under pure share uniform tractions and angular deflection parallel to a RVE face, and loaded by hydrostatic pressure as well as uniform triaxial displacements. These tests are aimed to obtain the relation between average stresses and average deformations in way to define homogenized elastic properties of the porous RVE.
Analyses performed under uniform displacements give as result the average stress tensor while the average deformation tensor is directly deduced by uniform displacements applied at the RVE surface. Thus, the elastic constants, such as the first and second Lamé constant, anisotropic shear modulus and bulk modulus, of the porous RVE are calculated.

In case of normal displacements, in a coordinate system parallel to cubic sides, the elastic constants are defined by the meaning of:

$$<\begin{bmatrix}\sigma_x\\ \sigma_y\\ \sigma_z\\ \tau_{xy}\\ \tau_{yz}\\ \tau_{xz}\end{bmatrix}>=\begin{bmatrix}\lambda+2G & \lambda & \lambda & 0 & 0 & 0\\ \lambda & \lambda+2G & \lambda & 0 & 0 & 0\\ \lambda & \lambda & \lambda+2G & 0 & 0 & 0\\ 0 & 0 & 0 & 2G' & 0 & 0\\ 0 & 0 & 0 & 0 & 2G' & 0\\ 0 & 0 & 0 & 0 & 0 & 2G'\end{bmatrix}\cdot<\begin{bmatrix}0\\ 0\\ \varepsilon_z\\ 0\\ 0\\ 0\end{bmatrix}>, \quad (4.1)$$

where λ and G are first and second Lamé constant, respectively, G' is a further elastic constant which defined the cubic symmetry of the material and, calling L the RVE cubic cell side length, $w=<\varepsilon_z>\cdot L$ is the applied displacement on positive z normal cubic cell face in z direction, see figure 4.7.
In case of angular deflection:

$$<\begin{bmatrix}\sigma_x\\ \sigma_y\\ \sigma_z\\ \tau_{xy}\\ \tau_{yz}\\ \tau_{xz}\end{bmatrix}>=\begin{bmatrix}\lambda+2G & \lambda & \lambda & 0 & 0 & 0\\ \lambda & \lambda+2G & \lambda & 0 & 0 & 0\\ \lambda & \lambda & \lambda+2G & 0 & 0 & 0\\ 0 & 0 & 0 & 2G' & 0 & 0\\ 0 & 0 & 0 & 0 & 2G' & 0\\ 0 & 0 & 0 & 0 & 0 & 2G'\end{bmatrix}\cdot<\begin{bmatrix}0\\ 0\\ 0\\ 0\\ \varepsilon_{yz}\\ 0\end{bmatrix}>, \quad (4.2)$$

where $\gamma=2\cdot<\varepsilon_{yz}>$ is the applied angular deflection on x and y normal cubic cell faces in the xy plane, see figure 4.7.
When a uniform triaxial displacements is applied to the cubic RVE, the bulk modulus is

$$k=\frac{<\sigma_x>+<\sigma_y>+<\sigma_z>}{3}\cdot\frac{1}{<\varepsilon>}, \quad (4.3)$$

where $<\varepsilon>\cdot L=<\varepsilon_x>\cdot L=<\varepsilon_y>\cdot L=<\varepsilon_z>\cdot L$ is the uniform displacement applied normally to three adjacent faces of the cubic RVE.
The analyses performed under uniform tractions give as result the average deformation tensor while the average stress tensor is directly deduced by uniform tractions applied at the RVE surface. Thus, the elastic constants, such as Young modulus, Poisson ratio, anisotropic shear modulus and bulk modulus, of the porous RVE are calculated.

In case of normal tractions, constants are defined by the meaning of:

$$<\begin{bmatrix}\varepsilon_x\\ \varepsilon_y\\ \varepsilon_z\\ \varepsilon_{xy}\\ \varepsilon_{yz}\\ \varepsilon_{xz}\end{bmatrix}>=\begin{bmatrix}\frac{1}{E} & -\frac{\nu}{E} & -\frac{\nu}{E} & 0 & 0 & 0\\ -\frac{\nu}{E} & \frac{1}{E} & -\frac{\nu}{E} & 0 & 0 & 0\\ -\frac{\nu}{E} & -\frac{\nu}{E} & \frac{1}{E} & 0 & 0 & 0\\ 0 & 0 & 0 & \frac{1}{2G'} & 0 & 0\\ 0 & 0 & 0 & 0 & \frac{1}{2G'} & 0\\ 0 & 0 & 0 & 0 & 0 & \frac{1}{2G'}\end{bmatrix}\cdot<\begin{bmatrix}0\\ 0\\ \sigma_z\\ 0\\ 0\\ 0\end{bmatrix}>, \quad (4.4)$$

where E and v are Young's modulus and Poisson ratio respectively, and $p=\frac{<\sigma_z>}{L^2}$ is the applied traction over positive z normal cubic cell face in z direction.

In case of shear tractions:

$$<\begin{bmatrix}\varepsilon_x\\ \varepsilon_y\\ \varepsilon_z\\ \varepsilon_{xy}\\ \varepsilon_{yz}\\ \varepsilon_{xz}\end{bmatrix}>=\begin{bmatrix}\frac{1}{E} & -\frac{\nu}{E} & -\frac{\nu}{E} & 0 & 0 & 0\\ -\frac{\nu}{E} & \frac{1}{E} & -\frac{\nu}{E} & 0 & 0 & 0\\ -\frac{\nu}{E} & -\frac{\nu}{E} & \frac{1}{E} & 0 & 0 & 0\\ 0 & 0 & 0 & \frac{1}{2G'} & 0 & 0\\ 0 & 0 & 0 & 0 & \frac{1}{2G'} & 0\\ 0 & 0 & 0 & 0 & 0 & \frac{1}{2G'}\end{bmatrix}\cdot<\begin{bmatrix}0\\ 0\\ 0\\ 0\\ \tau_{yz}\\ 0\end{bmatrix}>, \quad (4.5)$$

where $t=\frac{<\tau_{yz}>}{L^2}$ is applied pure shear traction over x and y positive normal cubic cell faces.

When hydrostatic pressure p is applied to the cubic RVE, the bulk modulus k is:

$$k = \frac{p}{<\varepsilon_x> + <\varepsilon_y> + <\varepsilon_z>}, \tag{4.6}$$

where $p = \dfrac{<\sigma_x> + <\sigma_y> + <\sigma_z>}{3}$.

According to Voigt and Reuss theory, prescribed tractions and prescribed displacement numerical tests give the upper and lower bounds of the investigated elastic properties, respectively. The models is tested in the available volume fraction range by a wide number of FE analyses. Both prescribed displacements and tractions tests are performed whether to obtain elastic isotropic characterization or to define cubic constant. Totally 20 finite element porous RVE models are processed under 6 different load cases.

Two constant are needed to describe isotropic elastic behaviour for all of the porous RVE cavity types, that is the Lamé constants λ and G or equivalently, the Young's modulus E and the Poisson ratio ν. A generic uniform normal displacement is applied over a face of the cubic RVE cell on a wide range of density, that means applying the average deformation tensor to the RVE. Finite element analysis gives as result the RVE average stress tensor, it allows direct calculation of the Lamé constants by means of the equation (4.1). Furthermore, a generic pressure is applied over a face of the cell, to perform tractions prescribed isotropic analysis. As results RVE average deformation tensor is obtained; starting from imposed average stress tensor Young's modulus and Poisson's ratio are directly calculated by means of the equation (4.4). As well known, the two couples of elastic constants λ and G, and E and ν are related by the following laws

$$\begin{cases} \lambda = \dfrac{\nu \cdot E}{(1+\nu)\cdot(1-2\nu)} \\ G = \dfrac{E}{2(1+\nu)} \end{cases}, \quad \begin{cases} E = \dfrac{G(3\lambda + 2G)}{\lambda + G} \\ \nu = \dfrac{\lambda}{2\lambda + G} \end{cases},$$

and both of them can equivalently characterize RVE isotropic elastic behaviour. In the follow Young's modulus and Poisson's ratio will be used.

Moreover, it is here recall the relationship between the bulk modulus and the two isotropic elastic constants E and ν:

$$k = \frac{E}{3(1-2\nu)}. \tag{4.7}$$

In the follow, they are reported three graphs that shown the variation of the Young's modulus, Poisson's ratio and bulk modulus with the volume fraction. The Young's moduli are normalized by defined value of the Young's modulus of the matrix.

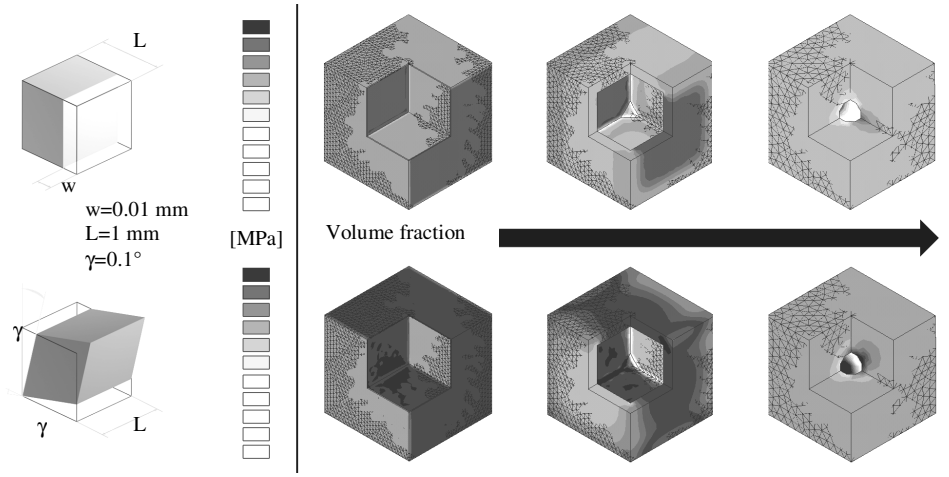

Fig. 4.7.

FE contour plot results of displacement applied test on porous RVE models, an inspection hole let see the interior, spots of the FE mesh are even highlighted. In the upper section first direction stresses are plotted in case of normal displacement for three different density type model; on the left, respective cinematic conditions are sketched. In the lower section shear stresses in deflection plane are plotted in case of angular deflection for three different density type model; on the left, respective cinematic conditions are sketched.

The graph in figure 4.8. shows that the normalized modulus tends to unit value when volume fraction is close to one, whereas while volume fraction diminishes results give values gradually lower and lower.

The graph in figure 4.9. shows the dependence of the Poisson's ratio by the volume fraction. The values are normalized by the value of the Poisson's ratio of the matrix, and, as expected, coincide to unit when cell is a full matrix RVE, instead, for lower value of the volume fraction, tend to a specific not zero value. Although the processed RVE model shows a cubic anisotropy, the bulk modulus depends upon the sole constants of the first diagonal block of its elasticity tensor – that is the Young's modulus and Poisson's ratio. This evidence is remarked by the correspondence between bulk modulus calculated by means of the law (4.7) and which one calculated by means of the results of triaxial FEM analyses. The graph in figure 4.10. shows that the normalized modulus tends to unit value when volume fraction is close to one, whereas while volume fraction diminishes results give values gradually lower and lower.

According to Voight and Reuss theory, the elastic constant calculated by means of prescribed displacements analyses are grater then which ones calculated by prescribed tractions ones.
Figure 4.7 shows FE results through contour value range related to normal displacement applied test on dice porous RVE model with volume fraction 0.2%.

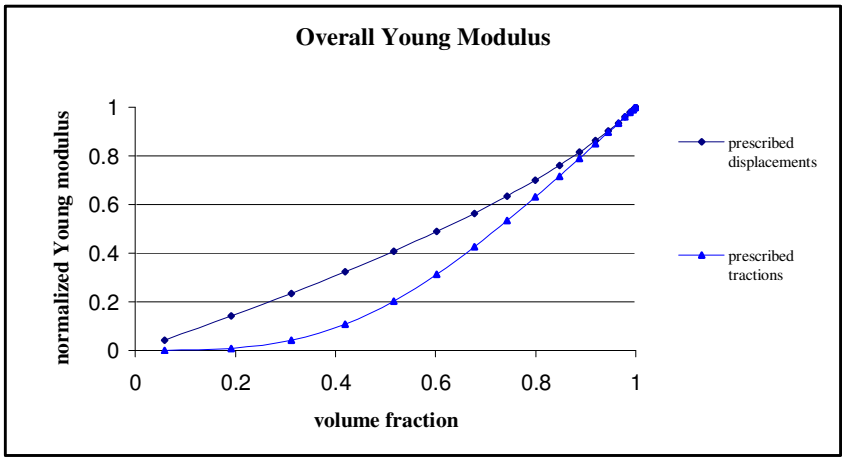

Fig. 4.8.
Volume fraction trend of Young's modulus normalized over matrix value in FE analyses of a cubic RVE showing a centred dice cavity.

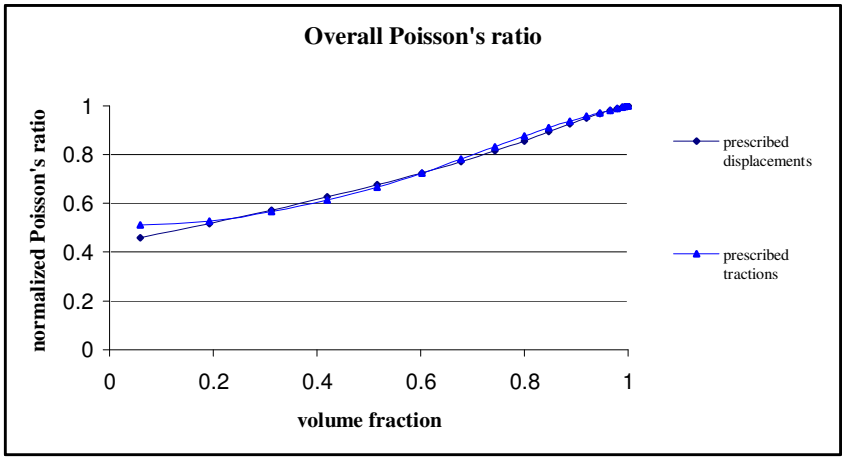

Fig. 4.9.
Volume fraction trend of Poisson's ratio normalized over matrix value in FE analyses of a cubic RVE showing a centred dice cavity.

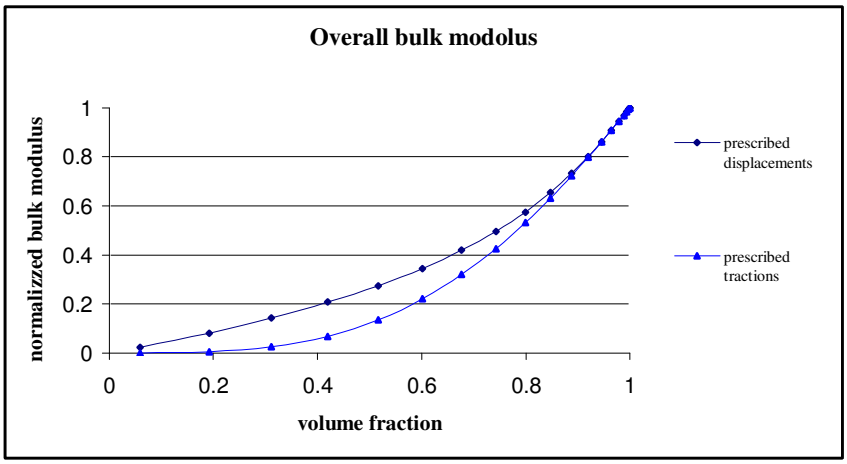

Fig. 4.10.
Volume fraction trend of bulk modulus normalized over matrix value in FE analyses of a cubic RVE showing a centred dice cavity.

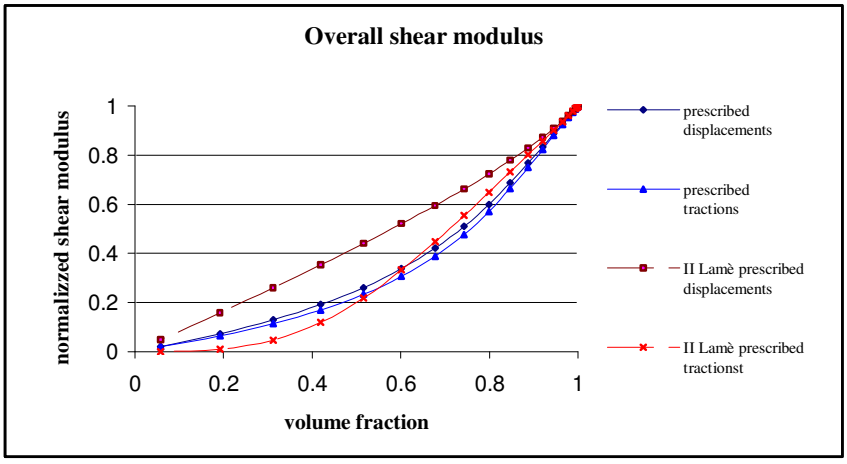

Fig. 4.11.
Volume fraction trend of shear modulus normalized over matrix value in dice cavity RVE. The normalized II Lamé constant trend is also highlighted.

Due to the cubic symmetry of the RVE, more numerical tests has been necessary to estimate the only anisotropic constant, that is G', the shear modulus. A prescribed pure shear and angular deflection tests are implemented. In both of case, elastic constants dependence on the volume fraction is obtained through the relations (4.2) and (4.5).

The analyses show significant difference between the two considered load conditions – prescribed tractions and displacements – (see figure 4.11.). However, in both of cases, normalized modulus rise with density from zero to the unit. In the graph in figure 4.11. is even represent the second Lamé constant variation, normalized by the corresponded matrix one.

1.2.e. Cavity's shape influence

Numerical mechanical tests are performed on porous RVEs characterized by three different cavity types, with the volume fraction variable in quite all the range zero-one, in way to obtain a density function of all the homogenized elastic constants of the porous RVEs. Two of the three porous RVEs model types shows a cavity geometry realized by spheres, one is a single centred sphere cavity, the other is a polar symmetric eight sphere union (see section 1.2.c.). In both cases the models may be considered isotropic and so two sole constants are needed to define the elastic homogenized RVE behaviour. In the third model, the cavity is made of seven centred polar symmetric ellipsoides (see section 1.2.c.). This model shown a cubic symmetry and so one more constant is needed to define its elastic behaviour.
Each model is tested both under uniform tractions and uniform displacements normal to a face of the RVE cubic cell. Moreover, cubic symmetric RVE models are even tested both under pure share uniform tractions and angular deflection in a plane parallel to a RVE face. These tests are aimed to obtain the relation between average stresses and average deformations in way to define homogenized elastic properties of the porous RVE, following the same procedure above described.
Each of three cavity's types models are tested in the available volume fraction range by 20 analyses per type. Both prescribed displacements and tractions tests are performed in order to obtain the homogenised elastic constants of the RVEs. Totally 60 finite element porous RVE models are processed under 6 different load cases. All this data set is added to one obtained through dice cavity RVE models tests in way to estimate cavity shape influence on elastic constants density trend.
In the graph in figure 4.12., the variation of the normalized Young modulus within the volume fraction is reported. It is possible to note that the normalized moduli tend to unit value when volume fraction is closed to one, and decrease when the volume fraction decreases. This trend is quite the same for both prescribed displacement and tractions tests. In figure 4.12. the difference between these two calculation methods is highlighted; according to Voight and Reuss theory, the Young modulus evaluated in prescribed traction tests is always greater than that one evaluated in prescribed displacements tests. However, not relevant differences in Young modulus density function are detected both in prescribed displacements and tractions tests throughout different cavity shapes.

In the graph in figure 4.13, Poisson's ratio variation within volume fraction is plotted for one sphere, eight spheres and seven ellipsoides cavity types. The homogenized Poisson's ratios are normalized by constant value of matrix Poisson's ratio. As the volume fraction goes down, values trend goes from unit to specific lower value in case of applied displacement tests for every cavity types but not for the seven ellipsoides cavities that has seems to rich zero value corresponding to zero volume fraction. Instead, for prescribed traction, the values remain close to unit, thus they appear grater then traction prescribed ones for all types of cavity but not for dice cavity one, whose trend is displacement like. Each kind of results seems to be significantly affect from cavity shape.
The same graphic is performed for bulk modulus. The moduli related to each cavity's shape are normalized by constant value of matrix bulk modulus. In the graph in figure 4.14. a regular trend is highlighted, where applied displacement applied tests values are grater than prescribed tractions ones. In both of case the results are similar for every cavity types, and when volume fraction decreases the normalized bulk modulus goes from unity to zero.

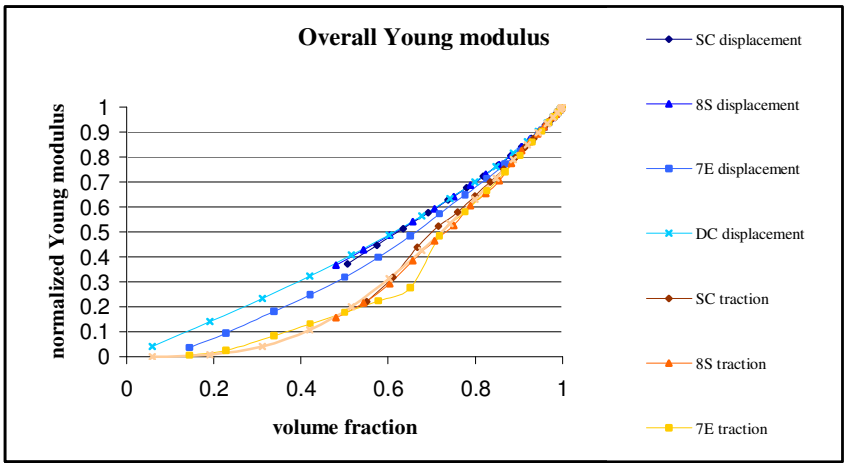

Fig. 4.12.

Volume fraction trend of Young modulus normalized over matrix value in FE analyses performed on RVE showing different cavity's shapes. (SC one sphere, 8S eight spheres, 7E seven ellipses, DC dice).

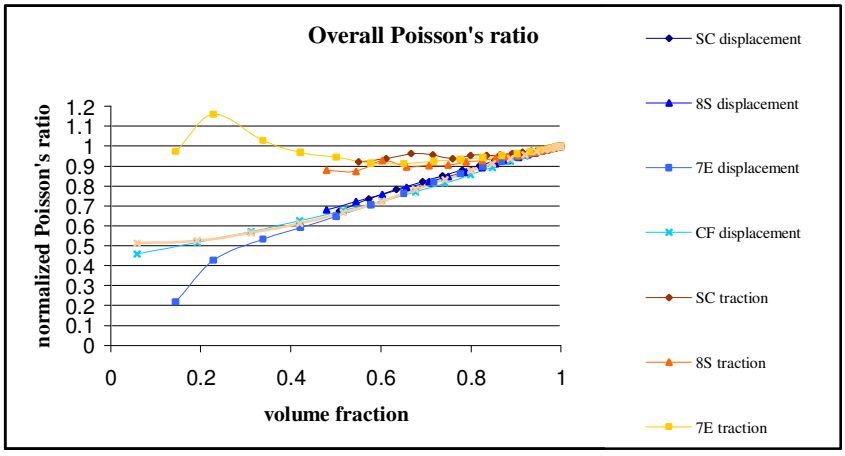

Fig. 4.13.

Volume fraction trend of Poisson's ratio normalized over matrix value in FE analyses performed on RVE showing different cavity's shapes. (SC one sphere, 8S eight spheres, 7E seven ellipses, DC dice).

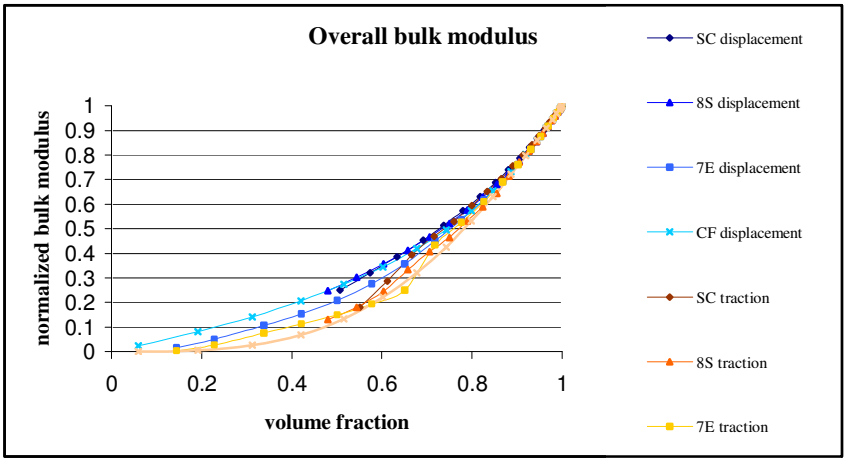

Fig. 4.14.

Volume fraction trend of bulk modulus normalized over matrix value in FE analyses performed on RVE showing different cavity's shapes. (SC one sphere, 8S eight spheres, 7E seven ellipses, DC dice).

1.2.f. Algebraic formulation

In scientific literature, it is available a self-consistent evaluation of the elastic moduli of porous media in case of dilute distribution of voids – that is for high value of the volume fraction (Christensen, 1979). On the other hand, Flugge's model (Flugge, 1972) allows to evaluate the homogenized elastic properties of a RVE made of three dimensional orthogonal shell arrangement and so that shown an high value of porosity. In particular, by means of the above mentioned theory, the following expressions of the homogenized bulk modulus as function of the volume fraction are found out:

$$\frac{k}{k_0}=\begin{cases}\varphi(\gamma)=c\cdot\gamma & \gamma\in[0,0.15]\\ \eta(\gamma)=1+\dfrac{(\gamma-1)}{c} & \gamma\in[0.85,1]\end{cases} \tag{4.8}$$

where k_0 is the matrix's bulk modulus, γ is the volume fraction and $c=\frac{2}{3}\cdot\frac{(1-2\nu)}{(1-\nu)}$ with ν equal to the matrix's Poisson's ratio. So, the equations (4.8) allow to calculate the overall elastic constants when the volume fraction is closed to one or to zero.
By starting from these theories, it is possible to establish a single law of variation for the overall elastic constant valid all over the range $[0,1]$ of the volume fraction.
In particular, the experimental results previously presented are interpolated by a third polynomial regression $\chi(\gamma)$.

$$\chi(\gamma)=C_1+C_2\cdot\gamma+C_3\cdot\gamma^2+C_4\cdot\gamma^3 \qquad \gamma\in[0,1]. \tag{4.9}$$

The four polynomial constants are determined by imposing that in limit condition – when $\gamma=0$ and $\gamma=1$ – the interpolation polynomial function have to verified the relations (4.8). So, the boundary conditions are

$$\begin{aligned}&\chi(0)=\varphi(0), \qquad &&\frac{\partial\chi}{\partial\gamma}(0)=\frac{\partial\varphi}{\partial\gamma}(0)=c\\ &\chi(1)=\eta(1), \qquad &&\frac{\partial\chi}{\partial\gamma}(1)=\frac{\partial\eta}{\partial\gamma}(1)\end{aligned} \tag{4.10}$$

and furnish the follow values of the polynomial constants

$$C_1=0,\quad C_2=c,\quad C_3=-\frac{1-3\cdot c+2\cdot c^2}{c},\quad C_4=-\frac{-1+2\cdot c-c^2}{c}. \tag{4.11}$$

In this way, the function $\chi(\gamma)$ is consistent with the theories above mentioned and it is defined all over the volume fraction range.

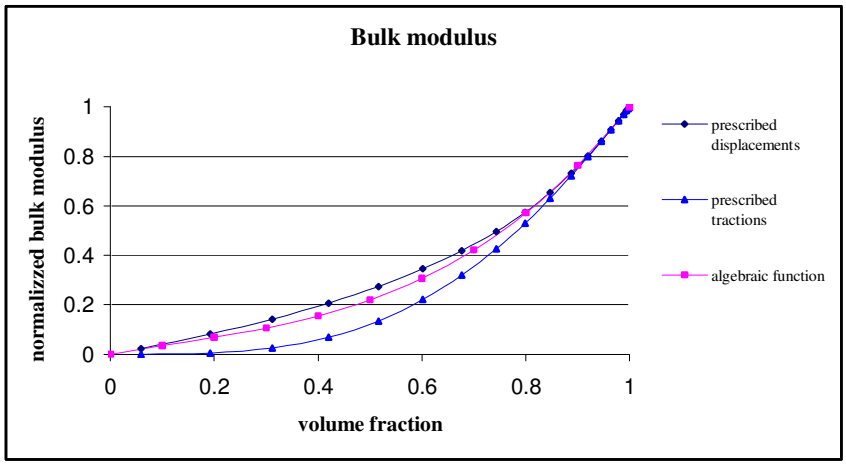

Fig. 4.16.

Confrontation between the algebraic function and the experimental ones of the overall bulk modulus. The experimental functions are obtained by means of prescribed displacements and tractions tests, respectively.

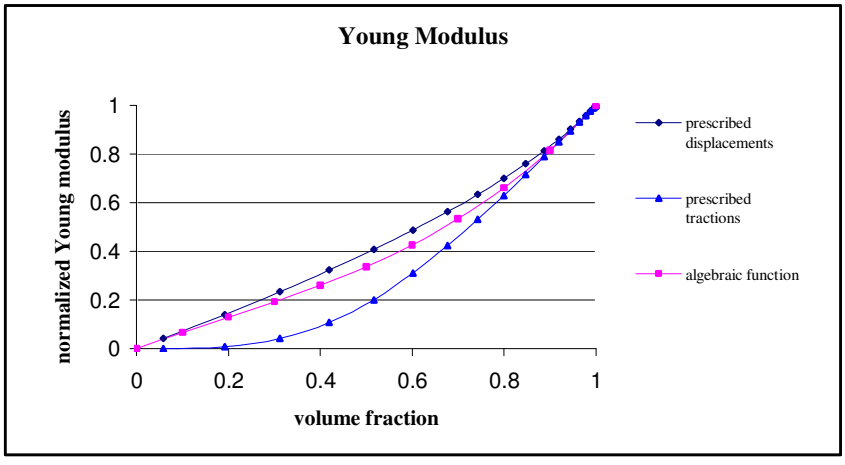

Fig. 4.17.

Confrontation between the algebraic function and the experimental ones of the overall Young modulus. The experimental functions are obtained by means of prescribed displacements and tractions tests, respectively.

Through an analogous procedure and utilizing the Christensen and Flugge's solutions for the Young modulus, it is possible to obtained an algebraic function which well interpolates the experimental results for the Young modulus, too.
In graphs in figure 4.16 and 4.17 the results obtained for the bulk modulus and Young modulus in case of RVE with dice cavity are shown. In both cases the algebraic functions well match the experimental results.
It is important to note that although in scientific literature some laws for the determination of the overall elastic constant of isotropic porous materials were proposed, they are not of general validity. In fact, the proposed laws – e.g. the Rho's law for bone tissue – are found out by means of experimental tests and then they are valid for the sole considered material. On the contrary, the laws proposed in this section have general validity being determine independently from the specific material or microstructural morphology.

2. EVALUATION OF THE ELASTIC MODULI FOR POROELASTIC SOLIDS: ORIENTED MICROSTRUCTURE

In this section materials that shown an orientated microstructure are treated. Such materials may be considered inhomogeneous and anisotropic because of the orientation of the microstructure.
In scientific literature, continuum models are proposed to describe the mechanical behaviour of anisotropic poroelastic materials, some of which are illustrated in Chapter II and III. Particular attention is here given to the micromechanical approach based on fabric tensor which, in spite of the mechanical consistency, is difficult to employ because it requires the evaluation of the fabric tensor which is variable with the position.
In the follow, some procedures to mechanically characterize anisotropic poroelastic materials are shown. In particular, the oriented microstructure materials with low and high volume are studied separately because in the first case the anisotropic behaviour is governed by the microstructural architecture, while in the second case by the voids orientation.
For poroelastic materials with low volume fraction a constitutive relationship is given starting from Flugge's solution generalized to the orthotropic case. This strategy conducts to an identification of the fabric eigenvalues which suggests to identify the fabric tensor with the inertia tensor opportunely normalized. In the complementary case – high volume fraction – the constitutive relation are found starting from the elastic solution of an ellipsoidal void in an infinite linear elastic solid.
In order to bear out the hypotheses of identifying the fabric tensor with the inertia tensor, some examples shown the analogies and the differences between the mean intercept length tensor and the inertia tensor for bidimensional RVE. Such examples seem to confirm the advisability to use the inertia tensor like microstructural parameter.

2.1. Flugge's solution for orthotropic porous material – Low Volume Fraction (LVF)

In this section, it is derived the overall elasticity tensor for the idealized porous material shown in Figure 4.18, (Flugge, 1972). It consists of many thin isotropic and homogeneous walls of different thickness, say $t_i \ll a$, parallel to the coordinate planes of a Cartesian system $\{x_1, x_2, x_3\}$. Then, t_i represents the thickness of the wall whose unit normal vector is coaxial with the x_i-axis, while the size a of the regularized pores have to be assumed small compared with the characteristic length L of the cubic RVE.

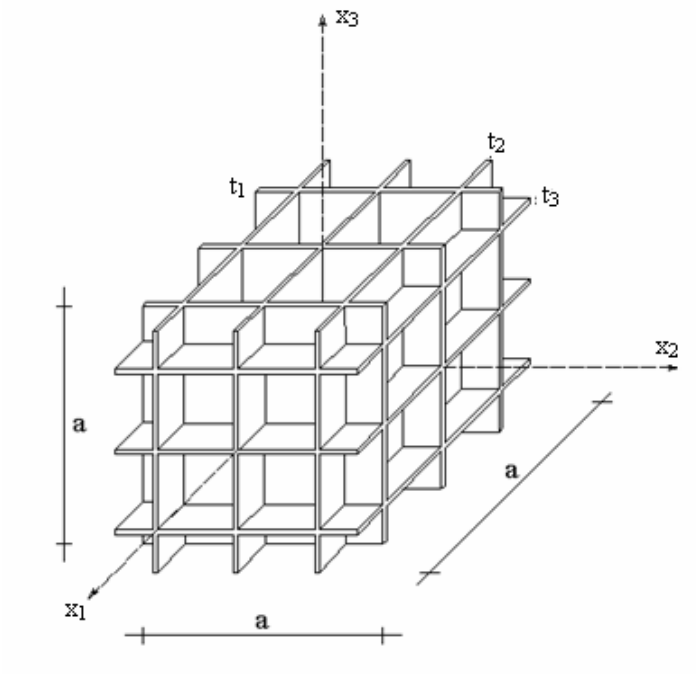

Fig. 4.18.
Flugge's idealized porous RVE

In each of the walls a plane stress system is possible. This means that, for example, the Hooke's stress-strain laws in the walls parallel to the $x_1 - x_2$ plane can be written in the following form

$$\begin{aligned}\sigma_{11} &= \frac{E}{(1-\nu^2)}(\varepsilon_{11}+\nu\varepsilon_{22}),\\ \sigma_{22} &= \frac{E}{(1-\nu^2)}(\varepsilon_{22}+\nu\varepsilon_{11}),\\ \sigma_{12} &= \frac{E}{2(1+\nu)}\varepsilon_{12},\end{aligned} \tag{4.12}$$

where E and ν are the Young modulus and the Poisson ratio of the isotropic and homogeneous matrix, respectively.

By starting from the micro-mechanical approach, it is immediately evident that the architecture of the considered RVE exhibits three planes of mirror symmetry. Then, by recalling that an element with sides parallel to the planes of elastic symmetry, after deformation under the action of any normal stress, remains a rectangular parallelepiped, it is easy to verify that all the coefficients of mutual influence and the coefficients of Chentsov vanish in a coordinate system the direction of whose axes coincides with the principal directions of elasticity. Then, in order to determine the overall elasticity tensor in Voigt contracted notation for the porous RVE, a classical homogenization procedure is employed and the equivalent orthotropic material is obtained.

To prove this, consider the RVE under several boundary conditions. In particular, to explore the elastic behaviour of the porous material, we assign several states of strain, applying corresponding forces on the faces of the porous cube, assuming the side characteristic length $L = n\,a$, with n $\{n \in \mathbb{N}, n \gg 1\}$ representing the number of walls for side. Then, we first consider the case in which a simple stretching is imposed, i.e. ε_{11} in the horizontal x_1 direction, with $\varepsilon_{22} = \varepsilon_{33} = 0$, as well as $\{\varepsilon_{ij} = 0,\ \forall i \neq j\}$. On the face $x_1 = \text{const}$ this requires stresses σ_{11} in the vertical and in the horizontal walls, from which we can write

$$\Sigma_{11} = n^2 a (t_2 + t_3)\sigma_{11} = n^2 a (t_2 + t_3)\frac{E}{1-\nu^2}\varepsilon_{11}, \tag{4.13}$$

where Σ_{11} represents the total force in the x_1 direction on the face whose normal is x_1. In general, in the follows, we will consider Σ_{ij} as the total force acting on a face whose normal is parallel to the x_i axis, in the x_i direction.

All the vertical walls normal to the x_1 axis have no strains and no stresses, while on the faces $x_2 = \text{const}$ and $x_3 = \text{const}$ there is only a contribution from the horizontal and vertical walls, respectively:

$$\Sigma_{22} = n^2 a t_3 \sigma_{22} = n^2 a t_3 \frac{\nu E}{1-\nu^2}\varepsilon_{11},$$
$$\Sigma_{33} = n^2 a t_2 \sigma_{33} = n^2 a t_2 \frac{\nu E}{1-\nu^2}\varepsilon_{11}. \tag{4.14}$$

It is worth to note that no shear forces are present. Now, in order to define for the porous material the "gross stresses", or equivalently the "macro-stresses", we have to divide each force by the nominal area $A = L^2 = (n a)^2$ of the face in which it is transmitted. By following this procedure we obtain

$$\Sigma_{11} = \frac{(t_2 + t_3)}{a}\frac{E}{1-\nu^2}\varepsilon_{11},$$
$$\Sigma_{22} = \frac{t_3}{a}\frac{\nu E}{1-\nu^2}\varepsilon_{11}, \tag{4.15}$$
$$\Sigma_{33} = \frac{t_2}{a}\frac{\nu E}{1-\nu^2}\varepsilon_{11},$$

where Σ_{ij} represents the macro-stresses. Moreover, considering the other two strains producing simple stretching in x_2 and x_3 directions and combining all the three conditions, we obtain

$$\Sigma_{11} = \frac{E}{(1-\nu^2)a}[(t_2 + t_3)\varepsilon_{11} + \nu(t_3\varepsilon_{22} + t_2\varepsilon_{33})] \tag{4.16}$$

as well as the analogous normal macro-stresses in the other two directions. The shear gross stresses in the walls can be found as follows

$$\Sigma_{12} = \Sigma_{21} = \frac{t_3}{a}\frac{E}{1+\nu}\varepsilon_{12},$$
$$\Sigma_{23} = \Sigma_{32} = \frac{t_1}{a}\frac{E}{1+\nu}\varepsilon_{23}, \tag{4.17}$$
$$\Sigma_{13} = \Sigma_{31} = \frac{t_2}{a}\frac{E}{1+\nu}\varepsilon_{13}.$$

Finally, we are able to define the overall elasticity tensor for the porous media, that shows the orthotropic symmetry in the Cartesian coordinate system. Then, by means of some algebraic manipulations, the Voigt elasticity tensor can be expressed in the following matrix form

$$\mathbb{C}=\begin{bmatrix} \frac{E(t_2+t_3)}{a(1-\nu^2)} & \frac{\nu E t_3}{a(1-\nu^2)} & \frac{\nu E t_2}{a(1-\nu^2)} & 0 & 0 & 0 \\ \frac{\nu E t_3}{a(1-\nu^2)} & \frac{E(t_1+t_3)}{a(1-\nu^2)} & \frac{\nu E t_1}{a(1-\nu^2)} & 0 & 0 & 0 \\ \frac{\nu E t_2}{a(1-\nu^2)} & \frac{\nu E t_1}{a(1-\nu^2)} & \frac{E(t_1+t_2)}{a(1-\nu^2)} & 0 & 0 & 0 \\ 0 & 0 & 0 & \frac{E t_1}{a(1+\nu)} & 0 & 0 \\ 0 & 0 & 0 & 0 & \frac{E t_2}{a(1+\nu)} & 0 \\ 0 & 0 & 0 & 0 & 0 & \frac{E t_3}{a(1+\nu)} \end{bmatrix} \tag{4.18}$$

It is worth to note that if the thickness of the different walls are all the same, that means $t_1=t_2=t_3=t$, the overall elasticity tensor becomes

$$\mathbb{C}=\begin{bmatrix} \frac{2E}{(1-\nu^2)}\frac{t}{a} & \frac{E\nu}{(1-\nu^2)}\frac{t}{a} & \frac{E\nu}{(1-\nu^2)}\frac{t}{a} & 0 & 0 & 0 \\ \frac{E\nu}{(1-\nu^2)}\frac{t}{a} & \frac{2E}{(1-\nu^2)}\frac{t}{a} & \frac{E\nu}{(1-\nu^2)}\frac{t}{a} & 0 & 0 & 0 \\ \frac{E\nu}{(1-\nu^2)}\frac{t}{a} & \frac{E\nu}{(1-\nu^2)}\frac{t}{a} & \frac{2E}{(1-\nu^2)}\frac{t}{a} & 0 & 0 & 0 \\ 0 & 0 & 0 & \frac{E}{2(1+\nu)}\frac{t}{a} & 0 & 0 \\ 0 & 0 & 0 & 0 & \frac{E}{2(1+\nu)}\frac{t}{a} & 0 \\ 0 & 0 & 0 & 0 & 0 & \frac{E}{2(1+\nu)}\frac{t}{a} \end{bmatrix} \tag{4.19}$$

and so the RVE shows a cubic symmetry.

2.2. Constitutive relations for LVF porous material by means of inertia tensor

Let consider a RVE of a real material that show a low volume fraction and an oriented microstructure. In order to describe the mechanical behaviour of such material, an heuristic approach is followed. This means to select *a priori* some parameters the mechanical response of material depends on. Here, they are chosen the volume fraction and the inertia tensor which naturally gives information about the distribution of the mass inside the RVE. It should be noted that both volume fraction and inertia tensor may be easily evaluated by means of specific software – e.g. AUTOCAD, RHINOCEROS, ANSYS – from a vectorial image of the RVE.
The real cell of considered material is reduced to an equivalent Flugge's cell showing the same volume fraction and inertia tensor of the real RVE, but the regular microstructure of Flugge's model – isotropic and homogeneous walls of different thickness orthogonal to each other. Two different morphologies are considered for the equivalent cell, following denoted with the letters *A* and *B* (see figure 4.19).

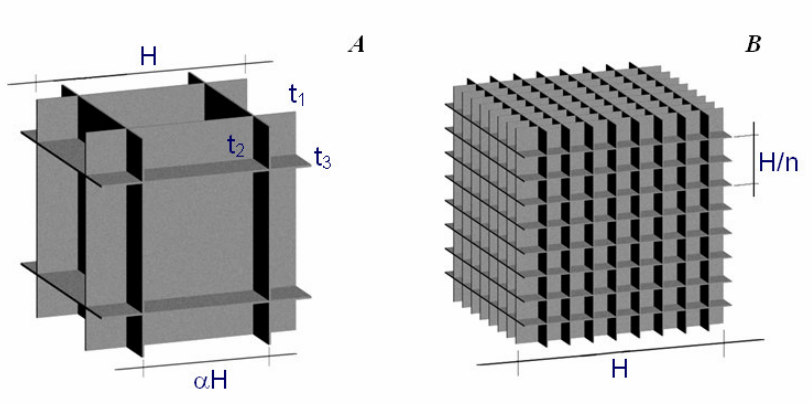

Fig. 4.19.
The two different morphologies of the equivalent Flugge cell; A) the RVE of size H is made of two parallel walls for each direction; the cell's geometry is completely described by the three thicknesses t_i and the pitch α; B) the RVE of size H is made of n parallel walls for each direction; the cell's geometry is completely described by the three thicknesses t_i and the number n.

In the case *A* the thicknesses t_i and the parameter α which characterizes the pitch of the walls, have to be determine under the conditions that the volume fraction and the inertia tensor of the ideal cell is the same of the real RVE.

In other words, the four unknown parameters – t_i and α – are calculated by solving the following system of equations

$$\begin{cases} I_{11} = \dfrac{H^4}{12}\left(t_1 + \left(t_1 + t_2 + t_3\right) + 3\left(t_2 + t_3\right)\alpha^2\right) = J_{11} \\ I_{22} = \dfrac{H^4}{12}\left(t_2 + \left(t_1 + t_2 + t_3\right) + 3\left(t_1 + t_3\right)\alpha^2\right) = J_{22} \\ I_{33} = \dfrac{H^4}{12}\left(t_3 + \left(t_1 + t_2 + t_3\right) + 3\left(t_2 + t_1\right)\alpha^2\right) = J_{33} \\ f = \dfrac{t_1 + t_2 + t_3}{H} = \gamma \end{cases} \tag{4.20}$$

where J_{11}, J_{22}, J_{33} and γ are the three eigenvalues of the inertia tensor and the volume fraction of the real RVE – estimated by means of specific software – while I_{11}, I_{22}, I_{33} and f are the eigenvalues of the inertia tensor and the volume fraction of the equivalent RVE computed as function of the geometric characteristics of the cell – that is the thicknesses t_i, the size H and the pitch α. The solution of the (4.20) gives

$$\begin{cases} t_1 = \sqrt[5]{2h}\,\gamma + \dfrac{2}{3}\dfrac{\sqrt[5]{2h}\,h}{k}\gamma^2 + \dfrac{2\sqrt[5]{2h}}{k}\gamma J_{11} \\ t_2 = \sqrt[5]{2h}\,\gamma + \dfrac{2}{3}\dfrac{\sqrt[5]{2h}\,h}{k}\gamma^2 + \dfrac{2\sqrt[5]{2h}}{k}\gamma J_{22} \\ t_3 = \sqrt[5]{2h}\,\gamma + \dfrac{2}{3}\dfrac{\sqrt[5]{2h}\,h}{k}\gamma^2 + \dfrac{2\sqrt[5]{2h}}{k}\gamma J_{33} \\ \alpha = \sqrt{1 - \dfrac{2}{3}\gamma - \dfrac{k}{h\gamma}} \end{cases} \tag{4.21}$$

with $h = Tr\left[\boldsymbol{J}^c\right] = H^5/2$ where $\boldsymbol{J}^c$ is the inertia tensor of a cubic cell of side H, and $k = Tr\left[\boldsymbol{J}^c\right]\gamma - Tr\left[\boldsymbol{J}\right]$.

In case of morphology *B* the thicknesses t_i and the number n of parallel walls completely characterize the geometry of the equivalent cell whose side is equal to H as in the previous case.

By solving the system of equations

$$\begin{cases} I_{11} = \dfrac{H^4}{12n}\left[\left(t_1+t_2+t_3\right)\left[1+2\left(n^2-1\right)\right]+t_1\right] = J_{11} \\ I_{22} = \dfrac{H^4}{12n}\left[\left(t_1+t_2+t_3\right)\left[1+2\left(n^2-1\right)\right]+t_2\right] = J_{22} \\ I_{33} = \dfrac{H^4}{12n}\left[\left(t_1+t_2+t_3\right)\left[1+2\left(n^2-1\right)\right]+t_3\right] = J_{33} \\ f = \dfrac{t_1+t_2+t_3}{H} = \gamma \end{cases} \tag{4.22}$$

the four unknowns are calculated

$$\begin{aligned} t_1 &= n\sqrt[5]{\frac{2}{h^4}}\left(3k-2h\gamma+6J_{11}\right) \\ t_2 &= n\sqrt[5]{\frac{2}{h^4}}\left(3k-2h\gamma+6J_{22}\right) \\ t_3 &= n\sqrt[5]{\frac{2}{h^4}}\left(3k-2h\gamma+6J_{33}\right) \\ n &= \sqrt{\frac{h\gamma}{3k}} \end{aligned} \quad . \tag{4.23}$$

Known the geometric characteristics of the two kinds of ideal cells, by means of Flugge's solution it is possible to determine the elasticity tensor of the real RVE as function of the parameters chosen as significant for the mechanical response of the material – that is the volume fraction and the inertia tensor of the real RVE. So, the elastic constants are expressed as function of the matrix elasticity and of the microstructural parameters J_{11}, J_{22}, J_{33} and γ

$$\begin{aligned} C_{1111} &= \frac{4\mu h}{3(1-\nu)k}\ \gamma^2 - \frac{4\mu}{(1-\nu)k}\gamma J_{11}; \\ C_{2222} &= \frac{4\mu h}{3(1-\nu)k}\ \gamma^2 - \frac{4\mu}{(1-\nu)k}\gamma J_{22}; \\ C_{3333} &= \frac{4\mu h}{3(1-\nu)k}\ \gamma^2 - \frac{4\mu}{(1-\nu)k}\gamma J_{33}; \end{aligned}$$

$$
\begin{aligned}
C_{2233} &= \frac{2\mu\nu}{(1-\nu)}\gamma - \frac{4\mu\nu h}{3(1-\nu)k}\gamma^2 + \frac{4\mu\nu}{(1-\nu)k}\gamma J_{11};\\
C_{1133} &= \frac{2\mu\nu}{(1-\nu)}\gamma - \frac{4\mu\nu h}{3(1-\nu)k}\gamma^2 + \frac{4\mu\nu}{(1-\nu)k}\gamma J_{22};\\
C_{1122} &= \frac{2\mu\nu}{(1-\nu)}\gamma - \frac{4\mu\nu h}{3(1-\nu)k}\gamma^2 + \frac{4\mu\nu}{(1-\nu)k}\gamma J_{33};\\
C_{2323} &= 2\mu\gamma - \frac{4\mu h}{3k}\gamma^2 + \frac{4\mu}{k}\gamma J_{11};\\
C_{1313} &= 2\mu\gamma - \frac{4\mu h}{3k}\gamma^2 + \frac{4\mu}{k}\gamma J_{22};\\
C_{1212} &= 2\mu\gamma - \frac{4\mu h}{3k}\gamma^2 + \frac{4\mu}{k}\gamma J_{33}.
\end{aligned}
\tag{4.24}
$$

It is important to note that the elastic constants do not depend on the morphology of the equivalent RVE. In fact, by choosing the morphology *A* or *B* the same value of elastic constants is obtained. However, the ultra-elastic response of the considered porous material could depend on such choice – e.g. the RVE called *B* is not able to describe the buckling because of its specific morphology.
Finally, it must be highlight that the comparison between the expression of the elastic constant in the form (4.24) and which one proposed by Cowin (Turner and Cowin, 1987), suggests to identify the *fabric tensor* with an appropriate normalization of the inertia tensor. In fact, the Cowin's solutions rewritten in the easier form $c = f_1(\gamma) + f_2(\gamma)G + f_3(\gamma)G^2$ – where *c* denotes the generic elastic constant, the $f_i(\gamma)$ are function of the volume fraction and G are the eigenvalues of the fabric tensor – show the same structure of the (4.24) provided that the second order terms G^2 are neglected.

2.3. Compliance tensors of ellipsoidal inclusions – High Volume Fraction (HVF)

The Kachanov's elastic solution for ellipsoidal inclusions having arbitrary elastic constants is here presented, (Sevostianov and Kachanov, 1999).
It is considered an ellipsoidal inclusion V^*, with boundary ∂V^* and compliance tensor $\mathbb{D}_0^*$ in an infinite linear elastic solid with compliance tensor $\mathbb{D}_0$ and assume that, in its absence, the stress field would have been uniform and equal to stress σ_{ij}^0 at infinity. The overall strain per certain reference volume V bounded by surface ∂V containing the inclusion is

$$\varepsilon_{ij} = D_{ijkl}^0 \sigma_{kl}^0 + \Delta\varepsilon_{ij} \tag{4.25}$$

where $\Delta\varepsilon_{ij}$ is the extra strain due to inclusion (it vanishes if the elastic "contrast" between the inclusion and the matrix vanishes).
Due to linear elasticity, $\Delta\varepsilon_{ij}$ is a linear function of applied stress σ^0_{ij}:

$$\Delta\varepsilon_{ij} = H_{ijkl}\sigma^0_{kl} \tag{4.26}$$

thus defining the *inclusion compliance tensor* $\mathbb{H}$. Tensor $\mathbb{H}$ can be derived in various ways. It is here expressed in terms of the elastic constant between the matrix and the inclusion, using the solution of Eshelby's problem in the form given by Kunin and Sosnina (1971) that does not use Eshelby's concept of equivalent eigenstrain. The results are as follows.
If σ^0_{ij} is a uniform stress at infinity, the resulting uniform stress inside the ellipsoidal inhomogeneity can be represented in the form

$$\sigma^{(\mathrm{int})}_{ij} = B_{ijkl}\sigma^0_{kl}, \text{ with } B_{ijkl} = \left[J_{ijkl} + Q_{ijmn}\left(D^*_{mnkl} - D_{mnkl}\right)\right]^{-1} \tag{4.27}$$

where $J_{ijkl} = \left(\delta_{ik}\delta_{lj} + \delta_{il}\delta_{kj}\right)/2$ is the unit fourth rank tensor and the inverse of symmetric fourth rank tensor X^{-1}_{ijkl} is defined as $X^{-1}_{ijmn}X_{mnkl} = X_{ijmn}X^{-1}_{mnkl} = J_{ijkl}$.
Tensor $\mathbb{Q}$ is expressed in terms of Eshelby's tensor $\mathbb{S}$ as follows:

$$Q_{ijkl} = B_{ijmn}\left(J_{mnkl} - S_{mnkl}\right) \tag{4.28}$$

Utilizing this solution yields tensor $\mathbb{H}$:

$$\mathbb{H} = \frac{V^*}{V}\left(\mathbb{D}^*_0 - \mathbb{D}_0\right) : \mathbb{B} = \frac{V^*}{V}\left[\left(\mathbb{D}^*_0 - \mathbb{D}_0\right)^{-1} + \mathbb{Q}\right]^{-1} \tag{4.29}$$

It is now analyzed the case of oblate and prolate spheroids. Let us consider a spheroid with semiaxes $a_1 = a_2 = a$ and a_3. The following notations will be used:

$$k = \frac{1}{2(1-2\nu)}, \quad f_0 = \frac{\alpha^2(1-g)}{2\left(\alpha^2-1\right)}, \quad f_1 = \frac{k\alpha^2}{4\left(\alpha^2-1\right)^2}\left[\left(2\alpha^2+1\right)g - 3\right] \tag{4.30}$$

where the shape coefficient g is expressed in terms of aspect ratio $\alpha = a/a_3$:

$$g=\begin{cases}\dfrac{1}{\alpha\sqrt{1-\alpha^2}}\arctan\sqrt{\alpha^2-1}, & \text{oblate shape}\\ \dfrac{1}{2\alpha\sqrt{\alpha^2-1}}\ln\left(2\alpha^2-1+2\alpha\sqrt{\alpha^2-1}\right), & \text{prolate shape}\end{cases} \tag{4.31}$$

In the case of spheroidal inhomogeneity, it is convenient to express the fourth-rank tensors that appear in (4.28) and (4.29) in terms of the following tensorial basis (m denotes the unit vector along the spheroid's axis of symmetry and $\theta_{ij}=\delta_{ij}-m_i m_j$)

$$\begin{aligned}&T^{(1)}_{ijkl}=\theta_{ij}\theta_{kl},\quad T^{(2)}_{ijkl}=\left(\theta_{ik}\theta_{lj}+\theta_{il}\theta_{kj}-\theta_{ij}\theta_{kl}\right)/2,\quad T^{(3)}_{ijkl}=\theta_{ij}m_k m_l\\ &T^{(4)}_{ijkl}=m_i m_j\theta_{kl},\quad T^{(5)}_{ijkl}=\left(\theta_{ik}m_l m_j+\theta_{il}m_k m_j+\theta_{jk}m_l m_i+\theta_{jl}m_k m_i\right)/4\\ &T^{(6)}_{ijkl}=m_i m_j m_k m_l\end{aligned} \tag{4.32}$$

In terms of this basis, tensors $\mathbb{Q}=G\sum_{k=1}^{6}q_k\mathbb{T}^{(k)}$ and $\mathbb{H}=\sum_{k=1}^{6}h_k\mathbb{T}^{(k)}$ have the following coefficients:

$$\begin{aligned}&q_1=4k-1-2(3k-1)f_0-2f_1,\\ &q_2=2\left[1-(2-k)f_0-f_1\right],\\ &q_3=q_4=2\left[(2k-1)f_0+2f_1\right],\\ &q_5=4\left[f_0+4f_1\right],\quad q_6=8\left[k f_0-f_1\right].\end{aligned} \tag{4.33}$$

$$\begin{aligned}&h_1=\frac{V^*}{V}\frac{1}{2\Delta}\left[\delta K+\frac{4}{3}\delta G+q_6\right];\quad h_2=\frac{V^*}{V}\frac{1}{2}\left[\delta G+\frac{q_2}{2}\right]^{-1};\\ &h_3=h_4=-\frac{V^*}{V}\frac{1}{\Delta}\left[\delta K-\frac{2}{3}\delta G+q_3\right];\quad h_5=\frac{V^*}{V}\left[\delta G+\frac{q_5}{4}\right]^{-1};\\ &h_6=\frac{V^*}{V}\frac{2}{\Delta}\left[\delta K+\frac{1}{3}\delta G+q_1\right]\end{aligned} \tag{4.34}$$

$$\delta K=\left(\frac{1}{K^*}-\frac{1}{K}\right)^{-1};\quad \delta G=\left(\frac{1}{G^*}-\frac{1}{G}\right)^{-1}$$

$$\Delta=2G\left[\frac{3\delta G\,\delta K}{G}+\delta K\left(q_1+q_6-2q_3\right)+\frac{\delta G}{3}\left(4q_1+q_6+4q_3\right)+G\left(q_1q_6-q_3^2\right)\right]$$

where K^*, G^*, K and G are the bulk and shear moduli of the inclusion and the matrix, respectively.

In the case of ellipsoidal cavity, $\delta K = \delta G = 0$ and

$$\begin{aligned} h_1 &= \frac{V^*}{V}\frac{1}{G}\frac{q_6}{4\left(q_1 q_6 - q_3^2\right)}; \quad h_2 = \frac{V^*}{V}\frac{1}{G q_2}; \\ h_3 &= h_4 = -\frac{V^*}{V}\frac{1}{G}\frac{q_3}{2\left(q_1 q_6 - q_3^2\right)}; \quad h_5 = \frac{V^*}{V}\frac{4}{G q_5}; \\ h_6 &= -\frac{V^*}{V}\frac{1}{G}\frac{q_1}{\left(q_1 q_6 - q_3^2\right)} \end{aligned} \tag{4.35}$$

Cartesian components of the tensor $\mathbb{H}$ in coordinate system x_1, x_2, x_3 (x_3 axis is along the spheroid's axis of symmetry) can be expressed in terms of h_i as follows:

$$\begin{aligned} &H_{1111} = H_{2222} = h_1 + \frac{1}{2}h_2; \quad H_{3333} = h_6; \\ &H_{1122} = H_{2211} = h_1 - \frac{1}{2}h_2; \\ &H_{1133} = H_{2233} = H_{3311} = H_{3322} = h_3 = h_4; \\ &H_{1212} = \frac{1}{2}h_2; \quad H_{1313} = H_{2323} = \frac{1}{4}h_5. \end{aligned} \tag{4.36}$$

So, from the (4.25) and (4.26), the overall compliance tensor $\bar{\mathbb{D}}$ is given by

$$\bar{\mathbb{D}} = \mathbb{D}_0 + \mathbb{H}\,. \tag{4.37}$$

2.4. Constitutive relations for HVF porous material by means of inertia tensor

Let consider a RVE of a real material characterized by an high volume fraction and an oriented microstructure. In order to describe the mechanical behaviour of such material a procedure analogous to which one presented for LVF porous materials is proposed. Thus, the volume fraction of the voids and the inertia tensor are *a priori* chosen as parameters meaningful for the mechanical response of the material. As already highlighted, these parameters may be easily evaluated by means of specific software – e.g. AUTOCAD, RHINOCEROS, ANSYS – from a vectorial image of the porous RVE.
The overall compliance tensor of the real material is found out starting from the analytical Kachanov's solution presented in the previous section. Specifically, the real cell of considered material is reduced to an equivalent cell showing the same porosity and inertia tensor of the real RVE, but a sole elliptic cavity for

which the overall compliance tensor is given by the (4.37). It is important to underline that the solution (4.37) is referred to an elliptic cavity in an infinity medium that means it is valid for dilute distribution of voids. This condition occurs in the considered equivalent RVE because of the hypothesis of HFV. Moreover, note that the *inclusion compliance tensor* $\mathbb{H}$ in the form (4.36) was obtained when two of the ellipse's diameters are equal. So, disposing of such analytical solution, it will be assumed that two diameters of the ellipse which characterizes the equivalent cell are equal to each other.
Firstly, the two different diameters – a and b – of the elliptic void inside the equivalent cell and the dimension H of the cell must be determined by imposing that the porosity and the inertia tensor of the equivalent RVE are the same of which ones of the real RVE here denoted with ϕ and $\boldsymbol{J}$, respectively. In other words the three unknowns are evaluated by solving the system:

$$\begin{cases} I_{11} = \dfrac{4}{15}\pi ab^2\left(a^2+b^2\right) = J_{11} \\ I_{33} = \dfrac{8}{15}\pi ab^4 = J_{33} \\ p = \dfrac{\frac{4}{3}\pi ab^2}{H^3} = \phi \end{cases} \tag{4.38}$$

where I_{11}, I_{33} and p are the moments of inertia and the porosity of the ellipsoidal cavity into the equivalent RVE – expressed as function of the two diameters a and b and of the size H of the cell – while J_{11}, J_{33} and ϕ are the moments of inertia and the porosity of the real RVE.
The solution of the (4.38) gives

$$\begin{cases} a = \sqrt[5]{\dfrac{15}{2^3\pi}}\sqrt[5]{\dfrac{\left(2J_{11}-J_{33}\right)^2}{J_{33}}} \\ b = \sqrt[5]{\dfrac{15}{2^3\pi}}\sqrt[10]{\dfrac{J_{33}^3}{2J_{11}-J_{33}}} \\ H = \sqrt[5]{5}\sqrt[15]{2\left(\dfrac{\pi}{3}\right)^2}\sqrt[3]{\dfrac{\sqrt[5]{\left(2J_{11}-J_{33}\right)J_{33}^2}}{\phi}} \end{cases} . \tag{4.39}$$

In particular, the aspect ratio $\beta = b/a$ is

$$\beta = \sqrt{\frac{J_{33}}{2J_{11}-J_{33}}} . \tag{4.40}$$

By considering the case of prolate spheroid where it results $J_{33} = \delta J_{11} < J_{11}$, the aspect ratio β may be expressed as function of the ratio between the moments of inertia $\delta = J_{33}/J_{11}$

$$\beta = \sqrt{\frac{\delta}{2-\delta}}\,. \tag{4.41}$$

By substituting the (4.41) inside the (4.37) and by means of a series expansion around the zero in δ arrested to the first order, the overall compliance tensor is determined whose independent components are

$$\begin{aligned}
D_{1111} &= D_{2222} = \frac{1}{E} + \phi\frac{1}{E}\left(\frac{3(1+\nu)(20\nu^2+8\nu-9)}{2(20\nu^2-4\nu-7)} + \frac{6(1+\nu)(140\nu^2-136\nu+33)(\delta-1)}{7(7-10\nu)^2}\right)\\
D_{3333} &= \frac{1}{E} + \phi\frac{1}{E}\left(-\frac{3(1+\nu)(20\nu^2+10\nu-9)}{2(20\nu^2-4\nu-7)} + \frac{12(1+\nu)(140\nu^2-136\nu+33)(\delta-1)}{7(7-10\nu)^2}\right)\\
D_{1122} &= -\frac{\nu}{E} + \phi\frac{1}{E}\left(-\frac{3+27\nu-36\nu^2-60\nu^3}{2(-20\nu^2+4\nu+7)} - \frac{6(17-87\nu+36\nu^2+140\nu^3)(\delta-1)}{7(7-10\nu)^2}\right)\\
D_{1133} &= D_{2233} = -\frac{\nu}{E} + \phi\frac{1}{E}\left(\frac{3+27\nu-36\nu^2-60\nu^3}{2(20\nu^2-4\nu-7)} + \frac{(1+\nu)(420\nu^2-312\nu+51)(\delta-1)}{7(7-10\nu)^2}\right)\\
D_{1212} &= \frac{1}{2\mu} + \phi\frac{15}{\mu}\left(\frac{1-2\nu}{4(7-10\nu)} + \frac{(2\nu-1)(14\nu-5)(\delta-1)}{7(7-10\nu)^2}\right)\\
D_{1313} &= D_{2323} = \frac{1}{2\mu} + \phi\frac{15}{\mu}\left(\frac{1-2\nu}{4(7-10\nu)} - \frac{(2\nu-1)(14\nu-5)(\delta-1)}{7(7-10\nu)^2}\right)
\end{aligned} \tag{4.42}$$

where ϕ is the porosity and E, ν and μ are the Young modulus, the Poisson's ratio and the second Lamé constant of the matrix.

2.5. Validation of the proposal for the Fabric Tensor – comparison between MIL tensor and inertia tensor

In this section MIL tensor and inertia tensor are compared with reference to porous bidimensional RVE. Specifically, the developed examples display that for particular microgeometries the inertia tensor is able to describe anisotropies that the MIL tensor do not reveal. Moreover, when the MIL tensor describes a material orientation, by showing an elliptic shape, the inertia tensor is elliptic too and the eigenvectors of the two tensors coincide. This last statement means that both tensors furnish the same directions of anisotropy.

It is firstly considered the case in which MIL tensor, unlike the inertia tensor, do not reveal material anisotropies.
In the first example it is considered a 2-D square cell of side $2H$ with a centred square cavity (fig. 4.20 A). By remembering that the MIL function $L(\theta)$ associates each orientation θ to the scalar given by the ratio between the length of the segment which intercepts the solid material and the total length of the segment which intercepts the RVE, it is easy verify that for the considered cell the MIL function is a circumference. For this specific geometry the inertia tensor is a circumference, too. Hence, the *degree of anisotropy A* – which is the ratio between the two eigenvalues of the tensor which describes the microstructure – is equal to one if it is used both the MIL and the inertia tensor to describe the microstructure. This result means that the microstructure does not show a particular orientation and than an anisotropic mechanical behaviour. The values of the geometric characteristics and of the degree of anisotropy shown in figure 4.20 A are obtained setting $H=1$ and the thickness of the matrix equal to 0.5 so that the radius of the MIL circumference is 0.5.

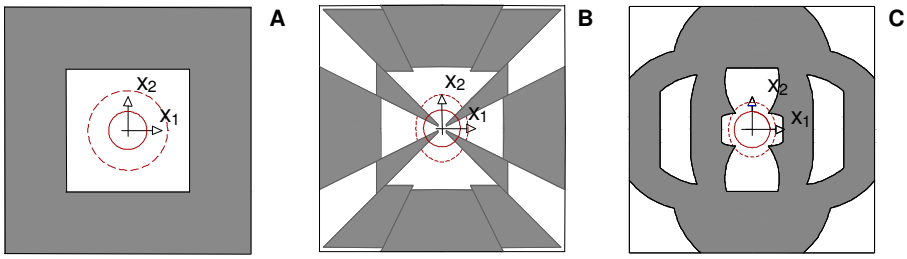

A	B	C
γ =0.75 L(θ)=0.5	γ =0.60 L(θ)=0.5	γ =0.59 L(θ)=0.5
I_{x1}=1.25 I_{x2}=1.25	I_{x1}=0.92 I_{x2}=0.71	I_{x1}=0.77 I_{x2}=0.66
A^{MIL} =1 A^{J} =1	A^{MIL} =1 A^{J} =0.77	A^{MIL} =1 A^{J} =0.85

Fig. 4.20

For the three bidimensional RVE's the MIL tensor (unbroken line) and the inertia tensor (broken line) are represented. For each microgeometries, they are also indicated the values of the volume fraction γ, of the mean intercept length functions $L(\theta)$, of the moments of inertia I_{x1}, I_{x2} and of the degree of anisotropy evaluated as ratio between the eigenvalues of the MIL tensor (A^{MIL}) or of the inertia tensor (A^{J}).
A) The matrix inside the RVE is not oriented; both MIL and inertia tensor are circumferences; B) and C) The matrix inside the RVE is oriented; the inertia tensor, unlike the MIL tensor, describes such material orientation showing an ellipsoidal shape and a degree of anisotropy minor than one.

The distribution of the material inside the square cell is now perturbed but preserving the value of the MIL function. The obtained geometries are shown in fig. 4.20 B and C where are also shown the inertia ellipse which are able to describe the evident orientation of the material that is not caught by the MIL function.
In order to correlate the mechanical anisotropy to the morphological one, let us consider a beam in bending regime. The *mechanical degree of anisotropy* α may be defined like

$$\alpha = \frac{k_1}{k_2} \tag{4.43}$$

where k_1 and k_2 are the stiffness in x_1 and x_2 directions, respectively. By remember the solutions for a bending beam, the degree of anisotropy α become

$$\alpha = \frac{I_2}{I_1} \tag{4.44}$$

where I_1 and I_2 are the moments of inertia respect x_1 and x_2 directions, respectively. Thus, by imaging that the cross section of the considered beam is the cell represented in fig. 4.20 B, the morphological and mechanical anisotropies A and α coincide.
It is also interested to note that by increasing the number of cells that compose the cross section of the beam the mechanical response of the structure becomes isotropic in the sense that I_1 and I_2 tend to assume the same value. In fact, with reference to figure 4.21, it is easy to prove that through Huygens' theorem I_1 and I_2 may be expressed as function of the number n^2 of elementary cells that composed the cross section of the beam as

$$\begin{aligned} I_1 &= n^2 I_1^c + \frac{\left(4n^2 - 1\right) H^4}{12n^2} \\ I_2 &= n^2 I_2^c + \frac{\left(4n^2 - 1\right) H^4}{12n^2} \end{aligned} \tag{4.45}$$

where $I_i^c \ \left(i = 1,2\right)$ is the inertia of elementary cell.
Figure 4.22 shows the parameter α as a function of n. The different curves are obtained for different value of the degree of anisotropy A of the elementary cell. In particular, the blue arrow indicates increasing value of A. Note that – for each value of A – α tends to one when n increases. This means that the effect of local orientation of the single cell – responsible of the anisotropic response of the

structure – vanishes when the number of cells increases. In other words, the material made of a great number of elementary cells is – from a mechanical point of view – like a material with microstructure randomly arranged which shows an isotropic behaviour.

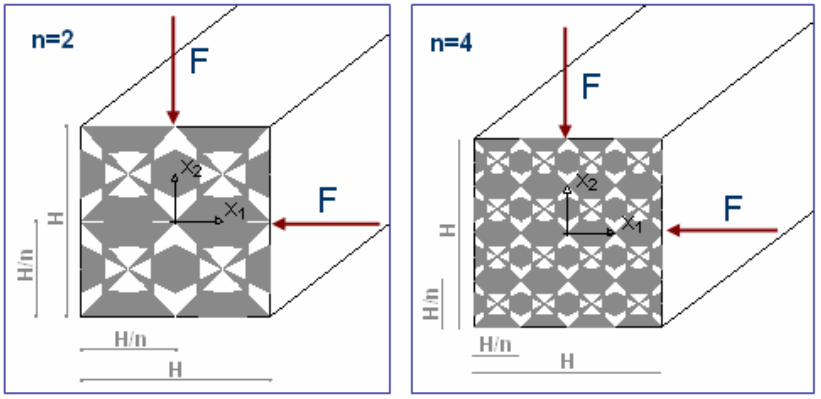

Fig. 4.21

Cross section of a bending beam made of n^2 elementary cells which show a morphological degree of anisotropy A.

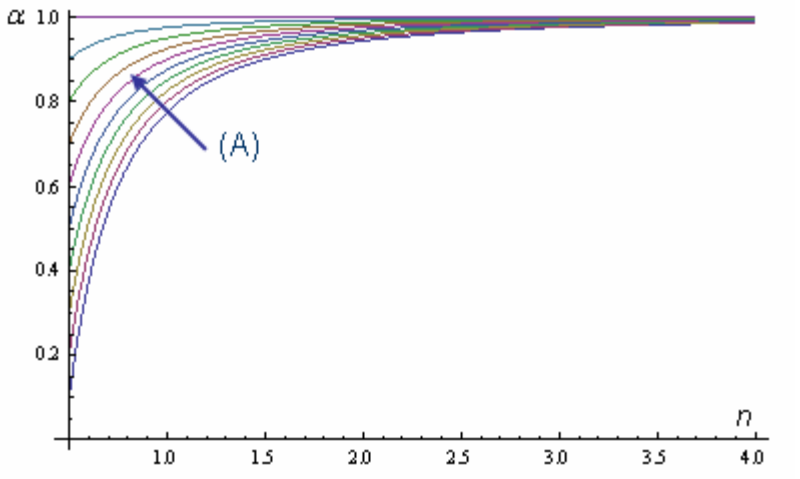

Fig. 4.22

Plot of the mechanical degree of anisotropy α as function of the number of cell that made the cross section of the bending beam. The different curves are obtained for different value of the degree of anisotropy A of the elementary cell. The blue arrow indicates increasing value of A. Independently on the value of A, α tends to one when n increases.

Let now analyze the case in which the MIL tensor shows an elliptical shape. The following examples point out possible correlation between the MIL tensor and the inertia tensor. In particular, by assuming that the elliptical MIL tensor is prescribed, the corresponding material distribution inside the RVE is evaluated. Thus, the inertia tensor of the RVE is calculated and compared with the MIL tensor. Remember that such study is motivated by the idea of using the inertia tensor to describe the microstructural arrangement of a porous material with the advantage that the inertia tensor may be more easily calculated than MIL one, e.g. by means of CAD programs.

The considered RVE are 2-D square cell of side $2H$ centred in the origin of the reference frame (x_1, x_2) with a centred cavity of unknown shape (fig. 4.23). The prescribed MIL function $L(\theta)$ – which represents the ratio between the length of the segment which intercepts the solid material and the total length of the segment for each orientation θ – is assumed to be an ellipse of equation

$$L(\theta) = \left(\frac{2a^2 b^2}{a^2 + b^2 + \left(b^2 - a^2\right)\mathrm{Cos}\left[2(\theta - \phi)\right]} \right)^{\frac{1}{2}} \tag{4.46}$$

where a and b are the semimajor and semiminor axes and ϕ is the angle between the semimajor axis a and the x_1-axis.

From the definition of MIL function just recalled, note the (4.46) and the total length of the segment $l(\theta)$ which intercepts the square cell for each orientation – easily computable being note the cell's dimension – the shape of the cavity may be evaluated in terms of a so-called *thickness function* $t(\theta)$ defined as

$$t(\theta) = L(\theta) l(\theta) \tag{4.47}$$

which represents the length of the segment that intercepts the solid material for each orientation.

Hence, note the distribution of the material inside the considered RVE, the corresponding inertia tensor is calculated.

In (fig. 4.23) they are reported the results obtained by setting $H = 1$, $a = 1/3$ $b = 1/6$ and considering eight different inclinations ϕ of the MIL ellipse. For each of the eight cases the inertia and MIL ellipse are coaxial even if the ratio between their eigenvalues – which furnish the *degree of anisotropy* α – is higher in the case of inertia tensor.

The obtained results highlight that when the MIL tensor describes an anisotropic attitude of the porous material, the inertia tensor is able to describe the same

attitude. Moreover, the coaxiality between the two tensors proves that both of them furnish the same directions of anisotropy.

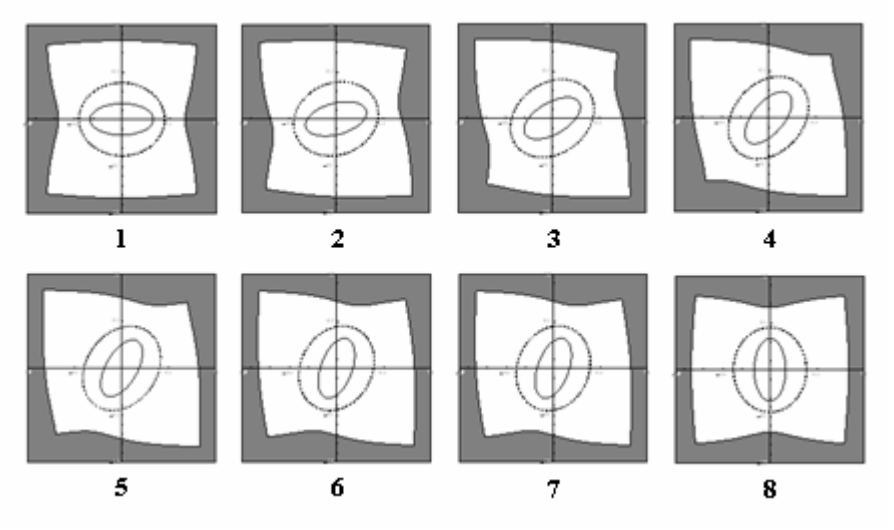

	ϕ	ψ	I_1	I_2	α^{MIL}	α^{J}	γ
1	0	0	0.90	0.77	0.50	0.85	0.39
2	$\pi/12$	0.39	0.92	0.76	0.50	0.82	0.40
3	$\pi/6$	0.62	0.95	0.74	0.50	0.77	0.40
4	$15\pi/54$	0.83	0.97	0.73	0.50	0.75	0.40
5	$\pi/3$	0.94	0.95	0.74	0.50	0.77	0.40
6	$21\pi/54$	1.08	0.93	0.75	0.50	0.80	0.40
7	$5\pi/12$	1.17	0.92	0.76	0.50	0.82	0.40
8	$\pi/2$	$\pi/2$	0.90	0.77	0.50	0.85	0.39

Fig. 4.23.

Coaxiality between MIL tensor (unbroken line) and inertia tensor (dot line) for eight different bidimensional RVE's.

In the table for each RVE's they are reported the direction cosines of the MIL and of the inertia tensors ϕ and ψ; the moments of inertia I_1 and I_2; the degree of anisotropy evaluated by means of MIL and inertia tensor α^{MIL} and α^{J}; the volume fraction γ.

CHAPTER V

OPTIMIZATION PROBLEMS FOR ENGINEERED MATERIALS

1. STANDARD TOPOLOGICAL OPTIMIZATION

The area of computational variable-topology shape design of continuum structures is presently dominated by methods which employ a material distribution approach for a fixed reference domain in the spirit of the so-called `homogenization method' for topology design, (Bendsøe *et al.*, 1988). That is, the geometric representation of a structure is similar to a grey-scale rendering of an image, in discrete form corresponding to a raster representation of the geometry. This concept has proven very powerful, but it does involve a number of difficulties. One is the issue of existence of solutions, another the issue of solution method.

In many applications, the optimal topology of a structure should consist solely of a macroscopic variation of one material and void, meaning that the density of the structure is given by a $(0-1)$ integer parametrization (often called a black-and-white design). Unfortunately, this class of optimal design problems is ill-posed in that, for example, nonconvergent, minimizing sequences of admissible designs with finer and finer geometrical details can be found, see (Cheng *et al.*, 1981; Kohn *et al.*, 1986). Existence of black-and-white solutions can be achieved by confining the solution space to limit the complexity of the admissible designs, making the designs dependent on the choice of parameters in the geometrical constraint. Such a restriction of the design space can be accomplished in a number of ways, e.g. by enforcing an upper bound on the perimeter of the structure (Ambrosio *et al.* 1993; Haber, *et al.*,1996; Petersson, 1998), one can introduce a filtering function that effectively limits the minimum width of a member, (Sigmund, 1994); or one can impose constraints on slopes on the parameters defining the geometry, (Chenais, 1975; Bendsøe, 1983; Niordson, 1983; Petersson *et al.*, 1998).

For reasonable raster representations of the $(0-1)$ black-and-white design, the solution of the resulting large-scale integer programming problem becomes a major challenge. Recently, dual methods have been shown to be effective, in the absence of local constraints, (Beckers, 1999). However, the most commonly used approach is to replace the integer variables with continuous variables, and then introduce some form of penalty that steers the solution to discrete $(0-1)$ values. A key part of these methods is the introduction of an interpolation function that expresses various physical quantities, e.g. material stiffness, cost, etc., as a function of continuous variables. The continuous variables are often interpreted as material densities, as in the so-called penalized, proportional “fictitious material” model. Inspired by the relaxed formulations

that introduce composites, some methods use interpolations derived from employing composite materials of some given form together with penalizations of intermediate densities of material.
Existence of solutions can also be achieved through relaxation, leaving the concept of a black-and-white design. Relaxation is sometimes attained by expanding the solution space to include microstructures and using homogenized properties to describe their behaviour, as seen in (Bendsøe *et al.*, 1988; Lurie *et al.*, 1982). In these formulations, the design is allowed to exhibit high-frequency oscillations at an indeterminate, microscopic length scale. Alternatively, we may describe these nonconventional designs through mathematical relaxation, e.g., quasi-convexification, etc. (Goodman *et al.*, 1986; Buttazzo *et al.*, 1993). In general, these approaches lead to designs that can only be realized by incorporating microstructure; however, there is no definite length scale associated with the microstructure. Relaxed formulations provide an appropriate basis for direct synthesis where composite materials are allowed to constitute part of the final design, simply because microstructure is admissible. Indeed, the demand for ``ultimate'' performance can lead one to consider all possible materials in the design formulation, (Ringertz, 1993; Bendsøe *et al.*, 1994). In general, relaxation yields a set of continuously variable design fields to be optimized over a fixed domain, so the algorithmic problems associated with the discrete $(0-1)$ format of the basic problem statement are circumvented; this was one of the main motivations for the initial use of the relaxation concept. Sometimes, a subset of the design fields is optimized analytically, leaving a reduced problem for numerical optimization, (Allaire *et al.*, 1993; Jog *et al.*, 1994). It should be emphasized that the continuum relaxation approach can be very involved theoretically. As of today, it has been mathematically fully worked for minimum compliance design of structures only (for both single and multiple loads) and for a broader class of problems involving the Laplace operator (Goodman *et al.*, 1986 ; Allaire *et al.*, 1993; Allaire *et al.*, 1997; Cox *et al.*, 1996; Díaz *et al.*, 1997; Olhoff *et al.*, 1998).

1.1. Basic problem statements

The continuum topology design problems considered are defined on a fixed reference domain Ω in R^2 or R^3. In this domain, we seek the optimal distribution of material, with the term `optimal' being defined through choice of objective and constraint functions, and through choice of design parametrization. The objective and constraint functions involve some kind of physical modelling that provides a measure of efficiency within the framework of a given area of applications, for example structural mechanics.
The basis for our discussion is the minimum compliance problem for a linearly elastic structure in 2-D (or 3-D, when specified as an example only; the micromechanical considerations in the sequel are not restricted to this

setting). We thus consider a mechanical element as a body occupying a domain Ω^m which is part of a the reference domain Ω, on which applied loads and boundary conditions are defined Fig. 5.1. This reference domain is often referred to as the ground-structure, in analogy with terminology in truss topology design, (Bendsøe, 1995). Referring to the reference domain Ω we can define the optimal topology-shape design problem as a minimization of force times displacement, over admissible designs and displacement fields satisfying equilibrium

$$\underset{u\in U,\Theta}{\text{minimize}} \quad \int_\Omega pu\, d\Omega + \int_{\Gamma_T} tu\, ds,$$

subject to:

$$\begin{aligned}
&\int_\Omega C_{ijkl}(x)\varepsilon_{ij}(u)\varepsilon_{kl}(v)\, d\Omega = \int_\Omega pv\, d\Omega + \int_{\Gamma_T} tv\, ds, \quad \text{for all } v\in U,\\
&C_{ijkl}(x) = \Theta(x)C^0_{ijkl},\\
&\Theta(x) = \begin{cases} 1 & \text{if } x\in\Omega^m,\\ 0 & \text{if } x\in\Omega/\Omega^m,\end{cases}\\
&\mathrm{Vol}(\Omega^m) = \int_\Omega \Theta(x)\, d\Omega \le V,\\
&\mathrm{Geo}(\Omega^m) \le K.
\end{aligned} \tag{5.1}$$

Here, the equilibrium equation is written in its weak, variational form, with U denoting the space of kinematically admissible displacement fields, u the equilibrium displacement, p the body forces, t boundary tractions and $\varepsilon(u)$ linearized strains. Moreover, $\mathrm{Geo}(\Omega^m)$ denotes a constraint function limiting the geometric complexity of the domain Ω^m, imposed here to obtain a well-posed problem.

In problem (5.1), C^0_{ijkl} denotes the stiffness tensor of a given elastic material from which the structure is to be manufactured, with a total amount of material V; $\Theta(x)$ denotes the pointwise volume fraction of this material, and for a black-and-white design this can only attain the values zero or one.

Problem (5.1) is a discrete optimization problem, and for many applications it is useful to consider reformulations in terms of continuous variables, with the goal of using derivative based mathematical programming algorithms. This means that one changes the model for material properties, i.e., the relations defined in (5.1) as

$$C_{ijkl} = \Theta C^0_{ijkl} = \begin{cases} \text{either} & C^0_{ijkl}, \\ \text{or} & 0, \end{cases} \tag{5.2}$$

to a situation where the volume fraction is allowed any value between zero and one. It may also involve finding an appropriate method for limiting geometric complexity, for example, exchanging the total variation of a density for the perimeter of a domain.

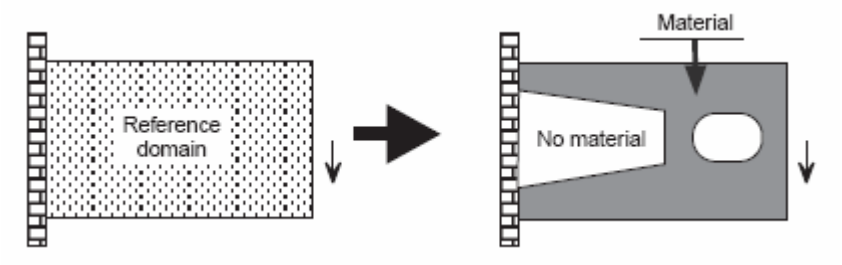

Fig. 5.1.
The generalized shape design problem of finding the optimal material distribution

In the subsequent sections we will concentrate solely on the interpolation models for the material properties, and will not address in further detail other aspects of the modelling and solution procedures connected with various choices of objective and constraint functions, physical modelling, discretization schemes, and optimization algorithms.

1.2. Isotropic models for solid-void interpolation in elasticity

In this section the so-called penalized, proportional "fictitious material" model, also names as the solid isotropic material with penalization model (SIMP), is presented (Bendsøe, 1989; Zhou *et al.*, 1991; Mlejnik *et al.*, 1993; Rozvany *et al.*, 1994). Here, a continuous variable γ, $0 \le \gamma_{\min} \le \gamma$, is introduced, resembling a density of material by the fact that the volume of the structure is evaluated as

$$\text{Vol} = \int_\Omega \gamma(x)\, d\Omega. \tag{5.3}$$

In computations, a small lower bound, $0 < \gamma_{\min} \le \gamma$, is usually imposed, in order to avoid a singular FEM problem, when solving for equilibrium in the full domain Ω.

The relation between this density and the material tensor $C_{ijkl}(x)$ in the equilibrium analysis is written as

$$C_{ijkl}(\gamma) = \gamma^p C^0_{ijkl}, \tag{5.4}$$

where the given material is isotropic, i.e. C^0_{ijkl} is characterized by just two variables, here chosen as the Young' s modulus E^0 and the Poisson ratio ν^0. The interpolation (5.4) satisfies that

$$C_{ijkl}(0) = 0, \quad C_{ijkl}(1) = C^0_{ijkl}. \tag{5.5}$$

This means that if a final design has density zero or one in all points, this design is a black-and- white design for which the performance has been evaluated with a correct physical model. For problems where the volume constraint is active, experience shows that optimization does actually result in such designs if one chooses p sufficiently big (in order to obtain true $(0-1)$ designs, $p \geq 3$ is usually required). The reason is that, for such a choice, intermediate densities are penalized; volume is proportional to γ, but stiffness is less than proportional.

1.3. Microstructure realizing the SIMP-model

For the SIMP interpolation (5.4), it is not immediately apparent that areas of grey can be interpreted in physical terms. However, it turns out that, under fairly simple conditions on p, any stiffness used in the SIMP model can be realized as the stiffness of a composite made of void and an amount of the base material corresponding to the relevant density. Thus using the term "density" for the interpolation function γ is quite natural.

The stiffness tensor $C_{ijkl}(\gamma)$ of the SIMP model is isotropic, with a Young's modulus varying with γ and a constant Poisson ratio, independent of γ. If this tensor is to correspond to a composite material constructed from void and the given material at a real density γ, the bulk modulus k and the shear modulus μ of the tensor $C_{ijkl}(\gamma)$ should satisfy the Hashin-Shtrikman bounds for two-phase materials, (Hashin *et al.*, 1963), written here for plane elasticity and for the limit of one phase being void

$$0 \leq k \leq \frac{\gamma k^0 \mu^0}{(1-\gamma)k^0 + \mu^0}, \quad 0 \leq \mu \leq \frac{\gamma k^0 \mu^0}{(1-\gamma)\left(k^0 + 2\mu^0\right) + k^0} \quad (\text{in } 2D). \tag{5.6}$$

Here k^0, μ^0 are the bulk and shear moduli, respectively, of the base material. This implies that the Young modulus should satisfy (Torquato *et al.*, 1998)

$$0 \le E \le E^* = \frac{\gamma E^0}{(3-2\gamma)} \quad (\text{in } 2D). \tag{5.7}$$

From (5.7), the SIMP model should satisfy

$$\gamma^p E^0 \le \frac{\gamma E^0}{(3-2\gamma)} \quad \text{for all } 0 \le \gamma \le 1, \tag{5.8}$$

which is true if and only if $p \ge 3$. However, the SIMP model presumes that the Poisson's ratio is independent of the density, and this leads to a stronger condition. From the relationship

$$k^0 = \frac{E^0}{2(1-\nu^0)}, \quad \mu = \frac{E^0}{2(1+\nu^0)} \quad (\text{in } 2D), \tag{5.9}$$

the condition (5.6) for the SIMP model can be written for all $0 \le \gamma \le 1$ as

$$\begin{aligned} 0 &\le \frac{\gamma^p E^0}{2(1-\nu^0)} \le \frac{\gamma E^0}{4-2(1+\nu^0)\gamma}, \\ 0 &\le \frac{\gamma^p E^0}{2(1+\nu^0)} \le \frac{\gamma E^0}{2(1-\gamma)(3-\nu^0)+2(1+\nu^0)}. \end{aligned} \tag{5.10}$$

After some algebra, this leads to a condition on the power p in the form

$$p \ge p^*(\nu^0) = \max\left\{\frac{2}{1-\nu^0}, \frac{4}{1+\nu^0}\right\} \quad (\text{in } 2D), \tag{5.11}$$

which in itself implies $p \ge 3$. The inequality $p \ge 2/1-\nu^0$ comes from the bulk modulus bound, while the inequality $p \ge 4/1+\nu^0$ is due to the shear modulus bound. Example values of p^* are

$$\begin{aligned} &p^*\left(\nu^0 = \tfrac{1}{3}\right) = 3; \quad p^*\left(\nu^0 = \tfrac{1}{2}\right) = 4; \quad p^*\left(\nu^0 = 0\right) = 4; \\ &p^*\left(\nu^0 = 1\right) = \infty; \quad p^*\left(\nu^0 = -1\right) = \infty \quad (\text{in } 2D), \end{aligned} \tag{5.12}$$

and $p^* = 3$ holds only for $\nu^0 = 1/3$.

It is important to note that the condition (5.11) implies that the SIMP model can be made to satisfy the Hashin-Shtrikman bounds, so that it makes sense to look for composites which realize the stiffness tensor for the model. The form of this composite can be computed through a design process, where the desired material properties of a periodic medium are obtained by an inverse homogenization process, (Sigmund, 1994; Sigmund, 1995). The geometry of the composite may depend on the density, and one can normally not expect to obtain the wanted properties by analytical methods.

It is still an open problem if all material parameters satisfying the bounds also can be realized as composites of the given materials. For two materials, one infinitely stiff, one infinitely soft, it is shown in (Milton *et al.*, 1995) that composites can be build for any positive definite material tensor. However, in topology design the stiffness is restricted and the density specified.

2. ANISOTROPIC TOPOLOGICAL OPTIMIZATION

Minimization of the strain energy density is of considerable significance when stiff structures or structured materials must be achieved for a given loading, whereas its maximization is an outstanding feature when a large amount of energy absorption under impact loading is demanded. Contrary to isotropic solids, in presence of elastic anisotropy the strain energy density changes when any material element is rotated to the principal directions of stress or strain. Accordingly, the orientation of the material axes can be employed as design variable to achieve the desired maximum or minimum value of the strain energy density. In designing living tissues, nature somehow employs this kind of strategy, and adjusts the microstructure of the material (i.e., its anisotropy), to enhance the mechanical performances. On the other hand, the same idea is artificially adopted when some man-made materials are produced. Among these, fibrous composites represent the most common example of materials intrinsically anisotropic and susceptible to be properly designed for given purposes.

In literature some procedures were proposed with the aim to rationalize the problem of finding the extrema for the strain energy density, with reference to linear elastic solids in presence of material symmetries (Rovati, *et al.*, 2003).

Referring to a linearly elastic anisotropic solid, defined by an elasticity tensor with components C_{ijhk}, subjected to a constant strain state characterized by given principal strains, this goal can be achieved by answering to the following questions: (a) which conditions must be satisfied by the stress and the strain fields to make the strain energy density stationary, and (b) which are explicitly the corresponding mutual orientations of the strain and the elasticity tensors that satisfy these conditions?

The answer to the first question is partially known. The results obtained up to now, which will be briefly reviewed later, concern essentially the determination of qualitative conditions to be satisfied by absolute maxima and minima for the strain energy density, and the number of such critical points. The problem of the explicit evaluation of the orientations corresponding to all the stationarity values of the strain energy density has only partially been solved. On the last point in following section it is widely explained a procedure proposed by Rovati *et al.* (2003), where for some classes of anisotropy (namely, tetragonal system, transverse isotropy and cubic symmetry) *all* the orientations of the principal directions of strain to the material symmetry axes at the critical points are found and discussed.

2.1. State of – the – art

Pioneering works where extreme values of the strain energy density in anisotropic bodies are sought are those by Banichuk (1981, 1983). Here, the problem of simultaneously evaluating the most efficient shapes for anisotropic rods in torsion and the orientation of the anisotropy axes which minimize the structural compliance is dealt with. The problem of defining the local values of the elastic coefficients, with fixed directions of material axes, which minimize the energy density is also considered in plane elasticity. These results have been extended in Banichuk and Kobelev (1987) to the case of ideally elastic-plastic solids. Anisotropic plates with variable elastic moduli and material axes orientation have been also studied by Kartvelishvili and Kobelev (1984), referring to optimal design for compliance and natural vibrational frequency.
Beside these structural formulations, the study of the best positioning of elastic symmetry planes in three-dimensional orthotropic bodies for minimum potential energy of deformation has been carried out in a general way in Seregin and Troitskii (1981). In this work, through the application of the Lagrangian multipliers method, it is shown that the solution is locally characterized by a mechanically meaningful condition, that is, *coaxiality of the stress and strain tensors.* Contrary to isotropic elasticity, where the strain and stress tensors are always coaxial, in anisotropic elasticity this feature is, in general, lost. The non-trivial result obtained by Seregin and Troitskii emphasizes a requirement that must always be fulfilled when extreme values of the global stiffness are sought; consequently, it should be assumed as a guidance for an optimal spatial arrangement of the material symmetry axes.
Later, but independently, the same problem has been dealt with in Rovati and Taliercio (1991, 1993) where orientations of the material symmetry axes which maximize or minimize the global elastic stiffness of a generally anisotropic three-dimensional continuum are sought. Necessary stationarity conditions for the strain energy density are directly computed, assuming the strain state to be given, and their mechanical interpretation (that is, collinearity of principal directions of stress and strain) is highlighted. Some closed form solutions for

cubic and transversely isotropic materials are found, and a material parameter, responsible of the relative shear stiffness of the solid, is introduced. It is shown how two classes of solutions can be defined according to its value: one, where stationarity of the strain energy density is accompanied by full collinearity of principal directions of stress, strain and material axes; the other one, where this collinearity is only partially preserved.

Due to pertinence to practical applications, much effort has been devoted to two-dimensional solids. In particular, the elastic problem previously described has been reformulated for plane elasticity in Sacchi Landriani and Rovati (1991), and conditions for absolute maximum and minimum structural stiffness are found; an extension to plates in bending is given as well. Careful investigations in this direction should be mentioned, such as those given by Pedersen (1989), where it is found that the best orientations of the material axes depend on a dimensionless material parameter, plus the ratio of the two principal strains. Coaxiality of the material axes and the principal strain directions always corresponds to stationary values for the energy density (trivial solutions); however, in some strain conditions, stationarity can also be achieved at some non-trivial orientations. In addition to these considerations referred to any material point, analyses are also carried out for the whole solid (Pedersen, 1990), through applications of sensitivity analysis, finite element analysis, and optimization procedures. Homogenization techniques, coupled with finite element analyses and design for optimal structural performances, have led to the very effective method of topology optimization (see Eschenauer and Olhoff, 2001, and the references therein).

A modern formulation of the problem of finding the best orientations of the material symmetry axes in a three-dimensional continuum is given by Banichuk (1996), where the application of spectral methods of tensor analysis makes it possible to clarify general features of the problem itself, and to discuss some qualitative properties. Further accounts on spectral decomposition of the anisotropic elasticity tensor can be found in Sutcliffe (1992) and Theocaris and Sokolis (2000a,b). Banichuk deals with several problems, such as minimization of the compliance functional, the dynamic stiffness and the distortion energy. These problems are then generalized to the case of bodies consisting of several anisotropic phases; accordingly, the medium is represented as a polycrystalline aggregate.

The problem of extremizing the strain energy density by varying the mutual orientation of a fixed stress state to the material symmetry axes (regardless of the considered symmetry class) has also been developed by Cowin (1994). After showing that the stress and strain tensors commute at the stationarity (or critical) points of the strain energy, Cowin looks for absolute maxima and minima of the energy in a subset of orientations at which the gradient of the strain energy density vanishes respect to a second-order orthogonal tensor, representing the coordinate transformation. It is shown that the symmetry coordinate system of cubic symmetry is the only situation in linear anisotropic elasticity for which a

strain energy density extremum can exist for all stress states. The stationarity conditions for materials with other symmetries depend on the given stress state. In particular, the conditions for the energy extrema for transversely isotropic and orthotropic solids are found for uniaxial stress states. In Vianello (1996a) and Sgarra and Vianello (1997a,b) attention is paid to showing the *existence* of rotations of the material axes with respect to the principal directions of strain, at which the energy density is stationary. By means of Weierstrass' theorem the existence of at least two such rotations is proved, which parametrically depend on the strain tensor for any material symmetry. At a first glance, this result seems to contradict the statement given in Cowin (1994); nevertheless, the difference with Cowin's formulation is that here the elastic symmetry is held fixed for a *specific* strain state, whereas in Cowin (1994) a *general* state is considered. This difference is exhaustively clarified in Cowin (1997). The extension to finite anisotropic elasticity is tackled by Blume (1994). and Vianello (1996b), where the properties of the extrema are shown to be the same as in the linear case. Further developments in this direction concern the problem of extremizing the strain energy density, with respect to both the orientation of the anisotropy axes and the type of material symmetry (Cowin and Yang, 2000), for a given, but arbitrary, stress state. This formulation reveals a strict connection with analogous problems concerning the generation of optimal topologies (Eschenauer and Olhoff, 2001), where it is essentially the microstructure of the solid that plays the role of design variable.

Finally, it is interesting to notice that the previously illustrated problems spontaneously arise not only in the study of the behaviour of man-made materials, but also in the mechanics of living tissues. For instance, Fyhrie and Carter (1986) develop a relationship between cancellous bone apparent density, trabecular orientation and applied stress, assuming the bone to be an orthotropic, self-optimizing material. It is shown that the trajectories of the material axes and the apparent density can be described by a unifying minimization principle involving a quadratic functional, similar to the strain energy density, and a purely quadratic Tsai-Wu failure criterion. The results predict the alignment of the material axes to the principal stress directions, in agreement with the previously reviewed results. Mechanisms of local changes in anisotropic properties, that more efficiently allow the living bone to carry the loads, are shown in Cowin (1987, 1995). These results suggest that .the bone is designed by nature to have the greatest stiffness in axial direction and the greatest impact load resistance in the transverse one. The intimate relationship between trabecular architecture of cancellous bone and mechanics is also described by Odgaard *et al*. (1997).

2.2. Stationarity of the strain density for some classes of anisotropic solids

The problem of finding critical points of the strain energy density function, in linearly elastic anisotropic solids, is dealt with. In this problem, the local

orientation of the anisotropy axes is assumed to be varying from a point to another through the body, and it is conceived as variable of the problem itself. The solid is supposed to be endowed with a positive definite strain energy. At first, no restriction on the type of elastic anisotropy is made. In an orthogonal reference system $z_1 z_2 z_3$, the constitutive law can be written in the form of the generalized Hooke's law:

$$T_{ij} = C_{ijhk} E_{hk} \tag{5.13}$$

where T_{ij} and E_{hk} are the Cartesian components of the symmetric second-order stress and linearized strain tensors, respectively. C_{ijhk} are the components of the elasticity tensor of rank 4. From here onwards, summation over repeated indices (here ranging from 1 to 3) is understood. The type of anisotropy of the material is reflected by the symmetry group to which the elasticity tensor belongs (Smith and Rivlin, 1958; Gurtin, 1972). Symmetry of the strain and stress tensors, along with the postulated existence of an energy function, lead to the usual symmetries of the elasticity tensor:

$$C_{ijhk} = C_{jihk} = C_{ijkh} = C_{hkij} . \tag{5.14}$$

In the most general case, the elasticity tensor depends on 21 independent coefficients (triclinic system; Gurtin, 1972): this is the case of complete anisotropy, and no restriction is placed on the elasticities C_{ijhk} by any material symmetry property. Conversely, if the material possesses some planes or axes of elastic symmetry, the number of independent elastic coefficients is accordingly reduced. Constraints imposed by material symmetry on the elasticity tensor, classification of symmetry classes, and number of the different types of anisotropy, are topics widely discussed in the literature (see, among others, Love, 1994; Hearmon, 1961; Gurtin, 1972; Ting, 1996; Forte and Vianello, 1996; Huo and Del Piero, 1991; Cowin and Mehrabadi, 1995; Chadwick *et al.*, 2001). For any material symmetry, it is customary to define, at each point *P* of the body, a 'principal', or 'material', orthogonal reference system $x_1 x_2 x_3$ in which the elasticity tensor shows the fewest number of independent non-vanishing components.

The relationship between the Cartesian components of the elasticity tensor in the global frame $z_1 z_2 z_3$, and those in the local material system $x_1 x_2 x_3$, denoted by $\hat{C}_{mnpq}$, is given by the transformation law:

$$C_{ijhk} = Q_{im} Q_{jn} Q_{hp} Q_{kq} \hat{C}_{mnpq} \tag{5.15}$$

where Q_{ij} are the components of a proper orthogonal second-order tensor $\boldsymbol{Q}$.
The anisotropy of the solid is supposed to be *given.* The state of strain at each point *P* of the solid is characterized by the *given* values of the three principal strains and by the orthogonal principal strain directions $x_I x_{II} x_{III}$.
Accordingly, at each point *P* of the solid *three* Cartesian orthogonal systems of axes are defined: $z_1 z_2 z_3$, parallel to the global system of coordinates, which form a set of axes common to all points in the body; $x_1 x_2 x_3$, aligned with the material axes, which can vary point by point; and $x_I x_{II} x_{III}$, the system of the principal directions of strain.
When the material symmetry axes are locally rotated at any point in the body with respect to the fixed system $z_1 z_2 z_3$, the local orientations of the principal directions of strain change as well. Thus, any change in the energy density

$$W = \tfrac{1}{2} C_{ijhk} E_{ij} E_{hk} = \tfrac{1}{2} Q_{im} Q_{jn} Q_{hp} Q_{kq} \hat{C}_{mnpq} E_{ij} E_{hk} \tag{5.16}$$

is due to a change in the mutual orientation between material axes $x_1 x_2 x_3$ and principal axes of strain $x_I x_{II} x_{III}$. Accordingly, in equation (5.16) the Q_{ij} must be understood as components of a proper orthogonal tensor that rotates the material axes with respect to the principal directions of strain.
It is expedient to replace the three-dimensional formulation adopted so far with a suitable formulation of the constitutive law in the six-dimensional space. Different possible notational conventions can be found in the literature to express the stress-strain relationship (Walpole, 1984; Cowin and Mehrabadi, 1987; Mehrabadi and Cowin, 1990; Nadeau and Ferrari, 1998; Ting, 1996; Helnwein, 2001). Here, the description adopted is given by the following linear transformation is six dimensions (Walpole, 1984; Rychlewski, 1984; Cowin and Mehrabadi, 1992):

$$\boldsymbol{t} = \mathbb{C}\boldsymbol{e} \tag{5.17}$$

where the two arrays $\boldsymbol{t}$ and $\boldsymbol{e}$ gather the six independent stress and strain components, respectively:

$$\boldsymbol{t} = \left(T_{11}\ T_{22}\ T_{33}\ \sqrt{2}T_{23}\ \sqrt{2}T_{31}\ \sqrt{2}T_{12} \right)^T \tag{5.18}$$

$$\boldsymbol{e} = \left(E_{11}\ E_{22}\ E_{33}\ \sqrt{2}E_{23}\ \sqrt{2}E_{31}\ \sqrt{2}E_{12} \right)^T \tag{5.19}$$

The elasticity tensor is then consistently transformed into the 6×6 matrix, $\mathbb{C}$:

$$\mathbb{C} = \begin{pmatrix} C_{1111} & C_{1122} & C_{1133} & \sqrt{2}C_{1123} & \sqrt{2}C_{1131} & \sqrt{2}C_{1112} \\ C_{1122} & C_{2222} & C_{2233} & \sqrt{2}C_{2223} & \sqrt{2}C_{2231} & \sqrt{2}C_{2212} \\ C_{1133} & C_{2233} & C_{3333} & \sqrt{2}C_{3323} & \sqrt{2}C_{3331} & \sqrt{2}C_{3312} \\ \sqrt{2}C_{1123} & \sqrt{2}C_{2223} & \sqrt{2}C_{3323} & 2C_{2323} & 2C_{2331} & 2C_{2312} \\ \sqrt{2}C_{1131} & \sqrt{2}C_{2231} & \sqrt{2}C_{3331} & 2C_{2331} & 2C_{3131} & 2C_{3112} \\ \sqrt{2}C_{1112} & \sqrt{2}C_{2212} & \sqrt{2}C_{3312} & 2C_{2312} & 2C_{3112} & 2C_{1212} \end{pmatrix} \tag{5.20}$$

According to this representation, the stress and strain tensors are mapped into the six-dimensional space in the same manner, contrary to the more frequently adopted Voigt's notation where only the shearing strains are affected by a multiplicative factor 2 (Love, 1994; Lekhnitskii, 1981; Sirotin and Chaskolkaïa, 1984; Mehrabadi and Cowin, 1990). The advantage of the Voigt's choice is that the components of the strain vector have the physical meaning of engineering strains. It has been proved by Mehrabadi and Cowin (1990) that the 6×6 matrix in (5.17) contains the components of a second-order tensor in six dimensions, whereas this tensorial character is lost in the Voigt's notation (Nye, 1957; Hearmon, 1961; Fedorov, 1968; Ting, 1996).

For the sake of conciseness, vector and tensor components in six dimensions will be denoted by lowercase letters, and the usual contraction of indices, which replaces any pair of indices with a single index $\left(\text{i.e.}, 11=1, 22=2, 33=3, 23=32=4, 31=13=5 \text{ and } 12=21=6\right)$ is assumed. In such a way the matrix representation (5.17) can be explicitly written as

$$\begin{pmatrix} t_1 \\ t_2 \\ t_3 \\ t_4 \\ t_5 \\ t_6 \end{pmatrix} = \begin{pmatrix} c_{11} & c_{12} & c_{13} & c_{14} & c_{15} & c_{16} \\ c_{12} & c_{22} & c_{23} & c_{24} & c_{25} & c_{26} \\ c_{13} & c_{23} & c_{33} & c_{34} & c_{35} & c_{36} \\ c_{14} & c_{24} & c_{34} & c_{44} & c_{45} & c_{46} \\ c_{15} & c_{25} & c_{35} & c_{45} & c_{55} & c_{56} \\ c_{16} & c_{26} & c_{36} & c_{46} & c_{56} & c_{66} \end{pmatrix} \begin{pmatrix} e_1 \\ e_2 \\ e_3 \\ e_4 \\ e_5 \\ e_6 \end{pmatrix} \tag{5.21}$$

The components of the elasticity tensor in six-dimensions referred to the material symmetry axes will be denoted by $\hat{c}_{ij}\left(i,j=1,...,6\right)$ and collected into the matrix $\hat{\mathbb{C}}$. To express the components of the second-rank elasticity tensor in any reference frame, c_{ij}, in terms of the elastic constants $\hat{c}_{ij}$, a suitable rotation tensor $\boldsymbol{q}$ in six dimensions must be defined, such that

$$c_{ij} = q_{im} q_{jn} \hat{c}_{mn} \ . \tag{5.22}$$

This equation represents the six-dimensional counterpart of the equation (5.15). The definition of the orthogonal tensor $\boldsymbol{q}$ can be found in Mehrabadi and Cowin (1990), where its matrix representation is given as

$$\boldsymbol{q} = \begin{pmatrix} \boldsymbol{q}_{AA} & \boldsymbol{q}_{AB} \\ \boldsymbol{q}_{BA} & \boldsymbol{q}_{BB} \end{pmatrix} \tag{5.23}$$

with

$$\boldsymbol{q}_{AA} = \begin{pmatrix} Q_{11}^2 & Q_{12}^2 & Q_{13}^2 \\ Q_{21}^2 & Q_{22}^2 & Q_{23}^2 \\ Q_{31}^2 & Q_{32}^2 & Q_{33}^2 \end{pmatrix} \tag{5.24}$$

$$\boldsymbol{q}_{AB} = \begin{pmatrix} \sqrt{2}Q_{12}Q_{13} & \sqrt{2}Q_{13}Q_{11} & \sqrt{2}Q_{11}Q_{12} \\ \sqrt{2}Q_{22}Q_{23} & \sqrt{2}Q_{23}Q_{21} & \sqrt{2}Q_{21}Q_{22} \\ \sqrt{2}Q_{32}Q_{33} & \sqrt{2}Q_{33}Q_{31} & \sqrt{2}Q_{31}Q_{32} \end{pmatrix} \tag{5.25}$$

$$\boldsymbol{q}_{BA} = \begin{pmatrix} \sqrt{2}Q_{21}Q_{31} & \sqrt{2}Q_{22}Q_{32} & \sqrt{2}Q_{23}Q_{33} \\ \sqrt{2}Q_{31}Q_{11} & \sqrt{2}Q_{32}Q_{12} & \sqrt{2}Q_{33}Q_{13} \\ \sqrt{2}Q_{11}Q_{21} & \sqrt{2}Q_{12}Q_{22} & \sqrt{2}Q_{13}Q_{23} \end{pmatrix} \tag{5.26}$$

$$\boldsymbol{q}_{BB} = \begin{pmatrix} Q_{22}Q_{33}+Q_{23}Q_{32} & Q_{21}Q_{33}+Q_{23}Q_{13} & Q_{21}Q_{32}+Q_{22}Q_{31} \\ Q_{32}Q_{13}+Q_{33}Q_{12} & Q_{31}Q_{13}+Q_{33}Q_{11} & Q_{31}Q_{12}+Q_{32}Q_{11} \\ Q_{12}Q_{23}+Q_{13}Q_{22} & Q_{11}Q_{23}+Q_{13}Q_{21} & Q_{11}Q_{22}+Q_{12}Q_{21} \end{pmatrix} \tag{5.27}$$

When the problem is written in the six-dimensional space, the energy density function (5.16) takes the form

$$c_{ij} = \tfrac{1}{2} c_{ij}\, e_i e_j = \tfrac{1}{2} q_{im} q_{jn}\, \hat{c}_{mn}\, e_i e_j \tag{5.28}$$

with $i, j = 1, 2, ..., 6$.

In the following the necessary condition for stationarity of the strain energy density is first briefly reviewed. This condition can be obtained in several ways (Seregin and Troitskii, 1981; Rovati and Taliercio, 1991, 1993; Cowin, 1994; Banichuk, 1996). Here it is preferred to recall the direct approach that makes use of the formulation in three dimensions (Cowin, 1994), where the physical

meaning of the stationarity condition turns out in explicit form.
The objective stated in the previous section is to find stationarity points for the strain energy density function (5.16), according to the orthogonality constraint on tensor $\boldsymbol{Q}$, which, in terms of components, reads

$$Q_{ik}Q_{jk} = \delta_{ij} \tag{5.29}$$

where δ_{ij} is the Kronecker's delta. By means of the Lagrangian multipliers method, this constrained probleml can be reformulated as an unconstrained one, consisting into the search for the stationarity of the augmented (or Lagrangian) function $\mathscr{L}$ (Cowin, 1994), defined as

$$\mathscr{L}\left(Q_{ij};\Lambda_{ij}\right) = \tfrac{1}{2}C_{ijhk}E_{ij}E_{hk} - \Lambda_{ij}\left(Q_{ik}Q_{jk} - \delta_{ij}\right), \tag{5.30}$$

where Λ_{ij} are the components of a symmetric tensor $\boldsymbol{\Lambda}$ of rank 2. Stationarity of function $\mathscr{L}$ with respect to the Lagrangian multipliers Λ_{ij} restores the constraint (5.29), whereas stationarity with respect to variables Q_{ij} that is, with respect to the local orientation of the anisotropy axes, is given by

$$\frac{\partial \mathscr{L}}{\partial Q_{rs}} = 2\left(\hat{C}_{mspq}Q_{im}Q_{hp}Q_{kq}E_{ir}E_{hk} - \Lambda_{rj}Q_{js}\right) = 0, \tag{5.31}$$

where minor and major symmetries (5.14) of the elasticity tensor have been taken into account. After some a1gebraic manipulations, it is not difficult to show that

$$T_{ik}E_{ir} = \Lambda_{rk}, \tag{5.32}$$

which, by virtue of the symmetry of tensors $\boldsymbol{T}$, $\boldsymbol{E}$ and $\boldsymbol{\Lambda}$ allows one to write

$$\boldsymbol{TE} = \boldsymbol{ET}. \tag{5.33}$$

The commutativity of this product implies that the two tensors $\boldsymbol{T}$ and $\boldsymbol{E}$ are coaxial. Thus, the stationarity points of the strain energy density correspond to those orientations of the principal directions of strain to the material symmetry axes which make the principal directions of strain collinear with the principal directions of stress. Two second-order tensors are coaxial if they have a common triad of orthogonal eigenvectors. In isotropic elasticity, tensors $\boldsymbol{T}$ and $\boldsymbol{E}$ are always coaxial; this does not apply to anisotropic solids unless special conditions are fulfilled, which will be explicitly derived later for some classes of elastic symmetries.

This coaxiality requirement is the starting point for the solution procedure leading to the analytical determination of the orientation of the anisotropy axes to the principal directions of strain here proposed.
When the strain energy density is stationary, at each point P of the anisotropic body and in the Cartesian coordinate system $x_I x_{II} x_{III}$ of the principal directions of stress and strain, condition (5.33) implies

$$\begin{pmatrix} t_I \\ t_{II} \\ t_{III} \\ 0 \\ 0 \\ 0 \end{pmatrix} = \begin{pmatrix} c_{11} & c_{12} & c_{13} & c_{14} & c_{15} & c_{16} \\ c_{12} & c_{22} & c_{23} & c_{24} & c_{25} & c_{26} \\ c_{13} & c_{23} & c_{33} & c_{34} & c_{35} & c_{36} \\ c_{14} & c_{24} & c_{34} & c_{44} & c_{45} & c_{46} \\ c_{15} & c_{25} & c_{35} & c_{45} & c_{55} & c_{56} \\ c_{16} & c_{26} & c_{36} & c_{46} & c_{56} & c_{66} \end{pmatrix} \begin{pmatrix} e_I \\ e_{II} \\ e_{III} \\ 0 \\ 0 \\ 0 \end{pmatrix} \tag{5.34}$$

which can be written, for notational purposes only, in concise form as

$$\begin{pmatrix} \boldsymbol{t}_p \\ \boldsymbol{0} \end{pmatrix} = \begin{pmatrix} \boldsymbol{C}_{AA} & \boldsymbol{C}_{AB} \\ \boldsymbol{C}_{BA} & \boldsymbol{C}_{BB} \end{pmatrix} \begin{pmatrix} \boldsymbol{e}_p \\ \boldsymbol{0} \end{pmatrix} \tag{5.35}$$

(with $\boldsymbol{C}_{BA} = \boldsymbol{C}_{AB}^T$). Therefore, coaxiality of the stress and strain tensors can be expressed as

$$\boldsymbol{C}_{BA}\boldsymbol{e}_p = \boldsymbol{0} \;\Rightarrow \begin{cases} c_{14}e_I + c_{24}e_{II} + c_{34}e_{III} = 0, \\ c_{15}e_I + c_{25}e_{II} + c_{35}e_{III} = 0, \\ c_{16}e_I + c_{26}e_{II} + c_{36}e_{III} = 0. \end{cases} \tag{5.36}$$

Clearly, system (5.36) is identically satisfied *for any* value of the principal strains e_I, e_{II}, e_{III} if all the coefficients $c_{14}, c_{24}, ..., c_{36}$ simultaneously vanish. This occurrence may happen only for those material symmetry classes for which at least a material coordinate system can be found where all the entries of submatrix $\boldsymbol{C}_{BA}$ vanish (Cowin, 1994, 1997), provided that, at the same time, these material axes are aligned with principal directions of stress and strain. These elastic symmetries correspond to the cubic system (characterized by 3 elastic coefficients), hexagonal(5) system (transverse isotropy, *5* coefficients), tetragonal(6) system (6 coefficients) and orthorombic symmetry (9 coefficients) (see Gurtin, 1972). For the other elastic symmetries, i.e. hexagonal (with 6 and 7 elastic coefficients), tetragonal (7 coefficients), monoclinie (13 coefficients) and triclinic (complete anisotropy, 21 coefficients), in any reference system the submatrix $\boldsymbol{C}_{BA}$ is different from the null matrix (Gurtin, 1972). Therefore, for such symmetries, no particular reference frame exists in which system (5.36) can

be satisfied *for any* non-vanishing value of the principal strains. Equations (5.36) show that, for those elastic symmetries such that $\boldsymbol{C}_{BA} = \boldsymbol{0}$ in some coordinate system, stationarity of the energy can be achieved, in particular, for simultaneous coaxiality of principal directions of stress, strain and material symmetry axes. This is the special case considered by Cowin (1994).

2.3. Cowin-Taliercio minimization of the strain energy involving Inertia-Fabric tensors: an explicit strategy

In the previous section it was shown that the necessary condition for stationarity of the strain energy density may be written in the form (5.33) which implies that the two tensors $\boldsymbol{T}$ and $\boldsymbol{E}$ are coaxial. Thus, as above underlined, the stationarity points of the strain energy density correspond to those orientations of the principal directions of strain to the material symmetry axes which make the principal directions of strain collinear with the principal directions of stress. Two second-order tensors are coaxial if they have a common triad of orthogonal eigenvectors. In anisotropic elasticity, tensors $\boldsymbol{T}$ and $\boldsymbol{E}$ are not always coaxial unless some specific classes of elastic symmetries are considered – orthotropic symmetry.
In the following, an explicit strategy of optimization of the elastic constant of an orthotropic material based on the minimization of the strain energy is developed. To this aim, it is considered the constitutive relation

$$\boldsymbol{T} = \overline{\mathbb{C}} : \boldsymbol{E} \tag{5.37}$$

where $\overline{\mathbb{C}}$ is the overall elasticity tensor expressed in the form (see Chapter IV)

$$\overline{\mathbb{C}} = \overline{\mathbb{C}}\left(\gamma, m_i\right), \qquad i = 1 \text{ to } 3 \tag{5.38}$$

where γ is the volume fraction of the material and the m_i -s are the eigenvalues of the fabric tensor in the main reference frame. Remember that in the (5.38) the anisotropy is governed by the eigenvalues of the fabric tensor in the sense that if all the m_i -s are different, the corresponding material symmetry is the orthotropy, if only two of the m_i -s are different, the corresponding material symmetry is the transverse isotropy, while if the m_i -s are all equal the corresponding material symmetry is the isotropy.
The energy density function is

$$W = \tfrac{1}{2} C_{ijhk} E_{ij} E_{hk} = \tfrac{1}{2} C_{ijhk}\left(\gamma, m_i\right) E_{ij} E_{hk} \tag{5.39}$$

and the problem of the minimization of the energy density function $W(\gamma, m_i)$ may be written as

$$\min \tfrac{1}{2} \int_{\Omega} C_{ijhk}(\gamma, m_i) E_{ij} E_{hk} \, dV \tag{5.40}$$

subject to

$$\int_{\Omega} \gamma dV = \overline{V} = \overline{\gamma} V < V \, . \tag{5.41}$$

With specific reference to the results obtained in Charter IV in cases of both LVF and HVF, namely by identifying the fabric tensor with an appropriate normalization of the inertia tensor, the eigenvalues m_i -s takes the form

$$m_i = f(\gamma) J_{ii} \tag{5.42}$$

where $f(\gamma)$ is a function to determine, while J_{ii} are the eigenvalues of the inertia tensor. In particular, it was shown that

$$J_{ii} = J_{ii}(\xi_j) \tag{5.43}$$

The parameters ξ_j depend on the specific microstructure and are hare considered

$$\xi_j = \begin{cases} (t_i, \gamma) & \text{for LVF,} \\ (\beta, \gamma) & \text{for HVF,} \end{cases} \tag{5.44}$$

where t_i are the thicknesses of the walls of the Flugge's equivalent RVE (see Chapter VI, Section 2.2.), β is the ratio the diameters of the equivalent ellipsoidal void (see Chapter VI, Section 2.4.) and γ is the volume fraction. Note that in Section 2.4. of the Chapter VI, with reference to the study of HVF materials, the porosity ϕ is considered instead of the volume fraction γ but because of the relation $\phi = 1 - \gamma$ choosing a parameter rather that the other is substantially the same.

By virtue of the relations (5.42), (5.43) and (5.44), the minimization of the energy density (5.40) is reduced to solving the set of $j+1$ equations

$$\begin{cases} \dfrac{\partial W}{\partial \gamma} \\ \dfrac{\partial W}{\partial \xi_i} \end{cases} \tag{5.45}$$

under the constrain $\int_\Omega \gamma dV = \overline{\gamma} V$.

In order to better clarifying the illustrated procedure, later on it will be developed a simple example.

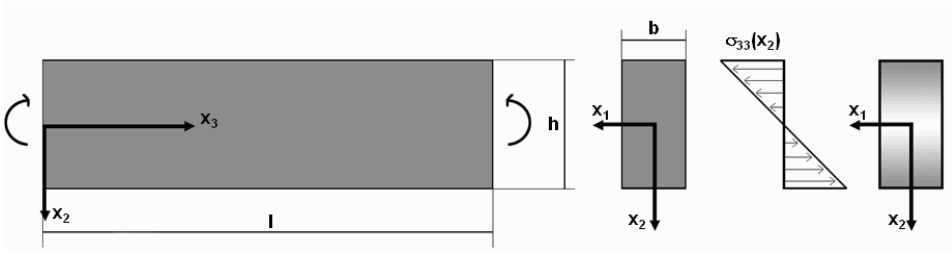

Fig. 5.2.

Beam in bending regime. Rectangular cross section before and after the optimization which gives a density linear in x_2.

Let us considered a beam of length l in bending regime (see Fig. 5.2). The rectangular cross section of the beam have the dimensions b and h. It is well known that the sole non-zero stress component inside the beam is the σ_{33} given by

$$\sigma_{33} = \frac{M}{I} x_2 . \tag{5.46}$$

The volume fraction inside the considered body is in general variable with the position $\boldsymbol{x}$ but it is here assumed variable with the sole component x_2

$$\gamma(\boldsymbol{x}) = \gamma(x_2) . \tag{5.47}$$

The energy density W takes the form

$$W = \tfrac{1}{2}\int_V \sigma_{33}\varepsilon_{33} dV = \tfrac{1}{2}\int_V \frac{\sigma_{33}^2}{\overline{E}} dV \tag{5.48}$$

where $\overline{E}$ is the overall Young modulus.
In order to give an explicit form to $\overline{E}$, the transverse strains are neglected – that means to assume $\nu = 0$. In this way the term the term C_{1111} of the elasticity tensor coincides with the Young modulus. Moreover, with reference to the Flugge's overall elasticity tensor for the cubic case - $t_i = t$ - we may conclude that

$$\overline{E} = C_{1111} = \frac{2}{3} E\gamma = k\gamma \tag{5.49}$$

where E is the Young modulus of the matrix, $\gamma = 3t/a$ and $k = 2E/3$.
By substituting the (5.46) and the (5.49) inside the (5.48), the strain energy density becomes

$$\begin{aligned} W = \frac{1}{2}\int_V \frac{M^2}{I^2 k}\frac{x_2^2}{\gamma(x_2)}dV = \frac{1}{2}\frac{M^2}{I^2 k}\int_V \frac{x_2^2}{\gamma(x_2)}dV = \\ \frac{1}{2}\frac{M^2}{I^2 k}\int_0^l \int_{-b/2}^{b/2}\int_{-h/2}^{h/2} \frac{x_2^2}{\gamma(x_2)}dx_1 dx_2 dx_3 = \frac{1}{2}\frac{M^2}{I^2 k} lb\int_{-h/2}^{h/2}\frac{x_2^2}{\gamma(x_2)}dx_2 \end{aligned} \tag{5.50}$$

By setting $A = \frac{1}{2}\frac{M^2}{I^2} lb$, the (5.50) becomes

$$W = A\int_{-h/2}^{h/2}\frac{x_2^2}{k\gamma(x_2)}dx_2 . \tag{5.51}$$

The optimal distribution of material inside the cross section of the beam - $\gamma(x_2)$ - is found out by means of the minimization of the energy density (5.51) according the constraint

$$\int_V \gamma(x_2)\,dV = lb\int_{-h/2}^{h/2}\gamma(x_2)dx_2 = \overline{V} = \overline{\gamma} V < V \tag{5.52}$$

By means of the Lagrangian multipliers method, this constrained probleml can be reformulated as an unconstrained one, consisting into the search for the stationarity of the augmented (or Lagrangian) function $\mathscr{F}$, defined as

$$\mathscr{F}(\gamma, \lambda) = A\int_{-h/2}^{h/2}\frac{x_2^2}{k\gamma(x_2)}dx_2 + \lambda\, lb\int_{-h/2}^{h/2}\gamma(x_2)dx_2 \tag{5.53}$$

where λ is the Lagrangian multiplier. The stationarity of the function $\mathscr{F}$ with respect to the volume fraction γ is given by

$$\delta\mathscr{F} = \left(-A\frac{x_2^2}{(k\gamma)^2}k + B\lambda \right)\delta\gamma = 0 \qquad \forall\,\delta\gamma . \tag{5.54}$$

The (5.54) gives

$$\gamma = \sqrt{\frac{Ax_2^2}{Bk\lambda}} = |x_2|\sqrt{\frac{A}{Bk\lambda}} \tag{5.55}$$

The substitution of the (5.55) into the constrain condition (5.52) gives

$$lb\int_{-h/2}^{h/2} |x_2|\sqrt{\frac{A}{Bk\lambda}}\,dx_2 = \bar{V} \tag{5.56}$$

which solved furnishes the value of the Lagrangian multiplier as

$$\lambda = \frac{ABh^2}{4k\bar{V}} . \tag{5.57}$$

By substituting the (5.57) into the (5.55), it results

$$\gamma = \frac{2}{Bh}\sqrt{\bar{V}}\,|x_2| . \tag{5.58}$$

The optimal distribution of the volume fraction inside the cross section of the beam is linear in x_2 as well as the stress σ_{33}.

CONCLUSIONS AND PERSPECTIVES

In this work the problem of the mechanical characterization of porous-elastic material is dealt with. Two different class of porous materials are separately treated, namely the porous materials that show randomly arranged and oriented microstructure.

In the first case, thanks to the presence of symmetry planes, the porous material shows an isotropic mechanical behaviour and the non-homogeneity may be described by the sole scalar parameter γ which represents the RVE volume fraction. By means of numerical analyses based on Finite Element Method, constitutive relations are built up. The results are indeed interpolated by algebraic functions which match the analytical solutions furnished for low volume fraction (Flugge's solutions) and high volume fraction (dilute distribution of voids) by literature. It is worth to note that, although some scientific papers present laws for estimating the overall elastic moduli of isotropic porous materials, they are however not valid in general. In fact, the literature proposals – e.g. the Rho modulus/density relationships for bone tissue – are found out by means of interpolations made over experimental tests related to specific anatomic sites and therefore only valid for those tissues and the corresponding void distribution within the specimens. On the contrary, the laws here proposed have general validity, being determined independently from the specific material or microstructural morphology.

Materials that exhibit an oriented microstructure may be considered inhomogeneous and anisotropic. They are commonly studied by means of micromechanical approaches based on fabric tensors which, in spite of the mechanical consistency, are difficult to employ because their involving requires the point-wise evaluation of the fabric tensor eigenvalues and eigenvectors.

In the present work the case of porous materials with oriented microstructure with low and high volume fraction are analysed separately, being in the first case the anisotropic behaviour governed by the matrix structure, while in the second case by the voids orientation.

For poro-elastic materials with low volume fraction a constitutive relationship is given starting from Flugge's solution, generalized to the orthotropic case. This strategy conducts to an identification of the fabric eigenvalues which suggests to identify the fabric tensor with the inertia tensor, opportunely normalized. In the complementary case – high volume fraction – the constitutive relations are found starting from the elastic solution of an ellipsoidal void embedded into an infinite linear elastic solid. In order to bear out the hypotheses of identifying the fabric tensor with the inertia tensor, some examples are derived and illustrated to highlight analogies and differences between the mean intercept length tensor and the inertia tensor for bi-dimensional RVEs. Such examples seem to confirm the advisability to use the inertia tensor like microstructural parameter. This choice has the advantage that the inertia tensor is a parameters easy to evaluate by

means of specific software, if a vectorial image of a considered RVE is available.

The obtained results may be applied in a wide range of mechanical problems involving anisotropic heterogeneous materials, for example the characterization of granular media (soils and rocks), cellular conglomerates, ceramic materials, synthetic biomaterials or biological tissue (cancellous bone, soft tissue), with the aim of studying damage or remodelling phenomena in alive tissue, and solve optimization problems for engineered materials – as explicit shown in Chapter V.

In conclusion, it is also worth to highlight that the constitutive models here presented are deferred to porous elastic materials where the presence of fluid is neglected. However, the effects of possible interstitial fluid in the solid matrix can be considered by invoking the classical linear and non-linear theories governing the coupling of the two phases.

REFERENCES

- Allaire, G., Kohn, R.V., 1993. Optimal design for minimum weight and compliance in plane stress using extremal microstructures. *Eur. J. Mech. A* **12**: 839-878.
- Alleire, G., Bonnetier, E., Francfort, G., Jouve, F., 1997. Shape optimization by the homogenization method. *Numer. Math.* **76**: 27-68.
- Alshits, V.I., Kirchner, O.K., 2001. Cylindrically anisotropic, radially inhomogeneous elastic materials. Proc. R. Soc., A 457, 671-693, London.
- Ambrosio, L., Buttazzo, G., 1993. An optimal design problem with perimeter penalization. *Calc. Var.* **1**: 55-69.
- Banichuk, N.V., 1981. Optimization problems for elastic anisotropic bodies. *Archives of Mechanics*, **33**: 347-363.
- Banichuk, N.V., 1983. Problems and Methods in Optimal Structural Design. Plenum Press, New York.
- Banichuk, N.V., 1996. Optimization of anisotropic properties for continuum bodies and structural elements using spectral methods of tensor analysis. *Mechanics of structure and Machines*, **24**: 71-87.
- Banichuk, N.V., Kobelev, V.V., 1987. On optimal plastic anisotropy. *Prikladnaja Matematika I Mekanika* **51**: 489-495. Traslated in: *Journal of Applied Mathematics and Mechanics* **51**: 381-385.
- Barber, J.R., 1992. Elasticity. Dordrecht, Boston, London, Kluwer Academic Publishers.
- Beckers, M., 1999. Topology optimization using a dual method with discrete variables. *Struct. Optim.* **17**: 14-24.
- Bendsøe, M.P., 1983. On obtaining a solution to optimization problems for solid elastic plates by restriction of the design space. *J. Struct. Mech.* **11**: 501-521.
- Bendsøe, M.P., 1989. Optimal shape design as a material distribution problem. *Struct. Optim.* **1**: 193-202.
- Bendsøe, M.P., 1995. Optimization of Structural Topology Shape and Material. Berlin Heidelberg: Springer Verlag.
- Bendsøe, M.P., Kikuchi, N., 1988. Generating optimal topologies in structural design using a homogeni- zation method. *Comput. Methods. Appl. Mechs. Eng.* **71**, 197-224.
- Bendsøe, M.P., Guedes, J. M., Haber, R.B., Pedersen, P., Taylor, J.E., 1994. An analytical model to predict optimal material properties in the context of optimal structural design. *J. Appl. Mech.* **61**: 930-937.
- Blume, J.A., 1994. Elastic materials with coincident principal stress and strain axes. *Journal of Elasticity* **35**: 275-280.
- Boehler, J.P., 1987. Application of Tensor Functions in Solid Mechanics. Springer, Wien.
- Bojarski, B., Iwaniec, T., 1983. Analytical foundations of the theory of quasi conformal mappings in R^n. *Annales Academiae Scientiarum, Ser. A.I. Mathematica*, **8**, 257-324.
- Budiansky, B., O'Connell, R.J., 1976. Elastic Moduli of a Cracked Solid. *Int. J. Solid Structure*, **12**: 81-97.
- Bunge, G., 1970. Texture Analysis in Material Science – Mathematical Methods. Butterworth, London.

References

- Buttazzo, G., Dal Maso, G., 1993. An existence result for a class of shape optimization problems. *Arch. Rational Mech. Anal.* **122**: 183-195.
- Cauchy, A.L., 1923. Rechercher sur l'équilibre et le movement intérieur des corps solides ou fluids, élastiques ou non élastique. *Bulletin de la Société Philomatique*, 9-13 (Oeuvres (2) 2, pp. 300-304, Gauthier-Villars, Paris, 1889).
- Cauchy, A.L., 1927a. De la pression ou tension dans un corps solide, *Exercices de Mathématiques* 2, 42-56 (Oeuvres (2) 7, pp. 60-93, Gauthier-Villars, Paris, 1889).
- Cauchy, A.L., 1927b. Sur les relations qui existent dans l'état d'équilibre d'un corps solide ou fluide (Oeuvres (2) 7, pp. 141-145, Gauthier-Villars, Paris, 1889).
- Cauchy, A.L., 1928. Sur les equations qui experiment les conditions d'équilibre ou les lois du movement intérieur d'un corps solide, élastique (Oeuvres (2) 8, pp. 195-226, Gauthier-Villars, Paris, 1890).
- Chadwick, P., Vianello, M., Cowin, S.C., 2001. A new proof that the number of linear elastic symmetries is eight. *Journal of the Mechanics and Physics of Solids* **49**: 2471-2492.
- Chenais, D., 1975. On the existence of a solution in a domain identification problem. *J. Math. Anal. Appl.* **52**: 189-289.
- Cheng, G., Olhoff, N., 1981. An investigation concerning optimal design of solid elastic plates. *Int. J. Solids Struct.* **16**: 305-323.
- Choquet-Bruhat, Y., Dewitt-Morette, C., Dillard-Bleick, M., 1977. Analysis Manifolds and Physics. North-Holland, Amsterdam.
- Christensen, R.M., 1979. Mechanics of Composite Materials. Wiley-Interscience, New York.
- Chung, M.Y, Ting, T.C.T, 1995. Line forces and dislocations in angularly inhomogeneous anisotropic piezoelectric wedges and spaces. Philos. Mag. A 71, 1335-1343.
- Cowin, S.C., 1985. The Relationship between the Elasticity Tensor and the Fabric Tensor, *Mechanics of Materials* **4**: 137-147.
- Cowin, S.C., 1986. Wolff's law of trabecular architecture at remodelling equilibrium. *Journal of Biomechanical Engineering*, **108**: 83-88.
- Cowin, S.C., 1987. Torsion of cylinders with shape intrinsic orthotropy. *J. Appl. Mech.*, **109**, 778-782.
- Cowin, S.C., 1994. Optimization of the strain energy density in linear anisotropic elasticity. *Journal of Elasticity* **34**: 45-68.
- Cowin, S.C., 1995. On the minimization and maximization of the strain energy density in cortical bone tissue. *Journal of Biomechanics* **28**: 445-447.
- Cowin, S.C., 1997. Remarks on coaxiality of strain and stress in anisotropic elasticity. *Journal of Elasticity* **47**: 83-84.
- Cowin, S.C., Mehrabadi, M.M., 1987. On the identification of material symmetry for anisotropic elastic materials. *Quarterly Journal of Mechanics and Applied Mathematics* **40**: 451-476.
- Cowin, S.C., Mehrabadi, M.M., 1992. The structure of the linear anisotropic elastic symmetries. *Journal of the Mechanics and Physics of the Solids* **40**: 1459-1471.
- Cowin, S.C., Mehrabadi, M.M., 1995. Anisotropic symmetries in linear elasticity. *Applied Mechanics Review* **48**: 247-285.
- Cowin, S.C., Yang, G., 2000. Material symmetry optimization by Kelvin modes. *J. Eng. Math* **37**: 27-43.
- Cox, S., Lipton, R., 1996. Extremal eigenvalue problems for two-phase conductors. *Arch. Rational Mech. Anal.* **136**: 101-118.

References

- Curran, D.R., Seaman, L., Shockey, D.A., 1987. Dynamic Failure of Soilds. *Physics Reports*, Nos. 5&6, **147**: 253-388.
- Díaz, Lipton, R., 1997. Optimal material layout for 3D elastic structures. *Struct. Optim.* **13**: 60-64.
- Edidin, A.A., Taylor, D.L., Bartel, D.L., 1991. Automatic assignment of bone moduli from CT data: a 3-D finite element study. *Trans. Orthop. Res. Soc.,* **16**: 491.
- Eschenauer, H.A., Olhoff, N., 2001. Topology optimization of continuum structures: a review. *Applied Mechanics Review* **4**: 331-390.
- Euler, L., 1757. Continuation des recherches sur la théorie du movement des fluids, *Hist. Acad. Berlin*, 316-361.
- Euler, L., 1771. Sectio tertia de motu fluidorum lineari potissimum aquae. *Novi Comm. Petrop.* 15: 219-360.
- Federer, H., 1969. Geometric measure theory, Springer- Verlag, New York.
- Fedorov, F.I., 1968. Theory of elastic waves in crystals. Plenum Press, New York.
- Flugge, W., 1972. Tensor Analysis and Continuum Mechanics, Sprinter-Verlag Berlin Heidelberg New York.
- Forte, S., Vianello, M., 1996. Symmetry classes for elasticity tensor. *Journal of Elasticity* **43**: 81-108.
- Fraldi, M., Cowin, S.C., 2004. Inhomogeneous elastostatic problem solutions constructed from stress-associated homogeneous solutions. *Journal of the Mechanics and Physics of Solids*, **52**, 2207-2233.
- Fraldi, M., Guarracino, F., 2001. On a general property of a class of homogenized porous media. *Mech.Res.Comm.*, **28**, 2, 213-221.
- Fyhrie, D.P., Carter, D.R., 1986. A unifying principle relating stress to trabecular bone morphology. *Journal of Orthopaedic Research* **4**: 304-317.
- Germain, P., 1972. Mécanique des milieux Continus. Tome I, Masson, Paris.
- Giangreco, E., 2003. Ingegneria delle strutture. UTET, 2 vol.
- Gonzáles, C., Segurado, J., Llorca, J., 2004. Numerical simulation of elasto-plastic deformation of composites: evolutions of the stress microfields and implications for homogenization models. *J. Mechanics and Physics of Solids* **52**, 1573-1593.
- Goodman, J., Khon, R.V., Reyna, L.: Numerical study of a relaxed variational problem from optimal design. *Comput. Methods Appl. Mech. Eng.* **57**:107-127.
- Gurtin, M. E., 1972. The Linear Theory of Elasticity, Handbbuch der Physik, Springer, Berlin.
- Gurtin, M.E., 1981. An introduction to continuum Mechenics. Academic Press, New York.
- Haber, R.B., Bendsøe, M.P., Jog, C.S., 1996. A new approach to variable-topology shape design using a constraint on the perimeter. *Struct. Optim.* **11**: 1-12.
- Harrigan, T.P., Mann R.W., 1984. Characterization of microstructural anisotropy in orthotropic materials using a second rank tensor. *Journal of Material Science*, **19**: 761-767.
- Hashin, Z., Shtrikman, S., 1963. A variational approach to the theory of the elastic behaviour of multiphase materials. *J. Mech. Phys. Solids* **11**: 127-140.
- He, Q.-C., Curnier, A., 1995. A more fundamental approach to damaged elastic stress-strain relations. *International J. of Solids and Structures*, **32**: 1433-1457.
- Hearmon, R.F.S., 1961. An introduction to applied anisotropic elasticity. Oxford University Press, Oxford.

References

- Helnwein, P., 2001. Some remarks on the compressed matrix representation of symmetric second-order and fourth-order tensors. *Computer Methods in Applied Mechanics and Engineering* **190**: 2753-2770.
- Hill, R., 1965a. A self-consistent mechanics of composite materials. *J. Mech. Phys. Solids*, **12**, 213-22.
- Hill, R., 1967. The essential structure of constitutive laws for metal composites and polycrystals. *J. Mech. Phys. Solids*, **15**, 79-95.
- Horii, H., Nemat-Nasser, S., 1983. Overall moduli of solids with microcracks: Load-induced anisotropy. *J. Mech. Phys. Solids*, Vol. **31**, 155-177.
- Huo, Y.Z., Del Piero, G., 1991. On the completeness of crystallographic symmetries in the description of symmetries of the elastic tensor. . *Journal of Elasticity* **25**: 203-246.
- Ilankamban, R., Krajcinovic, D., 1987. A Constitutive theory for Progressively Deteriorating Brittle Solids. *Int. J. Solids Structures*, **23**, 1521-1534.
- Jog, C., Haber, R. B., Bendsøe, M.P., 1994. Topology design with optimized, self-adaptive materials. *Int. J. Numeral Methods Eng.* **37**: 1323-1350.
- Jones, M.N., 1985. Spherical Harmonics and Tensors for Classical Field Theory. Wiley, New York.
- Kanatani, K., 1984. Distribution of directional data and fabric tensors. *Int. J. Engng Sci.* **22**, 149-164.
- Kartvelishvili, V.M., Kobelev, V.V., 1984. Rational schemes for reinforcing laminar plates from composite materials. *Prikladnaja Matematika I Mekanika* **48**: 68-80. Traslated in: *Journal of Applied Mathematics and Mechanics* **48**: 40-49.
- Keyak J.H., Meagher, J.M., Skinner, H.B., Mote, C.D., 1990. Automated three-dimensional finite element modelling of bone: a new method. *J. Biomed. Eng.,* **12**: 389-397.
- Khon, R.V., Strang,G., 1986. Optimal design and relaxation of variational problems. *Commun. Pure Appl. Math.* **39**: 1-25 (Part I), 139-182 (Part II), 353-377 (Part III).
- Kouznetsova, V., Brekelmans, W.A.M., Baaijens, F.P.T., 2001. An approach to micro-macro modeling of heterogeneous materials. *Computational Mechanics* **27**, 37-48.
- Krajcinovic, D., 1996. Damage Mechanics. North-Holland.
- Lelong-Ferrand, J., 1963. Géométrie Différentielle. Masson, Paris.
- Lekhnitskii, S.G., 1963. Theory of elasticity of an anisotropic elastic body, Holden Day Inc., San Francisco.
- Lekhnitskii, S.G., 1981. Theory of elasticity of an anisotropic elastic body, Mir Publisher, Moscow.
- Lemaitre, J., 1986. Local Approach of Fracture, *Eng. Fracture Mech.*, **25**: 523-537.
- Lemaitre, J., 1992. A Course on Damage Mechanics, Sprinter- Verlag, Berlin, Germany.
- Lemaitre, J., Chaboche, J.L., 1978. Aspect Phenomenologique de la Rupture par Endommagement, *J. Mech. Applique*, **2**: 317-365.
- Lemaitre, J., Dufailly, J., 1987. Damage measurement. *Engng Fracture Mech.*, **28**, 643-661.
- Lions, J.L., 1985. Les Methodes de l'Homogeneisation: Theorie et Applications en Physique, Saint Germain Paris, Eyrolles Ed.
- Love, A.E.H., 1994. A treatise on the mathematical theory of elasticity, fourth ed. Dover, New York.

- Lubarda, V., Krajcinovic, D., 1993. Damage Tensors and the Crack Density Distribution, *Int. J. Damage Mech.*, **48**: 2859-2877.
- Lurie, K.A., Cherkaev, A. V., Fedorov, A. V., 1982. Regularization of optimal design problems for bars and plates. JOTA, **37**: 499-522 (Part I), **37**: 523-543 (Part II), **42**: 247-282 (Part III).
- Malliavin, P., 1972. Géométrie Différentielle Intrinsèque. Hermann, Paris
- Mandel, J., 1971. Plasticité classique et viscoplasticité. Springer-Verlag, Vienna (CISM Lecture Notes, Udine, Italy).
- Marcus, M., Mizel, V.J. 1973. Transformations by functions in Sobolev spaces and lower semicontinuity for parametric variational problems, *Bull. Amer. Math. Soc.* **79**, 790-795.
- Mehrabadi, M.M., Cowin, S.C., 1990. Eigentensors of linear anisotropic elastic materials. *Quarterly Journal of Mechanics and Applied Mathematics* **43**: 15-41.
- Marom, S.A., Linden, M., Computed aided stress analysis of long bones utilizing computer tomography. *J. Biomech.* **23**:300-404.
- Marsden, J.E., Hughes, T.J.R., 1983. Mathematical foundations of elasticity. Prentice-Hall, Englewood Cliffs.
- Maugin, G.A.,1993. Material inhomogeneities in elasticity. Chapman & Hall.
- Milton, G.W., Cherkaev, A. V., 1995. Which elasticity tensor are realizable? *J. Eng. Mat. Tech.* **117**: 483-493.
- Mlejnik, H.P., Schirrmacher, R., 1993. An engineering approach to optimal material distribution and shape finding. *Comput. Methods Appl. Mech. Eng.* **106**: 1-26.
- Nadeau, J.C., Ferrari, M., 1998. Invariant tensor-to-matrix mappings for evaluation of tensorial expressions. *Journal of Elasticity*, **52**: 43-61.
- Nemat-Nasser, S., Horii, H., 1993. Micromechanics: Overall properies of heterogeneous materials. North-Holland.
- Niordson, F.I.: Optimal design of plates with a constraint on the slope of the thickness function. *Int. J. Solids Struct.* **19**:141-151.
- Noll, W., 1959. The foundation of classical mechanics in the light of recent advances in continuum mechanics, in The axiomatic method, with Special Reference to Geometry and Physics, pp. 266-281, North Holland, Amsterdam.
- Nye, J.F., 1957. Physical properties of crystals. Their Representation by tensors and matrices. Oxford University Press, Oxford.
- Odgaard, A., Kabel, J., van Rietbergen, B., Dalstra, M., Huiskes, R., 1997. Fabric and elastic principal directions of cancellous bone are closely related. *J. Biomechanics* **30**, 5: 487-495.
- Olhoff, N., Rønholt, E., Scheel, J., 1998. Toplogy optimization of three-dimensional structures using optimum microstructures. *Struct. Optim.* **16**: 1-18.
- Onat, E.T., 1984. Effective properties of elastic materials that contain penny shaped voids. *Int. J. Engng Sci.* **22**, 1013-1021.
- Onat, E.T., Leckie, F.A., 1984. Representation of mechanical behaviour in the Presence of Changing Internal Structure, *J. Appl. Mech.*, **55**: 1-10.
- Pedersen, P., 1989. On optimal orientation of orthotropic materials. *Struct. Opt.* **1**: 101-106.
- Pedersen, P., 1990. Bounds on elastic energy in solids of orthotropic materials. *Struct. Opt.* **2**: 55-62.
- Petersson, J., 1998. Some convergence results in perimeter-controlled topology optimization. *Comput. Methods Appl. Mechs. Eng.* **171**: 123-140.

References

- Petersson, J., Sigmund, O., 1998. Slope constrained topology optimization. *Int. J. Numeral Methods Eng* **41**:1417-1434.
- Rado, T., Reichelderfer, P.V., 1955. Continuous transformations in analysis. Springer- Verlag, Berlin.
- Rho, J.Y., Hobatho, M.C., Ashman, R.B., 1995. Relation of mechanical properties to density and CT number in human bone. *Med. Eng. Phys.,* **17**: 347-355.
- Ringertz, U., 1993. On finding the optimal distribution of material properties. *Struct. Optim.* **5**: 265-267.
- Rychlewski, J., 1984. On Hooke's law. *Prikladnaja Matematika i Mekanika* **48**: 420-435; Translated in: *J. Appl. Math. Mech.* **48**: 303-314.
- Rovati, M., Taliercio, A., 1991. Optimal orientation of the symmetry axes of orthotropic materials. In: Eschenauer, H.A., Mattheck, C., Olhoff, N. (Eds.), Engineering Optimization in Design Processes. Springer-Verlag, Heidelberg, pp. 127-154.
- Rovati, M., Taliercio, A., 1993. Bounds on the elastic strain energy density in 3-D bodies with material symmetries. In: Herskowits, J. (Ed.), Proceedings of Structural Optimization '93, Rio de Janeiro, August 2-6, pp. 353-360.
- Rovati, M., Taliercio, A., 2003. Stationary of the strain energy density for some classes of anisotropic solids. *Int. J. of Solids and Structures.*, **40**: 6043-6075.
- Rozvany, G.I.N., Zhou, M., Sigmund, O., 1994. Topology Optimization in Structural Design. In Adeli H (ed.): Advances in Design Optimization, pp. 340-399. London: Chapman and Hall.
- Sacchi Landriani, G., Rovati, M., 1991. Optimal 2-D structures made of composite materials. *J. Eng. Materials Technology*, Transactions of the ASME **113**, 88-92.
- Schwartz, L., 1967. Cours d'Analyse. Hermann, Paris.
- Seregin, G.A., Troitskii, V.A., 1981. On the best position of elastic symmetry planes in an orthotropic body. *Prikladnaja Matematika i Mekanika* **45**: 185-189; Translated in: *J. Appl. Math. Mech.* **45**: 139-142.
- Sevostianov, I., Kachanov, M., 1999. Compliance tensors of ellipsoidal inclusions. *International Journal of Fracture* **96**: L3-L7.
- Sgarra, C., Vianello, M., 1997a. Directions of coaxiality between pure strani and stress in linear elasticity. *Journal of Elasticity* **46**: 263-265.
- Sgarra, C., Vianello, M., 1997b. Rotations which make strain and stress coaxial. *Journal of Elasticity* **47**: 217-224.
- Sigmund, O., 1994. Design of Material Structures using Topology Optimization. DCAMM Special report S69, Department of Solid Mechanics, Technical University of Denmark, Lyngby.
- Sigmund, O., 1995. Tailoring materials with prescribed elastic properties. *Mech. Mat.* **20**: 351-368.
- Sirotin, Y., Chaskolkaïa, M., 1984. Fondements de la physique des cristaux. Éditions Mir, Moscow.
- Smith, K.T., 1983. Primer of Modern Analysis, Second Edition, Springer-Verlag, New York.
- Smith, G.F., Rivlin, R.S., 1958. The strain energy function for anisotropic elastic materials. *Transaction of American Mathematical Society* **88**, 175-193.
- Suquet, P., 1981a. Sur les equations de la plasticité: existence etrégularité des solutions. *J. Mécanique*, **20**, 3-40.
- Sutcliffe, S., 1992. Spectral decomposition of the elasticity tensor. *Journal of Applied Mechanics*, Transactions of the ASME **59**: 762-773.

References

- Theocaris, P.S., Sokolis, D.P., 2000a. Invariant elastic constants and eigentensors of orthorhombic, tetragonal, hexagonal and cubic crystalline media. *Acta Crystallographica Sect. A* **56**: 319-331.
- Theocaris, P.S., Sokolis, D.P., 2000b. Spectral decomposition of the compliance fourth-rank tensor for orthotropic materials. *Archives of Applied Mechanics* **70**: 289-306.
- Ting, T.C.T, 1996. Anisotropic elasticity- Theory and applications. Oxford.
- Torquato, S., Gibiansky, L.V., Silva, M.J., Gibson, L.J., 1998. Effective mechanical and transport properties of cellular solids. *Int. J. Mech. Sci.* **40**: 71-82.
- Tözeren, A., Skalak, R., 1989. Does fabric tensor exist for a fabric?, *Journal of Material Science*, **24**, 1700-1706.
- Truesdell, C., Noll, W., 1965. The non-linear field theories of mechanics. Handbuch der Physik, vol. III/3, Springer, Berlin.
- Truesdell, C., Toupin, R.A., 1960. The Classical Field Theory. Handbuch der Physik, vol. III/1, Springer, Berlin.
- Turner, C.H., Cowin, S.C., 1987. Dependence of elastic constants of an anisotropic porous material upon porosity and fabric. *Journal of Material Science*, **22**, 3178-3184.
- Vianello, M., 1996a. Coaxiality of strain and stress in anisotropic linear elasticity. *Journal of Elasticity* **42**: 283-289.
- Vianello, M., 1996b. Optimizetion of the stored energy and coaxiality of strain and stress in finite elasticity. *Journal of Elasticity* **44**: 193-202.
- Vilenkin, N.J., 1969. Fonctions Spéciales et Théorie de la Représentation des Groupes. Dunod, Paris.
- Vodopyanov, S.K., Goldshtein, V.M., Reshetnyak, Yu. G., 1979. On geometric properties of function with generalized first derivatives. *Russian Math. Surveys* **34**, 19-74.
- Voigt W., 1928. Lehrbuch der Kristallphysik. Leipzig: B.G. Teubner Verlag.
- Wagner, L.D., Gibson, L.J., 2000. The mechanical behaviour of interpenetrating phase composites - I: modelling. International Journal of Mechanical Science 42, 925-942.
- Walpole, L.J., 1984. Fourth-rank tensors of the thirty-two crystal classes: multiplication tables. Proceedings of the Royal Society of London A 391: 149-179.
- Wong, T.-f., 1985. Geometric Probability Approach to the Characterization and Analysis of Microcracking in Rocks, *Mech. of Materials*, **4**: 261-276.
- Zhou, M., Rozvany, G.I.N., 1991. The COC Algorithm, Part II: Topological geometrical and generalized shape optimization. *Comput. Methods Appl. Mechs. Eng.* **89**: 309-336.
- Zysset, P.K., Curnier, A., 1995. An alternative model for anisotropic elasticity based on fabric tensors, *Mech. of Materials*, **21**: 243-250.